

## ABSTRACT



# 31st Annual Computational Neuroscience Meeting: CNS\*2022

Published online: 3 January 2023

© Springer Science+Business Media, LLC, part of Springer Nature 2022

## K1 How full is the brain's petrol tank? Evidence from models of metabolic depletion

Michael Breakspear<sup>\*1</sup>

<sup>1</sup>The University of Newcastle Australia, School of Psychological Sciences, Newcastle, Australia

E-mail: michael.breakspear@newcastle.edu.au

Brain tissue is energy hungry and sensitive to disruptions, such that reduced supply of oxygen during ischemia, asphyxia, and stroke leads rapidly to severe neurological complications. Yet computational

neuroscience has focused almost exclusively on neural activity considered in isolation and has not considered neuronal coupling to an underlying metabolic reserve. Taking hypoxic insults to newborn infants as an exemplar, I will present our recent models of combined metabolic—neuronal coupling in metabolically compromised states. The models capture the essential features of normal and pathological activity observed empirically – seizures and paradoxical bursts - and identifies key homeostatic responses (Fig. 1). As a proof-of-principle, we further show that tracking the parameters of recovering versus poor outcome neonates is possible and predicts dynamics that mimic those seen in the clinic. Combined metabolic-neuronal modelling holds potential to uncover mechanisms in many pathological conditions such as adult stroke, epilepsy, and the altered neurovascular coupling in dementia and during anesthesia. More broadly, considering neuronal-metabolic

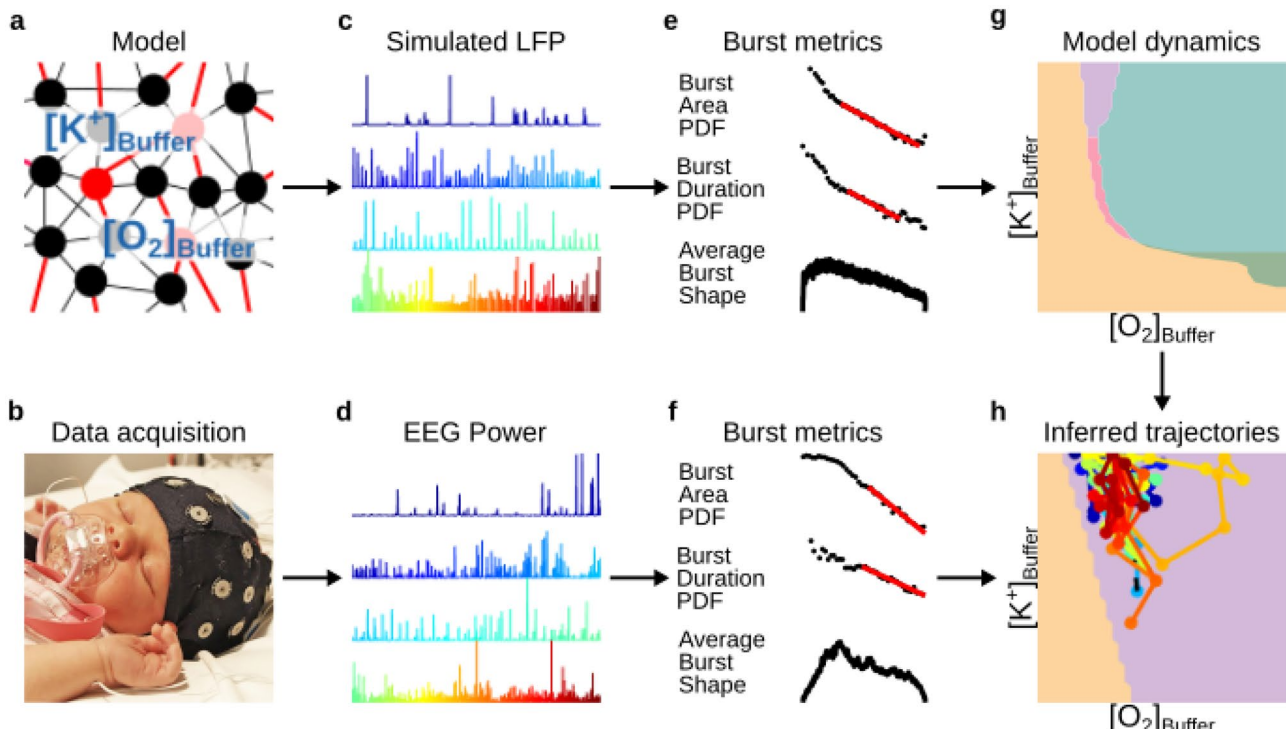


**Fig. 1** Overview of the analysis: **a** Local brain activity is modelled with a network of 400 modelled Hodgkin-Huxley neurons (320 excitatory in black and 80 inhibitory in red) with O<sub>2</sub> dynamics. **b** Two channel, biparietal EEG was recorded from 17 infants during recovery from ischemic-hypoxic insults at birth. **c** Model time series simulated under hypoxic conditions. **d** Infant EEG instantaneous power exhibiting burst suppression. **e–f** Six measures of burst statistics were estimated from the EEG and simulated time series: orders of magnitude and exponents of both the distribution of burst area and the dis-

tribution of duration (total 4 statistics); and asymmetry and sharpness of average burst-shapes from duration 1280 ms to 5120 ms (total 2 statistics). **g** We systematically mapped the emergent dynamical regimes (denoted by colors) in the parameter space of energy demand and supply. **h** By triangulating the infant EEG metrics within the corresponding model parameter space, we inferred likely parameter trajectories of individual infants. Panel (b) used with permission of photographer (Sampsaa Vanhatalo) and with permission to publish in public domain by guardian (Sampsaa Vanhatalo)

coupling in healthy states offers unique insights into the evolutionary constraints imposed by the brain's finite energy budget.

## K2 Enabling tools to model information processing in brains

Joseph Lizier<sup>\*1</sup>

<sup>1</sup>The University of Sydney, School of Computer Science, Sydney, Australia

\*Email: joseph.lizier@sydney.edu.au

The space–time dynamics of interactions in neural systems are often described using terminology of information processing, or distributed computation, in particular with reference to information being stored, transferred and modified in these systems. In this talk, I will introduce an information-theoretic framework – information dynamics – that we use to model each of these operations on information within a complex system, and their dynamics in space and time. Not only does this framework quantitatively align with natural qualitative descriptions of neural information processing, it provides multiple complementary perspectives on how, where and why a system is exhibiting complexity. Specifically, I will describe tools we have produced to enable quantitative analysis of such information processing in brain dynamics, including both theoretical advances (such as how to measure information flows between spike trains) and software toolkits (including JIDT and IDTxl). I will then review what these tools enable us to reveal about dynamics in brains. This will include characterizing behavioral regimes and responses in terms of information processing; revealing the space–time dynamics of information processing during cognitive tasks; and how we can model effective network structure in terms of information flows.

## K3 Moving beyond self-report: Longitudinal network mapping to track therapeutic progress in Interventional Psychiatry

Kristin Sellers<sup>\*1</sup>

<sup>1</sup>The University of California San Francisco, School of Medicine, California, USA

\*Email: kristin.sellers@ucsf.edu

Tracking of disease progression and efficacy of therapeutics in psychiatry often relies on a combination of patient self-report and clinician assessments. Self-report scales are valuable, as they provide insight into the patient's experience, but are also fundamentally lacking as they are sampled sparsely through time and are many steps removed from the biological processes underlying disease. However, self-reports can be used to tune and validate other metrics which in turn can provide more nuanced insight into disease progression and remission. Interventional Psychiatry is a growing subspecialty in which neurotechnology is used to identify dysfunctional brain circuitry underlying psychiatric disorders and brain stimulation is applied to therapeutically modulate that circuitry. In deep brain stimulation (DBS), electric current is delivered to modulate activity in specific neural circuits. Some DBS devices include the capability to measure neural activity via implanted electrodes. Such direct measure of biological processes provides a key window into circuits which can be monitored for evidence of disease progression and efficacy of treatment. Here, I will discuss ongoing research within the PRESIDIO clinical trial (NCT04004169), a study testing personalized closed-loop deep brain stimulation for the treatment of depression. Topics will include the application of computational approaches to identify network structure before and during therapeutic deep brain stimulation

as a way to monitor disease state and treatment efficacy. Looking at neural activity, and in particular network metrics, may provide an intermediate readout of potential therapeutic efficacy that complements and provides more insight than traditional self-report and clinician assessments.

## K4 Adventures in Neuroscience-enabled Technology: inside and outside the academy

Tara Hamilton<sup>\*1,2</sup>

<sup>1</sup>Cuvos, Sydney, New South Wales, Australia

<sup>2</sup>University Of Technology Sydney, School of Electrical and Data Engineering, Sydney, Australia

\*Email: Tara.Hamilton@uts.edu.au

I recently decided to end my (almost) 20-year academic career to dive into the choppy waters of a technology start-up. In this talk I will discuss my own research and how it might be leveraged commercially. Specifically, my research in neuromorphic hearing and learning algorithms holds much promise for commercial products but the road to developing something demonstrable is very bumpy! I will also discuss the field of computational neuroscience in general, and the plethora of commercial opportunities that currently exist. Throughout the talk I'll weave some thoughts and ideas surrounding the highs and lows of moving into private industry and the opportunities and pitfalls of private research and development.

## F1 Photoreceptor biophysics enables deep learning models to generalize across light levels

Saad Idrees<sup>\*1</sup>, Kiersten Ruda<sup>2</sup>, Lindsey Chew<sup>3</sup>, Greg Field<sup>3</sup>, Fred Rieke<sup>4</sup>, Joel Zylberberg<sup>1,5</sup>

<sup>1</sup>York University, Center for Vision Research, Toronto, Canada

<sup>2</sup>Harvard University, Beth Israel Deaconess Medical Center, Boston, United States of America

<sup>3</sup>Duke University, Department of Neurobiology, Durham, United States of America

<sup>4</sup>University of Washington, Department of Physiology and Biophysics, Seattle, United States of America

<sup>5</sup>York University, Department of Physics and Astronomy, Toronto, Canada

\*Email: idrees.sa@gmail.com

Under controlled experimental conditions, state-of-the-art deep learning models can predict retinal ganglion cell (RGC) responses to visual scenes well. However, challenges exist for these models in highly dynamic conditions of natural vision. For example, walking into a shaded area on a sunny day can instantly change the intensity of light reaching the retina by several orders of magnitude. These changes in light level dramatically alter RGC responses. Because current deep learning models of retina have no built-in notion of light level, they are unable to accurately predict RGC responses to light levels that they were not trained on. Our goal is to build retina models that [1] perform better than existing state-of-the-art retina predictors at a single light level, and [2] predict RGC responses to visual scenes at different light levels without training the model at each light level. To achieve this, we developed a deep learning model of retina that combines a biophysical front end capturing the phototransduction cascade with convolutional neural networks (CNNs) capturing the inner retina processing. In addition, we developed an

adaptive-conv layer, which dynamically adjusts the gain based on recent input history.

The front end photoreceptor layer with fast and slow adaptational mechanisms provided models with an in-built notion of light intensities by converting stimulus light intensities (rod isomerizations R\*rod-1 s-1) into photocurrents. Subsequent CNNs converted the photocurrents into RGC spiking. The adaptive-conv layer that we developed as part of this project further equipped the model to adapt to input dynamics. Here, the layer input was convolved with two temporal kernels which were combined divisively to form the output. The resulting model with a photoreceptor layer, adaptive-conv layer, conventional convolution layers and a dense output layer, when trained to predict rat RGC responses to stimuli at bright light levels (10,000 R\*rod-1 s-1), explained 91% variance in RGC responses. This is a significant improvement over previous state-of-the-art retina predictors based on McIntosh et al., 2016, that could only explain 79% of the variance in RGC responses to the same stimuli.

To evaluate if models with photoreceptor layer trained at bright light level could also predict retinal activity at a darker light level (1 R\*rod-1 s-1), we replaced the photoreceptor layer parameters representing cone dynamics with values representing rod dynamics. The CNN parameters were left unchanged from training at bright light level. This model could explain 54% of the variance in RGC responses. This generalization is exceptional given that this model was never trained on dark light level data. In contrast, retina models based solely on CNNs trained at bright light level failed to predict responses to stimuli at dark light levels.

Teaching artificial neural networks to adapt to dynamics of natural world is a first step in enabling models to generalize across conditions they were not trained on. This is significant for several applications, including visual prosthetics. With a trainable photoreceptor layer and the adaptive-conv layer, our deep learning model is already a better predictor of retinal activity than previous state-of-the-art deep learning models of the retina. Our next steps include evaluating the model at more light levels and evaluating these models in computer vision tasks which involve dynamic changes at multiple timescales.

## References

1. McIntosh, L. T., Maheswaranathan, N., Nayebi, A., Ganguli, S. & Baccus, S. A. Deep learning models of the retinal response to natural scenes. *Advances in Neural Information Processing Systems*. 2016; 1369–1377
2. Idrees, S., Baumann, M. P., Franke, F., Münch, T. A. & Hafed, Z. M. Perceptual saccadic suppression starts in the retina. *Nature Communications*. 2020; 11: 1977

## F2 Regional and circuit heterogeneity of brain abnormalities in psychiatric disorders

Ashlea Segal<sup>\*1</sup>, Linden Parkes<sup>2</sup>, Kevin Aquino<sup>3</sup>, Andrew Zalesky<sup>4,5</sup>, Ben J. Harrison<sup>6</sup>, Jeggan Tiego<sup>1</sup>, Murat Yucel<sup>1</sup>, Leah Braganza<sup>1</sup>, Chao Suo<sup>1</sup>, Mark Bellgrove<sup>1,7</sup>, Alex Fornito<sup>1,7</sup>, Seyed Mostafa Kia<sup>8</sup>, Thomas Wolfers<sup>9</sup>, Barbara Franke<sup>10</sup>, Martine Hoogman<sup>10</sup>, Christian F Beckmann<sup>11</sup>, Lars T Westlye<sup>9</sup>, Ole A Andreassen<sup>12</sup>, Christopher Davey<sup>6</sup>, Carles Soriano-Mas<sup>13</sup>, Narcís Cardoner<sup>14</sup>, Michael Berk<sup>15</sup>, Sue Cotton<sup>16</sup>, Andre F Marquand<sup>11</sup>

<sup>1</sup>Monash University, BrainPark, Turner Institute for Brain and Mental Health, School of Psychological Science, Melbourne, Australia

<sup>2</sup>University of Pennsylvania, Philadelphia, United States of America

<sup>3</sup>University of Sydney, School of Physics, Sydney, Australia

<sup>4</sup>The University of Melbourne, Department of Biomedical Engineering, and Department of Psychiatry, Melbourne, Australia

<sup>5</sup>The University of Melbourne, Department of Psychiatry, Melbourne, Australia

<sup>6</sup>The University of Melbourne and Melbourne Health, Melbourne Neuropsychiatry Centre, Department of Psychiatry, Melbourne, Australia

<sup>7</sup>Monash University, Monash Biomedical Imaging, Melbourne, Australia

<sup>8</sup>University Medical Center Utrecht, Department of Psychiatry, Utrecht, Netherlands

<sup>9</sup>University of Oslo, Department of Psychology, Oslo, Norway

<sup>10</sup>Radboud University Medical Center, Donders Institute for Brain, Cognition and Behaviour, Nijmegen, Netherlands

<sup>11</sup>Radboud University, Donders Centre for Cognitive Neuroimaging, Nijmegen, Netherlands

<sup>12</sup>University of Oslo & Oslo University Hospital, Norwegian Centre for Mental Disorders Research (NORMENT), Oslo, Norway

<sup>13</sup>Bellvitge University Hospital, Department of Psychiatry, Barcelona, Spain

<sup>14</sup>Parc Taulí University Hospital, Department of Mental Health and Institut d'Investigació i Innovació Parc Taulí (I3PT), Barcelona, Spain

<sup>15</sup>Deakin University, IMPACT – the Institute for Mental and Physical Health and Clinical Translation, Melbourne, Australia

<sup>16</sup>University of Melbourne, Centre for Youth Mental Health, Melbourne, Australia

\*Email: ashlea.segal@monash.edu

Psychiatric disorders are characterized by individual heterogeneity in patterns of divergent brain structure, which raises questions about the mechanisms driving phenotypic similarities between patients assigned the same diagnosis. One possible explanation is that anatomically heterogeneous brain abnormalities are functionally connected to common brain circuits across patients. To investigate this, we developed a framework for combining normative modeling [1] of grey matter volume (GMV) variations with elements of lesion network mapping [2] to map the functional brain circuits within which anatomical GMV deviations are embedded. This approach allowed us to derive a multiscale characterization of neural heterogeneity across patients diagnosed with six different disorders. We modelled age-, sex-, and site-related variation in GMV, in each of 1032 brain regions, in a training set of controls ( $n=1196$ ) using a hierarchical Bayesian model, as implemented in the PCNToolkit. An independent normative test sample of 269 controls was used. Individual-specific deviation maps, quantifying the degree to which GMV in a given region deviates from model predictions, were calculated. We evaluated heterogeneity at the regional level via permutation testing of patient-control differences in the proportion of individuals showing an extreme negative deviation ( $Z < -2.6$ ). We evaluated circuit-level heterogeneity by mapping areas that show significant functional connectivity with each extreme deviation in an independent healthy cohort. Group-differences in circuit-level overlaps across individuals were evaluated using permutation testing. At a regional level, no area in any disorder showed an extreme deviation in  $> 7\%$  of patients. Further, across patient groups, few regions showed significantly greater overlap than controls ( $pFDR < 0.05$ , two-tailed). Circuit-level overlap was higher, with maximum overlaps ranging between 39%–53%. The group-based permutation testing indicated that all disorders showed some statistical evidence of greater overlap than controls, with areas of lateral frontal and parietal cortex implicated across all disorders ( $pFDR < 0.05$ , two-tailed). However, many of these effects disappeared when using a second, spatially constrained permutation test that accounts for group differences in total deviation burden, indicating greater circuit-level overlap in patients is largely driven by a higher frequency of deviations ( $pFDR < 0.05$ , two-tailed). Collectively, these findings align with past research to indicate extreme heterogeneity of regional GMV abnormalities in psychiatric disorders.

We further show that these heterogenous loci are embedded within common functional circuits. However much of this elevated circuit level overlap was attributable to group differences in total deviation burden rather than the preferential involvement of a specific circuit. The consistent involvement of frontoparietal circuits across disorders may be a marker of transdiagnostic psychological distress associated with deviation burden, with variable involvement of other systems explaining phenotypic differences between disorders.

## References

1. Marquand, A. F., Rezek, I., Buitelaar, J. & Beckmann, C. F. Understanding Heterogeneity in Clinical Cohorts Using Normative Models: Beyond Case–Control Studies. *Biol. Psychiatry*. 2016; 80: 552–561
2. Boes, A. D. et al. Network localization of neurological symptoms from focal brain lesions. *Brain*. 2015; 138: 3061–3075

## F3 Activity-dependent infrared laser stimulation to assess its biophysical effects on single neurons

Alicia Garrido-Peña<sup>\*1</sup>, Pablo Sánchez-Martín<sup>2</sup>, Manuel Reyes-Sánchez<sup>1</sup>, Javier Castilla<sup>3</sup>, Jesús Tornero<sup>3</sup>, Rafael Levi<sup>1</sup>, Francisco B Rodriguez<sup>4</sup>, Pablo Varona<sup>4</sup>

<sup>1</sup>Universidad Autónoma de Madrid, Grupo de Neurocomputación Biológica, Madrid, Spain

<sup>2</sup>Universidad Autónoma de Madrid, Departamento de Ingeniería Informática, Madrid, Spain

<sup>3</sup>Hospital Los Madroños, Unidad Avanzada de Neurorrehabilitación, Brunete, Spain

<sup>4</sup>Universidad Autónoma Madrid, Ingeniería Informática, Madrid, Spain

\*Email: alicia.garrido@uam.es

Near-infrared (NI) laser stimulation has become popular in recent years as an effective neural stimulation technique [1]. Compared to other stimulation methods, the NI laser is less invasive and can be localized and focused on specific regions of the neural system including individual neurons. Thus, it has become a promising tool for medical treatments and a research topic in the last decade.

Most literature about NI laser stimulation has focused on its effective capability to elicit neural activity. Several works have explored its effect on neuronal membranes and discussed the source of the change in neural activity (temperature raise, photoelectric effect, etc.). Changes in capacitance, ionic channels among others [2, 3] have been proposed, but the biophysical source of these effects is not known in detail.

To further study the possible candidates generating this effect, we first explored continuous NI laser stimulation when focused on single neurons of *Lymnaea stagnalis*. During the laser stimulus, there is a strong and reversible change in the spike waveform, mainly affecting its duration by altering both the repolarization and depolarization phases. We have used conductance-based models [4] to reproduce these changes in a computational study and to discriminate candidates for the biophysical explanation of the observed changes.

In this work, we propose a new activity-dependent stimulation protocol that allows to illuminate the neuron only during the depolarization or repolarization phases. The activity is recorded and analyzed in real time. The shutter blocking the laser light is opened when the start of a given phase is detected, and then closed when the phase ends. The protocol uses the tracking of the accumulated activity over time and a threshold criterion to overcome problems derived from the latency of the shutter that controls the time during which the neurons are illuminated.

The real-time software RTXI was used to implement this protocol to avoid uncontrolled latencies allowing a precise detection of the onset of depolarization and repolarization phases. The stimulation protocol has been tested in a computer model study to help in constraining the biophysical candidates that can explain the biophysical effect of the laser stimulation on the ongoing dynamics of individual neurons. Thus, the effect of the laser on the activation and inactivation of different ionic channels can be assessed. We argue that the protocol can also be generalized for other kinds of activity such as bursts or subthreshold oscillations.

## Acknowledgements

This work was funded by AEI/FEDER PGC2018-095895-B-I00 and PID2020-114867RB-I00.

## References

1. Ford, S.M., Watanabe, M., & Jenkins, M.W. *Journal of Neural Engineering*. 2017; 15(1): 11001.
2. Shapiro, M.G., Homma, K., Villarreal, S., Richter, C.P., & Bezanilla, F. *Nature Communications*. 2012; 3(1): 1–11.
3. Li, X., Liu, J., Liang, S., Guan, K., An, L., Wu, X., Li, S., & Sun, C. *Cell Biochemistry and Biophysics*. 2013; 67(3): 1409–1419.
4. Vavoulis, D.V., Nikitin, E.S., Kemenes, I., Marra, V., Feng, J., Benjamin, P.R., & Kemenes, G. *Frontiers in Behavioral Neuroscience*. 2010; 4: 19.

## F4 Evidence of Criticality in Brain Neuronal Networks

Forough Habibollahi Saatlou<sup>1</sup>, Dechuan Sun<sup>2</sup>, Anthony Burkitt<sup>1</sup>, Chris French<sup>\*3</sup>

<sup>1</sup>The University of Melbourne, Biomedical Engineering, Melbourne, Australia

<sup>2</sup>The University of Melbourne, Electrical Engineering, Melbourne, Australia

<sup>3</sup>The University of Melbourne, Medicine, Melbourne, Australia

\*Email: frenchc@unimelb.edu.au

Dynamical systems exhibit transitions between ordered and disordered states. Criticality occurs when the system lies at the borderline between these states at which the input is neither strongly damped nor excessively amplified. Impairments in brain function such as dementia or epilepsy could arise from failure of adaptive criticality, and deviation from criticality may be a potential biomarker for cognition-related neurological and psychiatric impairments.

15-min episodes of widefield calcium imaging from hundreds of hippocampal CA1 neurons using Minisscopes in 8 freely-behaving mice were used to study criticality measures during rest, the cognitive task of novel object recognition (NOR), and NOR following scopolamine administration that greatly impairs spatial memory encoding. A Constrained Non-negative Matrix Factorization algorithm was performed to extract neuronal spatial footprints and temporal traces. Extracted temporal Calcium events were then used to identify neural avalanches using a thresholding step on the ensemble activity. Four independent criticality measures were calculated: power-law distribution, deviation from criticality (DCC), shape collapse error (SCe), and branching ratio (BR).

The 4 criticality metrics were measured during rest, NOR, and NOR-scopolamine sessions from 8 freely-behaving mice. We found that while the hippocampus neural network exhibits some characteristics of a near-critical system at rest (power law

expands less than 2 orders of magnitude,  $DCC = 1.115 \pm 0.182$ ,  $SCe = 0.263 \pm 0.035$ ,  $BR = 0.918 \pm 0.012$  in mean  $\pm$  SE), the network activity shifts significantly closer to a critical state when the mice engaged in cognitive tasks (power law expanded at least 2 orders of magnitude,  $DCC = 0.298 \pm 0.076$ ,  $SCe = 0.047 \pm 0.014$ ,  $BR = 0.976 \pm 0.014$  in mean  $\pm$  SE). The dynamics shift away from criticality when the animal's performance in the NOR test deteriorates due to scopolamine induced memory impairment (power law expands less than 2 orders of magnitude,  $DCC = 1.356 \pm 0.416$ ,  $SCe = 0.267 \pm 0.038$ ,  $BR = 0.832 \pm 0.160$  in mean  $\pm$  SE). The significance of all pairwise differences was established using a post-hoc Tukey's test (Fig. 1).

Our results utilizing a novel calcium imaging technique, for the first time, suggest that switching from inactivity to a cognitively active state modulates the hippocampal neural network's distance from criticality; meaning it decreases DCC and SCe while increasing BR. Additionally scopolamine induced-memory deficits tune the network away from criticality compared to saline controls.

Despite previous efforts we propose that hippocampus neural networks move closer to criticality when successfully processing increased cognitive load during a task such as Novel object recognition.

Our findings imply that being tuned near criticality is potentially the optimal state for the brain network while engaged in a cognitive task given at criticality, the dynamical range and the information content and transmission are maximized.

Neurodegeneration in pathologies such as Alzheimer's disease, Parkinson's disease, and Lewy Body Dementia (LBD) is an area where only a small number of studies have examined the role of critical phenomena. Thereby, it remains as our future path to investigate the deterioration of these criticality tuned dynamics in such pathologies. We aim to identify whether disruptions in the underlying

mechanisms which tune the brain neural network near criticality can act as potential biomarkers for a disease such as LBD.

## O1 Infomorphic Neurons: Locally learning pyramidal-inspired neurons derived from partial information decomposition

Abdullah Makkeh<sup>\*1</sup>, Michael Wibral<sup>2</sup>, Marcel Graetz<sup>3</sup>, Andreas Schneider<sup>4</sup>

<sup>1</sup>University of Göttingen, Göttingen Campus Institute for Dynamics of Biological Networks, Göttingen, Germany

<sup>2</sup>Georg-August-Universität, Campus Institut für Dynamik biologischer Netzwerke, Göttingen, Germany

<sup>3</sup>ETH Zurich, Department of Chemistry and Applied Biosciences, Zurich, Switzerland

<sup>4</sup>Max Planck Institute for Dynamics and Self-Organization, Neural Systems Theory, Göttingen, Germany

\*Email: abdullah.alimakkeh@uni-goettingen.de

Pyramidal neurons are neurons that have two separate trees of dendrites: apical and basal. These two distinct trees of dendrites are hypothesized to treat two classes of input with different roles, e.g. feedforward and feedback inputs. There is still, however, a lack of understanding of the roles of these distinct classes. Given that pyramidal neurons are abundant in the neocortex and can be found in various regions of the brain that serve inherently different tasks such as sensory, cognitive and motor tasks. It is safe to assume that pyramidal neuron architecture contributes in important ways to neocortical information processing capacity. Thus, a better understanding of the role of the two input classes promises to further our

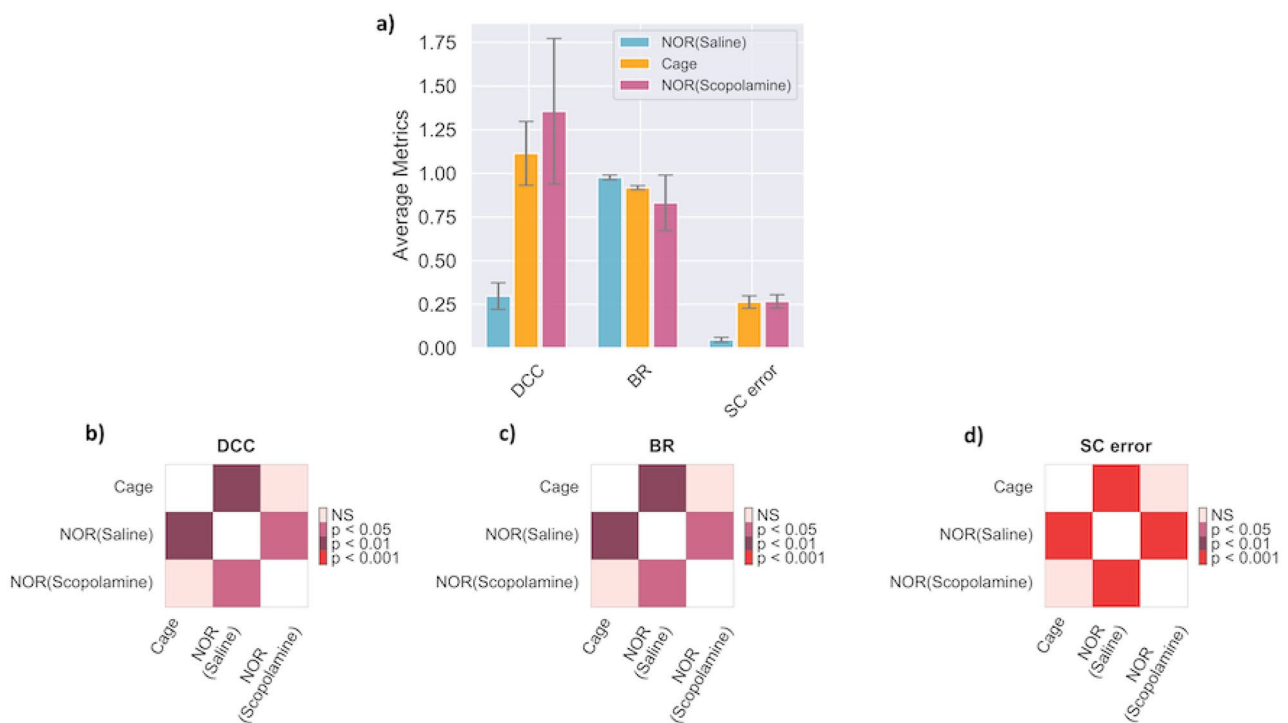


**Fig. 1** The recognition and spatial memory deficits induced by scopolamine injection tune the network away from criticality compared to saline controls showing dynamics more similar to rest periods in the home cage

understanding of cortical computation and to also improve the design of artificial neural networks.

To describe information processing in pyramidal cells independent of the semantics of the specific tasks above, their neural function can be formalized within the mathematical domain of information theory. Information theory is relevant to the description of pyramidal neurons with their input classes via its recent extension, partial information decomposition (PID). PID offers to characterize the information in the firing of the neuron as information that is (i) redundant in any of the two classes of input, (ii) unique to a specific class of input, (iii) synergistic requiring both classes of input jointly, and (iv) completely independent of the classes of input (i.e. driven by stochasticity). Thus, in this functional formulation, pyramidal neurons will tune their firing properties and synaptic weights to optimize types of information contributions relevant to their role. Therefore, building artificial neurons based on the PID formalism enables simulating various networks containing pyramidal-like neurons to gain new insights into the cortical computation.

To design such an artificial neuron based on the PID formalism, one requires a differentiable PID measure that quantifies the aforementioned types of information. We introduced such a measure in 2021 - enabling the design of “infomorphic” neurons inspired by pyramidal neurons that learn to fire by optimizing any prescribed combination of redundant, unique, synergistic information of their inputs and the stochastic information about their firing. In this work, we will explain the design of infomorphic neurons and demonstrate a minimalist infomorphic network built as a Hopfield-like memory network that significantly outperforms the memorization capacity of classical Hopfield networks (Fig. 1).

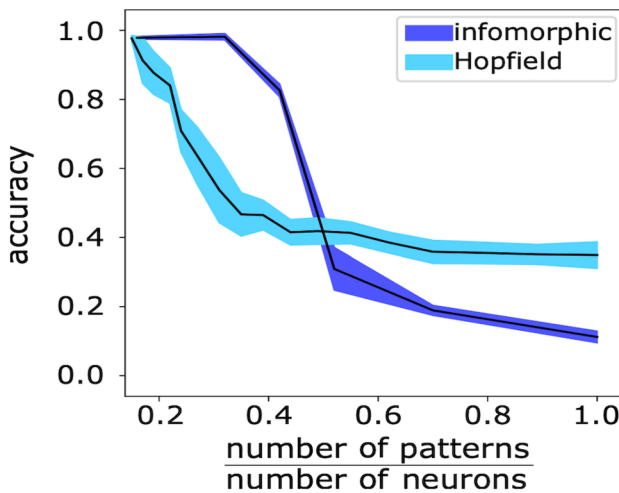


**Fig. 1** The memorization capacity of an Infomorphic network outperforms that of a Hopfield network. The networks were compared by increasing the patterns/neurons proportion. Infomorphic network maintains a more than 80% accuracy even as the patterns/neurons proportion reaches 0.45 whereas Hopfield network declines into catastrophic forgetting as early as its patterns/neurons proportion hits 0.25

## O2 Balancing sequence robustness and interval variability in minimal CPG bursting models

Blanca Berbel<sup>\*1</sup>, Pablo Sánchez-Martín<sup>1</sup>, Roberto Latorre<sup>1</sup>, Pablo Varona<sup>1</sup>

<sup>1</sup>Universidad Autónoma de Madrid, Departamento de Ingeniería Informática, Madrid, Spain

\*Email: blanca.berbel@uam.es

Many known CPGs produce bursting rhythms consisting of patterned activity built with robust sequential activations of their constituent neurons. Nevertheless, time intervals building such sequences cycle-by-cycle show variability that endows flexibility for motor coordination while guaranteeing the production of functional sequences. Some of these intervals display dynamical invariants in the form of robust linear relationships that are kept under extreme experimental conditions [1–3]. In this work, we studied CPG models with minimal circuit configurations to understand the presence of both robust sequence generation and interval variability in bursting rhythms. Model neurons implemented with the Komendantov-Kononenko conductance-based model were set into chaotic spiking-bursting regimes to induce intrinsic variability. CPG models considered slow and fast graded chemical synapses. We explored different parameters of CPG models that lead to interval variability while keeping robust sequential activations in the circuit. Interval variability was not easy to sustain in common CPG building-block architectures even when the intrinsic dynamics of model neurons are highly irregular. When such variability is present, dynamical invariants are difficult to find including those that display linear relationships of long intervals with the instantaneous cycle-by-cycle period. Variability of CPG patterned activity is part of living CPGs functional coordination mechanisms. CPG models tend to lack such variability whose origin relies on both in the intrinsic neuron and synapse dynamics. Our results show that chemical synapses contribute to shape the intervals building robust sequential activations in bursting CPGs.

## Acknowledgments

This work was funded by AEI/FEDER PGC2018-095895-B-I00.

## References

1. Elices, I., Levi, R., Arroyo, D., Rodriguez, F. B. F. B., & Varona, P. Robust dynamical invariants in sequential neural activity. *Scientific Reports*. 2019; 9(1): 9048.
2. Garrido-Peña, A., Elices, I., & Varona, P. Characterization of interval variability in the sequential activity of a central pattern generator model. *Neurocomputing*. 2021; 461: 667–678
3. Berbel, B., Garrido-peña, A., Elices, I., Latorre, R., & Varona, P. Effect of Electrical Synapses in the Cycle-by-Cycle Period and Burst Duration of Central Pattern Generators. In I. Rojas, G. Joya, & A. Català (Eds.), *Lecture Notes in Computer Science*. 2021; 12862: (pp. 81–92). Springer International Publishing.

## O3 Temporal scaling of neural trajectories in a multiple-timescale network

Tomoki Kurikawa<sup>\*1</sup>

<sup>1</sup>Kansai Medical University, Hirakata, Osaka, Japan

\*Email: labyrinth2shell@gmail.com

How temporal information is represented in the neural system is a crucial question for understanding various cognitive functions, such as working memory tasks. Recent experimental studies [1] revealed that the neural states moved at different speeds depending on the different context, but their trajectories are highly similar, which is called temporal scaling. Some theoretical studies have analyzed such temporal scaling of the neural representation by using reverse

engineering methods. However, the mechanism is a black box, and how the temporal scaling happens is still unclear. In our previous study [2], we developed a multiple-timescale neural network that generates robust sequential patterns to perform working memory tasks [3]. This network model is shaped through a simple learning rule that satisfies the locality (i.e., only pre- and post-synaptic information is required). Due to the simplicity of the learning rule, the structure of the neural dynamical systems after learning is clear. In this study, we used this model to clarify the mechanism underlying the temporal scaling of the neural representation across different contexts. We trained the network to generate a sequence under a certain context (here, different context is represented as different input strength of the external input and different gain parameter of the activation function in the neuron). After training, the temporal scaling across different contexts appears. We found that neural trajectories composed of pseudo fixed-point attractors and the stability of all attractors are simultaneously regulated by the strength of external input and/or gain parameter. The regulated stability of all attractors leads the neural states to transit from one attractor to another at different speeds depending on the input strength and/or the gain. We also found a network structure

allowing for global regulation of the stability of attractors. Our study suggests a new mechanism underlies the temporal scaling in the neural system.

### Acknowledgements

We thank JSPS KAKENHI (20H00123) and (20K07716) for supporting.

### References

- Wang, J., Narain, D., Hosseini, E. A., and Jazayeri, M. Flexible timing by temporal scaling of cortical responses. *Nature neuroscience*. 2018; 21(1): 102–110.
- Kurikawa, T., and Kaneko, K., Multiple-Timescale Neural Networks: Generation of History-Dependent Sequences and Inference Through Autonomous Bifurcations. *Frontiers in Computational Neuroscience*. 2021; 15.
- Kurikawa, T. Transitions among metastable states underlie context-dependent working memories in a multiple timescale network. In: International Conference on Artificial Neural Networks. Springer, Cham. 2021; p. 604–613.

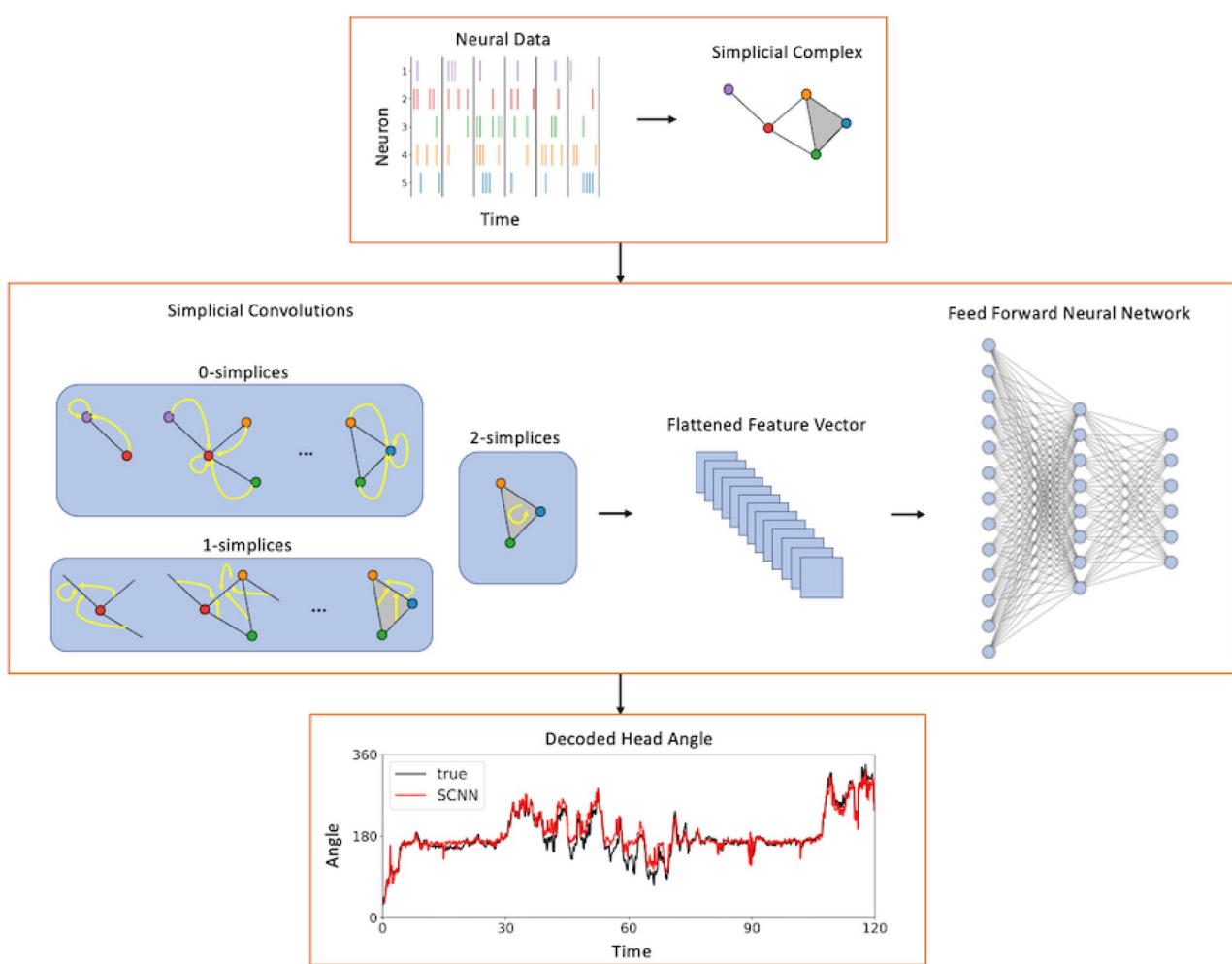


**Fig. 1** Workflow of simplicial convolutions for Head Direction Cell decoding

## O4 Deep Simplicial Manifold Learning for Neural Spike Train Decoding

Edward Mitchell<sup>\*1</sup>, David Boothe<sup>2</sup>, Piotr Franaszczuk<sup>2</sup>, Vasileios Maroulas<sup>1</sup>

<sup>1</sup>University of Tennessee, Department of Mathematics, Baltimore, MD, United States of America

<sup>2</sup>U.S. Army Research Laboratory, Human Research and Engineering Directorate, Aberdeen Proving Ground, MD, United States of America

\*Email: emitch39@vols.utk.edu

With new neurophysiological recording techniques increasing the number of neurons that can be simultaneously recorded, methods for decoding neural spike trains are drawing more interest. A growing number of decoding methods rely on deep learning tools, specifically artificial neural networks, which outperform statistical methods [1]. Manifold discovery, in which the high-dimensional activity of a group of cells is projected onto a low-dimensional manifold, has unlocked a new avenue for spike train decoding [2]. Artificial neural networks have been designed to handle a variety of data-types (e.g., vectors, matrices, graphs) as inputs, but only recently has work been done to allow for the input of simplicial complexes into neural networks for machine learning tasks [3, 4]. Simplicial complexes are topological spaces that use not only vertices and edges, but also higher-dimensional objects like triangles and tetrahedra to generalize graphs and capture more than just pairwise relationships. Thus, they naturally lend themselves to defining neural activity where ensembles of brain cells may work together to encode low-dimensional variables [5]. We devise a Simplicial Convolutional Neural Network (SCNN) framework for decoding neural spike train activity that combines unsupervised manifold discovery with the power of deep learning (Fig. 1).

The spike trains of a cell population are defined on a simplicial complex whose connectivity is generated by the intrinsic functional activity of the cells. This simplicial complex is called the *functional simplicial manifold*. Trajectories along the functional simplicial manifold correspond to neural activity over a period of time and are used as input to a SCNN which outputs the relevant decoded variables. The effectiveness of the framework is demonstrated by decoding Head Direction cells, which are brain cells that fire when the head is facing a certain direction (Fig. 1). A comparison to a naive feed forward neural network shows our method improves decoding accuracy and produces less outliers, which can be harmful in application.

### Acknowledgements

Edward Mitchell and Vasileios Maroulas would like to acknowledge funding from the U.S. Army Research Lab with CA number W911NF2120186.

### References

1. Xu Z, Wu W, Winter S, et al. A comparison of neural decoding methods and population coding across thalamo-cortical head direction cells. *Frontiers in Neural Circuits*. 2019; 13: 75.
2. Chaudhuri R, Gercek B, Pandey B, et al. The intrinsic attractor manifold and population dynamics of a canonical cognitive circuit across waking and sleep. *Nature Neuroscience*, 2019; 22(9):1512–1520.
3. Ebli S, Defferrard M, and Spreemann G. Simplicial neural networks, In NeurIPS Workshop on Topological Data Analysis and Beyond, 2020.
4. Hajij M, Zamzmi G, Papamarkou T, et al. Simplicial complex representation learning, Machine Learning on Graphs (MLoG) Workshop at 15th ACM International WSDM Conference, 2022.

5. Peyrache A, Lacroix M, Petersen P, et al. Internally organized mechanisms of the head direction sense. *Nature Neuroscience*, 2015; 18(4): 569–575.

## O5 Brain Wave Pattern Dynamics – Changes in Alzheimer’s Disease

Clarissa Hoffman<sup>\*1</sup>, Jingheng Cheng<sup>2</sup>, Daoyun Ji<sup>2</sup>, Yuri Dabaghian<sup>1</sup>

<sup>1</sup>The University of Texas McGovern Medical School at Houston, Neurology, Houston, TX, United States of America

<sup>2</sup>Baylor College of Medicine, Neuroscience, Houston, TX, United States of America

\*Email: clarissa.m.hoffman@uth.tmc.edu

Alzheimer’s Disease (AD) is a complex, progressive, and devastating neurodegenerative disease. Its detrimental effects span a variety of neurologic and cognitive functions. Major efforts, including computational modeling, are made to explain mechanisms of AD at various scales, from intracellular to network to organismal. We focus on the mechanism of synchronization and propose an alternative approach to EEG analysis that focuses on the rhythms’ patterns over a temporal mesoscale. Specifically, we use two “stochasticity scores” for quantifying structural regularity and irregularity of the recorded signals and correlate the outcomes with behavior. These methods stem from two independent mathematical frameworks, discovered by A. Kolmogorov in 1933 and V. Arnold in the 2000’s. The first approach quantifies a pattern’s consistency with its underlying mean behavior, and the second measures how “structured” (e.g., periodic-like or time-clustered) the pattern is. Our work in wild type mice revealed a coupling between the form, the patterns, of the hippocampal EEG waves and parameters of the animal’s activity, such as location, speed and acceleration. Specifically, we studied θ-waves, γ-waves, and sharp wave-ripple (SWR) events and found interdependencies between the θ-, γ-, and SWR patterns and the animals’ speed and acceleration. We also observed clustering of these hippocampal waves with spatially dependent morphologies along the animal’s trajectory which are reminiscent of hippocampal place fields. These are important observations because the θ-waves, γ-waves, and sharp wave-ripple (SWR) events coordinate hippocampal spiking activity, hence, may influence spatial and episodic memory encoding, consolidation, and retrieval. In AD-damaged synaptic circuits, the brain wave patterns are altered—we can distinguish the disordered structures in AD brains from those in healthy brains. Namely, the coupling between wave dynamics and speed/acceleration is weak and spatial selectivity is lost, suggesting that information exchange within the AD brain is compromised. Overall, these results offer a novel perspective on studying the structure, the dynamics, and the functionality of the brain waves and will provide a deeper understanding of AD at a neurocircuit level.

## O6 A large-scale survey of spatial and motion selectivity in an entire column in mouse V1

Reza Abbasi-Asl<sup>\*1</sup>, Roozbeh Farhoodi<sup>1</sup>, Josh Larkin<sup>2</sup>, Kevin Takasaki<sup>2</sup>, Daniel Millman<sup>2</sup>, Daniel Denman<sup>2</sup>, Jerome Lecoq<sup>2</sup>, Anton Arkhipov<sup>2</sup>, Nathan W. Gouwens<sup>2</sup>, Jack Waters<sup>2</sup>, R. Clay Reid<sup>2</sup>, Saskia E. J. de Vries<sup>2</sup>

<sup>1</sup>University of California, San Francisco, Neurology, Bioengineering and Therapeutic Sciences, San Francisco, CA, United States of America

<sup>2</sup>Allen Institute, Seattle, WA, United States of America

\*Email: reza.abbasiasl@ucsf.edu

Neurons in mouse V1 are shown to be selective to a wide variety of visual stimulus types including sparse noise, drifting and flashed gratings, natural images, and natural movies. This diverse selectivity profile reveals several distinct classes of response profiles including neurons that respond reliably to either motion features or localized spatial features. However, the exact organization of these distinct selectivity profiles to motion and spatial features is not well-understood in different visual layers in the brain. The detailed characterization of these response profiles could serve as a valuable resource to systematically build and assess biologically plausible models of neurons in visual cortex both from the biophysical and machine learning perspectives. As prior work suggests, the segregation of spatial and motion information may occur prior to the cortex as inputs from the lateral geniculate nucleus (LGN) show a similar segregation of spatial and motion information. Given the distinct spatial and motion information arriving in V1, and the evidence supporting distinct spatial and motion streams among the higher visual areas, we aim to characterize the distinct profiles of spatially-selective and motion-selective neurons in V1. Here, we systematically characterize the spatial and motion selectivity of neurons in an entire column in mouse V1. We have collected and analyzed a large-scale 2-photon and 3-photon volumetric imaging dataset from an  $800 \times 800 \times 600 \mu\text{m}^3$  volume in V1 of four mice spanning all visual layers from pia to white matter. The visual responses were recorded during presentation of a locally sparse noise stimulus and drifting gratings to efficiently reconstruct both spatial selectivity and motion selectivity profiles of neurons. We designed and implemented computational pipelines to identify responsive neurons to each stimulus type and determined the spatial and motion selectivity profile of each responsive neuron. Using these experimental and computational pipelines, we found that neurons in V1 are overall less responsive to spatial features compared to motion features (15% of the neurons were spatially-selective and 28% of neurons were motion-selective). The responsiveness ratio of motion-selective neurons increases up to  $\sim 300 \mu\text{m}$  depth and then decreased for the deeper planes. For the spatially-selective neurons, we found that the responsiveness ratio decreased in deeper planes starting at  $\sim 160 \mu\text{m}$  depth. Neurons in layer 2/3 were about 4 times more likely to respond to localized spatial features compared to neurons in layer 5. Finally, we found that 4% of the neurons are both spatially-selective and motion-selective which is about the chance level. Overall, our results show a distinct layer-specific profile for selectivity of neurons to spatial and motion features. These findings pave the road for the design and construction of detailed biophysical or machine learning models of visual cortex which are biologically plausible.

## O7 A new formalism relating kinematic intention readout to action processing

Kiri Pullar<sup>\*1</sup>, Eugenio Scaliti<sup>1</sup>, Giulia Borghini<sup>1</sup>, Andrea Cavalllo<sup>2</sup>, Stefano Panzeri<sup>3</sup>, Cristina Becchio<sup>4</sup>

<sup>1</sup>Istituto Italiano di Tecnologia, Center for Human Technologies, Genova, Italy

<sup>2</sup>Università degli Studi di Torino, Department of Psychology, Torino, Italy

<sup>3</sup>University Medical Center Hamburg-Eppendorf (UKE), Department of Excellence for Neural Information Processing, Center for Molecular Neurobiology (ZMNH), Hamburg, Germany

<sup>4</sup>University Medical Center Hamburg-Eppendorf (UKE), Department of Neurology, Hamburg, Germany

\*Email: kiri.pullar@iit.it

Trial-to-trial variations in movement kinematics convey intention-related information. Human observers can exploit this information

when explicitly prompted to do so. However, the question remains as to whether they spontaneously use this information to anticipate other people's actions. This question is difficult to address in part because of the lack of a formalism to relate the intention information that observers read out at the single trial level to action processing. Here we develop a novel computational analysis of motion tracking and psychophysical data to quantify kinematic intention information readout and relate it to action predictions. We demonstrate a new form of priming, which we term kinematic priming, and show that the amount of kinematic priming is determined by the amount of intention information read out at the single trial and single subject level. On each trial, participants ( $n=20$ ) observed either a reach-to-drink or reach-to-pour act (kinematic prime) followed by a static image of a person drinking or pouring (action probe). The prime-probe relationship was either congruent (same intention; 75% of trials) or incongruent (different intention; 25% of trials) and varied from trial-to-trial. Participants were asked to categorize the action depicted in the static image quickly yet accurately. Eye movements were monitored with an eye tracker. This task served to probe the kinematic priming of response latencies and initial fixations.

One hour later, participants performed a forced-choice intention discrimination task on the same reaching acts that were used as primes in the previous session. This task served to quantify intention information readout and obtain a measure of the intention information extracted by each participant from each reaching act. Using logistic regressions fitted to the intention discrimination data, we analyzed how intention information is encoded (mapping of kinematics to reaching act intention) and read out (mapping of kinematics to participant intention choices).

In the action categorization task participants were faster to respond on trials in which the intention encoded in the kinematic prime matched the action probe. Response time priming was further supported by eye tracking data, with the landing of initial fixations on the action probe picture varying systematically with the intention encoded in the prime. This kinematic priming phenomenon varied widely across trials and participants.

We next examined the relationship between variability in kinematic priming and kinematic intention encoding and readout. We found that kinematic readout of intention information at the single-participant single-trial level, but not kinematic encoding, predicted the extent of kinematic priming. These results collectively demonstrate that intention-related information encoded in movement kinematics is implicitly read out and spontaneously used to anticipate the actions of others.

## O8 Context-dependent hubs in multisensory perception revealed by computational modeling of large-scale cortical networks

Ronaldo Nunes<sup>1</sup>, Marcelo Reyes<sup>1</sup>, Raphael de Camargo<sup>1</sup>, Jorge Mejias<sup>\*2</sup>

<sup>1</sup>Universidade Federal do ABC, Center for Mathematics, Computing and Cognition, São Bernardo do Campo, Brazil

<sup>2</sup>University of Amsterdam, Swammerdam Institute for Life Sciences, Amsterdam, Netherlands

\*Email: jorge.f.mejias@gmail.com

Multisensory integration (MSI) is a crucial component of perception and cognition. Despite extensive research, there is still an intense debate on which brain region(s) are responsible for MSI, with evidence for multisensory processing pointing at regions as diverse as high cortical areas, subcortical areas or even primary sensory cortex [1, 2], often leading to contradicting hypotheses. In this communication, we present a theoretical and computational study to test the existence of 'hubs' for

MSI –i.e. brain regions in which coexisting signals from multiple sensory modalities evoke a response markedly larger than for unisensory signals. We first developed a data-constrained computational model of the large-scale mouse brain network, and then simulated a multisensory detection task in which mice must detect weak uni- or multi-sensory signals [3]. Our model revealed that, while some brain areas are indeed significantly better than others at MSI functions, the role of being such ‘multisensory hubs’ does not always fall upon the same areas, and the concrete set depends strongly on context-dependent conditions such as the level of ambient light. These changes in the response to multisensory signals are observed in many brain areas, indicating that the phenomenon is robust and distributed across the whole brain. Furthermore, with the help of a reduced model, we found that the existing variability of in-degree connectivity of different brain nodes (as indicated from the connectomics data) is the main cause for these context-dependent MSI hubs, as this variability impacts the working point of each brain area and therefore its nonlinear integrating abilities. Overall, our work provides a compelling explanation as of why it has not been possible to experimentally identify unique MSI areas even for a well-defined multisensory task, and suggests that MSI is, like other cognitive functions [4], highly distributed and context-dependent.

## References

- Stein BE, Rowland BA. Using superior colliculus principles of multisensory integration to reverse hemianopia. *Neuropsychologia*. 2020; 141: 107413
- Olcese U, Iurilli G, Medini P. Cellular and synaptic architecture of multisensory integration in the mouse neocortex. *Neuron*. 2013; 79: 579–593
- Meijer GT et al. Neural Correlates of Multisensory Detection Behavior: Comparison of Primary and Higher-Order Visual Cortex. *Cell Reports*. 2020; 31: 107,636
- Mejias JF and Wang X-J. Mechanisms of distributed working memory in a large-scale network of macaque neocortex. *eLife*. 2022; 11: e7236

## O9 The topochronic map of the human brain dynamics

Pierpaolo Sorrentino<sup>\*1,2</sup>, Spase Petkoski<sup>2</sup>, Fabio Baselice<sup>3</sup>, Viktor Jirsa<sup>4</sup>, Maddalena Sparaco<sup>5</sup>, Emahuel Troisi Lopez<sup>6</sup>, Elisabetta Signoriello<sup>5</sup>, Simona Bonavita<sup>5</sup>, Maria Agnese Pirozzi<sup>7</sup>, Mario Quarantelli<sup>7</sup>, Giuseppe Sorrentino<sup>6</sup>

<sup>1</sup>Parthenope University of Naples, Naples, Italy

<sup>2</sup>Aix-Marseille University, Institut de Neurosciences des Systèmes, Marseille, France

<sup>3</sup>Parthenope University of Naples, Biomedical Engineering, Naples, Italy

<sup>4</sup>INSERM & Aix-Marseille Université, Theoretical Neuroscience Group, Institut de Neurosciences des Systèmes, Marseille, France

<sup>5</sup>University of Campania Luigi Vanvitelli, Department of Advanced Medical and Surgical Sciences, Naples, Italy

<sup>6</sup>Parthenope University of Naples, Department of Motor Sciences and Wellness, Naples, Italy

<sup>7</sup>National Research Council, Biostructure and Bioimaging Institute, Naples, Italy

\*Email: ppsorrentino@gmail.com

Large-scale brain activity evolves dynamically over time, across multiple time-scales. The structural connectome imposes a spatial network constraint since two structurally connected brain regions are more likely to coordinate their activity [1, 2]. It also imposes a temporal network constraint by virtue of time delays via signal transmission, which has modulatory effects for oscillatory signals [3]. Specifically, the lengths of the structural bundles, their widths, myelination, as well as the overall organization of the structural scaffold, influence the timing of the interactions across the brain network. Here, we estimate the functional delays across the whole

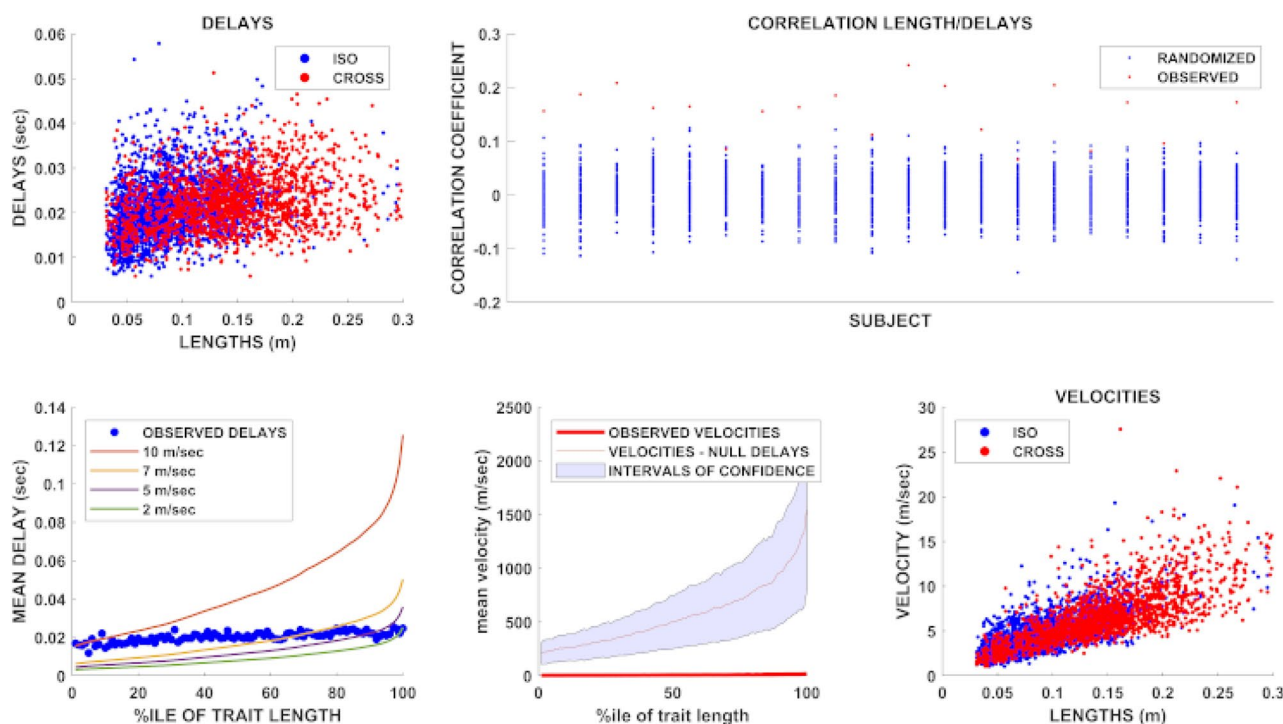


**Fig. 1** Top left: track lengths and functional delays Top right: individual lengths/delays relationship (red), corresponding nulls (blue). Bottom left: average delay across the nth percentile. Colored lines:

delays given constant velocities. Bottom middle: observed velocities (red); red line: velocity based on nulls). Bottom right: Relationship length/velocities

brain from magnetoencephalography—and integrate them with the structural connectome—derived from magnetic resonance imaging. We provide a map of the functional delays characterizing the connections across the human brain. Furthermore, we show in multiple sclerosis patients that demyelinating lesions correspond to higher transmission delays.

We introduce a novel *in vivo* approach for directly measuring functional delays across the whole brain using magneto/electro-encephalography and integrating them with the structural connectome derived from magnetic resonance imaging. Based on source-reconstructed magnetoencephalographic data from a cohort of healthy subject, we estimate neuronal avalanches. An avalanche was defined as starting when at least one region is above threshold, and as finishing when no region is active. The delays were estimated for each avalanche. In an avalanche, from the moment region activated, we recorded how long it took region  $j$  to activate. These are what we considered the delays. Hence, for each avalanche we obtained a matrix where rows and columns represent brain regions, and the entries contain the delays. We then averaged across all the avalanches belonging to one subject, obtaining an average  $ij$ th delay. We also obtained track length from MRI scans. Additionally, for each patient, a lesion map was obtained by segmentation of the 3D-FLAIR volume using the lesion prediction algorithm implemented in the Lesion Segmentation Tool for SPM. Finally, dividing the track lengths by the delays yielded velocities.

The functional delays are tightly regulated, showing, as expected, that larger structural bundles had faster velocities, with the delays varying much less than expected if they only depended upon distance (permutation test,  $p < 0.001$ ), both at the group and individual level. Then, we estimated the delays from magnetoencephalography (MEG) data in a cohort of multiple sclerosis patients, who have damaged myelin sheaths, and demonstrated that patients showed greater delays across the whole network than a matched control group (KS test,  $p < 0.001$ ). Furthermore, within each patient, individual lesioned connections were slowed down more than unaffected ones (permutation test,  $p < 0.001$ ). Our technique estimates functional transmission delays *in vivo* in health and disease, and provides empirical, subject-specific constraints to tailor brain models.

## References

1. P. Sorrentino, C. Seguin, R. Rucco, M. Liparoti, E. Troisi Lopez, S. Bonavita, M. Quarantelli, G. Sorrentino, V. Jirsa, A. Zalesky. The structural connectome constrains fast brain dynamics. *eLife*. 2021; 10: e67400
2. P. Sorrentino, R. Rucco, F. Baselice, R. De Micco, A. Tessitore, A. Hillebrand, L. Mandolesi, M. Breakspear, L. L. Gollo, G. Sorrentino. Flexible brain dynamics underpins complex behaviours as observed in Parkinson's disease. *Scientific Reports*. 2021; 11: 4051.
3. G. Deco, V. Jirsa, A. R. McIntosh, O. Sporns, R. Kötter. Key role of coupling, delay, and noise in resting brain fluctuations. *Proceedings of the National Academy of Sciences of the U. S. A.* 2009; 106: 10,302–10,307.
4. P. Sorrentino, et. al. On the topochronic map of the human brain dynamics. 2021; 2021.07.01.447872.

## O10 Spectral graph modeling of Alzheimer's disease neurophysiology

Parul Verma<sup>\*1</sup>, Kamalini Ranasinghe<sup>2</sup>, Chang Cai<sup>1</sup>, Xihe Xie<sup>1</sup>, Hannah Lerner<sup>2</sup>, Danielle Mizuiri<sup>1</sup>, Bruce Miller<sup>2</sup>, Katherine Rankin<sup>2</sup>, Keith Vossel<sup>3</sup>, Srikantan Nagarajan<sup>1</sup>, Ashish Raj<sup>1</sup>

<sup>1</sup>University of California San Francisco, Department of Radiology and Biomedical Imaging, San Francisco, United States of America

<sup>2</sup>University of California San Francisco, Department of Neurology, San Francisco, United States of America

<sup>3</sup>University of California Los Angeles, Department of Neurology, Los Angeles, United States of America

\*Email: parul.verma@ucsf.edu

Alzheimer's disease (AD) is the most common form of dementia, progressively impairing memory, cognition, as well as behavior. While various neuroimaging studies of the human brain have revealed functional abnormalities in patients with AD [1], how neuronal and synaptic functions are impaired remain unclear. Electrophysiological recordings that capture the local field potentials from pyramidal neuronal firing are the most direct techniques to record neuronal activity from human subjects non-invasively. Combined with mathematical models, empirical spectral data from electrophysiology will help uncover the abnormal biophysical mechanisms of neuronal activity which is otherwise intractable. In this work, we employed a spectral graph-theory based model (SGM) to identify abnormal biophysical markers of neuronal activity in AD [2].

SGM is a hierarchical and analytic model that describes the dynamics of excitatory and inhibitory neuronal activity. It models the coupled excitatory and inhibitory activity of local neuronal subpopulations, and the long-range excitatory macroscopic dynamics, for every brain region. It is parameterized by a small set of global parameters – we inferred these parameters for a well characterized clinical population of AD patients and a cohort of age-matched controls [3]. We estimated model parameters that best captured the regional MEG frequency spectra as well as the spatial distribution of the empirical alpha frequency oscillation. For both patients and controls, the modeled spectra closely match the empirical MEG spectra (Fig. 1A). Patients with AD have significantly elevated long-range excitatory neuronal time constant ( $\tau_G$ ) compared to controls ( $p = 0.0006$ ; Fig. 1B). Moreover, higher  $\tau_G$  is also associated with cognitive deficits in AD. Specifically, higher  $\tau_G$  is positively correlated with Clinical Dementia Rating – Sum of Boxes ( $p = 0.0117$ ; Fig. 1C), and is negatively correlated with Mini Mental State Exam score ( $p = 0.0016$ ; Fig. 1D).

These results indicate that abnormal spectral signatures in combination with SGM can reliably depict altered excitatory neuronal activity in AD patients. Importantly these abnormalities showed significant associations with cognitive deficits. These findings are intriguing given the context that neurofibrillary tangle pathology that is closely allied to cognitive deficits in AD have been shown to preferentially affect excitatory neurons in human neuropathological studies [4, 5]. Our findings provide critical insights about potential mechanistic links between abnormal neural oscillations and cellular correlates of impaired neuronal activity in AD.

## References

1. Jagust W. Imaging the evolution and pathophysiology of alzheimer disease. *Nature Reviews Neuroscience*. 2018, 19, 687–700.
2. Raj A, Cai C, Xie X, et al. Spectral graph theory of brain oscillations. *Human Brain Mapping*. 2020, 41, 2980–2998.
3. Ranasinghe K. G, Cha J, Iaccarino L, et al. Neurophysiological signatures in alzheimer's disease are distinctly associated with TAU, amyloid- $\beta$  accumulation, and cognitive decline. *Science Translational Medicine*. 2020, 12, eaaz4069.
4. Hyman B. T, Van Hoesen G. W, Damasio A. R, Barnes C. L. Alzheimer's disease: cell-specific pathology isolates the hippocampal formation. *Science*. 1984, 225, 1168–1170.
5. Fu H, Possenti A, Freer R, et al. A tau homeostasis signature is linked with the cellular and regional vulnerability of excitatory neurons to tau pathology. *Nature neuroscience*. 2019, 22, 47–56.

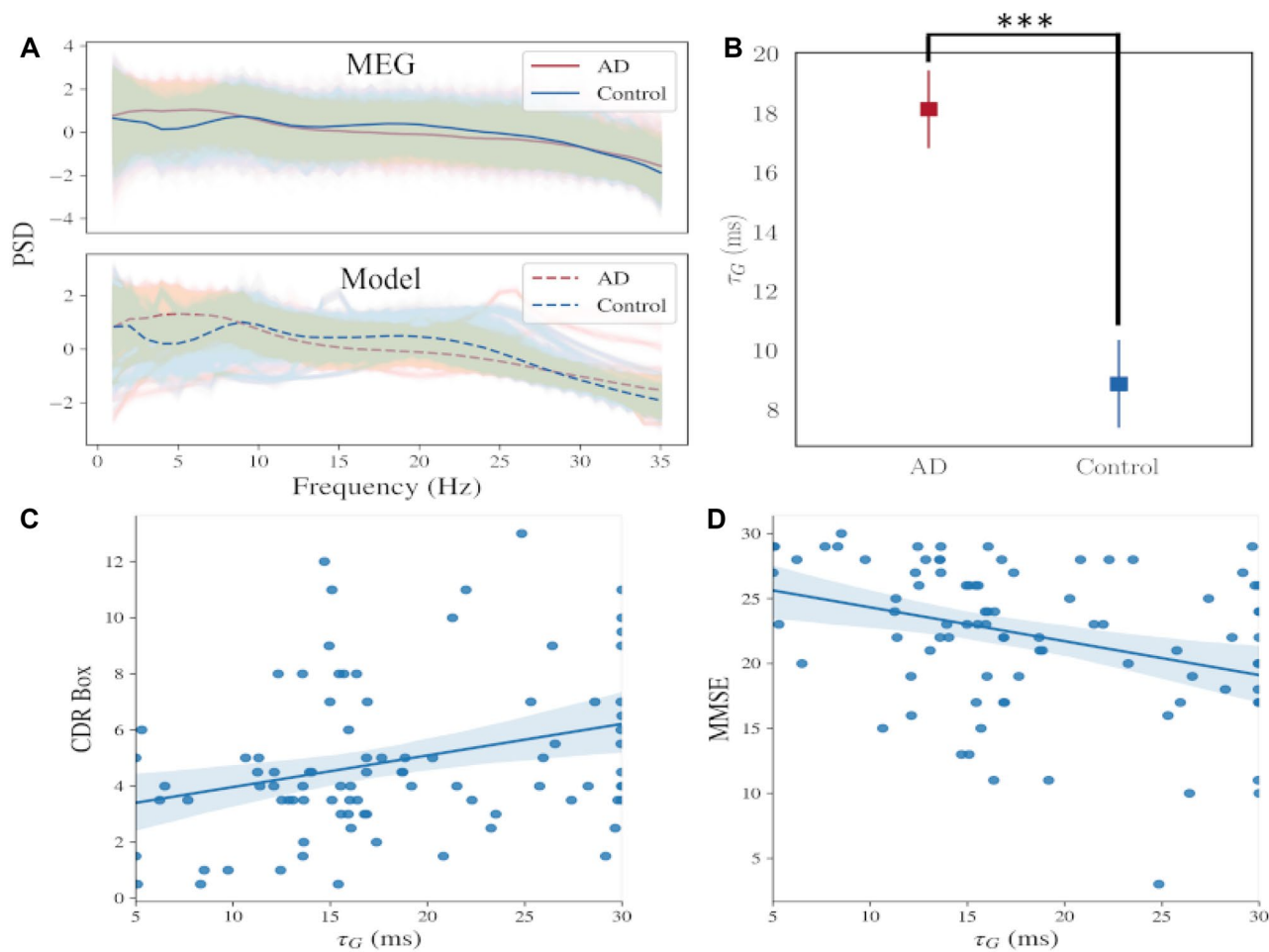


**Fig. 1** **A** Plot of scaled power spectral density (PSD) versus frequency for empirical MEG recordings of AD and control (top) and for the modeled spectra after inferring the model parameters (bottom). **B** Box plot comparing the excitatory time constant ( $\tau_G$ ) in

AD and controls. **C** Scatter plot showing the trend of association of  $\tau_G$  with Clinical Dementia Rating – Sum of Boxes (CDR Box) and **D** Mean Mental State Exam (MMSE)

#### O11 Perturbation-based approaches derived and tested in mathematical neural models generate biomarkers for seizure transitions in animal models

Wei Qin<sup>\*1</sup>, Anthony Burkitt<sup>1</sup>, Andre Peterson<sup>1</sup>

<sup>1</sup>The University of Melbourne, Department of Biomedical Engineering, Melbourne, Australia

\*Email: wqin1@student.unimelb.edu.au

Brain state transitions such as from a resting state to a seizure state, are often used to describe pathological brain dynamics observed in neurological diseases such as epilepsy. Epilepsy is a highly patient-specific disease which is characterized by seizure transitions, which are poorly understood. Brain imaging technology, such as Electro-encephalography (EEG), has been used to diagnose and study such pathological changes. When the brain gets closer to a transition, certain biomarkers (variance, autocorrelation and time for a perturbed system returning to baseline) are seen to increase. This has been observed in epileptic EEG data, which could be explained as

Critical Slowing Down (CSD). The underlying mechanism, however, cannot be mathematically verified because the principles governing brain dynamics are poorly described mathematically. In addition, state changes can be difficult to observe in raw EEG signals due to noise and signal complexity. In this project, we use a computational neural model to study the correlation between proposed biomarkers and state transitions. Understanding the nature of such brain state transitions is fundamental to uncovering the underlying cause of brain diseases.

The Wilson-Cowan model, a neural field model that describes the spike rate gathered from a population of neurons, is used to derive the state-transition biomarkers. This model is capable of producing a Hopf-bifurcation while being simple enough for theoretical analysis. In addition, this model has been well studied previously. Seven biomarkers are proposed, each of which is designed to capture the dynamical changes from time series data. The biomarkers consist of active perturbation-based biomarkers, passive summary statistics and Lyapunov exponents. Active biomarkers require external stimuli, so the evoked responses are repeatable and less likely to be interfered by noise. Passive summary statistics, on the other hand, do not require external inputs, which track the statistical features hidden in data. Lyapunov Exponents (LEs), the real part of the Floquet multiplier, indicate the stability of the system.

The performances of these biomarkers are evaluated as indicators of state transitions in both the Wilson-Cowan model and a tetanus toxin rat model. In analyzing numerical simulations of the Wilson-Cowan model, we found that biomarkers are associated with the stability of a system. LEs are observed to have a lower artifact tolerance when noise is added to the data. In the data from toxin-injected rats, both the long-term (over the animals' lifespan) and short-term (minutes before transitions) time scales were investigated. All the rats from the testing group exhibited clear state changes during the 8–10 week of recordings, while the control group did not. Clear increases of the biomarkers minutes before seizure events were also observed. In addition, we found that the increases are more pronounced for active biomarkers (i.e. those involving perturbations).

This study supports the use of biomarkers to evaluate brain state transitions. Several novel biomarkers are proposed, and we have shown active biomarkers outperform passive biomarkers in the evaluation of brain state transitions between seizure events. A small perturbation is shown to be an effective method to evaluate brain states without causing seizure events. These methods could be used to track brain dynamics for seizure prediction, epilepsy diagnosis and prognosis.

## O12 Linking connectivity to dynamics: How do coherent oscillations emerge in a partially random neural network?

Isabelle Harris<sup>\*1</sup>, Hamish Meffin<sup>2</sup>, Anthony Burkitt<sup>2</sup>, Andre Peterson<sup>2</sup>

<sup>1</sup>The University of Melbourne, Department of Medicine, Melbourne, Australia

<sup>2</sup>The University of Melbourne, Department of Biomedical Engineering, Melbourne, Australia

\*Email: iharris@student.unimelb.edu.au

Complex neural dynamics arises from a multitude of nonlinear network interactions in the brain. The nature of these dynamics is studied

to understand brain function, dysfunction, and the transition from one state to another, such as the transition to seizure. The current body of work studying seizure dynamics typically use neural field or mass models to mathematically describe transitions from normal brain activity to seizure activity. Though these models reproduce the clinically observed signal, the mathematical description of the normal brain state (a stationary equilibrium) and the seizure state (a stable limit cycle) do not correspond to our current clinical and biophysical understanding. We study the link between connectivity and dynamics in a local cortical network using a networked neural model with a connectivity matrix that captures the statistics of excitatory and inhibitory synaptic connections [1, 2, 3]. The model has been shown to exhibit intrinsically fluctuating dynamics for specific classes of connectivities. Developing this link between connectivity and dynamics, we aim to understand how pathological activity, such as coherent oscillations seen in seizures, emerge from normal brain activity in a random neural network. The nature of the dynamics and state transitions of the network is determined, in part, by the eigenvalues of the Jacobian, which for this model is a function of the connectivity matrix. Therefore, we study the eigenspectrum of the connectivity matrix and its relationship to the stability boundary. The connectivity matrix is defined as a partially random matrix with two (or more) distinct neural populations, following different but related Gaussian distributions. Mathematically, this corresponds to a class of rank-two perturbed random matrices that obey Dale's law. The eigenspectrum of a connectivity matrix depends on both the statistics of a random component and the deterministic component that partitions the neural populations. Consequently, tools from Random Matrix Theory are used to examine the statistical structure of the connectivity matrix and the anatomy of the corresponding eigenspectrum. A rank-two perturbed random matrix has an eigenspectrum that consists of a bulk and two eigenvalue outliers which for certain conditions exist as complex conjugate (cc) eigenvalues [4]. We find that there is an intimate interplay between the radius of the central eigenspectrum disc, and the existence and location of the cc eigenvalue outliers with the stability boundary. This interplay is vital to the study of the transition to seizure, as coherent oscillations emerge in the activity if the cc eigenvalue outliers lie on or near the stability

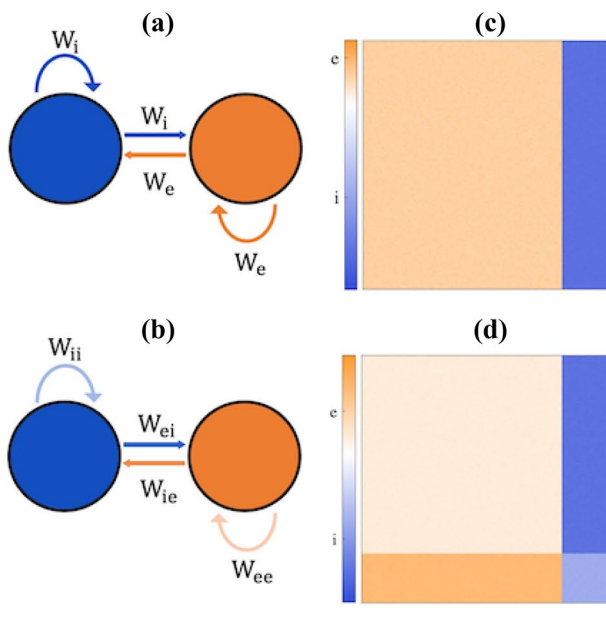
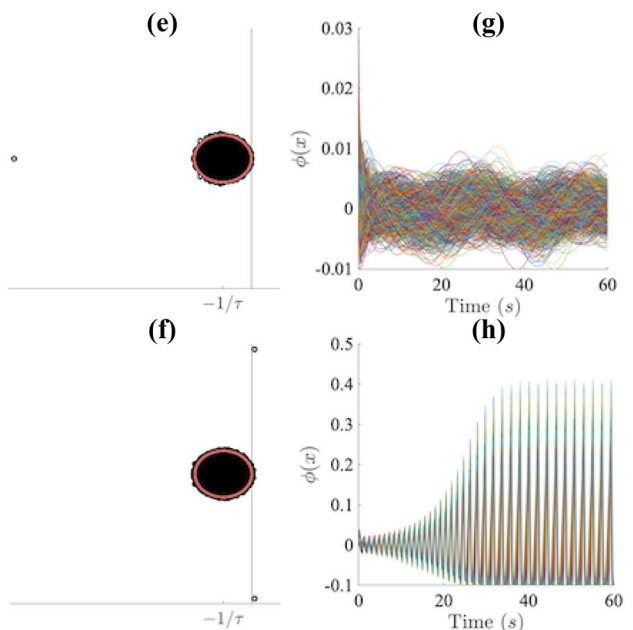


**Fig. 1** Illustrating the effects of introducing non-random structure into a random network, i.e., (top) excitatory-inhibitory two population network (bottom) a four-population network. (a, b) Neural network



populations (c, d) visualization of the partially random network connectivity matrices, (e, f) associated eigenspectrum, and (g, h) plot of simulated dynamics for the network model

boundary. The emergence of coherent oscillatory activity in a network exhibiting normal brain activity due to changes the connectivity matrix is a result that not only links connectivity to dynamics, but also shows that changes in connectivity can give rise to state-transitions in a partially random neural network. This mirrors more recent biophysical and clinical findings with respect to brain state-transitions in epilepsy.

## References

1. H. Sompolinsky, A. Crisanti, and H. J. Sommers. Chaos in random neural networks. *Physical Review Letters*. 1988; 61: 259–262
2. Kanaka Rajan and L. F. Abbott. Eigenvalue Spectra of Random Matrices for Neural Networks. *Physical Review Letters*. 2006; 97(18):188,104
3. Itamar Daniel Landau and Haim Sompolinsky. Coherent chaos in a recurrent neural network with structured connectivity. *PLOS Computational Biology*. 2018; 14(12):e1006309
4. Terence Tao. Outliers in the spectrum of iid matrices with bounded rank perturbations. *Probability Theory and Related Fields*. 2013; 155(1):231–263

## O13 Inhibitory stabilization in a cortical neural mass model

Parvin Zarei Eskikand<sup>\*1</sup>, Artemio Soto-Breceda<sup>1</sup>, Mark Cook<sup>2</sup>, Anthony Burkitt<sup>1</sup>, David Grayden<sup>1</sup>

<sup>1</sup>University of Melbourne, Department of Biomedical Engineering, Melbourne, Australia

<sup>2</sup>University of Melbourne, Department of Medicine, Melbourne, Australia

\*Email: pzarei@unimelb.edu.au

Recurrent excitatory connections in neural mass models can lead to runaway activity resembling epileptic seizures. Strong inhibitory recurrent connections can reduce the tendency for a network to become unstable, which is known as inhibitory stabilization. Networks that combine unstable excitatory recurrent connections with strong inhibitory feedback are known as Inhibition Stabilized Networks (ISNs) [1]. One of the characteristics of ISNs is their “paradoxical response”, where perturbing the inhibitory interneurons by increasing excitatory input results in a decrease in the activity of these neurons after a temporal delay instead of increasing their activity. Here, we develop a neural mass model of populations of neurons across cortical layers 2/3, 4 and 5. Within each layer, there is one population of inhibitory neurons and one population of excitatory neurons. The populations of neurons in layers 2/3 and 5 receive inputs from other cortical areas and the population of neurons in layer 4 receive thalamic input, all modelled as fixed input firing rates. The strengths and time constants of interconnections between the populations of neurons are derived from the Synaptic Physiology database available from the Allen Institute, USA. To investigate the presence of Inhibition-Stabilized Networks (ISNs) across different layers in the cortex, we measured the membrane potentials of the model neural populations after perturbing inhibitory populations with a step increase in the firing rate of their excitatory input.

The model shows the role of strong inhibitory-to-inhibitory connections in maintaining balance in the network. It shows that systematic variation in the connectivity strength between populations of neurons changes the excitatory and inhibitory balance across the cortical

layers. The differences in the levels of excitation-inhibition balance across the layers accords with neurophysiological data that shows that layer 2/3 has more inhibition-dominated connectivity than layers 4 and 5, which have more excitation-dominated connectivity [2]. The results show that layer 2/3 in the model does not operate in ISN regime as the mean membrane potential of the inhibitory interneurons increases with increased external excitatory input. However, layers 4 and 5 operate in the ISN regime as the membrane potential of the inhibitory interneurons decreases with increased excitation, after a transition period. These results accord with neurophysiological findings that explored the presence of ISNs across different layers in the cortex [3].

A disruption in excitation-inhibition balance in cortex is associated with emergence of epileptic seizures. The model may provide insights into how parameter changes may lead to bifurcations resembling epileptic seizures and the relationship of paradoxical response and seizure onset in epileptic brains.

## Acknowledgments

This work was funded by the Australian Government under the Australian Research Council’s Training Centre in Cognitive Computing for Medical Technologies (IC170100030).

## References

1. Sadeh S, Clopath C. Inhibitory stabilization and cortical computation. *Nature Reviews Neuroscience*. 2021; 22:21–37.
2. Markram H, et al., Reconstruction and simulation of neocortical microcircuitry. *Cell*. 2015; 163:456–492.
3. Mahrach A, et al., Mechanisms underlying the response of mouse cortical networks to optogenetic manipulation. *Elife*. 2020; e49967.

## O14 Consequences of Dale’s law on the stability-complexity relationship of partially random neural networks

Andre Peterson<sup>\*1</sup>, Jesper Ipsen<sup>2</sup>

<sup>1</sup>The University of Melbourne, Biomedical Engineering, Fitzroy, Australia

<sup>2</sup>The University of Melbourne, Mathematics and Statistics, Parkville, Australia

\*Email: peterson@unimelb.edu.au

One of the major difficulties in the study of brain dynamics and neurological disease is that it is highly patient-specific and varies significantly between individuals. One way of capturing these heterogeneous differences is to quantify different brain connectivities and examine their effects on brain network dynamics, particularly brain state transitions. Typically, this directed graph or networked dynamical system is described using neural mass models where the network connectivity is either averaged over, losing its individuation or via high dimensional brute force numerical simulations, which are not mathematically tractable. An alternative approach is to study randomly connected neural networks using mean-field theory [1], where it has been found that there is a rapid transition to a complex macroscopic ‘chaotic’ state [2]. Recently, in relation to this there have been two major developments: First, this transition has been described microscopically by Wainrib and Toboul [3] as an exponential explosion in the number of fixed points of the system. Second,

Rajan and Abbott [4] discovered that more anatomically realistic non-random connectivity structures such as Dale's law change the uniform density of the eigenspectrum. In this paper we combine these two seminal papers to show the effects of more anatomically realistic connectivity statistics on phase transitions.

In the study of randomly connected neural network dynamics there is a phase transition from a 'simple' state with few equilibria to a 'complex' state characterized by the number of equilibria growing exponentially with the neuron. Such phase transitions are often used to describe pathological brain state transitions observed in neurological diseases such as epilepsy. In this paper we investigate how more realistic heterogeneous network structures affect phase transitions using techniques from random matrix theory. Specifically, we parameterize the network structure according to Dale's Law and use the Kac-Rice formalism to compute the change in the number of equilibria when a phase transition occurs. We also examine the condition where the network is not balanced between excitation and inhibition causing outliers to appear in the eigenspectrum. The methods presented here enables us to compute the effects of different network connectivity on brain state transitions, which can provide new insights into pathological brain dynamics.

## References

1. H. Sompolinsky, A. Crisanti, and H. J. Sommers. Chaos in random neural networks. *Physical Review Letters*. 1988; 61: 259.
2. M. Stern, H. Sompolinsky and L. F Abbott. Dynamics of random neural networks with bistable units. *Physical Review E*. 2–14; 90: 062,710.
3. G. Wainrib and J. Touboul. Topological and dynamical complexity of random neural networks. *Physical Review Letters*. 2013; 110: 118,101.
4. K. Rajan and L. F. Abbott. Eigenvalue spectra of random matrices for neural networks. *Physical Review Letters*. 2006; 97: 188,104.

## O15 Evolutionary shaping of human brain dynamics

James Pang<sup>\*1</sup>, James Rilling<sup>2</sup>, James A Roberts<sup>3</sup>, Martijn van den Heuvel<sup>4</sup>, Luca Cocchi<sup>5</sup>

<sup>1</sup>Monash University, Turner Institute for Brain and Mental Health, Clayton, Australia

<sup>2</sup>Emory University, Department of Anthropology, Atlanta, United States of America

<sup>3</sup>QIMR Berghofer, Computational Biology, Brisbane, Australia

<sup>4</sup>Vrije Universiteit Amsterdam, Department of Complex Traits Genetics, Amsterdam, Netherlands

<sup>5</sup>QIMR Berghofer, Mental Health and Neuroscience, Brisbane, Australia

\*Email: james.pang1@monash.edu

The field of neuroscience has long sought to understand human brain features that have evolved to support our advanced behavioral and

cognitive functions [1]. This has been approached through comparative studies to uncover commonalities and variations in the brain anatomy of humans and other species. Neuroimaging studies have shown that human high-order association cortices are larger and more interconnected compared to other primates [2], which support complex logical and socio-cognitive functions [3]. Hence, it has been hypothesized that these expanded regions could be the evolutionary origin of distinctly human cognitive abilities. However, how does this difference in neuroanatomy endows the human brain with adaptive complex functions?

Here, we used unique diffusion MRI data for 58 adult humans (*Homo sapiens*) and 22 sex-matched and age-equivalent chimpanzees (*Pan troglodytes*) to reconstruct species-specific connectomes. We combined the connectomic data with a biophysical neural mass model [4] to generate regional neural activity across time (*neural dynamics*) for each species. We then determined a brain region's response to global (brain-wide) modulations in excitability, with shape characterized in terms of the *neural dynamic range*.

We found that the response functions of human brain regions were more similar to one another compared to those of chimpanzees (Fig. 1A), translating to a narrower distribution of neural dynamics ranges (Fig. 1B). The contrasting distribution of dynamic ranges in humans versus chimpanzees extended to other non-human primate species (i.e., macaques and marmosets; data not shown). Neural dynamic ranges followed a dominant spatial gradient along the anterior–posterior brain axis, with anterior associative regions having higher values than posterior sensory regions (Fig. 1A insets). Finally, a narrower distribution of dynamic ranges in humans supports stronger functional integration between regions (Fig. 1C; see overlapping curves). Conversely, a broader distribution of dynamic ranges in chimpanzees facilitates brain processes relying on neural interactions within specialized local systems and limits brain network integration. In summary, our work shows that human brain connectivity appears to have evolved to support neural dynamics that maintain relatively high levels of integration between functionally segregated brain systems. The unique properties of human and chimpanzee brain dynamics may therefore be understood as an evolutionary tradeoff between functional segregation and integration in service of species-specific cognitive functions and behavior.

## References

1. Seyfarth RM, Cheney DL. The evolution of language from social cognition. *Current Opinion in Neurobiology*. 2014; 28: 5–9.
2. Ardesch DJ, Scholtens LH, Preuss TM, et al. Evolutionary expansion of connectivity between multimodal association areas in the human brain compared with chimpanzees. *Proceedings of the National Academy of Sciences of the U.S.A.* 2019; 116: 7101–7106.
3. Margulies DS, Smallwood J. Converging evidence for the role of transmodal cortex in cognition. *Proceedings of the National Academy of Sciences of the U.S.A.* 2017; 114(48): 12641–12643.
4. Wong KF, Wang XJ. A recurrent network mechanism of time integration in perceptual decisions. *Journal of Neuroscience*. 2006; 26(4): 1314–1328.

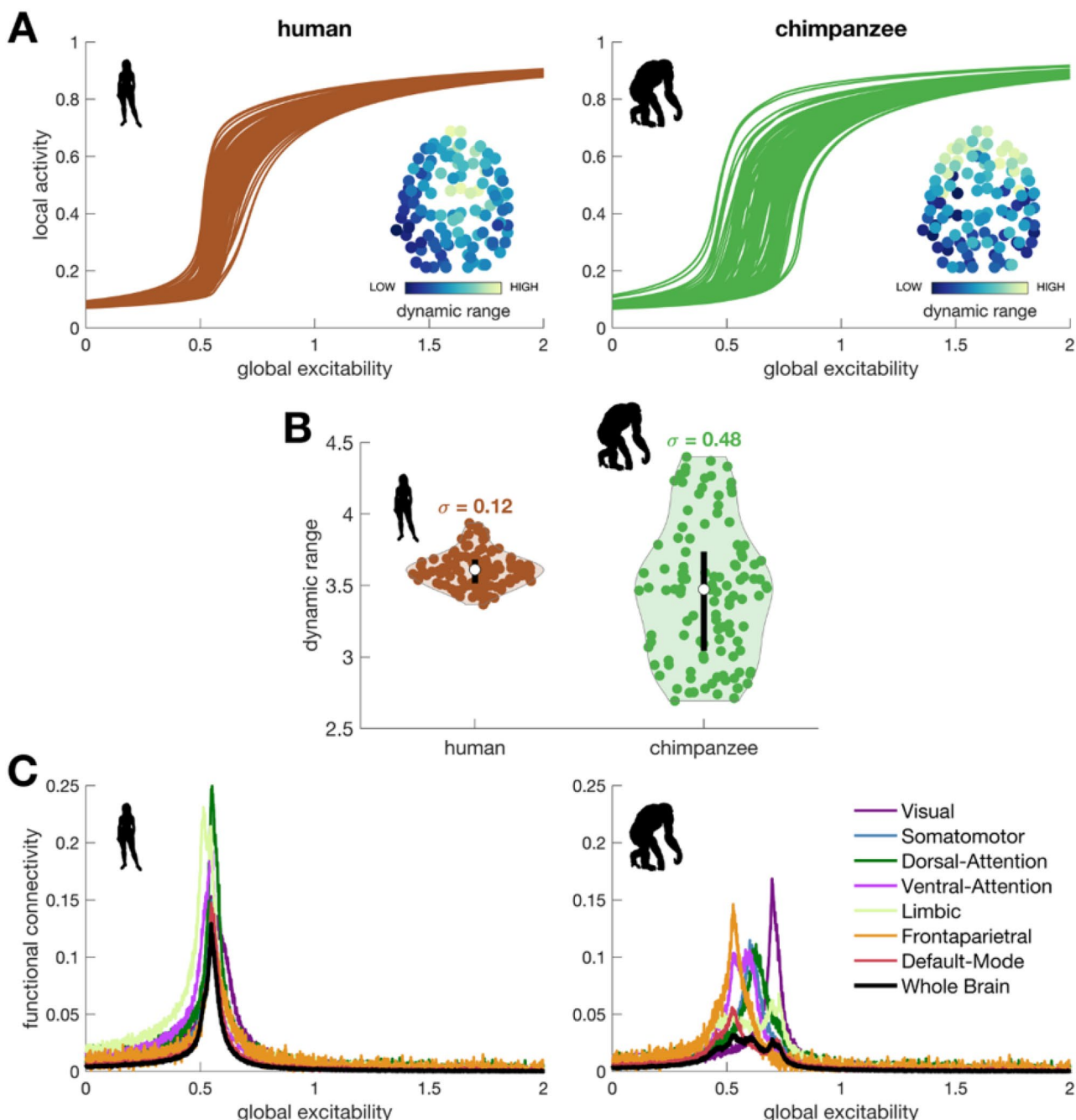


**Fig. 1** A Local activity response function vs global excitability for each brain region. The inset shows the spatial organization of dynamic ranges. B Distribution of dynamic ranges across brain

regions with standard deviation  $\sigma$ . C Changes in functional connectivity vs global excitability in the whole brain and canonical functional brain networks

#### O16 Exploiting brain critical dynamics to inform Brain-Computer Interfaces performance

Marie-Constance Corsi<sup>1</sup>, Pierpaolo Sorrentino<sup>2</sup>, Denis Schwartz<sup>1</sup>, Nathalie George<sup>1</sup>, Laurent Hugueville<sup>1</sup>, Ari E. Kahn<sup>3</sup>, Sophie Dupont<sup>1</sup>, Danielle S. Bassett<sup>3</sup>, Viktor Jirsa<sup>4</sup>, Fabrizio De Vico Fallani<sup>1</sup>

<sup>1</sup>Paris Brain Institute, Paris, France

<sup>2</sup>Institut de Neuroscience des Systèmes, Marseille, France

<sup>3</sup>University of Pennsylvania, Philadelphia, United States of America

<sup>4</sup>INSERM & Aix-Marseille Université, Theoretical Neuroscience Group, Institut de Neurosciences des Systèmes, Marseille, France

\*Email: marie.constance.corsi@gmail.com

Brain-Computer Interfaces (BCIs) constitute a promising tool but mastering non-invasive BCI remains a poorly-understood learned skill since the underlying brain processes and their reflection on

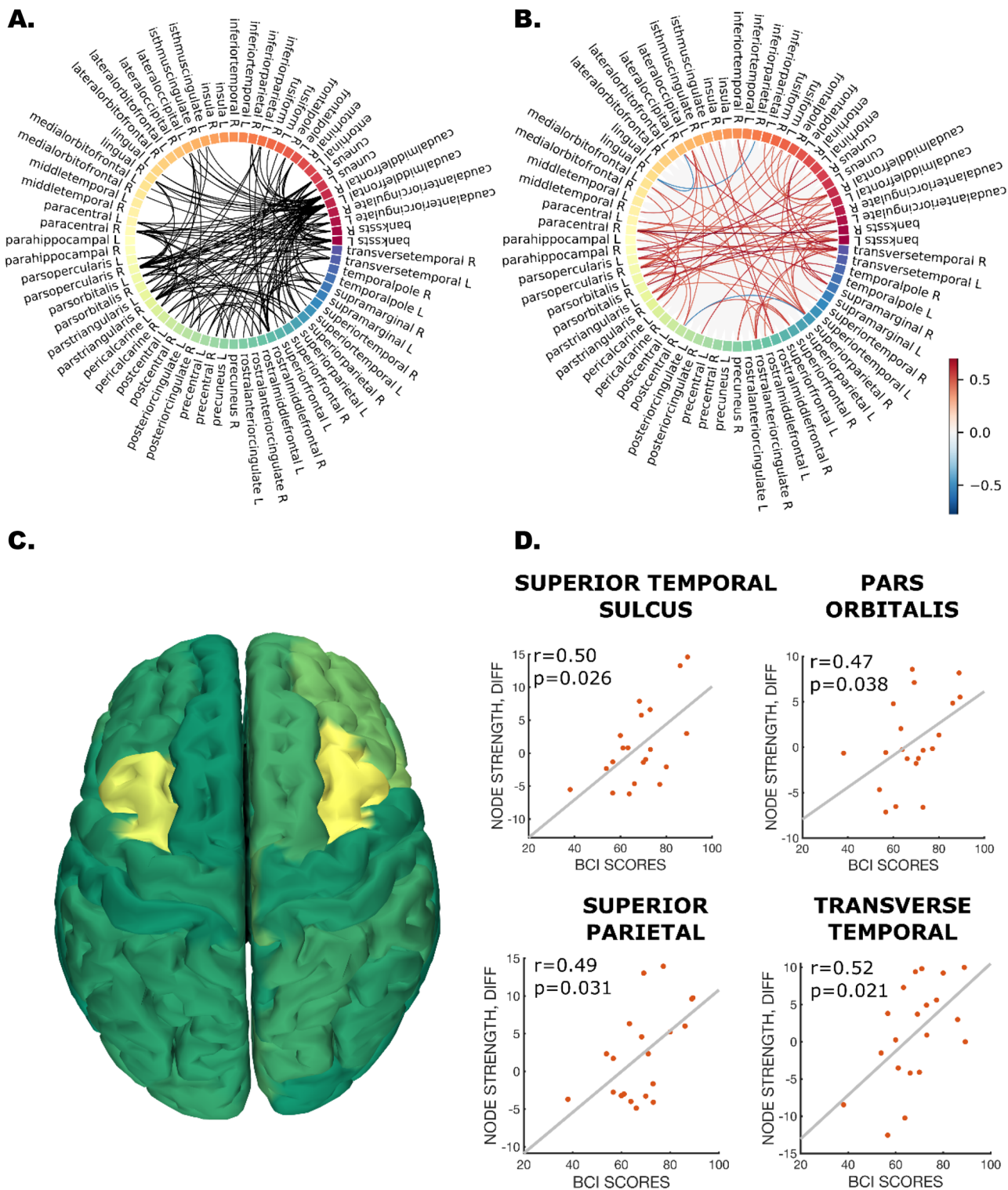


**Fig. 1** Main results. **A** Edge-wise analysis—Reliable task-based interactions over the subjects ( $p < 0.05$ , after correction for multiple comparison). **B** Edge-wise analysis—Correlation with BCI scores.

**C** Node-wise analysis—Reliable nodes over the subjects. **D** Node-wise analysis—Correlation with BCI scores

brain signals are unknown. Brain dynamic is characterized by aperiodic perturbations (i.e. “Neuronal Avalanches”) preferentially spreading across the white-matter bundles. Different avalanche trajectories might underlie different behaviors.

To test our hypothesis, we applied the neuronal avalanches approach to magnetoencephalography (MEG) data recorded in 20 healthy subjects ( $27.5 \pm 4.0$  years old, 12 men) during a motor-imagery (MI)-based BCI training session. We used avalanche transition matrices (ATM), containing the probability that region  $j$  would be active at time  $t+1$ , when region  $i$  was active at time  $t$ . For each subject, we computed the difference of the ATMs for the two experimental conditions. We randomly shuffled the labels of the transition matrices obtaining the null-distribution of the differences per each edge, and then Benjamini-Hochberg-corrected for multiple comparisons. We selected only those edges that were significant in a higher-than-chance number of subjects, highlighting “task-specific” regions. We related the differences in the transition probability corresponding to each of the edges incident upon the “task-specific” areas to the individual BCI scores. Finally, we summed the differences over edges per each “task-specific” node and related the corresponding difference (between tasks) to the BCI performance, defined as the proportion of successful trials over the session. Correlations were assessed using Spearman’s analysis.

Our results show that large-scale perturbations propagate differently according to the experimental condition. Figure 1A shows the edges which consistently differ between the two conditions across subjects. These “reliably different” edges selectively cluster on premotor regions bilaterally and, in particular, upon the caudal middle frontal gyri bilaterally. Premotor areas are involved in the planning of motor actions, imagining of actions, allocating executive attention. We then focused on the differences in the transition probabilities in the edges incident upon the “task-specific” regions, relating it to the performance in the MI task. Figure 1B, shows the edges which are incident upon such regions (color code proportional to correlation). Firstly, nearly all differences correlate positively with performance. Hence, perturbations of activity spread more often across prefrontal regions if a subject is tasked with MI, as compared to resting-state. Finally we have moved into nodal space. To this end, we have summed the differences corresponding to all the edges which are incident upon each “task-specific” region (shown in Fig. 1C), obtaining an overall difference per each such node, which was then correlated with the BCI scores. Four regions showed strong direct correlation with the BCI, as shown in Fig. 1D, notably, the superior parietal lobe, which is known to be involved during motor imagery tasks.

By selectively focusing on higher-order large-scale activity, we spotted a number of edges whose dynamics is affected by the execution of a motor imagery task. Our results suggest that avalanches capture functionally-relevant processes which are of interest for alternative BCI designing.

### O17 Latent Equilibrium: A unified learning theory for arbitrarily fast computation with arbitrarily slow neurons

Paul Haider<sup>\*1</sup>, Benjamin Ellenberger<sup>1</sup>, Laura Kriener<sup>1</sup>, Jakob Jordan<sup>1</sup>, Walter Senn<sup>1</sup>, Mihai A. Petrovici<sup>1,2</sup>

<sup>1</sup>University of Bern, Department of Physiology, Bern, Switzerland

<sup>2</sup>Heidelberg University, Heidelberg, Baden-Württemberg, Germany

\*Email: paul.haider@unibe.ch

Fast processing across the cortical hierarchy allows animals to act successfully in quickly changing environments. Simultaneously, efficient learning under such conditions needs to tackle the issue of credit assignment continuously, in real time. Recent years have witnessed

a surge of cortical learning models which address this question by approximating the error backpropagation algorithm, the driving force behind much of modern machine learning. However, all of these models either require long relaxation phases following a change in sensory stimuli, which renders them unable to cope with the fast time scales imposed by, e.g., saccades, or impose some form of rapidly phased learning, which is difficult to reconcile with experimental observations. Fundamentally, the relaxation times in these models are determined by the response speed of the individual neurons. This problem is further exacerbated in hierarchical models of cortical networks, where each layer introduces a response lag that cumulatively delays processing of stimuli and thereby drastically slows the inference process. In addition, this causes a timing mismatch between network output and instructive signals, thus disrupting learning.

We introduce Latent Equilibrium, a unifying framework for inference and learning in networks of slow components which avoids these issues by harnessing the ability of biological neurons to phase-advance their output with respect to their membrane potential. This mechanism enables quasi-instantaneous inference independent of network depth and avoids the need for computationally expensive relaxation phases, allowing networks to learn from stimulus-target pairs with dynamics on near-arbitrarily short time scales. We derive neuron morphology, network structure, and in particular disentangled neuronal and synaptic weight dynamics from a single prospective energy function. The resulting model can be interpreted as a real-time, biologically plausible approximation of error backpropagation in deep cortical networks with continuous-time, leaky neuronal dynamics and continuously active, local synaptic plasticity. We demonstrate successful learning from continuous input streams, achieving competitive performance with both fully-connected and convolutional architectures on standard benchmark datasets. We further show how our mathematical framework can be embedded within cortical microcircuits. Finally, we study the robustness of our model to spatio-temporal substrate imperfections to demonstrate its feasibility for physical realization, both *in vivo* and *in silico*.

### O18 Reward Bases: Instant reward revaluation with temporal difference learning

Rafal Bogacz<sup>\*1</sup>, Beren Millidge<sup>1</sup>, Mark Walton<sup>2</sup>

<sup>1</sup>University of Oxford, MRC Brain Network Dynamics Unit, Oxford, United Kingdom

<sup>2</sup>University of Oxford, Experimental Psychology, Oxford, United Kingdom

\*Email: rafal.bogacz@ndcn.ox.ac.uk

An influential theory posits that dopaminergic neurons in the mid-brain implement a model-free reinforcement learning algorithm based on temporal difference (TD) learning. A fundamental assumption of this model is that the reward function being optimized is fixed. However, for biological creatures the ‘reward function’ can fluctuate substantially over time depending on the internal physiological state of the animal. For instance, food is rewarding when you are hungry, but not when you are satiated. While a variety of experiments have demonstrated that animals can instantly adapt their behavior when their internal physiological state changes, under current thinking this requires model-based planning since the standard model of TD learning requires retraining from scratch if the reward function changes. Here, we propose a novel and simple extension to TD learning that allows for the zero-shot (instantaneous) generalization to changing reward functions. Mathematically, we show that if we assume the reward function is a linear combination of reward basis vectors, and if we learn a value function

for each reward basis using TD learning, then we can recover the true value function by a linear combination of these value function bases. This representational scheme allows instant and perfect generalization to any reward function in the span of the reward basis vectors as well as possesses a straightforward implementation in neural circuitry by parallelizing the standard circuitry required for TD learning. We demonstrate that our algorithm can also reproduce behavioral data on reward revaluation tasks, predict dopamine responses in the nucleus accumbens, as well as learn equally fast as successor representations while requiring much less memory.

## P1 Simulated responses of a model Marmoset pFC

Bernard Pailthorpe<sup>\*1</sup>

<sup>1</sup>University of Sydney, Physics, Sydney, Australia

\*Email: bernard.pailthorpe@sydney.edu.au

Model simulation of a significant cluster in the Marmoset pre-Frontal Cortex (pFC) exhibits a transition in oscillatory behavior due to simulated

pulses from the visual cortex. The cluster was identified using network analysis of the Marmoset cortex connectivity data. Tracing of local links identified a closely coupled, compact cluster of 6 anatomical areas within the Dorso lateral pFC, containing one out- (A10) and two in-hubs (A32V, A11). The other nodes are A32, A9 and A46D. Unlike other motifs in the network this cluster had a 3D star shape. Simulation was performed using Jansen-Ritt (JR) models of neural masses representing each of the six nodes in the pFC cluster.

Heterogeneity arose from differing size and local link weight measures for each anatomical area. Nodes were connected with directed; weighted links derived from the Marmoset connectivity data. Signals assumed to travel at a velocity of 1 m/s. Each node was modelled as 3 neural assemblies, following Wilson-Cowan (WC) and JR. The sigmoidal voltage to firing rate conversion,  $S(v)$ , was modelled using both a distribution of firing thresholds (erf) and of synaptic weights (erfc), as initially discussed by WC. Only the latter showed the results reported. Other model parameters were consistent with the original WC and JR studies and tuned to oscillate in the alpha band.

This six-node cluster exhibits a range of nonlinear oscillations and phase plane behavior familiar from earlier studies of neural masses, with added complexity due to the link weights and signal delays. The complex outputs arise from constructive and destructive interference of the outputs of the linked oscillators. Model outputs are the time

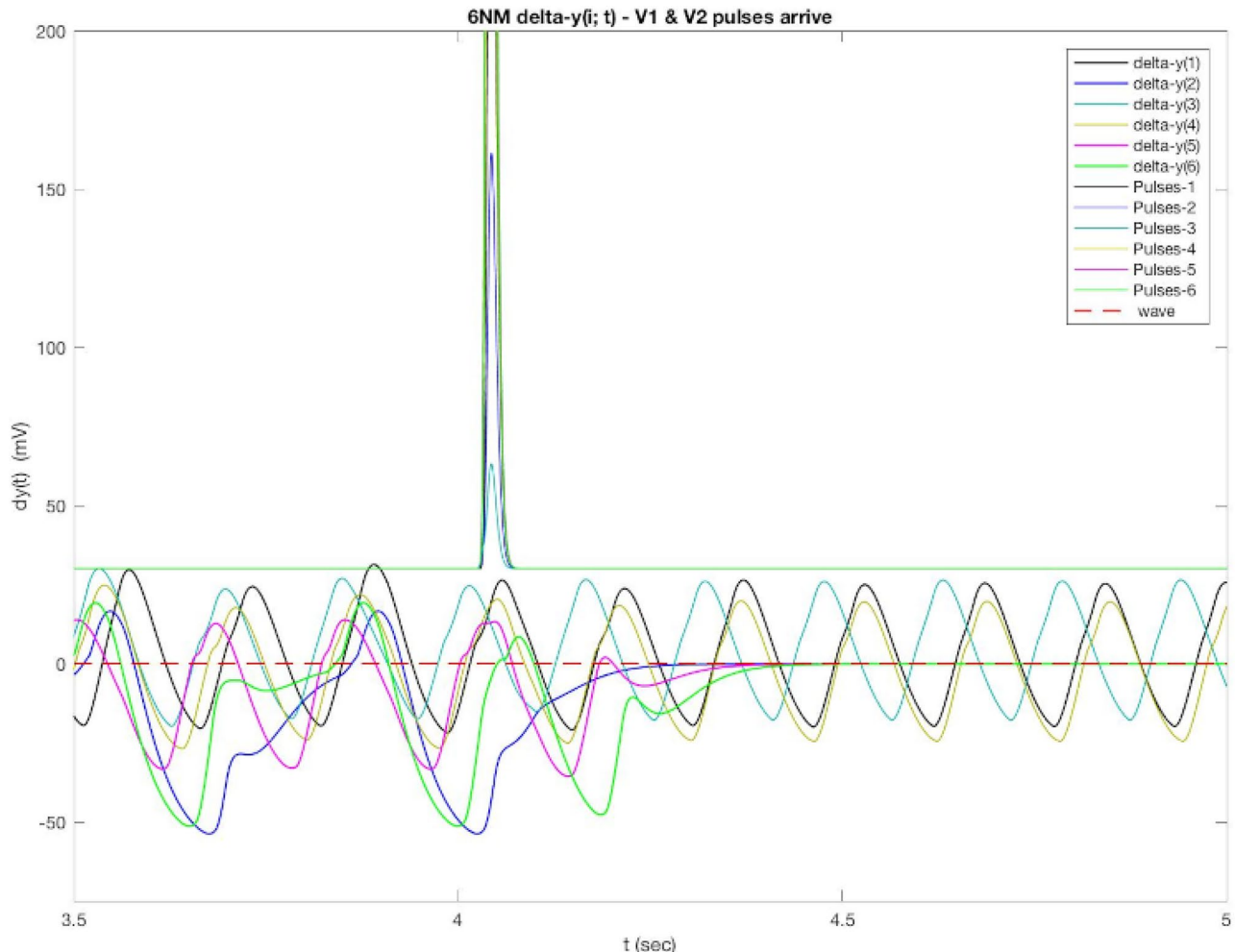


**Fig. 1** Model output for each neural mass in the pFC cluster near the transition (lower plot), showing individual waveforms and stimulus pulses (units s-1), modelling signals from V1 and V2, arriving at 4.0 s (upper plot)

dependent local field potential for each node, and the average for the cluster. The most useful measure for monitoring the system was the Inter Spike Interval (ISI).

The simulation protocol aligned with traditional experimental probes, such as stimulating primary senses and measuring emergent pulse trains and cortical responses. A single neural pulse originating from V1 and/or V2 and travelling directly, or via intervening waypoints thus forming 2-step links, to the 6 neural masses was assembled. This was based on the experimentally measured marmoset weighted link list and inter-areal distances. The 5 direct links from V1 and V2 to the pFC cluster are long range and weak and, alone, elicit no response. The V1-V2 link is short range and strong. From V2 there are possible 2-step links to the pFC cluster via 22 intermediate waypoints. Together these elicit a dynamic response in the pFC cluster (Fig. 1).

As in relevant experiments, selected inputs can be silenced in the simulations, to probe the role of key areas. Omitting pathways via a selected lobe (eg. PPC, Cing/RSP) preserved the response in the model, indicating redundancy. Restricting the V2 pulses to only those arriving to A46D is also sufficient to elicit the response, indicating a possibly essential role for A46D. These results illustrate the power of computational studies to complement experiments.

## P2 Consolidating memory storage and retrieval

Anu Aggarwal<sup>\*1</sup>

<sup>1</sup>The University of Illinois Urbana-Champaign, Department of Electrical and Computer Engineering, Champaign Urbana, IL, United States of America

\*Email: aaagganu@gmail.com

Since the time of patient H.M., the role of temporal lobe in memory formation has been appreciated. The case highlighted the importance of hippocampal formation in the synthesis of new episodic memories. It also raised questions as to why the pre-event memories were still intact and led researchers to hypothesize that pre-frontal cortex stores long-term memories. With the demonstration of medial entorhinal cortex grid cells [1] as input provider to the hippocampal place cells [2], we proposed the sensorimotor model of the place cells [3]. This model says that the place cells combine sensory and motor inputs from lateral and medial entorhinal cells. Through the current paper, we extend that model and hypothesize that the reciprocal connections formed directly between the pre-frontal cortex, motor cortex, thalamus, hypothalamus and the sensory areas consolidate the episodic memories that are conceived in the hippocampal place cells and presented to the pre-frontal cortex, thalamus and hypothalamus. And that there is an emotional component of memory formation due to involvement of the hypothalamus in the process.

## References

1. T. Hafting, M. Fyhn, S. Molden, M.B. Moser, E.I. Moser. Microstructure of a spatial map in the entorhinal cortex. *Nature*. 2005; 436: 801–806.
2. J. O’Keefe, D.H. Conway,. Hippocampal place units in the freely moving rat: why they fire where they fire. *Experimental Brain Research*. 1978; 31: 573–590.
3. A. Aggarwal. The sensori-motor model of the hippocampal place cells. *Neurocomputing*. 2016; 185: 142–152.

## P3 Oscillatory local field potential signatures associated with chemosensory processing in the accessory olfactory bulb

Marc Spehr<sup>1</sup>, Yoram Ben-Shaul<sup>\*2</sup>, Oksana Cohen<sup>2</sup>, Sebastian Malinowski<sup>3</sup>, Kahan Anat<sup>2</sup>

<sup>1</sup>RWTH Aachen University, Chemosensation, Aachen, Germany

<sup>2</sup>The Hebrew University, Faculty of Medicine, Medical Neurobiology, Jerusalem, Israel

<sup>3</sup>Institute for Biology II, RWTH Aachen University, Department of Chemosensation, Aachen, Germany

\*Email: yoramb@ekmd.huji.ac.il

Local field potential (LFP) oscillations have been widely described in the context of the main olfactory system. However, their role in information processing by the vomeronasal system (VNS) is considerably less understood. Here, we use our controlled stimulus delivery paradigm to reveal the existence of prominent theta band (~5–8 Hz) LFP oscillations in the accessory olfactory bulb (AOB), the first processing stage of the VNS. To objectively quantify these LFP signatures in light of a noisy recording across multiple electrodes, we developed a two-stage approach in which we first manually define oscillatory events, and then scan the entire record to find similarity to these patterns. Then, we use this similarity signal as a measure of the LFP patterns. We find that these LFP oscillations are associated with stimulus delivery and their magnitude reflects stimulus intensity. Several lines of analysis indicate that these oscillations are locally generated, are not a simple artifact of spiking activity, and that times of individual neurons are phase locked to these sweep-like events. This suggests that these oscillations may help to coordinate spiking activity of AOB output neurons to affect downstream processing regions more effectively.

## Acknowledgements

This work was funded by the Deutsche Forschungsgemeinschaft (DFG, German Research Foundation) – 378,028,035 (YBS & MS); The German-Israeli Foundation for Scientific Research and Development (1–1193–153.13/2012, YBS & MS).

## P4 A multiscale characterization of cortical shape asymmetries in early psychosis

Yu-Chi Chen<sup>\*1</sup>, Jeggan Tiego<sup>1</sup>, Ashlea Segal<sup>1</sup>, Sidhant Chopra<sup>2</sup>, James Pang<sup>1</sup>, Alex Fornito<sup>1</sup>, Kevin Aquino<sup>3</sup>

<sup>1</sup>Monash University, Turner Institute for Brain and Mental Health, Melbourne, Australia

<sup>2</sup>Yale University, Department of Psychology, New Haven, United States of America

<sup>3</sup>University of Sydney, School of Physics, Sydney, Australia

\*Email: yu-chi.chen@monash.edu

Abnormalities in cerebral asymmetry have been reported in numerous studies of patients with psychosis. Most anatomical studies have used point-wise or region-of-interest approaches, aiming to find the precise locations in the brain that differ between case and control groups. However, patients with psychosis have heterogeneous characteristics and

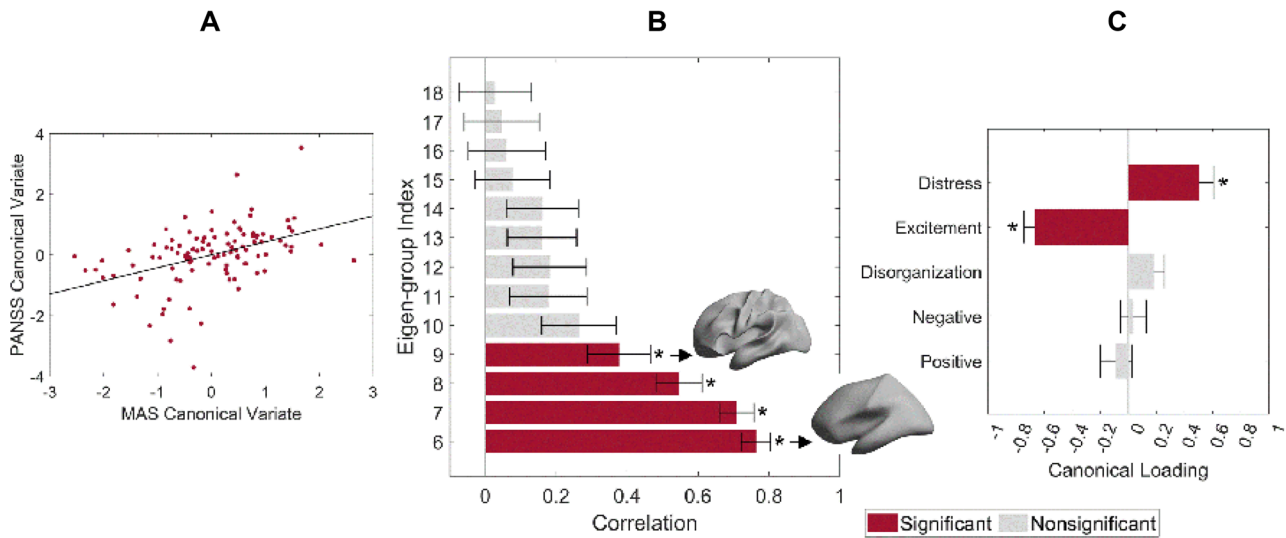


**Fig. 1** Cortical shape asymmetries are correlated with psychotic symptoms. **A** Association between shape asymmetry and psychotic symptom canonical variates. **B** Correlations between the original

inter-hemispheric shape correlations of each eigen-group and the asymmetry canonical variate. **C** Canonical variate loadings of the PANSS factors. Error bars show  $\pm 2$  bootstrapped standard errors

may show minimal overlap in the specific location of their brain deviations. Moreover, point-wise approaches are not sensitive to diffuse brain abnormalities and often conflate size-related measures with shape. We have recently shown that multiscale spectral descriptions of shape asymmetry across the whole cortex are highly personalized, akin to a cortical fingerprint [1]. Here, we use spectral shape analysis to examine abnormal cortical shape asymmetries in patients with early psychosis (EP).

We used the Human Connectome Project for Early Psychosis dataset (56 healthy controls (HC) and 113 EP patients) and quantified shape variations of each hemisphere over different spatial frequencies using the eigenfunction spectrum of the Laplace–Beltrami Operator [2]. We then calculated maximum Pearson’s correlations between the left- and right-eigenfunctions as a measure of hemispheric divergence in shapes at different spatial frequencies. We then took the mean of the correlation across each harmonic eigen-group, which describes shape variations with similar spatial wavelengths. We applied a GLM with permutation testing to examine the differences between the HC and EP groups. We further used a canonical correlation analysis (CCA) to examine associations between cortical asymmetry and clinical symptoms measured by the Positive and Negative Syndrome Scale (PANSS).

Cortical shape asymmetries across 6–18 eigen-groups, spanning wavelengths between 22–75 mm, were significantly different between the two groups ( $PFDR < 0.05$ ; Cohen’s  $d = 0.28 – 0.51$ ), with patients showing greater shape asymmetry than controls. We found a single canonical mode linking asymmetries to symptoms ( $CCAr = 0.45$ ;  $PFWER < 0.001$ ; Fig. 1A), with the 6–9 groups positively correlated with the canonical variate ( $PFDR < 0.05$ ; Fig. 1B). The loadings of the PANSS factors on the canonical variate were negative in excitement and positive in emotional distress ( $PFDR < 0.05$ ; Fig. 1C). Thus, EP patients with a higher cortical shape asymmetry show more severe excitement symptoms and less severe emotional distress. In contrast, commonly used morphological descriptors, such as those based on cortical thickness and surface area, at both global and regional levels, were not different between groups.

Differences in cortical shape asymmetry in EP are apparent at coarse spatial scales. These shape asymmetry features are also related to

psychiatric symptoms. Our findings underscore the advantage of discovering sscae-specific effects across the whole cortex, which may be ignored by traditional point-wise approaches.

## References

- Chen, Y.-C., et al. The individuality of shape asymmetries of the human cerebral cortex. *BioRxiv*. 2021.
- Reuter, M., et al. Laplace–Beltrami Eigenvalues and Topological Features of Eigenfunctions for Statistical Shape Analysis. *Computer-Aided Design*. 2009; 41(10): p. 739–755.

## P5 Radiomic Features Predictive of Treatment Response in HGG treated with CAR-T Therapy

Aleksandr Filippov<sup>\*1</sup>, Lawrence Shaktah<sup>2</sup>, Chi Wah Wong<sup>2</sup>, Christine Brown<sup>3</sup>, Behnam Badie<sup>4</sup>

<sup>1</sup>City of Hope, Surgery, Duarte, CA, United States of America

<sup>2</sup>City of Hope, Precision Medicine, Duarte, CA, United States of America

<sup>3</sup>City of Hope, Immunotherapy, Duarte, CA, United States of America

<sup>4</sup>City of Hope, Neurosurgery, Duarte, CA, United States of America

\*Email: afilippov@coh.org

High-Grade Glioma (HGG) is a heterogeneous primary CNS neoplasm with a high recurrence rate and poor outcomes [1]. Many studies are exploring the use of therapies that utilize a patient’s own immune system to combat the disease including monoclonal antibodies and Chimeric Antigen Receptor T cells. Radiomic models have shown value in identifying biomarkers predictive of tumor genetic burden, prognosis, and even treatment response. In this study, we explore radiomic features from 4 clinical sequences and 2 volumes: edema and enhancing tumor to predict whether a patient will progress during their first three doses of CAR-T therapy. In this IRB-approved phase 1 clinical trial, patients underwent surgical resection of the tumor and received

CAR-T cell therapy. Of the patients accrued, 59 (39 males, median age = 49) completed 3 cycles of therapy and had high quality, 3 T field strength MRI scans where imaging artifacts were minimal. Enhancing tumor and edema volumes were generated in a semi-automatic manner and reviewed by 3 readers with a combined 17 years' experience. T1 weighted pre-contrast, T1 weighted post-contrast, T2 weighted, and T2 FLuid Attenuated Inversion Recovery (FLAIR) sequences were used to generate 3D and 2D radiomics features. In total 28,541 radiomic features were generated per patient using post-surgery, pre-CAR-T imaging dates. Each patient's response to treatment after 3 cycles was determined to be either Stable Disease (SD) (29 patients), labeled '1', or Progression (PD), labeled '0' (per RANO guidelines) [2]. The radiomic feature set dimensionality was reduced through selecting features that had Pearson correlation values with an absolute value greater than 0.3, generating 100 radiomic features of interest. Logistic regression (LR), linear discriminant analysis (LDA), k-nearest neighbors (KNN), decision tree classifiers (DTC), gaussian naïve Bayes (GNB), and support vector machines (SVM) were examined for their utility in predicting treatment response using said 100 radiomic features. Of the six models, LDA performed the best with an accuracy of 83%, an F-1 score predicting Stable Disease and Progression of 0.75, and 0.88, respectively. Despite the small study size, our model can serve as a potential basis for optimizing clinical trial design through more personalized treatment planning and more precise patient screening.

## References

1. Krex D, Klink B, Hartmann C et-al. Long-term survival with glioblastoma multiforme. *Brain*. 2007;130 (Pt): 2596–606.
2. Wen PY, Macdonald DR, Reardon DA et-al. Updated response assessment criteria for high-grade gliomas: response assessment in neuro-oncology working group. *Journal of Clinical Oncology*. 2010; 28 (11): 1963–72

## P6 When local alterations meet collective oscillatory dynamics: On the causes of functional connectivity changes

Sophie Benitez Stulz<sup>\*1</sup>, Matthieu Gilson<sup>1</sup>, Demian Battaglia<sup>1</sup>

<sup>1</sup>Aix-Marseille University, Institut de Neurosciences des Systèmes (INS, UMR1106), Marseille, France

\*Email: sophie.benitez-stulz@etu.univ-amu.fr

Neuronal populations within local regions frequently undergo oscillatory modulations of their activity. The oscillations of distant populations coupled by long-range connections can lock in various patterns of stable phase differences and the flexible change of such phase locking patterns has been hypothesized to modulate communication and functional connectivity (FC) between them. It is therefore important to understand which factors can affect and control the established inter-regional phase relations (e.g., FC). Here, we emphasize that while the details of applied local alterations (stimulation or SC link changes) are important, we cannot neglect the global system's dynamics when predicting effects on FC. A tool which has proved useful to model and predict the behavior of coupled oscillating populations is the phase response curve (PRC). The PRC is a local transformation function that determines the phase-dependent response of an oscillator to any given external or internal input. Importantly, the PRC exclusively depends on parameters of the local regional microcircuit such as the relative strengths of recurrent excitation (E) and inhibition (I) but is ignorant of the oscillatory dynamics of the surrounding large-scale network or the inter-regional

connectivity parameters. However, in a complex system of many interacting populations, local and global dynamics are non-trivially coupled and the PRC may be more dependent on them than previously assumed. Considering specific examples of multi-scale circuits, we first show that equivalent changes in FC can be induced by either modifying local connectivity parameters and thereby the PRC, or by modifying features of the long-range inter-regional SC. In this way, diffuse changes of local E and I strengths (induced e.g., by neuromodulation or pharmacological treatments) may be used to compensate for a disrupted connectome (due e.g., to neurodegeneration). Secondly, we show that the phase-shifting effects of local pulse perturbations do not depend uniquely on the phase at which perturbation is applied, as postulated by the PRC concept, but also on the collective configuration of dynamic FC which the system is transiently visiting. Thus, accounting for changes in collective dynamics beyond local dynamics and structure, is vital for understanding and predicting how the brain will react to internal or external perturbations.

## Acknowledgements

Funded by Agence National de la Recherche (France; Grant "ERMUNDY", ANR-18-CE37-0014-02) and Centre de Calcul Intensif d'Aix-Marseille is acknowledged for granting access to its high-performance computing resources.

## P7 Structure or dynamics? On the role of the canonic circuit in the emergence of cortical multi-frequency oscillations

Samy Castro<sup>\*1</sup>, Demian Battaglia<sup>2</sup>

<sup>1</sup>Universite de Strasbourg, Strasbourg, France

<sup>2</sup>Aix-Marseille University, Institut de Neurosciences des Systèmes (INS, UMR1106), Marseille, France

\*Email: castro.novo.samy@gmail.com

Bottom-up and top-down functional connectivity (FC) between cortical regions are mediated by faster and slower frequency oscillations. Eventually, different cortical layers also oscillate at different frequencies. Therefore, it has been proposed that FC in different directions operates at different frequencies because of the distinct resonance frequencies of the source and target layers. Based on a systematic modelling analysis, we propose here on the contrary that the frequency specialization of directed FC stems as an emergent by-product of self-organized collective dynamics rather than of hardwired anatomy and intraneuronal diversity. Specifically, we analyze rate models of coupled cortical regions embedding a realistic multi-layer anatomical organization. Every layer includes an excitatory and a unique inhibitory population of the fast-spiking type, resonating at a fast gamma-range frequency. Despite this intrinsic resonance, we can obtain a great diversity of possible dynamical states as a function of contextual inputs and the relative strength of excitation and inhibition. Regimes in which faster and slower frequency oscillations predominate respectively in superficial or deeper layers arise spontaneously and robustly due to non-linear inter-layer interactions. However, we also find that the strength and the dominant frequencies of directed FC can be flexibly adjusted by modulating the dynamical regime of the network, without the need of structural changes. We furthermore show that dynamical regimes allowing such a multi-frequency adaptivity of directed functional interactions are extremely unlikely to arise in randomized networks. We thus speculate that the canonic circuit wiring may be optimized to favor the frequency multiplexing of inter-regional information routing.

## P8 Optimisation for initialising Kalman Filter to estimate neural model parameters from M/EEG data

**Yun Zhao**<sup>\*1</sup>, Phillipa Karoly<sup>2</sup>, Simon Teshuva<sup>1</sup>, David Grayden<sup>2</sup>, Phuc Luong<sup>1</sup>, Mario Boley<sup>1</sup>, Levin Kuhlmann<sup>1</sup>

<sup>1</sup>Monash University, Department of Data Science and AI, Melbourne, Australia

<sup>2</sup>University of Melbourne, Department of Biomedical Engineering, Melbourne, Australia

\*Email: yun.zhao@monash.edu

The Kalman filter (KF) is known as the optimal state estimator in the minimum mean square error sense under gaussian assumptions. Due to its global optimality and simple recursive structure, many methods are proposed based on the KF to estimate parameters of neural mass models of brain function. According to the KF theory, the distribution of the initial state,  $p(x_0)$ , is assumed to be known, but we often face a dilemma of insufficient or even unknown information about  $p(x_0)$ . Then, one will end up with a “guess” of the mean and increase the covariance to accommodate for the uncertainty. The problem becomes tougher when one applies the KF to electromagnetic source imaging time-series data from the whole brain since different brain regions are with varying states and a universal KF initialization cannot fit different brain states.

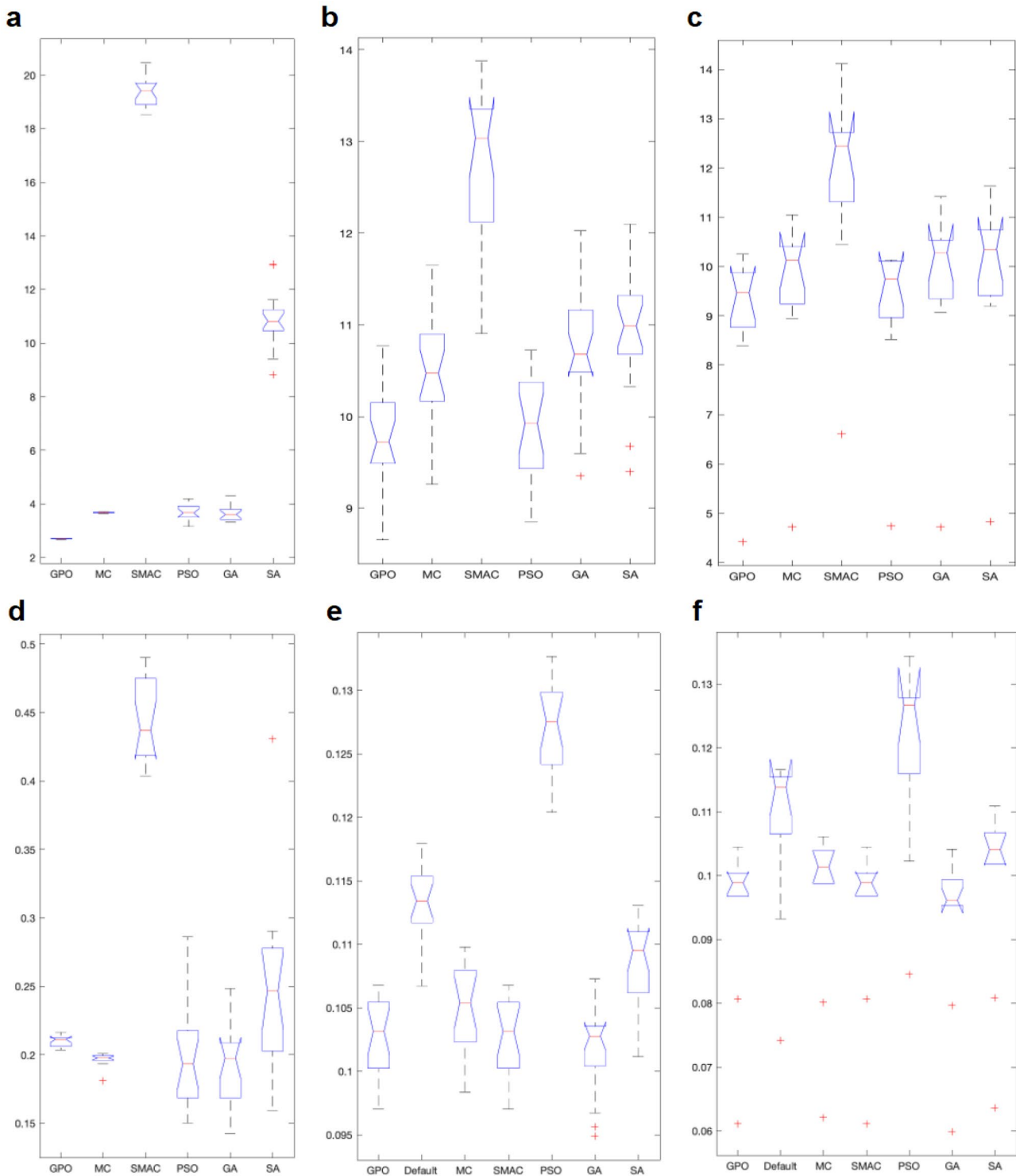
In this study, we propose a novel KF initialization framework using Gaussian process Bayesian optimization (GPO). Specifically, GPO is applied to find the most probable parameters of the model by minimizing the objective function (e.g., normalized root mean square error) between the data recording and the KF’s data prediction.  $p(x_0)$  can be derived from the model with the suggested parameters. We verified this design by applying it to synthetic data generated by forward simulating the model with parameters taken from a pre-defined parameter space. Simultaneously, we compared GPO with sequential model-based algorithm configuration (SMAC), particle swarm optimization (PSO), genetic algorithm (GA), simulated annealing (SA), and Monte Carlo sampling (MC). Besides, the proposed framework can suggest the most optimal KF initialization for different parts of the brain. For example, in terms of magnetoencephalographic (MEG) source data containing thousands of virtual voxels, we applied GPO to the strongest source point in one brain region and suggest the most probable KF initialization and further applied it to all voxels in that brain region. We evaluated the precision by applying this design to MEG source imaging data and compare GPO with SMAC, PSO, GA, SA, MC.

As we value efficiency of the framework, we used the area under the regret curve (AURC) to evaluate which optimizer can suggest the best KF initialization in a timely manner. For simulation data, normalized-root-mean-square-error (NRMSE) between the ground truth of parameters and parameter estimates was noted and for MEG data, NRMSE between the actual measurement and KF’s data prediction was calculated to further show the improvement that can be achieved with the framework. Specifically, we ran the simulation data experiment for 30 times with different random seeds, and statistical significance test shows GPO is the most efficient in finding optimal KF initialization ( $p\text{-value} < 0.05$ , averaged AURC = 2.6) and the parameter estimation error is trivial with variance 1.5e-5. We ran the MEG data experiment on two datasets (resting and deep anesthesia), and both show that GPO is the most efficient optimizer, and the data prediction error is only 10% of the parameter magnitude. (See Fig. 1 and Table 1 for statistics and boxplots).

In summary, the proposed framework makes KF more robust by suggesting an optimal initialization and more importantly the proposed whole-brain estimation scheme works for both resting state and deep anesthesia data, which indicates a broad application to MEG source data and different brain states.

**Table 1** ANOVA shows the aforementioned six optimisers lead to significantly different statistics of interest (AURC, NRMSE). The following multiple comparison tests indicated GPO was always the most efficient optimiser and thereby suitable for suggesting KF initialisation for MEG data

Scenario	Statistic of interest	Sample size	F	Prob > F
Simulation data	Area under the regret curve	30	2753.79	5.59E-102
Simulation data	Parameter estimation error	30	141	1.14E-42
Real clinical data, resting state	Area under the regret curve	22	50.67	8.73E-27
Real clinical data, resting state	Data prediction error	22	135.4	1.81E-52
Real clinical data, deep anesthesia	Area under the regret curve	11	3.08	0.0161
Real clinical data, deep anesthesia	Data prediction error	11	5.02	0.0003



#### P9 Sub-optimal modulation of gain by the cognitive control system in young adults with early psychosis

Bjorn Burgher<sup>\*1</sup>, Nikitas Koussis<sup>2</sup>, Genevieve Whybird<sup>3</sup>, James Scott<sup>1</sup>, Luca Cocchi<sup>1</sup>, Michael Breakspear<sup>4</sup>

<sup>1</sup>QIMR Berghofer Medical Research Institute, Mental Health and Neuroscience, Brisbane, Australia

<sup>2</sup>The University of Newcastle, School of Psychological Sciences, Newcastle, Australia

<sup>3</sup>Metro-North Hospital and Health Service, Mental Health, Brisbane, Australia

**Fig. 1** Boxplots and ANOVA tests table. Abbreviation: Gaussian process Bayesian optimisation (GPO); Monte Carlo sampling (MC); sequential model-based algorithm configuration (SMAC); particle swarm optimisation (PSO); genetic algorithm (GA); simulated annealing (SA); area under the regret curve (AURC); normalised-root-mean-square-error (NRMSE). **a** Boxplot of AURC of 30 simulation experiments. **b** Boxplot of AURC of resting-state MEG data with 22 subjects. **c** Boxplot of AURC of deep anaesthesia MEG data with 11 subjects. **a–c** indicate GPO was with the least AURC, meaning GPO can suggest an optimal KF initialisation efficiently. **d** Boxplot of NRMSE between the ground truth of parameters and parameter estimates of 30 simulation experiments. The KF initialisation suggested by GPO leads to a small parameter estimation error with trivial variance. **e** Boxplot of NRMSE between the actual measurement and KF's data prediction of resting-state MEG data with 22 subjects. **f** Boxplot of NRMSE between the actual measurement and KF's data prediction of xenon-induced deep anaesthesia MEG data with 11 subjects. **e–f** show the KF initialisation suggested by GPO lead to only 10% error of the parameter magnitude for both brain states

<sup>4</sup>The University of Newcastle, College of Engineering Science and Environment, College of Health and Medicine, Newcastle, Australia

\*Email: bjorn.burgher@qimrberghofer.edu.au

Executive dysfunctions in early psychosis (EP) are subtle but persistent, hindering recovery. We asked whether changes in the cognitive control system (CCS) disrupt the response to increased cognitive load in persons with EP. 30 EP and 30 control participants undertook multi-modal MRI. Computational models of structural and effective connectivity amongst regions in the CCS were informed by cortical responses to the multi-source interference task, a paradigm that selectively introduces stimulus conflict. EP participants showed greater

activation of CCS regions, including the superior parietal cortex, and were disproportionately slower at resolving stimulus conflict in the task. Computational models of the effective connectivity underlying this behavioral response suggest that the normative (control) group resolved stimulus conflict through an efficient and direct modulation of gain between the visual cortex and the anterior insula (AI). In contrast, the EP group utilized an indirect path, with parallel and multi-region hops to resolve stimulus conflict at the AI. Individual differences in task performance were dependent on initial linear gain modulations in the EP group versus a single nonlinear modulation in the control group. Effective connectivity in the EP group was associated with reduced structural integration amongst those connections critical for task execution. CCS engagement during stimulus conflict is hampered in EP due to inefficient use of higher order network interactions, with high tonic gain impeding task relevant (phasic) signal amplification.

#### P10 Exploring evolutionary constraints on human connectomes through randomized networks

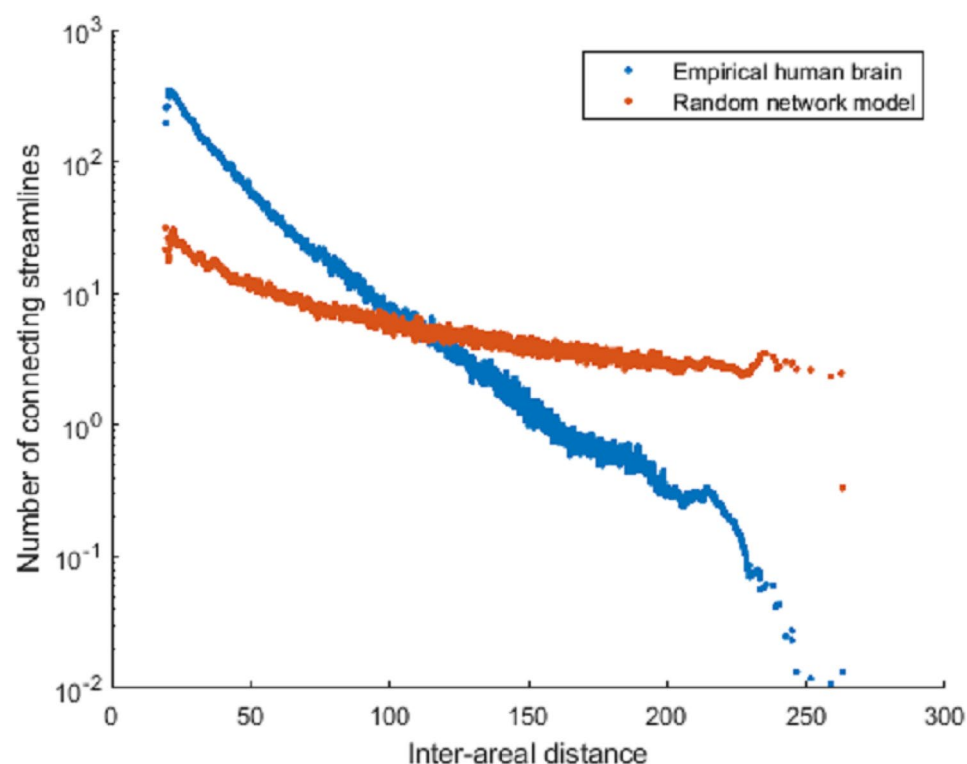
Jayson Jeganathan<sup>\*1</sup>, Michael Breakspear<sup>1</sup>

<sup>1</sup>The University of Newcastle, School of Psychology, School of Medicine and Public Health, Hunter Medical Research Institute, Newcastle, Australia

\*Email: jayson.jeganathan@gmail.com

Structural connectivity in the human brain is underpinned by the need for high throughput communication in the context of evolutionary constraints on wiring cost. How these fundamentals contribute to network features such as clustering and the inverse relationship between inter-node distance and connectivity strength, remains unclear.

**Fig. 1** Relationship between inter-areal distance and connectivity strength in empirical human networks and in random networks constrained to preserve wiring cost alone. Connectivity strengths are averaged across subjects



To capture the trade-off between communication needs and wiring cost, we developed a network measure called fiber efficiency, the ratio of total number of fibers to wiring cost. To test network features that can be explained by wiring cost constraints alone, we developed a random network model that preserves wiring cost while allowing the distance-strength relationship to vary, thus exploring a larger null model space than previous network models. The procedure is based on sampling from a simplex surface but can be understood intuitively as involving redistributed edge weights instead of edge swaps.

Network measures were compared between 3 network types: empirical networks from human diffusion data, our random network model, and a surrogate network which preserves the distance-strength relationship. Human networks had a steeper distance-strength relationship than the random network model which preserves wiring cost, demonstrating that the empirical relationship does not arise from wiring cost constraints alone (Fig. 1). We then asked whether the empirical distance-strength relationship reflects the demands of communication efficiency rather than wiring cost. The empirical distance-strength relationship could not be explained by optimization of previous measures of network efficiency based on multi-step communication but produces superior fiber efficiency compared to the random network model. Finally, we asked whether network features in the human brain are consequences of the distance-strength relationship. In support of this hypothesis, high clustering, modularity, and the existence of network hubs were similar between human data and the surrogate network model. However, hubs are placed more peripherally than expected under optimization principles, reflecting their co-evolution within neocortex on top of stable subcortical structures.

The human brain has evolved to balance the need for information processing with the energy costs of greater connectivity. This evolutionary pressure, quantifiable through fiber efficiency, is optimized by the co-location of connected brain regions, resulting in the relationship between inter-areal distance and connectivity. These principles account for a range of network properties in the human brain, but hub placements additionally reflect the idiosyncrasies of our unique evolutionary history.

#### P11 Cognitive control system gates insula subregion processing of affective stimuli in early psychosis

Nikitas Koussis<sup>\*1</sup>, Bjorn Burgher<sup>2</sup>, Jayson Jeganathan<sup>3</sup>, James Scott<sup>2</sup>, Luca Cocchi<sup>2</sup>, Michael Breakspear<sup>3</sup>

<sup>1</sup>The University of Newcastle, New Lambton Heights, Australia

<sup>2</sup>QIMR Berghofer Medical Research Institute, Mental Health and Neuroscience, Brisbane, Australia

<sup>3</sup>The University of Newcastle, School of Psychology, School of Medicine and Public Health, Hunter Medical Research Institute, Newcastle, Australia

\*Email: nikitas.koussis@gmail.com

Emotional disturbances appear in the prodrome and early psychosis (EP) stages of major psychotic disorders. Deficits in emotional processing manifest as dysfunctions in emotional expression, emotional experience, and emotional recognition. Classic computational accounts of psychosis suggest that the top-down influence of the cognitive control system (CCS) on expectations and precisions of the external milieu contribute to delusions and other positive symptoms. We hypothesized that a similar effect takes place in processing of emotion during conflict in the insula, influenced by the CCS, leading to emotional disturbances in early psychosis.

The emotional Go/No-Go task was used to probe brain responses to motor inhibition during calm or fearful faces. Computational

modelling of fMRI data was performed using Dynamic Causal Modelling (DCM). Different mechanisms regarding the top-down influence of the CCS on processing of affect in the insula were tested using Parametric Empirical Bayes (PEB).

When inhibiting motor response to fearful faces, EP participants showed higher brain activity in the right posterior insula (PI). Across both groups, PEB showed an important role of dorsolateral prefrontal cortex (DLPFC) in cognitive control on neural interactions between anterior insula (AI) and PI. This mechanism differs between groups however, such that EP participants require more top-down influence of DLPFC to maintain similar performance. Effective connectivity between visual cortex and regions of the cognitive control network was inhibited in EP participants with higher negative symptom burden.

Our study suggests CCS gates AI-PI processing of affective stimuli through modulation of gain in EP. Negative symptoms associate strongly with strength of inhibition in CCS and visual cortex, perhaps linking to affective blunting. Further work should examine this cognitive and limbic network in tasks of interoceptive awareness or social cognition.

#### P12 Decomposing neural circuit function into information processing primitives

Demian Battaglia<sup>\*1</sup>, Nicole Voges<sup>2</sup>, Andrea Brovelli<sup>2</sup>

<sup>1</sup>Aix-Marseille University, Institute for Systems Neuroscience, Marseille, France

<sup>2</sup>Aix-Marseille University, Institut de Neurosciences de la Timone, Marseille, France

\*Email: demian.battaglia@univ-amu.fr

Cognitive functions must arise from the coordinated activity of neural populations distributed over large-scale brain networks. However, it is challenging to understand (and measure) how specific aspects of neural dynamics translate into operations of information processing, and, ultimately, cognitive function. An obstacle is that simple circuit mechanisms –such as self-sustained or propagating activity and non-linear summation of inputs– do not directly give rise to high-level functions, even if they do, nevertheless, already implement simple transformations of the information carried by neural activity.

Here we show that distinct neural circuit functions, such as stimulus representation, working memory or selective attention stem from different combinations and types of low-level manipulations of information, or information processing primitives. To prove this hypothesis, we combine approaches from information theory with computational simulations of canonical neural circuits involving one or more interacting brain regions and emulating well-defined cognitive functions. More specifically we track the dynamics of information emergent from dynamic patterns of neural activity, using suitable quantitative metrics to detect where and when information is actively buffered (“active information storage”), transferred (“information transfer”) or non-linearly merged (“information modification”), as different possible modes of low-level processing. We thus find that neuronal subsets maintaining representations in working memory or performing attention-related gain modulation are signaled by their boosted involvement in operations of, respectively, active information storage or information modification.

Thus, information dynamics metrics, beyond detecting *which* network units participate in cognitive processing, also promise to specify *how* they do it, i.e. through which type of primitive computation, a capability that could be exploited for the parsing of actual experimental recordings.

### P13 Neural model simulations of the efficacy and safety of a neural activity shaping strategy for visual prostheses

Martin Spencer<sup>\*1</sup>, Tatiana Kameneva<sup>2</sup>, David Grayden<sup>3</sup>, Hamish Meffin<sup>3</sup>, Anthony Burkitt<sup>3</sup>

<sup>1</sup>The University of Melbourne, Melbourne, Australia

<sup>2</sup>Swinburne University of Technology, School of Science, Computing and Engineering Technologies, Melbourne, Australia

<sup>3</sup>The University of Melbourne, Department of Biomedical Engineering, Melbourne, Australia

\*Email: martin.spencer@unimelb.edu.au

Bionic eyes use implanted electrode arrays to stimulate neural tissue responsible for visual perception, usually in the retina or visual cortex. Conventional stimulation strategies sequentially activate individual electrodes to induce perception in local regions, known as phosphenes. Combinations of phosphenes are used to build up an image that implants can use to navigate or perceive objects as bright and dark regions. More difficult tasks, such as reading or face recognition, are difficult with existing visual prostheses because phosphenes overlap leading to low visual acuity. The Neural Activity Shaping (NAS) strategy uses a calibrated linear-nonlinear model of the neural activation profile (i.e., the neural spiking rate at each retinal location) of each electrode array to create a closed-loop approach [1]. Electrodes are activated simultaneously to induce neural activation and to attenuate undesired neural activation from neighboring electrodes in a “push–pull” arrangement. This simultaneous stimulation strategy relies on analysis of the *inverse* linear-nonlinear model calibrated for each implant.

While simulations provide a value for the level of neural activation associated with different positions in the visual field, these patterns of neural activation do not directly provide a measure of visual acuity. We have previously produced a method to convert patterns of neural activation into a clinical visual acuity score such as the Snellen ratio or the Minimum Angle of Resolution measure.

Simulations were performed that combined the acuity measure with the NAS strategy. These were used to assess the clinical significance of different parameter choices in visual prostheses.

Results were obtained for: a) different methods of managing inevitable errors in the calibrated forward model, b) the effect on visual acuity of different choice of safe electrode amplitude, and c) cases in which there are lost electrodes, a relatively frequent occurrence in clinical and pre-clinical devices (Fig. 1).

It was found that: a) model error could be managed using eigenvalue selection while maintaining improved visual acuity, b) while reducing the maximum safe electrode amplitude did lead to reduced visual acuity, the NAS gave higher visual acuity than the conventional strategy, and c) lost electrodes could lead to an increase in neural activation, however this was limited to the amplitude associated with a single electrode.

The results showed that the NAS can be made robust to model error and clinical safety limitations while providing improved visual acuity in comparison to the conventional sequential stimulation strategy.

### References

1. M.J. Spencer, T. Kameneva, D. B. Grayden, H. Meffin, and A. N. Burkitt. Global activity shaping strategies for a retinal implant. *Journal of neural engineering*. 2019; 16(2): 026008.

### P14 Unifying sparse coding, predictive coding, and divisive normalization

Yanbo Lian<sup>\*1</sup>, Anthony Burkitt<sup>1</sup>

<sup>1</sup>University of Melbourne, Department of Biomedical Engineering, Melbourne, Australia

\*Email: yanbo.lian@unimelb.edu.au

Sparse coding [1], predictive coding [2] and divisive normalization [3] are thought to be underlying principles of neural circuits across the brain, supported by much experimental evidence. However, the connection among these three principles is still poorly understood. In this study, we aim to unify sparse coding, predictive coding, and divisive normalization in the context of a two-layer neural model. Sparse coding assumes that the model linearly represents the incoming input using neurons with low activity levels, which can learn properties of neurons in different brain areas such as visual system, auditory system, and navigational system. The predictive structure of predictive coding provides an error-correction mechanism that is used to explain many brain phenomena, such as extra-classical receptive field properties in the visual cortex. Divisive normalization provides a simple mathematical framework that explains considerable experimental data in different brain areas such as the visual system and area MT and can provide an account of multisensory integration. Though sparse coding, predictive coding and divisive normalization have been used to account for properties of neurons in different systems, there are fundamental differences between them: sparse coding focuses on the sparsity of the neuronal activity; predictive coding focuses on the model structure that gives prediction and prediction error; divisive normalization focuses on the mathematical equation that gives different nonlinearities with different values of model parameters.

Based on the cost function of sparse coding and predictive coding, sparse coding can be implemented by the predictive structure of predictive coding. Furthermore, sparse coding and predictive coding can be equivalent if the feedback activation function,  $f(x)$ , of the original predictive coding is linear:  $f(x) = x$ . Additionally, both sparse coding and predictive coding have the ability to learn from

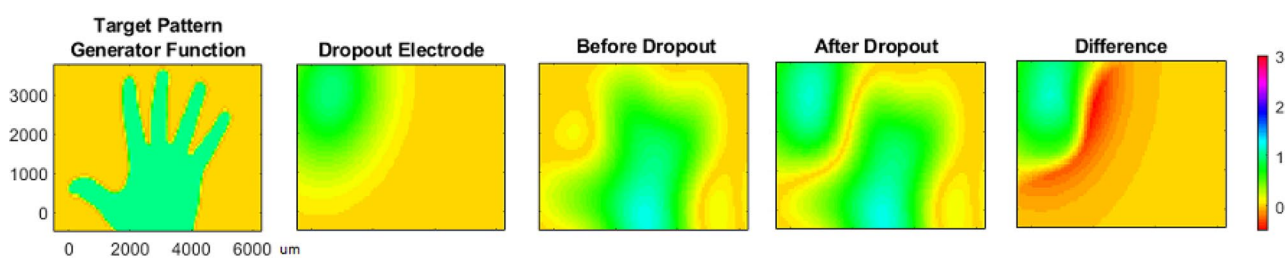


**Fig. 1** Simulated electrode drop-out. Colors indicate the combined linear combination of the influence of electrodes

input stimuli while divisive normalization is a physiological model that does not incorporate learning.

In this study, a two-layer model is constructed that implements sparse coding with the structure originating from predictive coding. Our results show that a homeostatic function (the derivative of the sparsity function in the original sparse coding model) in the model can shape the nonlinearity of neural responses, which can replicate different forms of divisive normalization.

We demonstrate that this model is equivalent to divisive normalization in a single-neuron scenario. Our simulation also shows that the model can learn simple cells with the property of contrast saturation that is previously explained by divisive normalization.

In summary, our study demonstrates that the three principles of sparse coding, predictive coding, and divisive normalization can be unified, such that the model has the ability to learn as well as display more diverse response nonlinearities. This framework may also be potentially used to explain how the brain learns to integrate input from different sensory modalities.

## References

- Olshausen BA, Field DJ. Emergence of simple-cell receptive field properties by learning a sparse code for natural images. *Nature*. 1996; 381: 607–609.
- Rao RP, Ballard DH. Predictive coding in the visual cortex: a functional interpretation of some extra-classical receptive-field effects. *Nature Neuroscience*. 1999; 2: 79–87.
- Heeger DJ. Normalization of cell responses in cat striate cortex. *Visual Neuroscience*. 1992; 9: 181–197.

## P15 Modelling Working Memory functions of the Basal Ganglia

Sandeep Nair<sup>\*1</sup>, Vigneswaran Chandrasekaran<sup>1</sup>, V Srinivasa Chakravarthy<sup>1</sup>

<sup>1</sup>Indian Institute of Technology, Madras, Department of Biotechnology, Chennai, India

\*Email: sandeepsathyandan@gmail.com

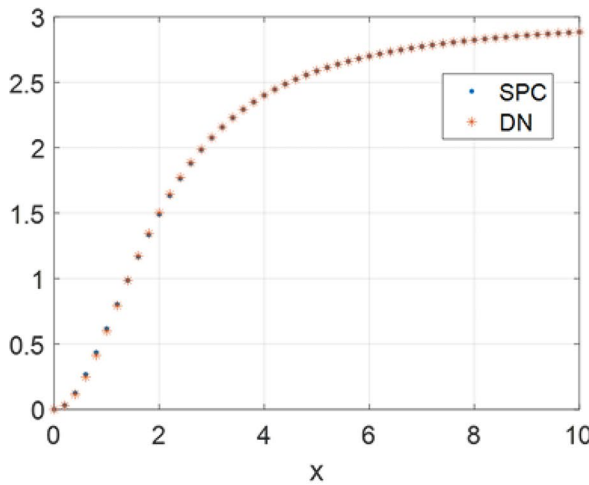
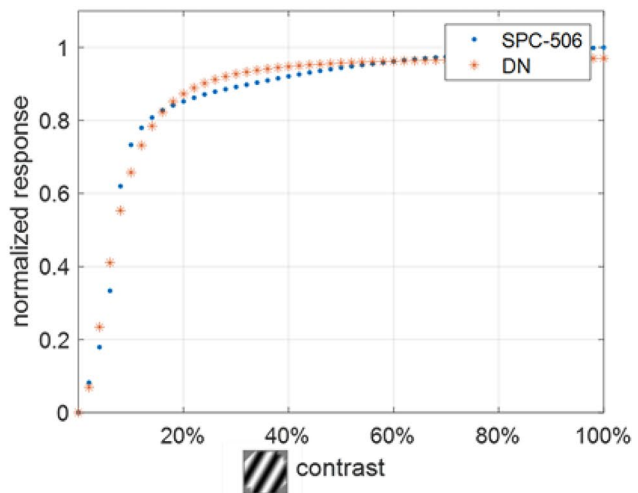


**Fig. 1** A Sparse predictive coding (SPC) can be equivalent to divisive normalization (DN) in a single-neuron scenario. x-axis represents the input and y-axis represents the model response. **B** Given natu-

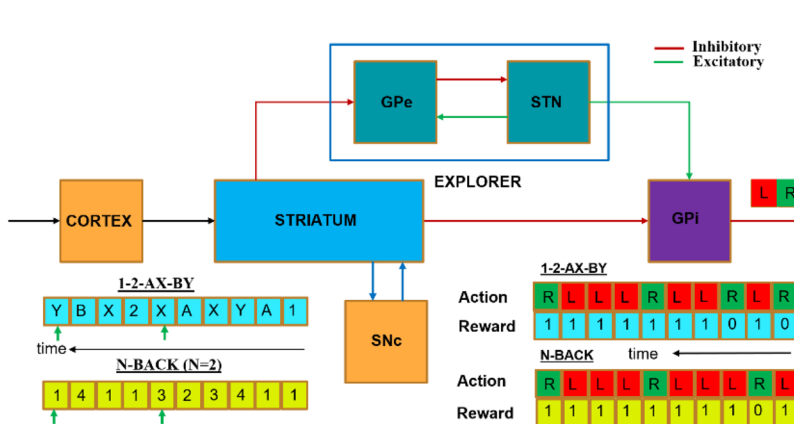
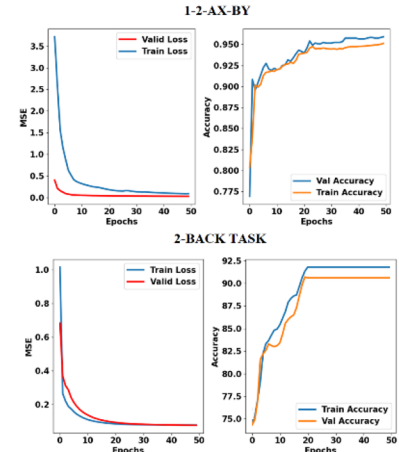
ral memory refers to the ability to temporarily store and manipulate information necessary to execute complex cognitive tasks. In computational terms, working memory is thought to be encoded in terms of stable neural activation patterns, distinguishing it from longer term memories based on synaptic update. Although the exact range of durations underlying is debated, working memory is believed to extend over seconds to tens of seconds. Two brain structures are thought to be crucially involved in working memory – the prefrontal cortex and the basal ganglia – both of which receive projections from the midbrain dopaminergic nuclei. In this study we focus on the working memory functions of the Basal Ganglia (BG).

The proposed BG model consists of the Striatum as the input port of the BG, which receives inputs from the cortex. The Striatum is connected to one of the key output ports viz, the Globus pallidus interna (GPI) directly, as well as indirectly through the Globus pallidus externa (GPe) and the subthalamic nucleus (STN). Training of the BG circuitry is cast in the reinforcement learning (RL) framework whereby the striatum acts as the Critic while the GPI performs action selection. Dopaminergic activity of the Substantia Nigra pars compacta (SNc) is interpreted as Temporal Difference (TD) error [1]. The STN-GPe subsystem acts as the explorer module, whose lateral weights and inter-connectivity weights modulates the degree of exploration [2]. The weights between the Striatum and the GPI are updated using Q-learning. The striatal medium spiny neurons (MSNs) capable of exhibiting UP-DOWN states are thought to be cellular substrates of working memory in the BG system. The MSNs are modelled using Flip-Flop neurons, which can store information gated by dopamine inputs from SNc. This ensures fast update of the new information into the working memory as well as the maintenance of existing information.

Using the aforementioned model, we simulated two standard working memory tasks: 1-2-AX-BY task and N-back. In case of the former the task is divided into two types of stimuli – the numeric stimuli and the alphabetical stimuli. When a numeric 1 is encountered, action ‘Right’ is the desired action only when A followed by an X had already appeared in the sequence. For all other alphabetical sequences, action ‘Left’ is the desired action. Similarly, when a numeric 2 is encountered, action ‘Right’ is the desired action only when B followed by a Y had already appeared in the sequence.



ral images as the training input, SPC can learn simple cells with the property of response saturation that is previously explained by DN

**A) Model Architecture & Tasks****B) Accuracy and Loss**

**Fig. 1** A Model Architecture of Cortico-Basal Ganglia circuitry. GPe-Global Pallidus Externa; GPi-Global Pallidus Interna; STN- Subthalamic Nucleus; SNC- Substantia Nigra pars compacta; L and R-Left and R-Right Action. B Plots indicating the Accuracy and Loss of 1-2-AX-BY task and 2-Back task

For all other alphabetical sequences, action ‘Left’ is the desired action. In case of N-back task, if the current stimulus matches the stimulus presented ‘N’ time steps back, the action ‘Right’ is the desired action, else action ‘Left’ is the desired action. The model was trained for respective tasks and a testing accuracy of 95.6% and 92.4% was attained for tasks 1-2-AX-BY and N-back (N = 2) tasks respectively.

**References**

1. W. Schultz. Predictive Reward Signal of Dopamine Neurons. *Journal of Neurophysiology*. 1998 Jul; 80(1): 1–27
2. V. S. Chakravarthy & A. A. Moustafa. Computational Neuroscience Models of the Basal Ganglia, 1st ed. Singapore: Springer Singapore, 2018.

**P16 Bifurcation of normal & AD brains detected by ensemble learning method applied to longitudinal EEG data**

Eunjin Hwang<sup>\*1</sup>, Sergey Leksikov<sup>1</sup>, Younghyun Yoon<sup>2</sup>, Yeayoung Kim<sup>3</sup>, Jee Hyun Choi<sup>4</sup>

<sup>1</sup>Lablup, Inc., Research Team, Seoul, South Korea

<sup>2</sup>Vanderbilt University, Department of Computer Science and Cognitive Science, Nashville, United States of America

<sup>3</sup>Catholic University, College of Medicine, Seoul, South Korea

<sup>4</sup>Korea Institute of Science and Technology, Brain Science Institute, Seoul, South Korea

\*Email: bluemoon@postech.ac.kr

In the aged society where the number of Alzheimer’s disease (AD) patients are increasing, delaying the onset or slowing the progress of the disease is important to reduce the socioeconomic costs of the disease. According to the hypothetical time course of AD, the behavior level functional decline is preceded by pathophysiological and structural changes in the brain. Since the examination of pathophysiological change in the brain is costly to be done through regular check-ups, there is an increasing demand for early and inexpensive diagnostic methods. EEG signals contain information about the architecture of

the neural network in the brain. EEGs are useful in diagnosing brain conditions such as seizure disorders and psychiatric diseases like schizophrenia but there is no established EEG time course or EEG biomarkers for AD yet. In this study we have investigated the longitudinal change of the brain using EEG, if there are any aspects of EEG that are changing with disease progression, and if so, what the aspects are, and how the change looks like, whether it is abrupt or gradual, and whether it has any characteristic time point. With a longitudinal EEG dataset acquired from AD model (5xFAD) mouse brains and normal mouse brains, we present a new approach to differentiate the change of diseased brain function from the normal by using random forest classifier. On a monthly basis, baseline EEGs and event-related EEGs with auditory stimuli was acquired in multiple trials for each mouse from four brain areas, bilateral frontal and parietal cortices. Individual features of EEG such as resting and evoked state band power, correlation between areas, and phase locking to auditory stimuli were acquired throughout the ages. Age-related EEG features were selected with Spearman’s correlation analysis and divided into training and testing datasets where the training set is acquired at the old age like 34 weeks. A random forest model was trained to distinguish AD mice from control and tested in 5-week windows sliding over the younger age dataset with 1-week step. In a test window, experiments were repeated 30 times with a random state seed for the RF model and the evaluation metrics were obtained by averaging over the results of 30 repetition. In the random forest model with the maximum average accuracy over testing windows, class probabilities were obtained and the divergence of probability distributions for AD and control mice were quantified with Kullback–Leibler divergence. Also, feature importance was determined with Gini impurity scores and visualized with a decision tree. The divergence of the predicted class between normal and AD brains was found dramatically increasing at the age of 6–7 months after birth, while the difference between two started to be observed as early as 4-month after birth which is the earliest age detected with EEG, and at which the memory impairment was reported to start. The features of high importance in predicting the class probability were inter-trial coherence of the responses, especially in gamma band, which band is known to participate in cognitive functions such as perception, attention and memory. We have presented a new method to quantify temporal changes of brain function in AD model mice using machine learning method and shown that the ensemble of EEG features could

capture the differentiation of diseased and normal brain states, which could not be done on an individual feature basis.

#### P17 Artificial speech sounds synthesized from intracranial recordings during overt and silent speech tasks

**Kevin Meng**<sup>\*1</sup>, Farhad Goodarzy<sup>2</sup>, Mark Cook<sup>3</sup>, David Grayden<sup>1</sup>, Eui-Young Kim<sup>4</sup>, June Sic Kim<sup>5</sup>, Chun Kee Chung<sup>6</sup>

<sup>1</sup>The University of Melbourne, Department of Biomedical Engineering, Melbourne, Australia

<sup>2</sup>The University of Melbourne, MDHS, Fitzroy, Australia

<sup>3</sup>The University of Melbourne, Department of Medicine, Melbourne, Australia

<sup>4</sup>Seoul National University, Interdisciplinary Program in Neuroscience, Seoul, South Korea

<sup>5</sup>Seoul National University, Research Institute of Basic Sciences, Seoul, South Korea

<sup>6</sup>Seoul National University Hospital, Department of Neurosurgery, Seoul, South Korea

\*Email: ksmeng@student.unimelb.edu.au

Speech neuroprostheses could help people who have lost their ability to speak [1]. To accelerate the development of such devices, we developed a closed-loop brain-computer interface (BCI) system that synthesizes artificial speech sounds from intracranial recordings [2]. Here, we characterize neural features that contribute to the reconstruction of continuous audio signals, evaluate the prediction accuracy of their spectrograms, and add further evidence regarding the feasibility of real-time synthesis of silent speech processes from intracranial signals [3].

Five patients with epilepsy were implanted with intracranial grid and depth electrodes for clinical monitoring purposes. They read the same list of 108 Korean words under three different speech conditions: overt (twice), mimed (once), and imagined (once). The first overt session was used to train a speech synthesis model. The remaining three sessions were used to test the model under different conditions. The synthesis model consisted of two parallel decoders operating with an update step of 16 ms. Inputs to both decoders were power spectral densities of recording sites and frequency bands of interest, extracted from raw intracranial signals at 2 kHz. The first decoder predicted 16-ms audio waveforms at 16 kHz. The second decoder estimated the probability of speech occurrence. An adjustable threshold was applied to the probability to mute or unmute the artificial sound output. Two patients performed the testing sessions with real-time feedback.

In terms of neural features, localized areas within the ventral sensorimotor cortex and the superior temporal gyrus contributed most to the reconstruction of audio spectrograms. Neural activations in various bands within high frequency range 70–170 Hz were most correlated with speech features. Accuracy of artificial speech sounds was assessed using voice recordings during overt sessions as a benchmark. Interestingly, our synthesis model, trained on overt speech, also predicted audible outputs during silent speech conditions. Similar activation patterns between overt and silent conditions may indicate the presence of efference copies during speech imagery tasks [4]. For patients who performed the testing sessions in a closed-loop fashion, post-hoc analyses improved the accuracy of artificial sounds delivered as feedback during initial data collection.

Future directions include the reduction in feedback delay time [2] and the development of robust metrics to evaluate speech intelligibility [5]. This will allow BCI users to experience a better sense of agency and to adapt their mental strategies during speech imagery.

#### References

1. Moses D, et al. Neuroprosthesis for decoding speech in a paralyzed person with anarthria. *New England Journal of Medicine*. 2021; 385(3): 217–227.
2. Meng K, et al. Implementation of a closed-loop BCI system for real-time speech synthesis under clinical constraints. In IEEE 10th International Winter Conference on Brain-Computer Interface (BCI). 2022; 1–6.
3. Angrick M, et al. Real-time synthesis of imagined speech processes from minimally invasive recordings of neural activity. *Communications biology*. 2021; 4(1): 1–10.
4. Tian X, et al. Mental imagery of speech implicates two mechanisms of perceptual reactivation. *Cortex*. 2016; 77: 1–12.
5. Verwoert M, et al. Speech Production in Intracranial Electroencephalography: iBIDS Dataset. *bioRxiv*. 2022; 487183.

#### P18 Decoding semantic categories in the anterior temporal lobe using intracranial recordings

**EuiYoung Kim**<sup>\*1</sup>, Kevin Meng<sup>2</sup>, June Sic Kim<sup>3</sup>, Chun Kee Chung<sup>4</sup>

<sup>1</sup>Seoul National University, Interdisciplinary Program in Neuroscience, Seoul, South Korea

<sup>2</sup>University of Melbourne, Biomedical Engineering, Melbourne, Australia

<sup>3</sup>Seoul National University, Research Institute of Basic Sciences, Seoul, South Korea

<sup>4</sup>Seoul National University Hospital, Department of Neurosurgery, Seoul, South Korea

\*Email: key411@snu.ac.kr

High-level linguistic processing in the human brain remains incompletely understood and constitute a challenging topic in the field of speech neuroscience. Using intracranial recordings of the human brain during speech perception, many studies focused on low-level phonetic components [1]. In contrast, few studies have attempted to decode high-level semantic components [2]. In their dual-stream model of speech processing from the auditory cortex to the frontal lobe, Hickok and Poeppel proposed that the dorsal stream is left-hemisphere dominant, while the ventral stream is mostly bilaterally organized [3]. Here, we are interested in better characterizing the ventral stream, particularly within the anterior temporal lobe, which is thought to process speech signals for comprehension. To address the existence of semantic hubs in the brain, we aimed to identify key neural features and train linear classifiers to discriminate between selected semantic categories during controlled listening tasks.

Ten patients with intractable epilepsy were implanted with intracranial grids, strips, and depths with variable coverage of the anterior temporal lobe. They participated in a question-answer task, which consisted of 144 trials. Questions were pre-recorded and delivered via headphones. There were four possible questions, each introducing a different semantic category (alive, not alive, body part, or not body part), but all ending with the same sentence (“which one is it?”). We focused our analysis of brain signals during the latter sentence and labelled trials by their semantic categories. In our preliminary results, we showed that recording sites in the posterior temporal lobe tracked acoustic and phonetic components of speech in the high-gamma frequency band (70–110 Hz). However, these localized neural features did not show any discriminative power. In contrast, combining numerous features in various frequency bands (1–200 Hz) in recording sites within the anterior temporal lobe improved classification accuracy, possibly illustrating the existence of nodes for encoding “yes-no” or specific semantic categories, such as living

things or body parts. An important limitation of our study is the lack of control on clinical electrode placement, which prevented us from generalizing patient-specific results. In future directions, our unique dataset may be further exploited using different approaches, such as connectivity analyses.

## References

- Mesgarani. Phonetic Feature Encoding in Human Superior Temporal Gyrus. *Science*. 2014; 343: 1006–1010
- Sato. Frequency-Dependent Cortical Interactions during Semantic Processing: An Electrocorticogram Cross-Spectrum Analysis Using a Semantic Space Model. *Cerebral Cortex*. 2021; 31: 4329–4339
- Hickok, Poeppel. The cortical organization of speech processing. *Nature Reviews Neuroscience*. 2007; 8: 393–402

## P19 Understanding hyperexcitability of cortical malformations through network analyses

Ana Aquiles<sup>\*1</sup>, Hiram Luna-Munguía<sup>1</sup>, Tatiana Fiordelisio<sup>2</sup>, Mirela Regalado<sup>1</sup>, Luis Concha<sup>1</sup>

<sup>1</sup>Neurobiology Institute, Cognitive Neurosciences, Querétaro, Mexico

<sup>2</sup>Faculty of Sciences, Neuroendocrinology, Mexico City, Mexico

\*Email: anaaquiles@ciencias.unam.mx

Several biological processes are involved in the morphological development of the cortex during early gestation. Genetic and epigenetic factors can alter cortical development and result in morphological

abnormalities collectively known as malformations of cortical development (MCD). One of these is focal cortical dysplasias (FCDs), characterized by a delaminated cortex, blurring of the interface between gray and white matter, and variable architectural abnormalities. Their clinical importance lies in the fact that they can result in refractory and drug-resistant epilepsy, with greater incidence in the pediatric population. Their variability in morphology, location, and extension are major hurdles to an early and accurate diagnosis. Moreover, the relation between their aberrant morphology and their epileptogenic activity remains obscure. Here, we used an animal model of cortical dysplasia [1] to investigate the functional network properties and their response to a hyperexcitable challenge.

Using calcium imaging with a large field of view, we can record a wide number of live cells throughout the primary motor cortex in an early stage of development (p30), at their basal activity, and before and after an external stimulus (pilocarpine - an acetylcholine agonist). We inferred connectivity using the cross-correlation method in five 150-s windows and, by generating a new dataset from the phase and amplitude of the wave, determined the significance of these correlations. We also checked significance using FDR correction to eliminate false positives. We evaluated five temporal windows (1-Before stimulus, 2-During stimulus, 3–5, After stimulus) describing global features by their degree of connectivity and position. We approach local description by measuring some network metrics, such as assortativity and cluster coefficient.

Compared to the cortical tissue of control animals, dysplastic cortices show remarkable values of connectivity density, especially around depth positions 0.4–0.8 (Fig. 1A), whereas in the control we observe lower density and wider distribution throughout the cortex, which is more evident in the later temporal windows. Suggesting that dysplasia cortices present more connections only in a focal region, while control cortices dissipate their connectivity across the cortex. In addition,

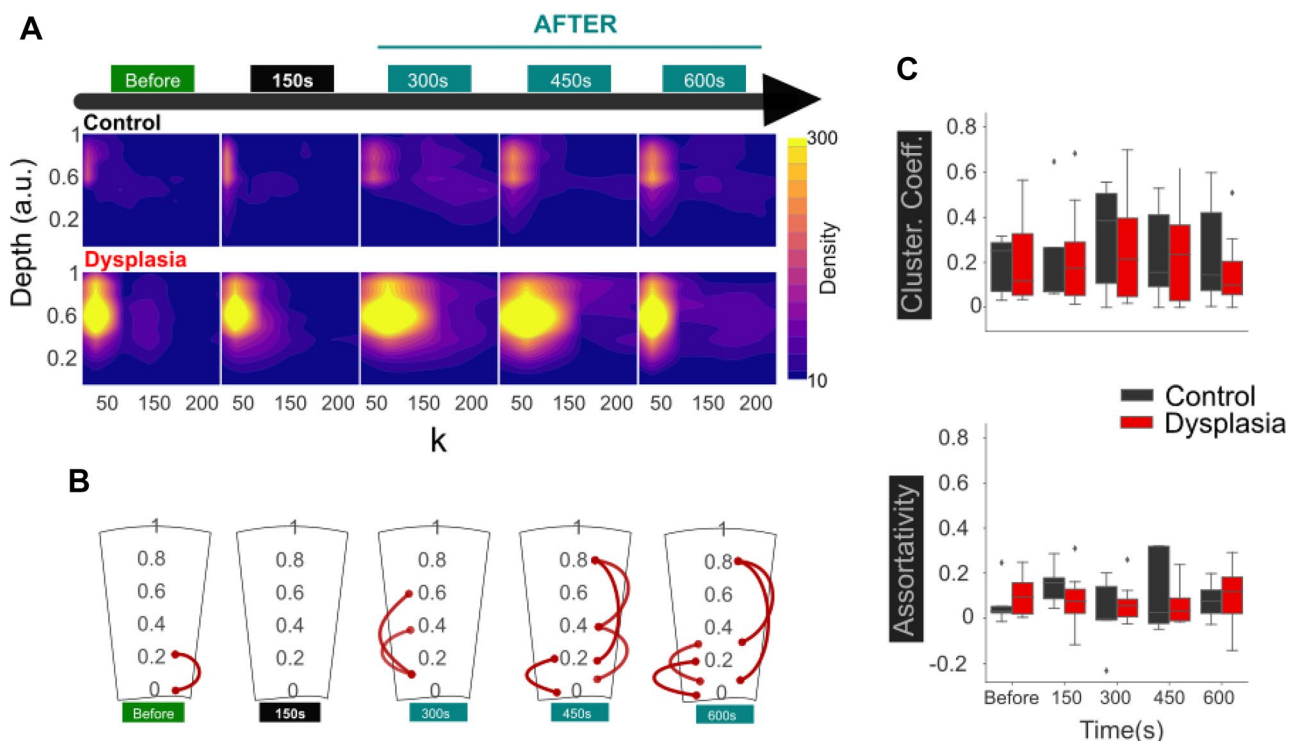


**Fig. 1** **A** Degree of connectivity ( $k$ ) and cortical depth (0=gray/white matter junction; 1=cortical surface) and its evolution over time in 150 s windows before (green), during (black), and after (aqua)

stimulus. **B** Intracortical connectivity between dysplastic cortex and control cortex (red lines, represent interactions with difference between groups Control > Dysplasia). **C** Network metrics

internal connectivity shows differences in interactions at different depths between groups, with an increase in interactions in the last windows, where activity is found after the stimulus. (Fig. 1B). Finally, we also explored connectivity by measuring two intrinsic network metrics, its ability to form clusters and its connectivity preference. In the first case we found that communication is very similar at the clustering level, in controls than in dysplasias. On the other hand, intra-cortical connectivity differs between groups in a depth-specific fashion before and after the hyperexcitable stimulus (Fig. 1C).

#### Acknowledgements

We thank Nydia Hernández-Ríos, Ericka de Los Ríos and Juan Ortiz-Retana for technical assistance.

#### Funding

UNAM-DGAPA (IN204720, IA200621).

#### References

1. Benardete E, Kriegstein A. Increased excitability and decreased sensitivity to GABA in an animal model of dysplastic cortex. *Epilepsia*. 2002; 43: 970–982

#### P20 Modeling roles of Ca<sup>2+</sup> dynamics in temperature coding mechanisms of *Drosophila* sensory neurons

Natalia Maksymchuk<sup>1</sup>, Akira Sakurai<sup>1</sup>, Daniel N. Cox<sup>1</sup>, Gennady Cymbalyuk<sup>\*1</sup>

<sup>1</sup>Georgia State University, Neuroscience Institute, Atlanta, GA, United States of America

\*Email: gcymbalyuk@gmail.com

Cold nociception is critical to animals' survival in environments with variable temperature. Capitalizing on the wealth of genetic tools provided by the *Drosophila* model system, we investigate larval Class III (CIII) primary afferents responsible for cold-sensing. In response to temperature decrease, these neurons produce patterns of activity with two distinct components bursting and spiking. Bursts are more frequently seen with a fast temperature drop to noxious cold, followed by tonic spiking with frequency adaptation. In contrast, the slow decrease to the same temperature value caused sparse bursting activity throughout the stimulation. Previously, our CIII neuron model with the phenomenological representation of thermosensitive TRP (thermo-TRP) currents, having temperature-dependent activation and calcium-dependent inactivation properties captured these phenomena. Our recent experimental data further implicate complex Ca<sup>2+</sup> dynamics including Calcium induced Calcium Release (CICR), and its interaction with Ca<sup>2+</sup>-activated ionic currents, Ca<sup>2+</sup>-activated Cl-channels [1] and Ca<sup>2+</sup>-activated K<sup>+</sup> channels (SK and BK), and hyperpolarization-activated current. Here, we developed a family of computational CIII models with these currents and processes incorporated. We investigated how thermoTRP currents interact with the CICR mechanism to induce amplified Ca<sup>2+</sup> response appropriate for neural coding of cold nociception. In this CIII model, intracellular [Ca<sup>2+</sup>] dynamics include ER as the main Ca<sup>2+</sup> store, mitochondrial Ca<sup>2+</sup> store, and cytosolic Ca<sup>2+</sup> binding proteins. The model describes the exchange of Ca<sup>2+</sup> between two cytosolic micro-domains, Ca<sup>2+</sup> stores and Ca<sup>2+</sup> binding proteins. For modeling of TRP channel-dependent CICR, we use a single electrical compartment and four Ca<sup>2+</sup> compartments (two cytosolic, and two calcium storage compartments). Our model

results show that Cl-ion homeostasis and interaction of the chloride and SK potassium currents play key roles in distinguishing between bursting and spiking components of the activity patterns generated by CIII neurons in response to cold temperature stimulation.

#### Acknowledgments

This research was supported by NIH grant 1R01NS115209 awarded to Daniel Cox and Gennady Cymbalyuk.

#### References

1. Himmel NJ, Sakurai A, Letcher JM, Patel AA, Bhattacharjee S, Benson MN, Gray TR, Cymbalyuk GS, and Cox DN. Chloride-dependent mechanisms of multimodal sensory discrimination and neuropathic sensitization in *Drosophila*. 2021; bioRxiv. 472093.

#### P21 Multi-compartmental reconstruction and simulations of an entire module of the mouse cerebellar cortex

Robin De Schepper<sup>\*1</sup>, Alice Geminiani<sup>1</sup>, Claudia Casellato<sup>1</sup>, Stefano Masoli<sup>1</sup>, Martina Rizza<sup>1</sup>, Alberto Antonietti<sup>1</sup>, Egidio D'Angelo<sup>1</sup>

<sup>1</sup>University of Pavia, Department of Brain and Behavioral Sciences, Pavia, Italy

\*Email: robingilbert.deschepper@unipv.it

Data-driven modelling of the brain unifies multiple multimodal datasets into functional constructs. Handling and processing such information into a network model - with cells, their morphologies, membrane mechanisms, and synapses - ready for simulation requires a framework catered to the neuroscientific nature of the data and the problem, with general solutions to accommodate experimental data at different scales. To this end, we have developed the Brain Scaffold Builder (BSB), a tool for structural and functional microcircuit modelling. The BSB provides a project based environment, an organized workflow with several stages, multiple generic strategies for cell placement and connectivity, a configuration system capable of including detailed neuronal and synaptic models, and support for multiple simulators. All stages, including reconstruction and simulation, can always be executed in parallel. It is provided as an open-source package, applicable for multi-scale modelling of different brain areas. The interfaces with several simulators (NEURON, NEST, Arbor) allow to investigate the same brain region at different levels of resolution, depending on the scientific question. The BSB's effectiveness was tested on the cerebellar network, which has a complex geometry and raises a broad set of modelling challenges. For the first time, an entire module of the mouse cerebellar cortex was reconstructed using morphologically realistic conductance-based multi-compartmental neuron models of granule, Golgi, Purkinje, stellate and basket cells. Different connection rules, based on population properties such as divergence and convergence, or rules based on morphological intersection, were used to generate the connectome, unifying a collection of scattered experimental data into a coherent construct. The model consists of 30 thousand cells and 1.5 million synapses. Baseline and sensory-burst stimulation were used for functional validation against *in vivo* recordings, monitoring the impact of subcellular and cellular mechanisms on signal propagation and spatio-temporal processing in the cerebellum. The integration of structural and functional properties through the model provides a new "ground truth" about cerebellar circuit organization capable of predicting neural dynamics *in vivo*.

**P22 Spatial representability of neuronal activity**Danil Akhtiamov<sup>1</sup>, Anthony Cohn<sup>2</sup>, Yuri Dabaghian<sup>\*3</sup><sup>1</sup>The Hebrew University, Mathematics, Jerusalem, Israel<sup>2</sup>University of Leeds, School of Computing, Leeds, United Kingdom<sup>3</sup>The University of Texas McGovern Medical School at Houston, Neurology, Houston, TX, United States of America<sup>\*</sup>Email: [yuri.a.dabaghian@uth.tmc.edu](mailto:yuri.a.dabaghian@uth.tmc.edu)

A common approach to interpreting spiking activity is based on identifying neuronal firing fields - regions in physical or configuration spaces that elicit action potentials. Common examples include hippocampal place cells that fire at preferred locations in the navigated environment, head direction cells that fire at preferred orientations of the animal's head (angular domains), view cells that respond to preferred spots in the visual field, etc. In all these cases, referencing an individual neuron's activity to a particular region in a suitable representing space is key for understanding its contribution and for reasoning about functions of neuronal ensembles in terms of the corresponding "maps". This raises a natural question: when is a spatial interpretation of neuronal activity at all possible, i.e., when might there exist a correspondence between the patterns of neuronal activity and regions in low-dimensional space?

Historically, all firing fields were discovered empirically, experimentally, by trial and error. We argue that the existence and a number of properties of the firing fields can be established theoretically, through topological analyses of the neuronal spiking activity that involve Leray criterion, persistent homology theory, Eckhoff conditions and Region Connection Calculus. Specifically, it can be demonstrated that spatial representability of neuronal responses an emergent phenomenon, and that the firing fields acquire their properties dynamically, through learning, which includes such fundamental properties and dimensionality [1].

**References**

1. Akhtiamov D, Cohn AG, Dabaghian Y. Spatial representability of neuronal activity. *Scientific Reports*. 2021; 11(1):20957.

**P23 Discrete brain rhythms, oscillons and rapid spectral dynamics**Ms Zobaer<sup>1</sup>, Carli Marie Domenico<sup>2</sup>, Luca Perotti<sup>3</sup>, Daoyun Ji<sup>2</sup>, Yuri Dabaghian<sup>\*1</sup><sup>1</sup>The University of Texas McGovern Medical School at Houston, Neurology, Houston, TX, United States of America<sup>2</sup>Baylor College of Medicine, Neuroscience, Houston, United States of America<sup>3</sup>Texas Southern University, Physics, Houston, United States of America<sup>\*</sup>Email: [yuri.a.dabaghian@uth.tmc.edu](mailto:yuri.a.dabaghian@uth.tmc.edu)

Neurons in the brain are submerged into oscillating extracellular field, which is one of the principal determinants of the brain activity and a key component of many neurophysiological mechanisms. The format of our understanding these rhythms' structure and functionality depends on the mathematical approaches used for analyzing the recorded potentials—the Local Field Potential (LFP). Currently, most methods are based on decomposing the signal into ad hoc selected components (sinusoids, wavelets, etc.), viewed as the LFP's basic building blocks. Since such decompositions are typically mathematically complete and useful in their own way, it may appear that the question about the "actual" structure of

the signal is of little importance if not at all meaningless. However, this is not the case: each method biases the overall picture in a particular way, highlighting some aspects of the data and obscuring others. As long as the physiological mechanisms of the LFP oscillations remain unknown, the search of a physically adequate description of the brain waves remains a matter of fundamental importance.

A novel approach to LFP analyses—Discrete Padé Transform (DPT)—proposed in [1] allows constructing the signals' prime components empirically, thus helping to capture the physical organization of synchronized neuronal oscillations. From the DPT perspective, hippocampal "brain waves" decompose into a superposition of a few phase modulated oscillatory processes, which we call *brain wave oscillons*. For example, there is a single discrete  $\theta$ -oscillon that corresponds to the standard  $\theta$ -rhythm, a couple of  $\gamma$ -oscillons that roughly correspond to slow and fast  $\gamma$ -rhythms, and so forth. Furthermore, it turns out the oscillons spectra exhibit complex dynamics, coupled with animal's speed and acceleration. In addition to the slow, undulatory spectral waves, we also observe rapid spectral kicks are localized not only in frequency, but also in time: a typical kick grows and abates over a few hundred msec period. While many peaks are recurrent, appearing and disappearing repeatedly at about the same frequency, others are isolated, which suggests that part of the oscillons' spectral changes is due to endogenous, regular network dynamics, while other is due to external cortical and parahippocampal inputs [2].

**References**

1. Perotti, L., DeVito, J., Bessis, D., Dabaghian Y. Discrete Structure of the Brain Rhythms. *Scientific Reports*. 2019; 9(1):1105
2. Zobaer, M., Domenico, C., Perotti, L., Ji, D. & Dabaghian, Y. Rapid spectral dynamics in hippocampal oscillons. *Frontiers in Computational Neuroscience*. 2022

**P24 Investigating the Mechanisms Behind Experience-Dependent Place Cell Shifting**Kathrine Clarke<sup>\*1</sup>, Anthony Burkitt<sup>1</sup>, Yanbo Lian<sup>1</sup>, Simon R Schultz<sup>2</sup>, Mary Ann Go<sup>2</sup>, Catherine Davey<sup>1</sup><sup>1</sup>The University of Melbourne, Department of Biomedical Engineering, Melbourne, Australia<sup>2</sup>Imperial College London, Department of Bioengineering, London, United Kingdom<sup>\*</sup>Email: [kathrine.e.c@gmail.com](mailto:kathrine.e.c@gmail.com)

The spatial receptive fields (place fields) of Hippocampal place cells rapidly learn and update their firing locations in response to experience of an environment. Past experimental observations suggest that when an animal repeatedly travels one trajectory, the firing locations of individual cells on average shift backwards relative to the motion path [1]. However, both forwards and backwards shifting place fields have been observed [2], and the range of magnitudes of shifting is not well understood. This backwards shifting effect is often attributed to the interaction between an asymmetric learning rule such as spike-timing dependent plasticity, and repeated sequential activation of place cells [3]. Place cells are strongly modulated by theta frequency oscillations, leading to the compression of location sequences into learning relevant time scales (dubbed theta sequences), which results in the fast learning rates observed in the hippocampus. We propose that the broad distribution of place field shifting can be explained by variability in the order of spikes in this sequence compression. Using two-photon imaging we observe the activity of place cells in the CA1 hippocampal region as head-fixed mice repeatedly run

around an airlifted circular track (using methods described in [4]). By tracking the firing locations of many place cells over successive laps, we investigate the distribution of shifting, and how it changes with familiarity and time spent within the environment. This analysis is compared to a theoretical model derived from the interaction of place fields with theta oscillations with spike timing dependent a plasticity learning rule. After a theoretical exploration that variations in the theta timescale can result in a wide distribution of shifts, we then use simulation to explore the effect of this shifting distribution over many laps, comparing this experimentally observed firing locations of place cells as they change of many laps.

Preliminary findings suggest that while place fields shift backwards on average, the shifting of individual cells falls within a wide distribution, with individual cells exhibiting both backwards and forwards shifting. Through our simulation we demonstrate how a broad distribution of place field shifts can emerge from a network with the fast learning-rates seen in the hippocampus. Simulated sequences of place cell firing locations over repeated laps of are similar to those observed experimentally.

## References

1. Mehta M, Barnes A, McNaughton, B. Experience-dependent, asymmetric expansion of hippocampal place fields. Proceedings of the National Academy of Sciences of the USA. 1997; 89:18–8921
2. Lee I, Rao G, Knierim J. A double dissociation between hippocampal subfields: Differential time course of CA3 and CA1 place cells for processing changed environments. Neuron. 2004; 40:803–815
3. Mehta M, Quirk M, Wilson M. Experience-dependent asymmetric shape of hippocampal receptive fields. Neuron. 2000; 70:7–715
4. Go A et al. Place Cells in Head-Fixed Mice Navigating a Floating Real-World Environment. Frontiers in Cellular Neuroscience. 2021; 1–16

## P25 Modelling the resonant neural activity evoked by deep brain stimulation of the subthalamic nucleus using a network of Kuramoto oscillators with STDP

James Sermon<sup>\*1</sup>, Rafal Bogacz<sup>2</sup>, Benoit Duchet<sup>2</sup>, Christoph Wiest<sup>1</sup>, Huiling Tan<sup>1</sup>, Timothy Denison<sup>1,3</sup>

<sup>1</sup>University of Oxford, Nuffield Department of Clinical Neurosciences, Oxford, United Kingdom

<sup>2</sup>University of Oxford, MRC Brain Network Dynamics Unit, Oxford, United Kingdom

<sup>3</sup>University of Oxford, Department of Engineering Science, Oxford, United Kingdom

\*Email: jjsermon0@gmail.com

Evoked resonant neural activity (ERNA) is the appearance of high frequency oscillations (250–350 Hz) that decay in both amplitude and frequency with time, following the onset of deep brain stimulation (DBS) of the subthalamic nucleus (STN). While the appearance of the ERNA has been consistently and well documented in several clinical studies of STN DBS, its biophysical origins remain unclear. We demonstrate that the high frequency, time-decaying oscillations of the ERNA can be captured through a simple model of Kuramoto oscillators. In order to recreate the time-dependent characteristics of the ERNA, we introduce spike-timing-dependent-plasticity (STDP). In the presence of stimulation and with STDP we observe an increase of the coupling in the network, which induces a high frequency signal due to the increased coherence between the oscillators. We verify features of the ERNA at variable stimulation parameters, investigate

STDP parameters compatible with the data and how the ERNA signal might change with more complex neuromodulation patterns. These results reveal that complex neuronal responses to stimulation can be captured and explained through simple models. Better understanding the effects of DBS will allow us to further refine and tailor neuromodulation protocols. Furthermore, investigating the origins of the ERNA will allow us to explore the use of the phenomenon as a potential diagnostic tool.

## Acknowledgements

The authors would like to acknowledge the use of the University of Oxford Advanced Research Computing (ARC) facility in carrying out this work. <https://doi.org/10.5281/zenodo.22558>. We thank the Medical Research Council for support with grants MC\_UU\_00003/1, MC\_UU\_00003/2, MC\_UU\_00003/3 and MR/V00655X/1, as well as the Rosetrees trust.

## P26 Large-scale and topographically detailed model of the sensorimotor thalamus with bidirectional connections to M1 and S1

Joao Moreira<sup>1</sup>, Fernando Borges<sup>2</sup>, William W Lytton<sup>2</sup>, Salvador Dura-Bernal<sup>\*2</sup>

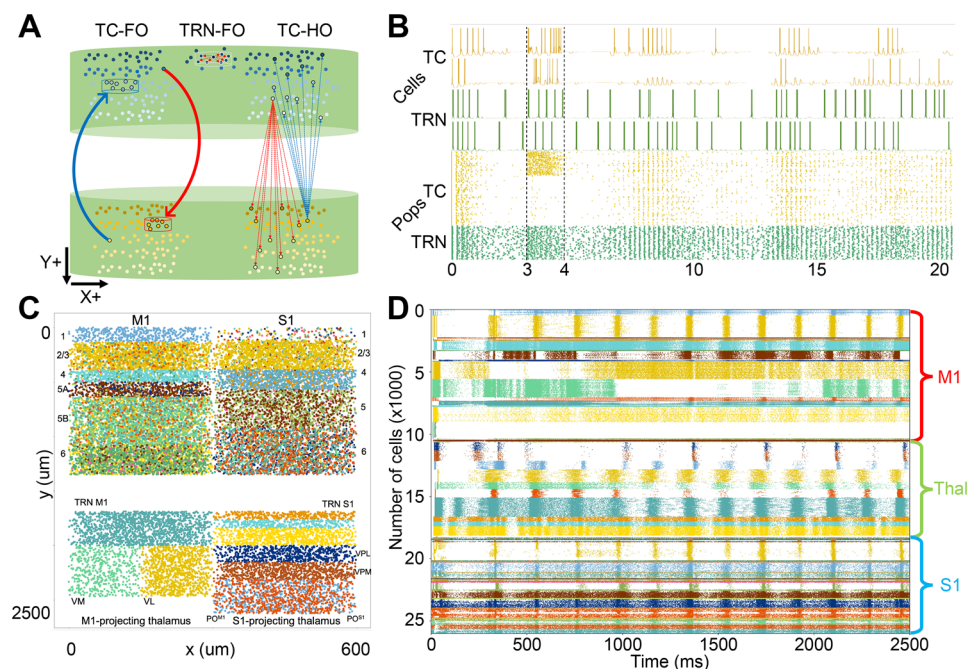
<sup>1</sup>SUNY Downstate Health Sciences University, School of Graduate Studies, Brooklyn, NY, United States of America

<sup>2</sup>SUNY Downstate Health Sciences University, Department of Physiology and Pharmacology, Brooklyn, NY, NY, United States of America

\*Email: salvadordura@gmail.com

The thalamus is often referred to as a relay center, forwarding information between the cerebral cortex and the periphery of the body. Thalamic relay cells fire at two different regimes, known as tonic- and burst-firing mode, which have been a major focus of experimental preparations and computational models. However, it is only in recent years that researchers were able to have a better understanding of the network dynamics that take place in different nuclei. Each nucleus has a specific pattern of connections, with functional implications which are not yet fully understood. We developed a large-scale model of the motor and somatosensory thalamus, with ~2,250 neurons and ~33,000 connections, which incorporated recent data on projection targets and circuit architecture. Our objective was to reconcile the single cell dynamics of thalamic relay and reticular nuclei cells with circuit-level observations and integrate it with two large-scale models of the primary motor (M1) and somatosensory (S1) cortices. The model was built using the NetPyNE tool (<http://www.netpyne.org>) and the NEURON simulator (<https://www.neuron.yale.edu>). It is composed of four first-order (core) excitatory nuclei: the motor cortex projecting ventral anterior/ventrolateral and ventromedial nuclei; and the somatosensory cortex projecting ventral posterolateral and ventral posteromedial nuclei. It also includes a higher-order (matrix) excitatory posterior medial nucleus with separate motor and somatosensory projecting sectors. First-order nuclei distributed topographical projections in a columnar fashion, with higher-order nuclei connected via a divergence rule as an approximation due to incomplete anatomical data. All excitatory nuclei are interconnected within the thalamus via the reticular nucleus, represented here by a single-layered motor sector and a three-layered somatosensory sector (Fig. 1A). We used single-compartment cell models based on Destexhe [1] with adjusted parameters. Both cell types feature Hodgkin-Huxley-type mechanisms, including Na<sup>+</sup> and K<sup>+</sup>, low-threshold transient Ca<sup>2+</sup>, and K<sup>+</sup> leak currents, and relay cells also have a hyperpolarization-activated cationic current and a rapidly-inactivating and transient K<sup>+</sup> current. The connectivity rules

**Fig. 1** Large-scale model of the sensorimotor thalamus, M1 and S1. **A** Schematic of the topological connectivity in the thalamus model (TC: thalamocortical; TRN: thalamic reticular nucleus; FO: first order; HO: higher order); **B** Voltage traces and raster plot for two interconnected TC and TRN populations, highlighting the dynamic interactions taking place in the network. Dashed lines represent a 1 s stimulation in a subset of TC cells; **C** 2D plot of the cell positions for the thalamus, M1 and S1 models, with different colors for each population; **D** Raster plot for the full M1-thalamus-S1 circuit



were based on data of axonal and dendritic footprints for each nucleus, and probability and weight of connections were tuned within biological constraints to match dynamics observed experimentally. The results show our model reproduces key dynamical features: 1. tonic- and burst-firing behavior at single-cell level; 2. rhythmic bursting and spindle oscillations at circuit level; 3. stable self-sustained rhythmic activity; 4. responsiveness to driver inputs, with shift in dynamics through external modulation (Fig. 1B). Integration with M1 and S1 exhibited synchrony between the neuronal activity of the two cortical regions and the thalamus, consistent with animal experimental data (Fig. 1C-D). Together, these models will provide a framework to study neural coding, information flow and learning mechanisms in the cortico-thalamo-cortical circuits of the sensorimotor pathway with an unprecedented level of detail, allowing us to make predictions about the mechanisms underlying physiological and pathological sensorimotor dynamics in the brain.

## References

- Destexhe, A., Bal, T., McCormick, D. A., & Sejnowski, T. J. (1996). Ionic mechanisms underlying synchronized oscillations and propagating waves in a model of ferret thalamic slices. *Journal of Neurophysiology*, 76(3), 2049–2070.

## Acknowledgements

This work was funded by the following grants: NIH U24EB028998, NSF 1904444-1042C, NIH U01EB017695, NYS SCIRB DOH01-C32250GG-3450000.

## P27 Closed-loop brain-inspired meta-learning rules for action suppression in artificial agents

Federica Robertazzi<sup>1</sup>, Matteo Vissani<sup>1</sup>, Guido Schillaci<sup>1</sup>, Egidio Falotico<sup>1</sup>

<sup>1</sup>Sant'Anna School of Advanced Studies, The BioRobotics Institute and Department of Excellence for Robotics & AI, SSSA, PISA, Italy

\*Email: federica.robertazzi@santannapisa.it

Cognitive control is the ability to adapt behavior to current demands by promoting relevant information regardless of interference with the internal urge [1]. Action suppression – the disengagement from a motor response – is an important component of cognitive control involved in the transition between cognitive demands. However, although artificial agents have been becoming extremely efficient to repeat the execution of a single task, demanding the action suppression of an already-planned motor command is an unexpected constraint to fulfill [2, 3]. Meta-learning (ML) systems can be exploited to integrate flexible learning in artificial agents. In ML the learning loop is continuously adjusted by meta-parameters which reflect computational changes in the artificial agent-environment interaction [4, 5]. Neurophysiological knowledge can lay the basis for the development of brain-inspired meta-parameters rules that mimic the neurotransmitter dynamics in the brain, such as acetylcholine, serotonin, dopamine, and noradrenaline, as previously suggested by Doya and colleagues [6–8]. In a previous work [9], we developed a brain-inspired meta-learning framework (i.e., basal ganglia and prefrontal cortex areas) for action inhibition that includes differential dopamine ( $D_1$  and  $D_2$ ) effect and an open-loop dopamine concentration regulation driven by serotonin. We tested the model in two well-known action inhibition tasks: NoGo Paradigm and Stop-Signal Paradigm [10–13]. The artificial agents learned how to successfully countermand the motor command in case of contingency, i.e., the appearance of a hold signal. Moreover, serotonin concentration was found to regulate the impulsive behavior of the agent. Here, in this work, we expanded the aforementioned model evaluating the role of the  $D_1/D_2$  ratio in action inhibition. Briefly, we investigated the computational role of the dopamine meta-parameter, both in terms of concentration and efficacy. We found that  $D_1$  and  $D_2$  provoked differential and asymmetrical effects in the network's activity as well as in the behavioral performance. Indeed, setting the same  $D_1/D_2$  ratio – by increasing  $D_2$  and decreasing  $D_1$  – led to different artificial agent's behavioral state. Then, we implemented a closed-loop serotonin-dopamine interaction. We included monotonic linear and non-linear (e.g., logarithmic) interaction functions that mediate the concentration of the two neurotransmitters according to the ongoing demand of the learning in the artificial agent. Inhibition performances in terms of right inhibition, stop-signal reaction time (i.e., the time required to implement the inhibition command), and accuracy

increased in the closed-loop scenario compared to the previous open-loop implementation. We demonstrated that ML brain-inspired rules may pave the way for the deployment of robust and flexible cognitive inhibition control in artificial agents.

## References

1. J.-C. Dreher & K. F. Berman. Fractionating the neural substrate of cognitive control processes. *Proceedings of the National Academy of Sciences*. 2002; 99(22): 14595–14600
2. R. Pfeifer, M. Lungarella, & F. Iida. Self-Organization, Embodiment, and Biologically Inspired Robotics. *Science*. 2007; 318(5853): 1088–1093
3. E. S. Spelke & K. D. Kinzler. Core knowledge. *Developmental Science*. 2007; 10(1): 89–96
4. S. Thrun & L. Pratt. 'Learning to Learn: Introduction and Overview' in *Learning to Learn*. Pub Boston, MA: Springer US. 1998; 3–17.
5. J. X. Wang et al., Learning to reinforcement learn. *arXiv:1611.05763*. 2017; 25(2021). [Online]. Available at: <http://arxiv.org/abs/1611.05763>
6. K. Doya. Metalearning and neuromodulation. *Neural Networks*. 2002; 15(4–6): 495–506
7. K. Doya. Reinforcement learning: Computational theory and biological mechanisms. *HFSP Journal*. 2007; 1(1): 30–40
8. N. Schweighofer & K. Doya. Meta-learning in *Reinforcement Learning*. *Neural Networks*. 2003; 16(1): 5–9
9. F. Robertazzi, M. Vissani, G. Schillaci, & E. Falotico. Brain-inspired meta-reinforcement learning cognitive control in conflictual inhibition decision-making task for artificial agents. *Neural Networks*. 2022; 154(283–302)
10. D. M. Eagle, C. Baunez, D. M. Hutcheson, O. Lehmann, A. P. Shah, & T. W. Robbins. Stop-Signal Reaction-Time Task Performance: Role of Prefrontal Cortex and Subthalamic Nucleus. *Cerebral Cortex*. 2008; 18(1): 178–188
11. M. Khamassi, S. Lallée, P. Enel, E. Procyk, & P. F. Dominey. Robot Cognitive Control with a Neurophysiologically Inspired Reinforcement Learning Model. *Front. Neurorobot.* 2011; 5
12. M. Khamassi, P. Enel, P. F. Dominey, & E. Procyk. Medial prefrontal cortex and the adaptive regulation of reinforcement learning parameters, in *Progress in Brain Research*. Elsevier. 2013; 202: 441–464
13. J. D. Schall, T. J. Palmeri, & G. D. Logan. Models of inhibitory control. *Phil. Trans. R. Soc. B*. 2017; 372(1718); 20160193

## P28 Disturbed hierarchical function in schizophrenia and early psychosis

Alexander Holmes<sup>\*1</sup>, Priscila Levi<sup>1</sup>, Kevin Aquino<sup>2</sup>, Yu-Chi Chen<sup>1</sup>, Sidhant Chopra<sup>3</sup>, James Pang<sup>1</sup>, Alex Fornito<sup>4</sup>

<sup>1</sup>Monash University, Turner Institute for Brain and Mental Health, Clayton, Australia

<sup>2</sup>The University of Sydney, School of Physics, Sydney, Australia

<sup>3</sup>Yale University, Department of Psychology, New Haven, United States of America

<sup>4</sup>Monash University, The Turner Institute for Brain and Mental Health, School of Psychological Sciences and Monash Biomed, Clayton, Australia

\*Email: alexander.holmes1@monash.edu

Functional networks of the human cerebral cortex are organized along a hierarchical axis, with unimodal sensorimotor areas at one end and trans-modal association areas at the other. Using mathematical and computational methods, this hierarchy and other axes of organization are often characterized as low-dimensional manifolds of inter-regional functional coupling estimates, termed gradients [1]. The

clinical features of schizophrenia and first-episode psychosis involve a constellation of positive, negative, and cognitive symptoms and have often been linked to dysfunctional interactions between association and sensorimotor areas, implying a disruption of hierarchical organization [2]. Here, we investigate how the unimodal-to-transmodal hierarchy differs in schizophrenia, first-episode psychosis, and health by comparing regional gradient scores across the first and second primary gradients, which explain the greatest proportion of variance in functional connectivity. Using 162 subjects from the Human Connectome Project - Early Psychosis (HCP-EP; 48 controls, 114 early psychosis) and 171 subjects from the Consortium for Neuropsychiatric Phenomics (CNP; 121 controls, 50 schizophrenia), we identified lower dimension manifolds via diffusion map embedding combined with a recently developed joint-alignment technique [3]. This produced a primary cortical gradient consistent with the classical sensory-fugal hierarchy observed in tract-tracing literature and a secondary gradient ranging from visual to other sensorimotor areas [4]. In the CNP cohort, we found significantly different regional gradient scores in the second, but not the first, gradient between individuals with schizophrenia and healthy individuals, predominantly driven by changes in visual areas. Gradient dispersion metrics further highlighted these differences; individuals with schizophrenia had lower within-network dispersion in the Frontoparietal (pFDR = .018), Limbic (pFDR = .020), Dorsal Attention (pFDR < .001), and Visual (pFDR = .003) networks, alongside lower between-network dispersion between the Visual network and all other 7 canonical networks (pFDR < .001). In contrast, there were no significant differences in the scores of the first two gradients between individuals with early psychosis and healthy individuals in the HCP-EP cohort. These findings provide new evidence to suggest distinct differences in hierarchical function in individuals with schizophrenia, primarily along the visual-sensorimotor axis rather than the sensory-fugal axis. The absence of any such differences in early psychosis suggests that abnormalities along the visual-sensorimotor axis may only emerge as the illness progresses.

## References

1. Margulies DS, Ghosh SS, Goulas A, Falkiewicz M, Huntenburg JM, Langs G, Bezgin G, Eickhoff SB, Castellanos FX, Petrides M, Jefferies E. Situating the default-mode network along a principal gradient of macroscale cortical organization. *Proceedings of the National Academy of Sciences*. 2016; 113:12574–9
2. Pearlson GD, Petty RG, Ross CA, Tien AY. Schizophrenia: a disease of heteromodal association cortex?. *Neuropsychopharmacology*. 1996; 14:1–7
3. Nenning KH, Xu T, Schwartz E, Arroyo J, Woehler A, Franco AR, Vogelstein JT, Margulies DS, Liu H, Smallwood J, Milham MP. Joint embedding: A scalable alignment to compare individuals in a connectivity space. *Neuroimage*. 2020; 222:117232
4. Mesulam MM. From sensation to cognition. *Brain: a journal of neurology*. 1998; 121:1013–52

## P29 The effects of different preprocessing steps and cortical parcellations on diffusion MRI connectomics

Mehul Gajwani<sup>\*1,3</sup>, Stuart Oldham<sup>2</sup>, James Pang<sup>1</sup>, Aurina Arnatkevičiūtė<sup>1</sup>, Jeggan Tiego<sup>1</sup>, Mark Bellgrove<sup>1,3</sup>, Alex Fornito<sup>1</sup>

<sup>1</sup>Monash University, Turner Institute for Brain and Mental Health, School of Psychological Sciences, Melbourne, Australia

<sup>2</sup>Monash Children's Research Institute, Developmental Imaging, Melbourne, Australia

<sup>3</sup>Monash University, Monash Biomedical Imaging, Melbourne, Australia

\*Email: mehul.gajwani1@monash.edu

Recent years have seen a surge in the use of diffusion MRI to map connectomes in humans and other species. This has been paralleled by a similar increase in the number of options to pre-process and analyze the data, but the effects of the different pre-processing and analysis steps on the resulting connectome are rarely compared systematically. Here, in a healthy adult population ( $n=294$ ), we characterize the impact of a broad range of analysis pipelines on one widely studied property of the human connectome; its degree distribution. We identified three key steps (streamline seeding, propagation constraint, and tractography reconstruction) and the associated options in the processing of diffusion MRI [1] and used these to generate 10 different pipelines. The effects of these pipelines – in conjunction with 4 parcellations [2–4], 5 group reconstruction regimes, and 11 reconstruction thresholds – on highly connected regions (so called ‘hubs’) were then evaluated. We find that hub location is highly variable between parcellation schemes (Fig. 1) and pipelines. The location of highly connected nodes can vary between frontal, parietal, or occipital areas depending on the parcellation used (with pre-processing options fixed; Fig. 1A). Similarly, a change in pipeline (whilst using a given parcellation) can likewise affect the location of hubs, largely based on the choice of deterministic or probabilistic tractography. Furthermore, hub connectivity is highly correlated with regional surface area in many of the assessed pipelines ( $\rho > 0.70$  in 69% of pipelines; Fig. 1B), particularly when using weighted networks. Unweighted network analysis has its own drawbacks, resulting in degree distributions that highly depend on the thresholding density, or have negative skewness (which are less biologically plausible). Overall, our results demonstrate the need for prudent decision making when processing diffusion MRI data, and for significant caution in the interpretation of findings where putative connectivity differences may (instead) be largely driven by inter-regional anatomical variation.

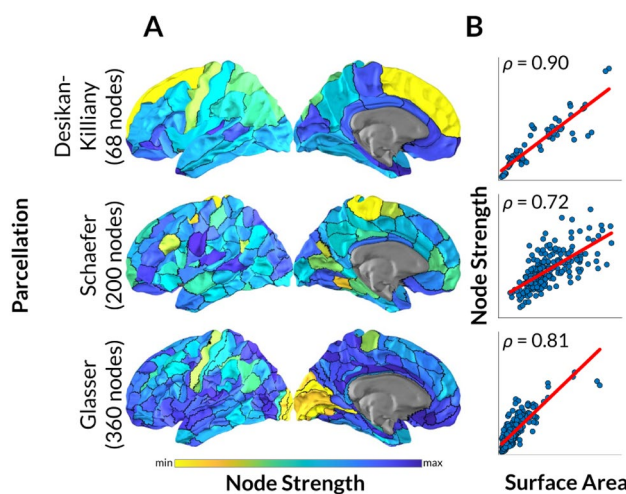


**Fig. 1** The effect of cortical parcellation on node strength. For an example pipeline using grey-white masking, dynamic seeding, and deterministic tractography, node strength (A) and correlation with surface area (B) are shown in three different parcellations

#### Acknowledgements

This work was supported by the National Health and Medical Research Council (ID: 1050504) and Sylvia and Charles Viertel Charitable Foundation.

#### References

- Oldham, S. et al. The efficacy of different preprocessing steps in reducing motion-related confounds in diffusion MRI connectomics. *NeuroImage*. 2020; 222: 117252
- Desikan, R. S. et al. An automated labeling system for subdividing the human cerebral cortex on MRI scans into gyral based regions of interest. *NeuroImage*. 2006; 31: 968–980.
- Glasser, M. F. et al. A multi-modal parcellation of human cerebral cortex. *Nature*. 2016, 536, 171–178.
- Schaefer, A. et al. Local–Global Parcellation of the Human Cerebral Cortex from Intrinsic Functional Connectivity MRI. *Cereb. Cortex*. 2018; 28: 3095–3114.

#### P30 Cortical geometry explains diverse patterns of brain activity

James Pang<sup>\*1</sup>, Kevin Aquino<sup>2</sup>, Alex Fornito<sup>1</sup>

<sup>1</sup>Monash University, Turner Institute for Brain and Mental Health, School of Psychological Sciences, Clayton, Australia

<sup>2</sup>University of Sydney, School of Physics, Sydney, Australia

\*Email: james.pang1@monash.edu

Several neuroimaging studies have explored how brain function is constrained by its underlying structure and anatomy. Attempts to understand this structure–function coupling have mostly focused on finding associations between the profiles of structural connectivity (i.e., strength of connections between regions derived from diffusion MRI) and functional connectivity (i.e., coordinated fluctuations between regions derived from functional MRI) [1]. However, such univariate analysis cannot fully explain the mechanisms of how the brain can flexibly produce diverse brain dynamics. Here, we ask whether the geometry of the human cortex can explain the emergence of diverse patterns of cortical activity (from task-evoked to spontaneous).

We derived the shape harmonics of the human cortical surface mesh from a population-averaged template (Fig. 1A left). Specifically, we solved the eigenvalue problem  $\Delta f = -\lambda f$  [2], where  $\Delta$  is the Laplace–Beltrami operator,  $\lambda$  is the eigenvalue, and  $f$  is the eigenmode. The eigenvalues are ordered from low to high values and proportional to the eigenmodes’ spatial frequency. Moreover, the eigenmodes are orthogonal and form a full basis set of the spatial profiles of cortical shape, similar to Fourier analysis harmonic modes. Hence, shape harmonics yield a multiscale description of how the geometry of the cortex varies in space (Fig. 1A).

We then used the shape harmonics to reconstruct task-evoked and resting-state data of 250 healthy subjects from the Human Connectome Project (HCP) [3]. For the task-evoked data, we extracted activation maps for 47 different task contrasts. For the resting-state data, we constructed functional connectivity using the HCP-MMP1 parcellation. Figure 1B shows that using 200 modes, shape harmonics can reconstruct the data with high accuracy (data vs reconstruction correlations  $> 0.9$ ). We then evaluated whether the same reconstruction accuracy can be achieved when the complex topology of the brain’s structural connectivity is accounted for or when a data-driven approach is used. Thus, we compared the performance of shape harmonics with the basis sets formed by connectome harmonics (from the graph Laplacian of structural connectome [4]) and principal component analysis (PCA) of the data themselves. Figure 1C shows that the reconstruction accuracy improves as more modes/components are used. Critically, after at least 50 modes, shape harmonics is consistently superior to other competing methodologies in explaining brain activity data.

In summary, we have shown that the geometry of the human cortex can successfully explain diverse aspects of brain function, providing strong

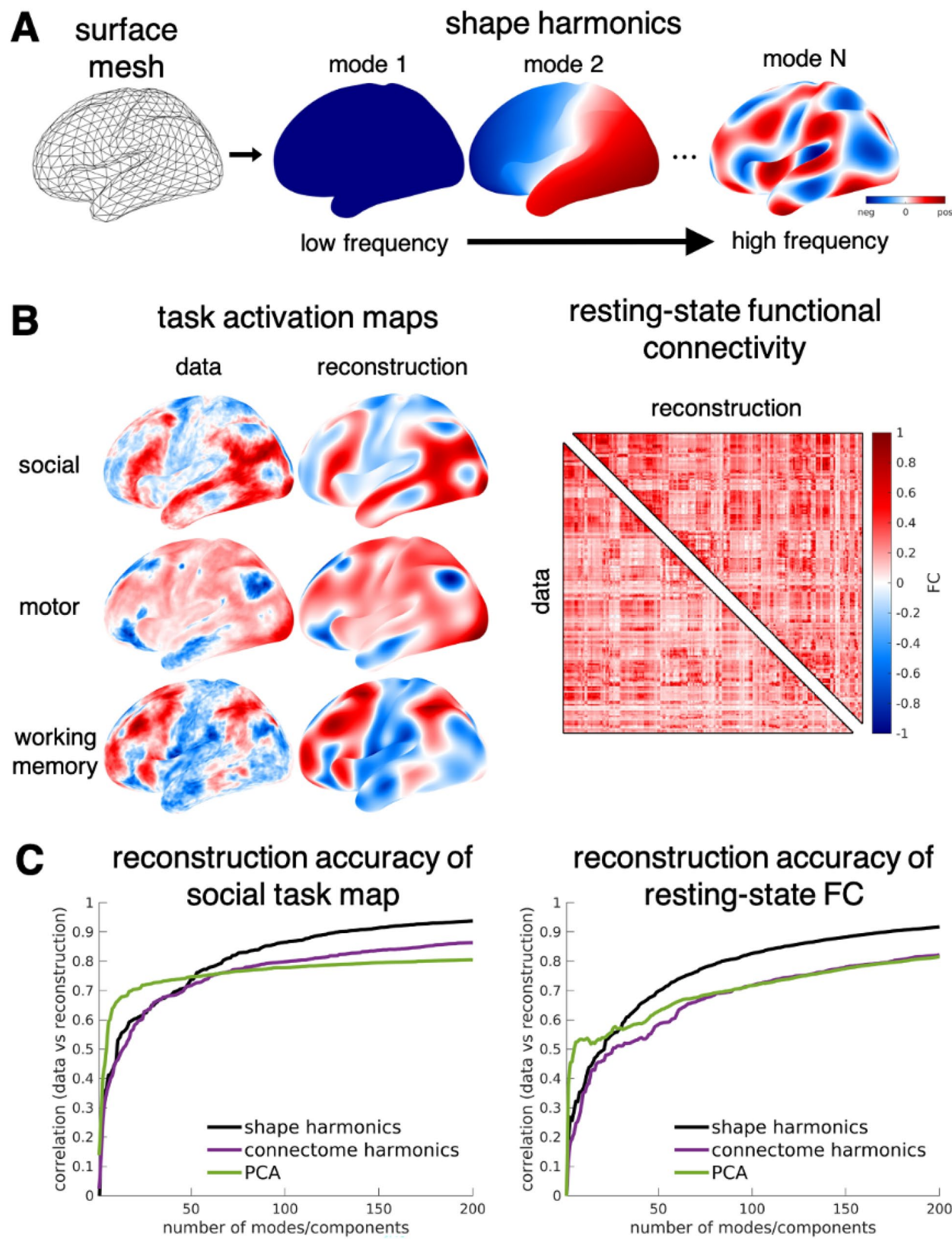


**Fig. 1** **A** Shape harmonics eigenmodes with low to high spatial frequency derived from the cortical surface mesh. **B** Shape harmonics reconstruction of task activation maps and resting-state func-

tional connectivity. **C** Comparison of reconstruction accuracies with increasing number of modes of basis sets: shape harmonics, connectome harmonics, and data-driven PCA

mechanistic evidence for the tight structure–function coupling in the brain. From a methodological point of view, shape harmonics offer a simple, robust, and anatomically-based basis set for explaining data without the need for more complex data and/or algorithms.

## References

- Honey CJ, et al. Predicting human resting-state functional connectivity from structural connectivity. *Proceedings of the National Academy of Sciences of the U.S.A.* 2009; 106(6): 2035–2040.
- Wachinger C, et al. BrainPrint: A discriminative characterization of brain morphology. *NeuroImage*. 2015; 109: 232–248.
- Van Essen DC, et al. The WU-Minn Human Connectome Project: An overview. *2013*; 80: 62–79.
- Atasoy S, et al. Human brain networks function in connectome-specific harmonic waves. *Nature Communications*. 2016; 7: 10340.

## P31 Mode-based morphometry: a new approach to mapping human neuroanatomy

Trang Cao<sup>\*1</sup>, James Pang<sup>1</sup>, Kevin Aquino<sup>2</sup>, Yu-Chi Chen<sup>1</sup>, Alex Fornito<sup>1</sup>

<sup>1</sup>Monash University, The Turner Institute for Brain and Mental Health, School of Psychological Sciences and Monash Biomed, Clayton, Australia

<sup>2</sup>University of Sydney, School of Physics, Sydney, Australia

\*Email: trang.cao@monash.edu

Cortical thickness (CT) has been studied extensively to investigate neuroanatomical variations between groups, such as differences between sexes, through development, or between psychiatric and neurological patients and healthy people. These analyses are typically performed at the level of individual surface vertices or a priori-defined regions-of-interest, thus defining a specific spatial resolution scale at which anatomical differences are examined. Here, we develop a new approach for mapping CT differences between groups that relies on the eigen-decomposition of the Laplace–Beltrami Operator of the cortical surface [1]. The resulting eigenmodes represent an orthonormal basis set of spatial patterns, ordered by wavelength, that can be used to obtain a multi-scale characterization of diverse brain maps (Fig. 1A). We leverage this property to model CT differences between two groups as linear combinations of eigenmodes, which allows us to identify characteristic

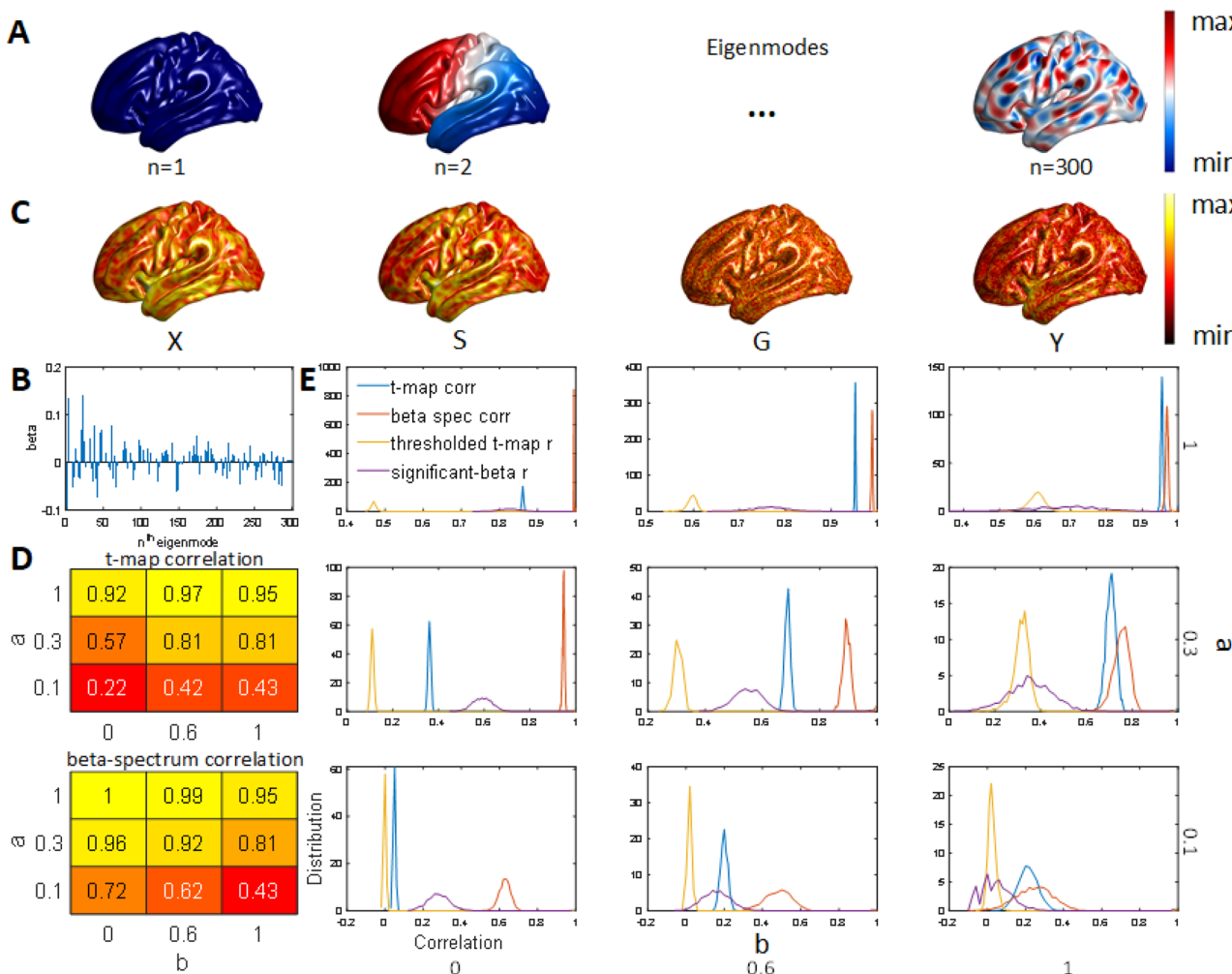


**Fig. 1** **A** Eigenmodes ordered by wavelength. **B** Example beta (coefficient) spectrum obtained from eigenmodes with a GLM. **C** Example model maps of X, S, G, and Y with coefficients a and b equal to 1 and 0.1, respectively. **D** Mean of the correlation between the t-map/

beta-spectrum of each simulation and the ground-truth CT difference. **E** Distributions of the correlations between simulated results and the ground truth across simulation runs

spatial scales of neuroanatomical variation through the resulting beta (coefficient) spectrum (Fig. 1B). To validate the approach, we develop a model with a known ground truth. We assume that a CT map of a subject in each group ( $Y$ ) is a linear combination of a group-specific map ( $X$ ), an individual-specific noise map ( $S$ ), and noise resulting from measurement errors ( $G$ ). In the model, the coefficient  $a$  controls the contribution of the group-specific CT phenotype,  $X$ , and the coefficient  $b$  controls the relative contributions of structured noise,  $S$ , and Gaussian noise,  $G$  (Fig. 1C). We sample  $X$  and  $S$  from CT maps of participants of the Human Connectome Project (HCP) [2] to ensure that they have the same spatial structure as real data. For each pair of  $a$  and  $b$ , we run 200 simulations. We simulate two experimental groups and study the resulting CT maps using a classical t-statistic vertex-based analysis and our mode-based morphometry (MBM) approach. To quantify the accuracy of each method with respect to the ground truth, we use the correlation between the t-map of each run and the ground-truth CT difference for the classical analysis; and between the beta spectra of the two difference maps for MBM (Fig. 1D). To evaluate sampling variability across simulations, we compare the distributions of correlations between t-maps, correlations between beta spectra, binary correlations (denoted by  $r$ ) [3] between thresholded t-maps, and binary correlations between statistically significant beta spectra identified through permutation testing (Fig. 1E). Figures 1 D-E show that our approach performs better when there is proportionally more structured than Gaussian noise ( $b \sim 1$ ) and significantly better when Gaussian noise is more dominant ( $b \sim 0$ ), especially, when the ratio between the ground truth and noise is small ( $a \sim 0.1$ ,  $b \sim 0$ ). Our results show that MBM is a more robust and accurate approach to mapping neuroanatomical variability than classical approaches and can identify characteristic spatial scales of such variations.

## References

1. Reuter, M., et al. Laplace–Beltrami eigenvalues and topological features of eigenfunctions for statistical shape analysis. Computer Aided Design. 2009; 41: 739–755.
2. Van Essen, D.C., et al. The Human Connectome Project: a data acquisition perspective. Neuroimage. 2012; 62: 2222–31.
3. Arnatkeviciute, A., et al. Hub connectivity, neuronal diversity, and gene expression in the *Caenorhabditis elegans* connectome. PLoS Computational Biology. 2018; 14: e1005989.

## P32 Disinhibition of muscarinic modulated potassium channels in a hippocampal CA1 model reproduces memory impairment observed in vivo

Dechuan Sun<sup>1,2</sup>, Ranjith Rajasekharan Unnithan<sup>2</sup>, Chris French<sup>\*3</sup>

<sup>1</sup>The University of Melbourne, Melbourne Medical School, Melbourne, Australia

<sup>2</sup>The University of Melbourne, Department of Electrical and Electronic Engineering, Melbourne, Australia

<sup>3</sup>The University of Melbourne, Department Medicine, Melbourne, Australia

\*Email: frenchc@unimelb.edu.au

The hippocampus and associated cholinergic inputs are important for neuronal function in memory, and cholinergic transmission at muscarinic acetylcholine receptors (mAChR) has been proposed to play critical roles [1]. Administration of muscarinic agonists is known to impair memory in animals and humans which has been ascribed to effects on neuronal network behavior. Although the role of mAChRs in

memory is not completely understood, it is likely that ion channels are a major substrate. Previous studies have discovered that mAChRs modulate various potassium channels [2], including muscarine sensitive “M currents” that strongly affect neuronal action potential threshold and repetitive firing. Thus, alteration of individual neural dynamics through modulation of potassium channels might impact memory by altering neuronal firing patterns and/or disrupting synchronization of the neural network. Here, we present a conductance based hippocampal model that reproduces our *in vivo* observations of scopolamine on place cell properties by varying M current amplitude.

## Results and methods

We first tested the effect of scopolamine on spatial memory of mice by observing the activity of place cells, which are hippocampal pyramidal neurons that activate in response to position. Mice were trained to traverse a familiar linear track and calcium activity of hippocampal neuronal populations was recorded using a miniaturized fluorescence microscope. Scopolamine significantly impaired neural dynamics with a decreased neural firing rate, and reduced number of place cells. We also measured spatial information content to quantify the precision level of neural coding. Scopolamine severely disrupted the precision level, reducing information content. Additionally, there was greatly increased variability of neuronal activity in observed neurons, both in place fields and surrounding areas.

We sought to reproduce these observations through modeling the scopolamine effect by increasing the amplitude of the M current in pyramidal cells and interneurons in a conductance based CA1 network composed of 130 pyramidal neurons and several interneuron subtypes based on a previous model [3]. In particular, an M-channel conductance was included in interneuron channel repertoire. The effect of scopolamine was modeled by increasing the M-channel total conductance of pyramidal cells and interneurons. Using this simple model strategy, remarkably the experimental results were reproduced.

In conclusion, we find that the prominent reduction of place cell numbers and impairment of spatial sensitivity is reproduced in a conductance based hippocampal circuit model by simple alteration of a potassium current amplitude. Although there are almost certainly other factors involved, these modeling results suggest a significant role of a voltage-gated potassium channel in producing the well-studied amnesic effects of scopolamine.

## References

1. Hasselmo. The role of acetylcholine in learning and memory. Current Opinion in Neurobiology. 2006; 16: 710–715.
2. Buchanan, Petrovic, Chamberlain, et al. Facilitation of long-term potentiation by muscarinic M1 receptors is mediated by inhibition of SK channels. Neuron. 2010; 68(5): 948–963.
3. Turi, Li, Chavlis, et al. Vasoactive intestinal polypeptide-expressing interneurons in the hippocampus support goal-oriented spatial learning. Neuron. 2019;101: 1150–1165.e1158.

## P33 Is catastrophic forgetting Bayes-optimal?

Noor Sajid<sup>\*1</sup>, Laura Convertino<sup>1</sup>, Victorita Neacsu<sup>1</sup>, Thomas Parr<sup>1</sup>, Karl Friston<sup>2</sup>

<sup>1</sup>University College London, Wellcome Centre for Human Neuroimaging, Queen Square Institute of Neurology, London, United Kingdom

<sup>2</sup>University College London, London, United Kingdom

\*Email: noor.sajid.18@ucl.ac.uk

Humans exploit highly complex cognitive processes that are apt for acquiring new knowledge, whilst protecting the old. However, under

specific circumstances, humans can disregard old for new information, i.e., exhibit catastrophic forgetting. In this paper, we pursue the notion that catastrophic forgetting is a misnomer and should be considered Bayes-optimal. For this, we commit to the Bayesian brain hypothesis, and related active inference theory, to categorise catastrophic forgetting as simply the internal (generative) model updating to best explain observations and minimise free energy (or maximise model evidence). Accordingly, any apparent failure or sub-optimality is defined relative to a generative model – and may be better explained as optimality under an appropriate model. Under this framework, we also establish that a Bayes-optimal arbitration between synaptic stability and plasticity ensures that information that does not affect the ability to make apt inferences is forgotten, whereas relevant information is not. We then illustrate the Bayes-optimal nature of catastrophic forgetting, the temporal and hierarchical separation of the generative model updates, and how they preserve the stability-plasticity constraint during the learning of a language identification task. These analyses suggest that catastrophic forgetting is a Bayes-optimal response to environmental changes that alters the structure of the generative model – mediated by parameter and structural learning in the brain.

#### P34 Characterizing schizophrenia neural dynamics using univariate time-series feature analysis

Annie Bryant<sup>\*1</sup>, Kevin Aquino<sup>2</sup>, Linden Parkes<sup>3</sup>, Trent Henderson<sup>1</sup>, Preethom Pal<sup>3</sup>, Adithya Vignaraja<sup>1</sup>, Alex Fornito<sup>3</sup>, Ben Fulcher<sup>1</sup>

<sup>1</sup>The University of Sydney, School of Physics, Sydney, Australia

<sup>2</sup>University of Sydney, School of Physics, Sydney, Australia

<sup>3</sup>Monash University, The Turner Institute for Brain and Mental Health, School of Psychological Sciences, Monash University, Clayton, Australia

\*Email: abry4213@uni.sydney.edu.au

Functional magnetic resonance imaging (fMRI) offers a window into region-specific neural dysfunction in disease based on the time series of blood oxygen level-dependent (BOLD) signaling. For example, recent studies comparing BOLD signals in individuals with schizophrenia versus cognitively healthy control subjects report high classification accuracies, largely using functional connectivity and/or deep learning methods<sup>1</sup>. Despite strong classification metrics, such approaches generally miss region-specific local dynamics and lack biologically interpretable insights due to their black-box nature.

Modern methods in univariate time-series feature extraction<sup>2</sup> enable the analysis of BOLD neural dynamics at the level of individual brain regions, offering both biological insight and classification abilities. To that end, here we present a systematic analysis combining diverse linear and nonlinear univariate time-series features<sup>3</sup> derived from BOLD signals in an open fMRI dataset of individuals with ( $N = 50$ ) and without ( $N = 121$ ) schizophrenia<sup>4</sup>. We investigated classification performance (using a linear support vector machine) across three distinct settings: (i) individual brain regions (across all time-series properties,  $N = 22$ ); (ii) individual time-series features (across all brain regions,  $N = 82$ ); and (iii) the combination of all regions and time-series features ( $N = 1,804$  combinations).

We report cross-validated classification accuracies of up to 72% using a single brain region with all 22 time-series features, up to 68% using a single time-series feature with all 82 brain regions, and up to 67% using the combination of all regions and time-series features (Fig. 1). This highlights the importance of examining region-specific BOLD dynamics (e.g. first local minimum of the autocorrelation function) to understand locally dysregulated neural activity in schizophrenia.

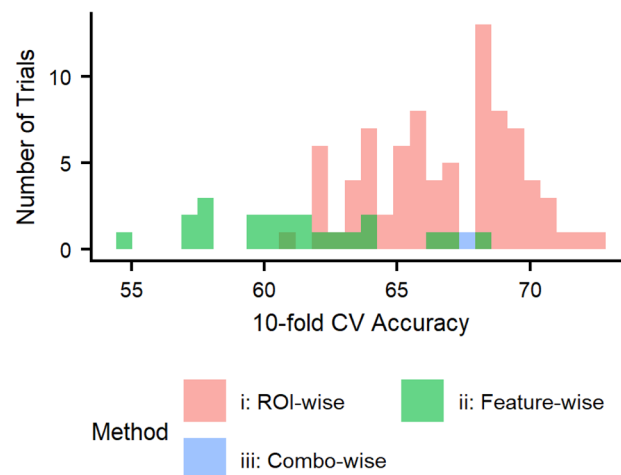


**Fig. 1** Distribution of tenfold CV accuracy for each of the three settings

Our findings demonstrate that systematically quantifying the dynamics of individual brain regions is a promising way of understanding how distributed brain activity is disrupted in neurological disease.

#### References

- Quaak, M., van de Mortel, L., Thomas, R. M. & van Wingen, G. Deep learning applications for the classification of psychiatric disorders using neuroimaging data: Systematic review and meta-analysis. *NeuroImage Clinical*. 2021; 30:102584
- Henderson, T. & Fulcher, B. D. An Empirical Evaluation of Time-Series Feature Sets. In: 2021 International Conference on Data Mining Workshops (ICDMW). 2021; 1032–1038
- Lubba, C. H. et al. catch22: Canonical Time-series Characteristics. *Data Mining and Knowledge Discovery*. 2019; 33, 1821–1852
- Gorgolewski, K. J., Durnez, J. & Poldrack, R. A. Preprocessed Consortium for Neuropsychiatric Phenomics dataset. 2017

#### P35 A feature-based transfer entropy approach to detect large-scale interactions in neural systems

Aria Nguyen<sup>\*1</sup>, Oliver Cliff<sup>2</sup>, Joseph Lizier<sup>2</sup>, Ben Fulcher<sup>1</sup>

<sup>1</sup>The University of Sydney, School of Physics, Sydney, Australia

<sup>2</sup>The University of Sydney, Centre for Complex Systems, Sydney, Australia

\*Email: aria.mt.nguyen@gmail.com

Quantifying relationships between elements of complex systems is critical to understanding their distributed dynamics. Many methods to infer dependencies between pairs of time series exist, such as Pearson correlation and transfer entropy [1], where the measure of dependency is calculated directly from time-series data. But in many systems the elements interact in complex ways on different timescales, making it challenging to learn and interpret statistical relationships directly from the time-series values using model-free, data-driven approaches.

A promising alternative involves transforming local segments of a time series into interpretable dynamical summary statistics, or ‘features’. In this work, we introduce a feature-based adaptation of conventional

statistical pairwise dependence methods, demonstrating that using the dynamics of time-series features can substantially increase the sensitivity and interpretability of pairwise inference in simulated and experimental data.

We demonstrate our method using the *thecatch22* set of 22 time-series features [2], using a given feature and window length of the source to define the response of the target. We use transfer entropy to measure dependencies between raw source and target data, and features of source and target data.

In simulation studies, we simulated interactions between processes governed by stochastic, autoregressive, and nonstationary oscillations, with time-series features of the ‘source’ dynamics influencing the ‘target’ dynamics. We first used an empirical null-testing procedure to verify that our statistical testing framework correctly controls for false positives across the multiple feature comparisons. We then investigated how interaction timescales and time-series length affect the sensitivity of inferring true underlying interactions. For example, for 1000-sample time series, the feature-based transfer entropy measurement captures 99.53% of true interactions, while the measurement computed on the raw source and target data only captures 50% of cases. Feature-based inference also requires far shorter time-series lengths, with robust performance down to just 50 observations, while 5000 observations are needed to achieve similar performance using the conventional method. We applied the method to a mouse fMRI dataset, demonstrating its ability to detect and interpret distributed relationships across the mouse brain, with potential applications for a diverse multivariate neural time series.

In summary, we have developed an efficient and sensitive method for detecting and understanding dependencies in complex dynamical systems by combining information-theoretic estimators with extracted time-series features. When interactions are mediated by properties of the dynamics, our method can efficiently detect dependencies between time series that are far shorter, and on longer timescales, with greater noise robustness than conventional model-free approaches. We anticipate this method being useful for many applications involving the characterization of dynamic interactions underlying neural systems.

## References

- Edinburgh T, et al. Causality indices for bivariate time series data: a comparative review of performance. *Chaos: An Interdisciplinary Journal of Nonlinear Science*. 2021.
- Lubba C, et al. *catch22*: Canonical time-series characteristics: Selected through highly comparative time-series analysis. *Data Mining and Knowledge Discovery*. 2019.

## P36 Summarizing non-stationarity in spatio-temporal neural data

Brendan Harris<sup>\*1</sup>, Ben Fulcher<sup>1</sup>

<sup>1</sup>The University of Sydney, School of Physics, Sydney, Australia

\*Email: bhar9988@uni.sydney.edu.au

Uncovering the patterns buried in high-dimensional spatio-temporal data is vital for investigating how environmental parameters translate to complex neuronal activity. Standard methods of dimensionality reduction excel at finding global low-dimensional structure, but do not provide crucial fine-grained information about how the dynamics of individual neural elements change over time. As an alternative, univariate time-series features measure the dynamical properties of local neural elements, but most assume stationary data in which dynamical properties are constant. We present a new method that combines time-series features with dimensionality reduction to produce interpretable, time-resolved summaries of non-stationary data. By exploiting the

correspondence between parameters and dynamics [1], we are then able to infer the parametric variation underlying non-stationarity in complex neural dynamics.

Our method (Fig. 1) first applies feature extraction [2] to windows of a time series, yielding a feature matrix that measures dynamical properties across time. We then infer parametric variation by applying dimensionality reduction to the feature matrix, extracting the trajectory of local time-series windows through a low-dimensional feature space. To ensure our feature-space embedding is unbiased with respect to feature-feature dependencies, we also developed an extension to PCA that generates orthonormal features by examining the dependency structure of a controlled, baseline, dataset. We verified our methods are able to accurately track non-stationarity and the underlying variation in ground-truth parameters using an extensive variety of simulated dynamical systems (correlations from 0.9 to 1.0).

We then investigated neural responses to visual stimuli by applying our method to the Allen Neuropixels dataset, a spatio-temporal set of electrophysiological recordings from the mouse brain [3]. As a visual stimulus changes over time, our method automatically reveals channels that transition between states with distinct patterns of activity. In a single subject, we are able to temporally resolve the dynamical regimes of regions such as the primary visual cortex and lateral posterior nucleus, which include slow, periodic theta oscillations and higher-frequency broadband fluctuations, without aggregating local readings over imposed anatomical divisions (as required by most conventional methods).

Our new method has further advantages over conventional approaches to dimensionality reduction: i) it does not require phase-synchronized time series; ii) it produces an informative low-dimensional representation of complex dynamics, resolved over space and time; and iii) it can be directly interpreted in terms of the dynamical properties encapsulated by each feature, without the need to identify a model for the underlying system. Our approach can be applied to many forms of spatio-temporal neural data to understand how the dynamics of neural components respond to changes in the environment.

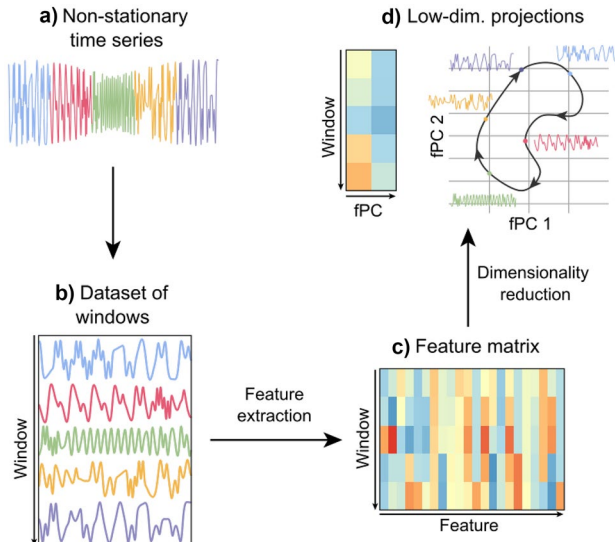


**Fig. 1** A schematic of our method. We divide a non-stationary time series (a) into pseudo-stationary windows (b), before summarizing the dynamical properties of each window in a feature matrix (c). Finally, we use dimensionality reduction on the feature matrix to represent the time series as a low-dimensional trajectory through feature space that corresponds to variation in the underlying parameters (d)

## References

- Güttler S, Kantz H, and Olbrich E. Reconstruction of the parameter spaces of dynamical systems. *Physical Review E*. 2001; 63: 056215
- Fulcher BD, Little MA, and Jones NS. Highly comparative time-series analysis: the empirical structure of time series and their methods. *Journal of the Royal Society Interface*. 2013; 10: 20130048
- Siegle JH, Jia X, Durand S, et al. Survey of spiking in the mouse visual system reveals functional hierarchy. *Nature*. 2021; 592: pp. 86–92.

### P37 Bayesian model-based strategies in spatial location tasks: is there knowledge transfer?

Chin-Hsuan Sophie Lin<sup>\*1</sup>, Trang Thuy Do<sup>1</sup>, Lee Unsworth<sup>1</sup>, Marta I. Garrido<sup>1</sup>

<sup>1</sup>The University of Melbourne, Melbourne School of Psychological Sciences, Melbourne, Australia

\*Email: chinhuan.sophie.lin@gmail.com

People make decisions under uncertainty by integrating their knowledge of the world (i.e. priors) with current sensory evidence (i.e. likelihood) based on their respective reliabilities in a Bayesian fashion [1]. However, it has been hotly debated whether optimal behaviors in humans are achieved by precise but exhaustive Bayes computations [2]. Behaviorally we can validate the use of explicit Bayes model by testing people's ability to instantaneously reach optimal performance when encountering learnt elements in a new context, a test called Bayesian transfer [3]. In two transfer experiments, we manipulated one cognitive factor at a time to better pinpoint whether exact Bayesian strategies are used in decision making.

Participants estimated hidden target locations drawn from Gaussian priors with different variances. In each trial, scattered dots sampled from Gaussian distributions provided likelihood information about target locations. After priors were learnt, participants encountered transfer conditions that paired trained priors with new likelihoods different from ones paired with priors in the training phase. In experiment 1, we manipulated the working memory load, such that one group of participants learnt two priors simultaneously (harder) and the other learnt the same priors serially (easier). We hypothesized that simultaneous learning requires a higher working memory capacity and would promote (less computationally demanding but suboptimal) non-Bayes strategies. In experiment 2, we compared situations where integrating one learnt prior with a new likelihood that was either within (interpolation) or outside (extrapolation) the range of their previous experience. We hypothesized that only explicit Bayesian observers would perform optimally in both interpolation and extrapolation conditions.

In exp 1, we found working memory load per se did not affect performance. Both high (simultaneous) and low (serial) cognitive demand groups showed equal levels of reliability-based weighting in the training and transfer phase, i.e. Bayesian transfer. Interestingly, participants consistently underweighted priors, irrespective of experimental phases and memory loads, as if priors were more variable than they truly were. In exp 2, participants demonstrated Bayesian transfer and optimal reliability-weighting in both interpolation and extrapolation conditions. We found evidence of Bayesian transfer, which supported the use of exact Bayesian model in both experiments. However, we observed optimality only when one prior was used (exp 2). When tasks involved learning multiple priors (exp 1), it may be too challenging for the learning of prior parameters to complete within experiments. Subjective prior uncertainty was thus higher than objective uncertainty (i.e.

the variances of priors) and therefore participants demonstrated prior under-weighting in behaviors.

## Acknowledgements

We thank the Australian Research Council Centre of Excellence for Integrative Brain Function for supporting MG and CSL (ARC Centre Grant CE140100007) and the University of Melbourne (2021ECR104) for supporting CSL.

## References

- Ma WJ., Bayesian Decision Models: A Primer. *Neuron*. 2019; 104: p.164–175
- Bowers JS, Davis CJ., Bayesian Just-So Stories in Psychology and Neuroscience. *Psychological Bulletin*. 2012; 138: p.389–414
- Maloney LT, Mamassian P., Bayesian decision theory as a model of human visual perception: Testing Bayesian transfer. *Visual Neuroscience*. 2009; 26: p.147–155

### P38 Mini EPSC analysis of synaptic integration to inform a Drosophila motor circuit model

Cengiz Gunay<sup>\*1</sup>, Patrick Del Rio<sup>2</sup>, Ekechi Nzewi<sup>1</sup>, Caleb Gebremeskel<sup>2</sup>

<sup>1</sup>Georgia Gwinnett College, School of Science and Technology, Lawrenceville, GA, United States of America

<sup>2</sup>Gwinnett School of Mathematics, Science, and Technology, Lawrenceville, GA, United States of America

\*Email: cengique@users.sf.net

Seizure disorders often exhibit motor symptoms. Fruit fly (*Drosophila*) offers an attractive model system to study motor systems because of established electrophysiological access to motor neurons and the availability of bang-sensitive seizure mutants. We are targeting to quantify changes in motor circuits of seizure mutants by analyzing synapses incoming to one motor neuron, aCC, in wildtype versus bang-senseless (bss) mutants. Changes that could be happening at pre-motor or motor neurons (pre- or post-synaptic sites, respectively) are parameters for vesicle pool size, quanta size, and frequency of release and absorption. To explore parameters and mechanisms of synaptic input change, we constructed a computer model of the aCC motoneuron at the first instar developmental stage [1]. This stage was chosen because of the available electron micrograph connectomics data that showed synapses incoming to aCC from different pre-motor interneurons. We developed two scripts in Python to identify and position synapses from different neurons. One script reads CSV files exported from CATMAID and converts them to SWC format that can be imported into the Neuron Simulator and also produces several additional CSV files. It uses different data structures including dictionaries, tuples, and lists to store specific information about the different neurons and their various synapses to be used in the Neuron simulation. The SWC file is manually imported into Neuron and an SES file export is made before running a second script to initialize the simulation. The second script initializes the simulation by importing the Python module of Neuron, loading the pre-generated SES file, and then reading the newly generated CSV files to create synapse objects attached to the correct morphological sections. The simulation still needs biological parameters to simulate synaptic inputs. Synaptic inputs were previously analyzed to quantify changes in spontaneous rhythmic current (SRC) inputs to aCC. We hypothesize that an SRC results from neurotransmitters causing several excitatory post-synaptic currents (EPSCs) and combining on the membranes of the neuron's dendrites [2]. In this study, we went one

more step to decompose each EPSC into one or more released neurotransmitter vesicles arriving at receptors on the postsynaptic membrane. Each vesicle causes one mini-EPSC (“mini”), or “quantal” event. To create models of minis, we observed spontaneous minis released when spiking was blocked via tetrodotoxin (TTX) only in wildtype fruit flies. Observing them from soma, minis exhibit different magnitudes. To measure these magnitudes, we developed scripts using the Pandora toolbox in MATLAB and analyzed the recordings. These scripts performed tasks such as filtering, normalization, and thresholding because the recordings were unsuitable for data analysis in their original form. By analyzing the mini structure, we aim to guide the simulations so we can compare changes in seizure mutants. We present results showing effects of simulated activity in several identified pre-motor neurons and discuss their relevance.

## References

1. Massaquoi BR, Gunay C. Investigating impact of synaptic inputs in seizure models. CNS\*2018, Seattle, WA. July 13, 2018.
2. Vu JK, Sugatapala DC, Gunay C. Motoneuron synaptic currents in a Drosophila seizure mutant. Program No. 066.06. 2019 Chicago, IL: Society for Neuroscience, 2019.

## P39 Modulation of dynamical interareal communication and visual attention

Shencong Ni<sup>\*1</sup>, Pulin Gong<sup>1</sup>

<sup>1</sup>The University of Sydney, School of Physics, Sydney, Australia

\*Email: shni2598@uni.sydney.edu.au

Brain functions fundamentally rely on communication between different brain areas, but the mechanism of interareal communication remains unclear. In this study we develop a large-scale circuit model consisting of a sensory area and an association area. We first demonstrate that localized activity patterns with complex propagating dynamics emerge from the circuit can account for a variety of neural response properties, including gamma oscillations and normalization. The localized patterns in the sensory and association area can have transient synchronization. We find that these synchronized patterns form a low-dimensional communication subspace, thus unifying the synchronization-based and subspace-based views of cortical communication. We further illustrate that such pattern-based communication is modulated during attention tasks, and that the modulation process can account for key neural effects of attention such as reduction of firing rate variability and noise correlations.

## P40 Computational modelling of optic flow sensitive neurons in the dragonfly

Edward Luong<sup>\*1</sup>, Benjamin Cazzolato<sup>2</sup>, Steven Grainger<sup>2</sup>

<sup>1</sup>The University of Adelaide, School of Biomedicine, Adelaide, Australia

<sup>2</sup>The University of Adelaide, School of Mechanical Engineering, Adelaide, Australia

\*Email: edward.luong@adelaide.edu.au

Insects make use of vision as an important source of sensory information for estimating self-motion and navigating their environment. Previous studies have reported on the properties of visual neurons sensitive to optic flow (wide field motion stimuli) in insects such as flies, moths

and bees. A recent electrophysiological study [1] was the first to characterize optic flow sensitive neurons in the dragonfly. The optic flow sensitive neurons in the dragonfly (termed lobula tangential cells or LTCs) exhibit novel properties not seen in other species. Optic flow neurons in other species typically show similar spatiotemporal and velocity tuning in response to drifting sinusoidal gratings and natural broadband imagery. In contrast, dragonfly LTCs can be grouped into clusters based on differential response to the same stimuli. LTC clusters show similar spatiotemporal and velocity tuning in the unadapted state but differential tuning in the motion adapted state. We propose two computational model variants to explain how such dynamic shifts in tuning may occur. One model proposes a dynamic delay time constant within the elementary motion detector stage of visual processing. The other proposed model is based on two parallel elementary motion detector pathways with different static delay time constants. We then address the question of the potential functions of the dragonfly LTCs. Our modelling demonstrates that the LTCs could function as a visual sensor measuring the angular velocity of the dragonfly. We also show that this sensor function could form part of a visuomotor feedback loop controlling angular velocity. We demonstrate the advantages of the dynamic differential velocity tuning in that it provides an unambiguous and extended range of measured velocities and produces more robust closed loop control.

## References

1. Evans BJE, O’Carroll DC, Fabian JM, Wiederman SD. Differential tuning to visual motion allows robust encoding of optic flow in the dragonfly. Journal of Neuroscience. 2019 October 9; 39(41):8051– 8063.

## P41 Using unlabelled self-supervised machine learning to reduce the amount of data required for seizure detection

Andisheh Partovi<sup>\*1</sup>, Farhad Goodarzy<sup>2</sup>, Anthony Burkitt<sup>1</sup>, David Grayden<sup>1</sup>

<sup>1</sup>The University of Melbourne, Department of Biomedical Engineering, Melbourne, Australia

<sup>2</sup>The University of Melbourne, Faculty of Medicine Dentistry and Health Sciences, Fitzroy, Australia

\*Email: apartovi@student.unimelb.edu.au

Machine Learning (ML) has proven to be a valuable tool in analyzing brain signals in Brain-Computer Interfaces and related tasks like seizure detection. However, one of the biggest challenges in using ML remains the lack of sufficient annotated data for supervised learning algorithms. There are computational methods that address data sparsity through the use of large amounts of unlabeled data, and they have gained popularity in image and audio analysis domains. In this research we have designed a self-supervised machine learning algorithm that when trained on large amounts of unannotated data, it can reduce the amount of labeled data required for supervised tasks. We have evaluated this method on the public seizure detection dataset of CHB-MIT, using large amounts of unlabeled EEG data we collected from Epilepsy patients.

Our self-supervised model is inspired by Pascual, Santiago, et al.’s PASE+ model [1], designed for audio processing. We have made a number of modifications to this model, namely changing the SincNet layer, the size of the embeddings, and the worker layers. We have also adapted the model to the multi-channel structure of EEG using the topological position of EEG electrodes in our montage. All models are trained up to 300 epochs with 32 batch size.

Our test dataset, the CHB-MIT dataset [2] is recorded from 23 pediatric patients with intractable seizures accepted at the Boston Children's Hospital. It is publicly available at PhysioNet's website for research. The montage used in this experiment is the International 10–20 System for electrode positioning in a bipolar configuration. The sample rate of the EEG is 256 Hz with a 16-bit depth. Trained specialists have annotated seizure events on this data. Due to the different channel numbers among these patients and to reduce the complexity of the task, we have decided to use the data from 10 patients. We studied 347 h of inter-ictal activity and 1 h of ictal activity from 51 annotated seizures.

The dataset we used to pre-train the embedding model is collected from 4 patients at the St Vincent's Hospital in Melbourne, Australia. The montage used in this experiment is also the International 10–20 System for 21 channels with the 256 Hz sample rate. We studied 286.1 h of inter-ictal activity and 7 min of ictal activity.

To evaluate our model, we trained a simple feedforward Convolutional Neural Network using a supervised training regime on the CHB-MIT dataset. We compared the results to an alternative which uses only a fraction of the CHB-MIT dataset but starts the training using the pre-trained self-supervised model trained on the St Vincent's data. In this comparison, we managed to reduce the amount of labeled data required to achieve the same level of performance to 20% of the original dataset. I.e. using only 20% of the training data in conjunction with the unsupervised training on another dataset achieved the same results as a full dataset.

This result indicates that we can reduce the amount of data required to train a supervised machine learning model significantly, by pre-training the model on large amounts of unlabeled data beforehand, even if the unlabeled data is from other subjects and acquired in different settings and with different technologies.

## References

1. Goldberger, A., Amaral, L., Glass, L., Hausdorff, J., Ivanov, P. C., Mark, R., & Stanley, H. E. PhysioBank, PhysioToolkit, and PhysioNet: Components of a new research resource for complex physiologic signals. *Circulation* [Online]. 2000; 101(23): e215–e220
2. Pascual, Santiago, et al. "Learning problem-agnostic speech representations from multiple self-supervised tasks". arXiv preprint. 2019; arXiv:1904.03416

## P42 An epileptic seizure prediction framework allowing for variable warning times

Jordan Chambers<sup>\*1</sup>, Mark Cook<sup>2</sup>, Anthony Burkitt<sup>1</sup>, David Grayden<sup>1</sup>

<sup>1</sup>University of Melbourne, Department of Biomedical Engineering, Melbourne, Australia

<sup>2</sup>University of Melbourne, Department of Medicine, Melbourne, Australia

\*Email: jordanc@unimelb.edu.au

Prediction of epileptic seizures can remove uncertainty and open the possibility of acute treatments for patients. However, individual patients require different warning times to remove uncertainty. Similarly, different acute treatments will also require different warning times to be effective. Currently, most seizure prediction systems are only capable of producing predictions based on assumptions regarding the optimal warning time. Attempts to alter the warning time often produce poor results because the features used to develop the model are unique to the initial warning time. Here, we developed a framework that can predict epileptic seizures with different warning times.

Electroencephalography (EEG) detects electrical activity in the brain and multiple observations produce a time series. To avoid feature engineering of the time series data, we used machine learning to process

the raw EEG data. Long-Short Term Memory (LSTM) neural networks are a type of machine learning architecture that can analyze time series data using recurrent connections. Our model comprised four LSTM layers separated by three average pooling layers. 10-s segments of raw EEG across 16 electrodes were fed into the LSTM models. The output of the final layer of LSTMs classified the EEG data in regards to the time before seizure. EEG data was obtained from long-term intracranial recordings of three patients from the NeuroVista dataset [1].

The LSTM models could classify raw EEG data for multiple labelling systems on unbalanced, unseen test data. For Patient 1, the LSTM models could provide a 1–24 h warning with sensitivity (S) of 52% and time in selectivity or warning (T) of 34% (> 5 times better S and = T compared to a random predictor), 15–75 min warning with 49% S and 15% T (> 100 times better S and > 2 times better T compared to a random predictor) and a 1–15 min warning with 47% S and 4% T (> 300 times better S and > 5 times better T compared to a random predictor). Preliminary results for two other patients indicate similar performance in terms of sensitivity across multiple warning times. The performance of this model is below the best published results using the same dataset [1–3] (for the same patient the best sensitivities are 65–83%), but direct comparison is difficult due to different warning times. None of the published models using the same dataset could change the warning times, which is the advantage of the current model.

LSTM models can process raw EEG data and classify it to produce seizure predictions. Using LSTMs to process raw EEG data can avoid feature engineering, thereby creating a method in which the seizure warning times can be easily varied while producing consistent results. The ability to change the warning times in this current model is an improvement on previous models, enables individual patients to meet their personal needs, and enables acute treatments with different time courses of action to be considered.

## References

1. Cook MJ, et al. Prediction of seizure likelihood with a long-term, implanted seizure advisory system in patients with drug-resistant epilepsy: a first-in-man study. *Lancet Neurology*. 2013; 12(6): 563–71.
2. Kiral-Kornek I, et al. Epileptic Seizure Prediction Using Big Data and Deep Learning: Toward a Mobile System. *EBioMedicine*. 2018; 27: 103–11.
3. Maturana MI, et al. Critical slowing down as a biomarker for seizure susceptibility. *Nature Communications*. 2020; 11(1): 2172.

## P43 The role of epidemic spreading in seizure dynamics and epilepsy surgery

Ana Millan<sup>\*1</sup>, Ida A Nissen<sup>1</sup>, Elisabeth C.W. van Straaten<sup>1</sup>, Cornelis J. Stam<sup>1</sup>, Sander Idema<sup>2</sup>, Johannes C. Baayen<sup>2</sup>, Piet Van Mieghem<sup>3</sup>, Arjan Hillebrand<sup>1</sup>

<sup>1</sup>Amsterdam University Medical Center, Clinical Neurophysiology and MEG Center, Amsterdam, Netherlands

<sup>2</sup>Amsterdam University Medical Center, Neurosurgery, Amsterdam, Netherlands

<sup>3</sup>Delft University Technology, Faculty of Electrical Engineering, Mathematics and Computer Science, Amsterdam, Netherlands

\*Email: a.p.millanvidal@amsterdamumc.nl

Epilepsy surgery is the treatment of choice for drug-resistant epilepsy patients, but only 2/3 of the patients are seizure-free (SF) one year after surgery [1]. Simulation of seizure dynamics and surgery on large-scale brain networks may help us improve outcome rates by finding resection strategies targeted for each patient [1–3]. However, modelling efforts

face significant conceptual and methodological problems, such as the choice of dynamical model, fitting and optimization algorithms. In order to simplify the modelling considerations, we have considered seizure propagation as a spreading process [2, 3]. Whilst too simplified to describe brain function, a spreading dynamics near criticality is sufficient to reproduce functional brain connectivity and information flow in the brain [4]. We developed an individualized seizure propagation model based on epidemic spreading that incorporated multi-modal patient-specific data, such as Magnetoencephalography (MEG), Diffusion Tensor Imaging (DTI) and invasive Electroencephalography (EEG) data. These data were used to construct the backbone networks for seizure propagation and to fit the model to the patient-specific seizure propagation patterns (see Fig. 1a,b). The model reproduced the seizure patterns for all patients ( $N=15$ ), with a significantly better fit for SF than non-SF patients, when using the resected area (RA) as the seed. Once fitted for each patient, the model was used to generate alternative hypotheses about the seizure onset zone (SOZ) by finding for each region the likelihood that it generated the observed seizures. RA regions were significantly more likely to start seizures than non-RA regions ( $\text{diff}=0.074, p=0.02$ ).

Finally, we simulated the effect of different resection strategies in the model. Using an optimization algorithm, we found that resections smaller than the RA but with similar predicted seizure reduction were possible by taking into account the patient's unique brain topology (Fig. 1c,d) [2, 3]. Moreover, when considering the ROIs with largest likelihood as seeds, we found that SF patients were more

likely to present a significant decrease in seizure propagation than non-SF patients after the surgery ( $\text{diff}=0.29, p=0.09$ ).

Our findings indicate that individualized epidemic spreading models may capture the fundamental aspects of seizure propagation, and can be used to generate alternative hypotheses about the SOZ. Resection strategies can be individualized in silico, with the goal of improving surgery outcome.

### Acknowledgements

APM and IAN were supported by ZonMw and the Dutch Epilepsy Foundation (n.95105006). The funding sources had no role in study design, data collection and analysis, or interpretation of results.

### References

1. Sinha, Dauwels, Kaiser, et al. Predicting neurosurgical outcomes in focal epilepsy patients using computational modelling. *Brain*. 2017; 140:319–332
2. Millán, van Straaten, Stam et al. Epidemic models characterize seizure propagation and the effects of epilepsy surgery in individualized brain networks based on MEG and invasive EEG recordings. *Scientific Reports*. 2022; 12:1–20
3. Nissen, Millán, Stam et al. Optimization of epilepsy surgery through virtual resections on individual structural brain networks. *Scientific Reports*. 2021; 11:1–18
4. Stam, van Straaten, van Dellen et al. The relation between structural and functional connectivity patterns in complex brain networks. *International Journal of Psychophysiology*. 2016; 103:149–160

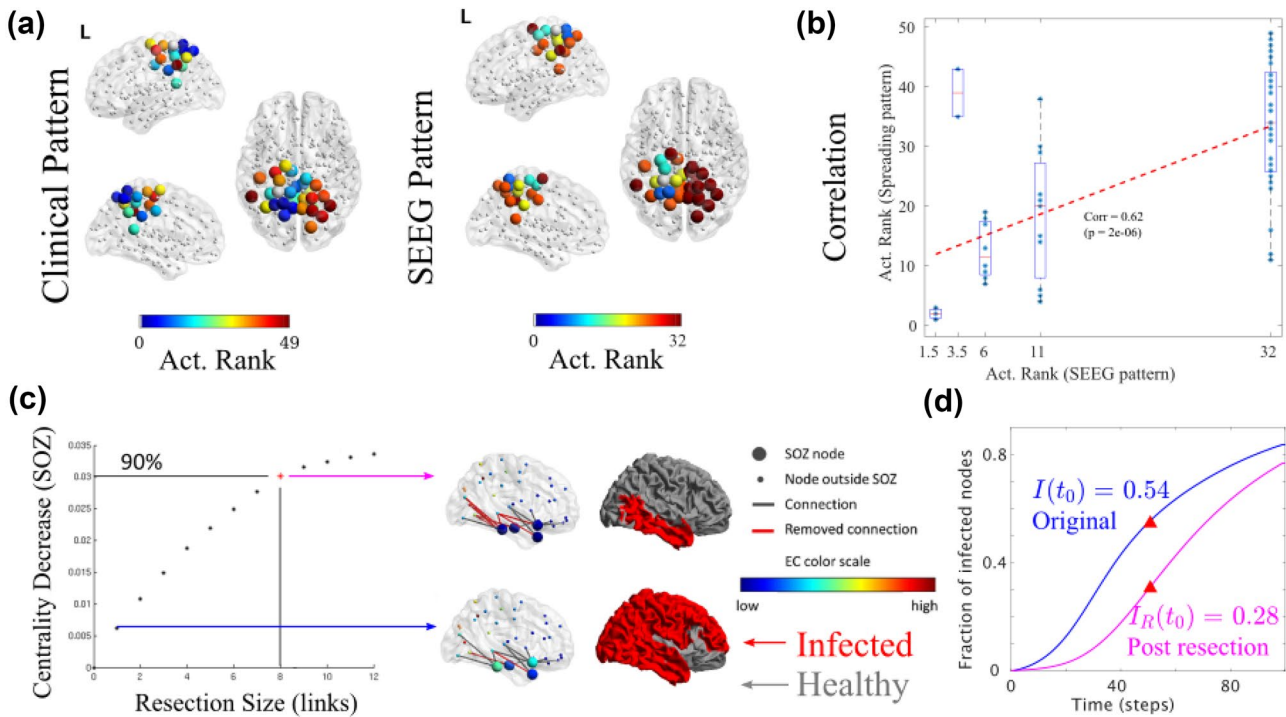


**Fig. 1** **a, b** The model parameters were fitted by maximizing the correlation between the clinical and modelled seizure propagation patterns. **c** Alternative resections were found using the Eigenvector cen-

trality of the RA (or SOZ). The optimal resection was defined as the one leading to a 90% decrease. **d** The effect of the surgery was calculated as the decrease in spreading at a given time,  $I(t_0)$

#### P44 A realistic neural network model of the optokinetic response to identify the neuronal circuitry responsible for the velocity storage mechanism

Yusuke Shinji<sup>\*1</sup>, Toshimi Yamanaka<sup>2</sup>, Yutaka Hirata<sup>2</sup>

<sup>1</sup>Chubu University, Department of Computer Science, Graduate School of Engineering, Aichi Kasugai, Japan

<sup>2</sup>Chubu University, Department of Robotic Science and Technology, Graduate School of Engineering, Aichi Kasugai, Japan

\*Email: tp19803-0969@sti.chubu.ac.jp

Most vertebrates present a reflexive eye movement called the optokinetic response (OKR). The OKR stabilizes our vision by smoothly following a large field visual motion to minimize image slip on the retina. OKR eye velocity is considered to be composed of two components: direct and indirect. In response to velocity step visual stimulation, the direct component forms an initial sudden increase in eye velocity followed by a rapid decay. By contrast the indirect component gradually builds up during the visual stimulation and decays slowly in the dark after the termination of the stimulus. The decaying continuous eye velocity in the dark is called the optokinetic after nystagmus (OKAN) which is postulated to reflect the output of a temporal integrator named the velocity storage mechanism (VSM). In goldfish and carp, it has been demonstrated that the OKR becomes predictive after prolonged exposure to temporally periodic visual stimulation [1]. The VSM was implicated to be necessary for the acquisition of this predictive behavior because zebrafish, medaka, and mice that do not present OKAN did not acquire the predictive OKR [2, 3]. Although the VSM has been localized in and around bilateral vestibular nuclei [4, 5], its neuronal circuit structure, mechanism to integrate incoming signals, and role in predictive OKR are remained unknown. Presently, we configured a neural network model of the OKR that explicitly describes the connectome subserving the OKR. We referred to the connectome identified in goldfish which is one of the animal species most thoroughly studied for visual and vestibular behavior and whose structural/functional understanding of oculomotor neurons and circuitry has accumulated for the past 25 years [4]. The model incorporated each neuron type characterized in the vestibular nuclei (VN), cerebellum, and other brainstem structures. Each neuron is described as a McCulloch-Pitts neuron model with ReLU as the activation function. The model containing 34 neuron models with 28 variable parameters and 21 constant parameters (synaptic weights and dc firing rates) was implemented on Simulink (Mathworks). A genetic algorithm was employed to determine their variable parameters that best reproduce velocity step OKR and OKAN measured in goldfish. Simulation of the model revealed that there are four neural loops enabling temporal integration as the function of the VSM to produce OKAN: 1 DO eIIhI\_exc  $\Rightarrow$  AII  $\Rightarrow$  DO eIIhI\_exc, 2 DO eIIhI\_exc  $\Rightarrow$  AII  $\Rightarrow$  DO eIIhI\_inh  $\rightarrow$  DO eIhII\_inh  $\rightarrow$  DO eIIhI\_exc, 3 DO eIIhI\_exc  $\Rightarrow$  AII  $\rightarrow$  DO eIhII\_inh  $\rightarrow$  DO eIIhI\_inh  $\rightarrow$  DO eIIhI\_exc, 4 DO eIhII\_inh  $\Rightarrow$  DO eIhII\_inh  $\Rightarrow$  DO eIhII\_inh, where, \_exc and \_inh represent excitatory and inhibitory neurons, respectively while e and h represent eye and head sensitivities of the neurons, respectively toward ipsi (I) or contralateral (II) directions. DO and AII are the descending octaval (vestibular) nucleus and the area II nucleus, respectively. All these pathways cross the midline and involve the bilateral vestibular nuclei as suggested in previous studies [4, 5]. Simulations of midline sections that selectively disconnects one or two of the four loops revealed that the pathways 1, 3, and 4 contribute significantly to produce OKAN while the pathway 2 plays a supplementary role. These results suggest that the VSM is formed by multiple commissural

neural loops involving both excitatory and inhibitory neurons in not only the vestibular nuclei but AII as well.

#### Acknowledgments

Supported by JSPS KAKENHI 20H04286, 19K06756, 18KK0286 (YH).

#### References

1. Miki S., Baker R., Hirata Y., Cerebellar role in predictive eye velocity initiation and termination. *J. Neuroscience*. 2018; 38(48): 10371–10383.
2. Miki S., Urase K., Baker R., Hirata Y., Velocity storage mechanism drives a cerebellar clock for predictive eye velocity control. *Scientific Reports*. 2020; 10: 6944.
3. Yamanaka T., Matsuzawa Y., Hernández R., Blazquez P., Yakusheva T., Katoh A., Ono S., Hirata Y., Acquisition of predictive optokinetic eye movements in mice and humans. *Society for Neuroscience*. 2021, November.
4. Pastor A. M., Calvo P. M., de la Cruz R. R., Baker R., Straka H., Discharge properties of morphologically identified vestibular neurons recorded during horizontal eye movements in the goldfish. *Journal of Neurophysiology*. 2019; 121: 1865–1878.
5. Holstein G. R., Martinelli G. P., Wearne S., Cohen B., Ultrastructure of vestibular commissural neurons related to velocity storage in the monkey. *Neuroscience*. 1999; 93: 155–170.

#### P45 Cross-comparison of state of the art morphologically detailed simulators on modern CPUs and GPUs using the Brain Scaffold Builder

Robin De Schepper<sup>\*1</sup>, Egidio D’Angelo<sup>1</sup>, Abigail Morrison<sup>2</sup>, Claudia Casellato<sup>1</sup>, Nora Abi Akar<sup>3</sup>, Thorsten Hater<sup>4</sup>, Brent Huisman<sup>4</sup>

<sup>1</sup>University of Pavia, Department of Brain and Behavioral Sciences, Pavia, Italy

<sup>2</sup>Forschungszentrum Jülich, Institute of Neuroscience and Medicine (INM-6), Jülich, Germany

<sup>3</sup>Swiss National Supercomputing Centre (CSCS), Scientific Software & Libraries, Zurich, Switzerland

<sup>4</sup>Jülich Supercomputing Centre (JSC), Simulation and Data Lab Neuroscience, Jülich, Germany

\*Email: robingilbert.deschepper@unipv.it

A variety of software simulators exist for neuronal networks, and a subset of these tools allow the scientist to model neurons in high morphological detail. The scalability of such simulation tools over a wide range in neuronal networks sizes and cell complexities is predominantly limited by effective allocation of components of such simulations over computational nodes, and the overhead in communication between them. In order to have more scalable simulation software, it is therefore important to develop a robust benchmarking strategy that allows insight into specific computational bottlenecks for models of realistic size and complexity. In this study, we demonstrate the use of the Brain Scaffold Builder [1] as a framework for performing such benchmarks. We perform a comparison between the well-known morphologically detailed simulator NEURON [2], CoreNEURON [3], and Arbor [4], a new simulation library developed within the framework of the Human Brain Project. The BSB can construct identical neuromorphological and network setups of highly spatially and biophysically detailed networks for each simulator. This ensures good coverage of feature support in each simulator, and realistic workloads. After validating the outputs of the BSB generated models, we execute the simulations on a variety of hardware configurations consisting of two types of nodes (GPU and CPU). We investigate performance

of two different network models, one suited for a single machine, and one for distributed simulation. We investigate performance across different mechanisms, mechanism classes, mechanism combinations, and cell types. Benchmarks with CoreNEURON are underway. Our benchmarks with NEURON show that, depending on the distribution scheme deployed by Arbor, a speed-up with respect to NEURON of between 60 and 400 can be achieved. Additionally, Arbor can be up to two orders of magnitude more energy efficient.

## References

1. De Schepper, R., Geminiani, A., Masoli, S., Rizza, M. F., Antonietti, A., Casellato, C., et al. Scaffold modelling captures the structure–function–dynamics relationship in brain microcircuits. *bioRxiv*. 2021
2. Carnevale, N. T. and Hines, M. L. *The NEURON book*. Cambridge University Press. 2006
3. Kumbhar, P., Hines, M., Fouriaux, J., Ovcharenko, A., King, J., Delalondre, F., et al. CoreNEURON: an optimized compute engine for the NEURON simulator. *Frontiers in neuroinformatics*. 2019; 13: 63
4. Abi Akar, N., Cumming, B., Karakasis, V., Kusters, A., Klijn, W., Peyser, A., et al. Arbor — A Morphologically-Detailed Neural Network Simulation Library for Contemporary High-Performance Computing Architectures. In 2019 27th Euromicro International Conference on Parallel, Distributed and Network-Based Processing (PDP). 274–282.

## P46 Endogenous and exogenous brain fluctuations induce and block alpha activity

Axel Hutt<sup>1</sup>

<sup>1</sup>INRIA Nancy Grand Est, MIMESIS, Strasbourg, France

\*Email: axel.hutt@inria.fr

Brain rhythms in the alpha frequency range [8 Hz-12 Hz] are present in idling conditions and sleep. A prominent occipital alpha wave emerges in mammals when the subject closes its eyes (alpha

generation) and it is blocked when opening its eyes (alpha blocking). This switch in alpha power is accompanied by an inverse switch in gamma activity [1]. With open eyes, the brain receives strong input from the external world and responds by strong gamma/weak alpha-activity, whereas disappearing input induces the inverse strong alpha/weak gamma-activity. Considering input as random input fluctuations, this switch may result from an alteration in exogenous fluctuations. The work proposes a mathematical mesoscopic neural mass model for the cortico-thalamic feedback (CTF) loop derived from a microscopic neuron network model. This model describes this fluctuations-induced switch as a phase transition induced by additive noise [2]. Figure 1A shows the time-dependent spectral power of model activity in the alpha- and gamma-frequency range (upper panel) subjected to experimental condition ‘eyes open’ and ‘eyes closed’ (lower panel). This result suggests that the well-known emerging and blocking of occipital alpha waves may result from the alternating level of random (exogenous) fluctuations in the brain.

A related emergence of alpha-activity has been also observed in the frontal lobe under general anaesthesia [3]. Under general anaesthesia, GABAergic anaesthetics induce loss of consciousness (LOC) in mammalian subjects and the corresponding frontal EEG exhibits enhanced alpha-power with diminished beta-power. Considering a similar hypothesis as in the previous study, we assume that the anaesthetics affect endogenous brain fluctuations [4]. We have implemented a CTF model and find that a level decrease of endogenous fluctuations generates the modulation from beta activity to alpha activity (see Fig. 1B). Physiologically, the endogenous fluctuations are controlled by the Ascending Reticular Arousal System (ARAS), that has been shown to be highly sensitive to anaesthetics. This hypothesized endogenous fluctuation control by the ARAS permits to describe the impact of multiple anaesthetics on the brain network without knowledge of their specific action on thalamus, cortex and between each other.

Finally, the endogenous fluctuation hypothesis has been applied very recently to describe action of transcranial Direct Current Stimulation and the non-GABAergic anaesthetic ketamine on frontal EEG as a model of psychosis [5]. This additional successful description of population action by endogenous fluctuations points to its importance in neural information processing.

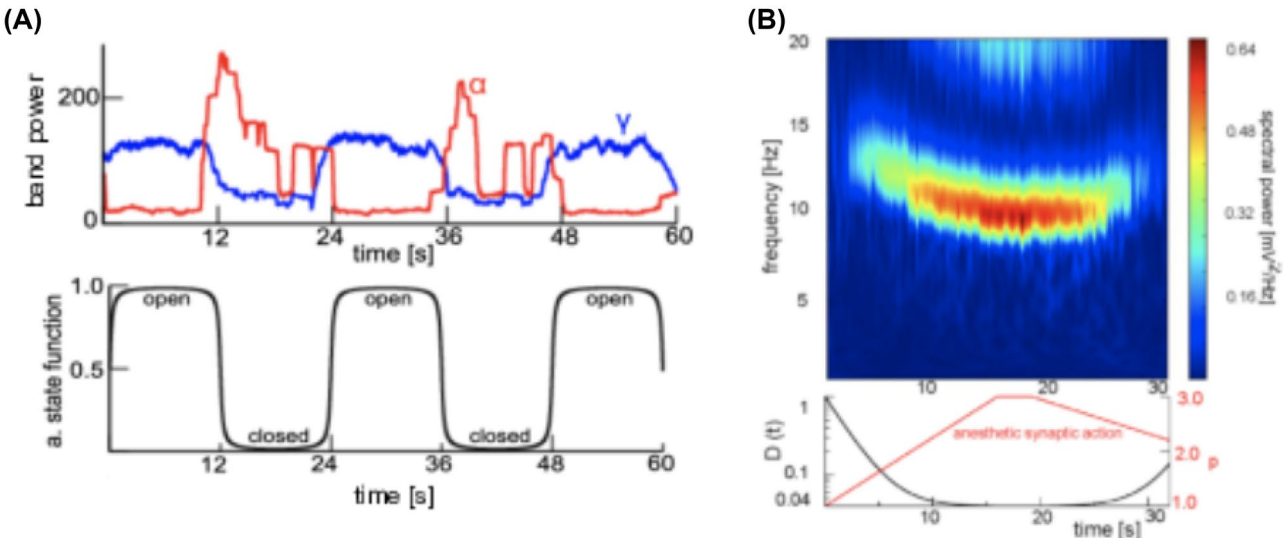


**Fig. 1** Model alpha generation and blocking by alternating fluctuations. **A** Time-dependent alterations between alpha and gamma power subject to the experimental behavioral condition ‘eyes open’ and ‘eyes closed’ induced by exogenous fluctuations [2]. **B** Time-dependent induction of alpha activity subject to the endogenous fluctuation level D and the anesthetic synaptic action p

‘eyes closed’ induced by exogenous fluctuations [2]. **B** Time-dependent induction of alpha activity subject to the endogenous fluctuation level D and the anesthetic synaptic action p

## References

1. Geller, A.S. et al. Clin. Neurophysiol. 2014; 125(9): 1764–1773.
2. A. Hutt and J. Lefebvre, Arousal fluctuations govern oscillatory transitions between dominant gamma- and alpha occipital activity during eyes open/closed conditions. Brain Topography. 2021; 35:108–120.
3. Purdon et al., PNAS. 2012; 110: E1142-1150
4. A. Hutt, J. Lefebvre, D. Hight and J. Sleigh, Suppression of underlying neuronal fluctuations mediates EEG slowing during general anesthesia. Neuroimage. 2018; 179: 414–428
5. J. Riedinger and A. Hutt. Mathematical model insights into EEG origin under transcranial direct current stimulation (tDCS) in the context of psychosis. Journal of Clinical Medicine. 2022; 11(7): 1845

## P47 Efficient analysis of combinatorial neural codes with algebraic, topological, and statistical methods

Thomas Burns<sup>\*1</sup>, Irwansyah Irwansyah<sup>2</sup>

<sup>1</sup>Okinawa Institute of Science and Technology, Okinawa, Japan

<sup>2</sup>University of Mataram, Department of Mathematics, Indonesia

\*Email: t.f.burns@gmail.com

Artificial and biological neural networks (ANNs and BNNs) can encode inputs in the form of combinations of individual neurons' activity. These combinatorial neural codes present a computational challenge for direct and efficient analysis due to their high dimensionality and often large volumes of data. Here we improve the efficiency – from exponential to quadratic time – of direct algebraic methods [1] previously applied to small, simulated neural codes and apply them to large, real, and simulated neural codes. We also introduce a procedure to perform hypothesis testing on the algebraic and topological features of neural codes using information geometry [2]. We apply these methods to neural activities from ANNs and BNNs to, without observing any inputs or outputs, estimate the structure,

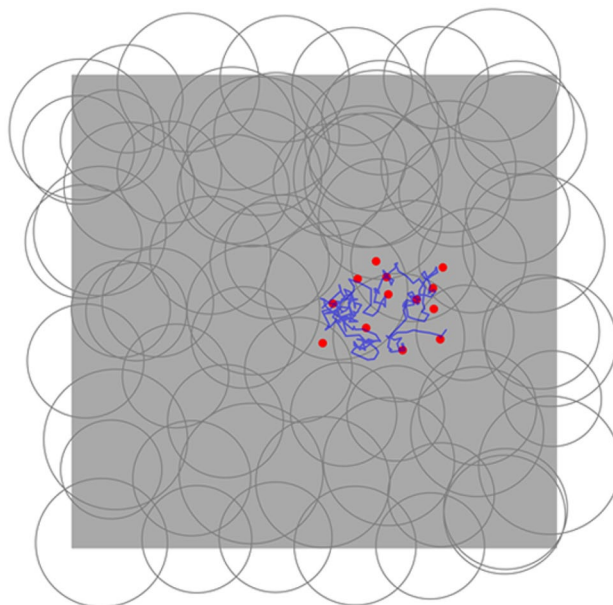


**Fig. 1** Example simulated 2D environment and trajectory where we apply our method

dimensionality, and connectedness of the stimulus or task space, e.g., of navigation environments (Fig. 1). Additionally, we show exploration trajectories which minimize uncertainties about such features and demonstrate that ANNs can follow such trajectories during learning. These methods provide a novel and efficient way of probing algebraic and topological characteristics of combinatorial neural codes and give insights on how such characteristics are related to learning and experience in neural networks.

## References

1. Curto C, Veliz-Cuba A, Youngs N. Analysis of combinatorial neural codes: An algebraic approach. In: Robeva R, Macauley M, editors. Algebraic and Combinatorial Computational Biology. 1st edition. Cambridge, USA: Academic Press; 2019, p.213–240.
2. Amari S. Information Geometry and Its Applications. 1st edition. Tokyo, Japan: Springer Publishing; 2016.

## P48 Yet Another Brain, a graph-based framework for neural simulation

Carlos Enrique Gutierrez<sup>\*1</sup>, Minoru Owada<sup>2</sup>, Izumi Kazutaka<sup>2</sup>, Atsuya Tange<sup>3</sup>, Hiroshi Kagawa<sup>2</sup>, Yuko Ishiwaka<sup>4</sup>

<sup>1</sup>SoftBank Corp., ATPO, Tokorozawa, Japan

<sup>2</sup>SoftBank Corp., ATPO, Tokyo, Japan

<sup>3</sup>SoftBank Corp., Tokyo, Japan

<sup>4</sup>SoftBank Corp., Technology Unit, Hakodate, Japan

\*Email: carlosenrique.gutierrez@g.softbank.co.jp

Models of the brain are frequently built as networks of interacting differential equations describing the evolution of variables like membrane potentials. On simulations of such networks, programs and data are considered as separated components. We introduce YAB (Yet Another Brain), a new framework for model building and simulation, where data and programs are combined within a graph and stored in a database. YAB incorporates its own programming language and runs on a virtual machine for Linux Ubuntu. The framework organizes neural networks as graphs, where nodes represent neurons and edges their synaptic connections. Within its structure, a node integrates data such as fixed parameters and variables, and programs such as methods for initialization, update of the membrane potential and spike transmission. Similarly, edges incorporate data attributes like connection weight and description tags. The model graph is generated and stored on a dedicated database called NDS (Neuro Data Store) during compilation, and thereafter accessed and maintained on simulation time. Thus, data and programs are unified, which significantly cuts down the memory consumption of neural network simulations. Simulations are managed by two YAB core components, clock and queue. The clock controls the logical simulation time, which can be paused for examining performance and results. The queue administers the execution of node methods and distributes the workload over workers for parallel processing on CPU or GPU. A YAB console provides a view of the running processes, allowing time-bin wise execution, as well as graph storage and retrieval. We have developed template nodes of leaky integrate-and-fire neuron models with alpha function-based synapses, and different connectivity modalities. Neurons are created and initialized as instances of a template node, while connectivity templates are used to generate few node instances for running wiring methods during compilation or execution time. For an efficient signal propagation over the graph, action-potentials trigger spike methods with axonal delay specifications to the queue, which manages the execution at the corresponding time. In this way, source nodes transmit spike events that update target nodes, avoiding node's

reading of presynaptic signals at every step of the simulation. The framework was tested on the building of a balanced spiking neural network model [1], with parameter specifications from [2], showing self-sustained asynchronous-irregular activity. We observed a steady memory consumption, indicating that simulation and storage simultaneously occurred. These results provide an initial verification of YAB as tool for neural simulation. YAB aims to serve as an efficient simulation engine. New node templates can be developed, implementing methods of different complexity. For example, few nodes may be used for modeling a single neuron at a biophysical level of abstraction, incorporating the dynamics of dendrites, soma, compartments, and axon. Furthermore, non-neural models could be implemented as well for combined simulations, such as models of the body, sensory organs, experimental settings, and others.

## References

1. Brunel, N. Dynamics of sparsely connected networks of excitatory and inhibitory spiking neurons. *Journal of Computational Neuroscience*. 2000; 8:3:183–208.
2. Kriener, B, et al. Dynamics of self-sustained asynchronous-irregular activity in random networks of spiking neurons with strong synapses. *Frontiers in Computational Neuroscience*. 2014; 8:136.

## P49 Motoneuron base firing pattern controller for skeletal muscle model

Shun Ogawa<sup>\*1</sup>, Tomohiro Yoshida<sup>2</sup>, Tadateru Itoh<sup>2</sup>, Yuko Ishiwaka<sup>2</sup>

<sup>1</sup>SoftBank Corp., Tokyo, Japan

<sup>2</sup>SoftBank Corp., Technology Unit, Hakodate, Hokkaido, Japan

\*Email: shun.ogawa01@g.softbank.co.jp

A decision to make a spontaneous motion is an output of brain activity. Signals produced in the brain propagate to the muscles through the spinal cord, and readiness potentials (RPs) are produced unconsciously before awareness of one's decision [1]. This work focuses on the part of the process after the signal has left the brain, from the spinal cord through to the muscles, and proposes an FPC (Firing Pattern Controller) that takes into account the delay coming from RPs for skeletal muscle models (Fig. 1, Top). The foundation of the model is the muscles controlled via motoneurons, spinal cord interneurons producing control signals, and the motoneurons propagating them to the muscle fibers. The motoneurons are modeled in terms of a Hodgkin-Huxley type equation which brings about the refractory period, inducing cooperative behavior in muscle fibers. It is well known that large and small motoneurons control slow and fast twitch elements respectively [2]. The muscle fibers are modeled with a Hill type model including fast and slow twitch elements. A target motion is acquired via the FPC with a multi-agent reinforcement learning method [3], a variant of Q-learning taking into account the time lag brought about by the existence of the time-to-peak before a muscle reaches full tension [4].

We perform the simulation with and without delay. The simulation results indicate that the target motion cannot be acquired without time delay because the firing patterns are evaluated before their result motion appears, while it can be achieved when the temporal delay is taken into account. This pre-firing is related to RP in the brain. We also simulate the model incorporating muscle growth and find that the fast and slow twitch elements cooperatively work to reach and maintain the target position (Fig. 1, Bottom) more efficiently when the muscle growth is taken into account, while the model not incorporating muscle growth resulted in fast twitch elements exclusively being used, and only reached the target position when the initial state of the muscle was sufficiently strong. We believe that this model has potential for applications in rehabilitation as a new method for controlling FES (Functional Electrical Stimulus), and also sheds light on how neonates develop motor skills.

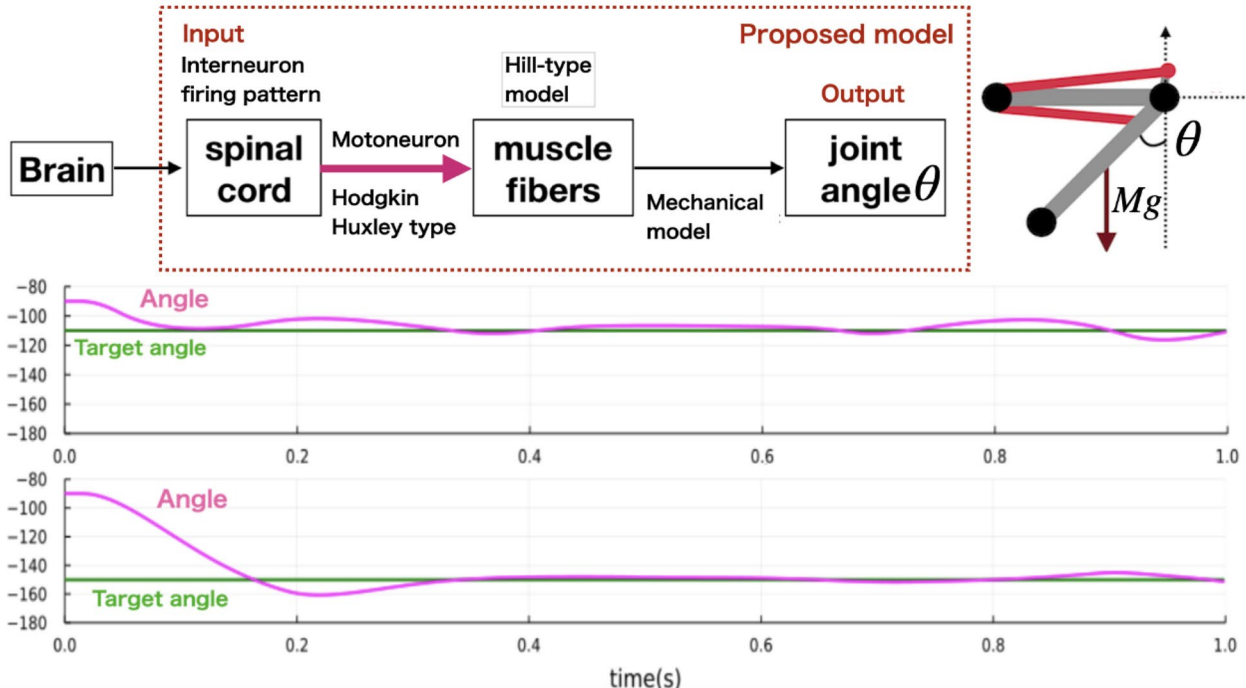


**Fig. 1** Top left: Schematic illustration of FPC model. This work deals with the part in the dotted rectangle. Top Right: Physical model of a leg. Gray and red bold lines indicate bones and muscles respectively. Bottom: Joint angle in an episode for each target motion after learning

## References

- Vercillo, T., O’Neil, S., and Jiang, F. Action-effect contingency modulates the readiness potential. *NeuroImage*. 2018; 183: 273–279.
- Kandel, E., Schwartz, J., Jessell, T., Siegelbaum, S., and Hudspeth, A. Principles of Neural Science, Fifth Edition. McGraw-Hill Education. 2012.
- Eccles, T., Bachrach, Y., Lever, G., Lazaridou, A., & Graepel, T. Biases for Emergent Communication in Multi-Agent Reinforcement Learning. In: Wallach H, Larochelle H, Beygelzimer A, Alche-Buc F, Fox E, Garnett R (eds) Advances in neural information processing systems 32, Curran Associates, Inc. 2019, pp 13111–13121.
- Zemková, E., Poór, O., and Pecho, J. Peak rate of force development and isometric maximum strength of back muscles are associated with power performance during load-lifting tasks. *American Journal of Men’s Health*. 2019; 13

## P50 Learning Algorithm of Synaptic Connections for a Parser Based on the Assembly Calculus

Atsuya Tange<sup>\*1</sup>, Tomohiro Yoshida<sup>2</sup>, Shun Ogawa<sup>1</sup>, Carlos Enrique Gutierrez<sup>3</sup>, Christos H. Papadimitriou<sup>4</sup>, Yuko Ishiwaka<sup>2</sup>

<sup>1</sup>SoftBank Corp., Tokyo, Japan

<sup>2</sup>SoftBank Corp., Technology Unit, Hakodate, Hokkaido, Japan

<sup>3</sup>SoftBank Corp., ATPO, Tokorozawa, Japan

<sup>4</sup>Columbia University, Department of Computer Science, New York, United States of America

\*Email: atsuya.tange01@g.softbank.co.jp

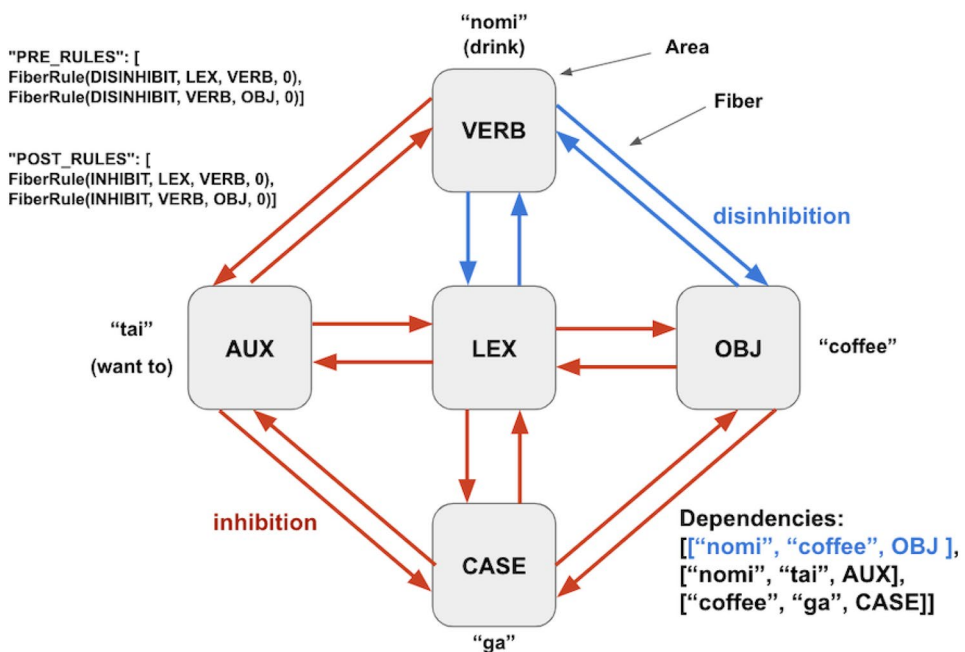
A computational neural model called the Assembly Calculus (AC) has been recently proposed [1], which is founded on basic tenets of neuroscience. The AC model consists of brain areas with recurrent synaptic connectivity, and fibers of synapses connecting them. Each fiber can be individually inhibited and disinhibited. Synaptic connectivity, both recurrently within the same area, or from one area to another via fibers, is assumed to be uniformly random. Inhibition with each area implies

that only k of the n neurons in each area fire at each time. The synaptic connections have initially weight one, and their weight is updating via a simple Hebbian rule. In the resulting dynamical system, neural assemblies emerge via an AC operation called projection; through which an assembly in one area is copied in another brain area.

Within this computational system, a biologically plausible parser has been implemented [2], which for several families of simple sentences correctly computes the dependency parse of the sentence. This parser consists of a lexicon area (LEX) residing in the left medial temporal lobe (MTL) and areas representing the syntactic role of words in the superior temporal gyrus (STG). The areas are assumed to be connected by an appropriate set of fibers. Each word in the language is represented in LEX by an assembly and has associated with it an action set of (dis)inhibition commands. When the word is input, the corresponding assembly is projected and the action set of executed. In this manner, the parser correctly identifies the dependencies between the words [2]. However, the parser in [2] is specific to English; for example, it exploits the fact that the subject always comes before the verb. Yet, each language parser requires a particular set of fiber rules. Discovering the complex word dependencies of the Japanese language is challenging. For instance, dependencies cannot be determined solely from adpositions like “ga,” because either subject or object may come before “ga,” and this is a well-known problem for Japanese parsing [3]. The problem remains in currently used Japanese parsers.

This work aims to solve the problem through AC and machine learning. By trial and error and linguistic insight (Fig. 1), one can design fiber and area rules to capture the correct dependencies for very simple sentences; it is however not practical to find such rules. We therefore propose a multi-agent reinforcement learning algorithm to acquire fiber rules for Japanese sentences. As a result, we successfully parsed short sentences containing subject and object before the same adposition. Our algorithm generates several valid fiber rule sets. The proposed algorithm can be applied to other language parsers if part of speech and dependency areas are designed. We believe that our work can contribute to elucidating a language parsing and acquisition model of the brain.

**Fig. 1** Schematic picture of the Japanese parsing process. English translations are written in parentheses. Pre-rules and Post-rules written on the left top are fiber rules applied before projection and after projection respectively. The word “nomi” is projected through LEX, VERB, and OBJ(object). The dependency “the object of ‘nomi’ is ‘coffee’” is recorded by projections in this figure



## References

- Papadimitriou, Vempala, Mitropolsky, Collins, et al. Brain computation by assemblies of neurons. *Proceedings of the National Academy of Sciences*. 2020; 117(25):14464–14472.
- Mitropolsky, Collins, Papadimitriou, et al. A Biologically Plausible Parser. *Transactions of the Association for Computational Linguistics*. 2021; 9: 1374–1388.
- Shibatani. “11 Grammatical structure”. In: Comrie, editors. “The languages of Japan”. 1st edition. Cambridge: Cambridge University Press. 1990; p.257–388.

## P51 Deciphering clock cell network morphology and its functional role within the biological master clock, suprachiasmatic nucleus

Kyoung Jin Lee<sup>\*1</sup>, In Hoi Jeong<sup>1</sup>

<sup>1</sup>Korea University, Department of Physics, Seoul, South Korea

\*Email: kyoung@korea.ac.kr

The suprachiasmatic nucleus (SCN) is a tiny nucleus located within a deep brain area, serving the role of the biological master clock for mammals [1, 2]. It is composed of approximately 10,000 (neuronal) clock cells and orchestrates all daily rhythms such as the sleep-wake cycle and heart-beat rate modulation. The SCN is a vitally important part of the brain, as any significant disruptions in the spatiotemporal circadian phase dynamics inside this small nucleus may potentially lead to circadian arrhythmia akin to cardiac arrhythmia. The clock cells are known to be heterogeneous with respect to their intrinsic circadian periods as well as to their biological characteristics, for example, different neuropeptides which they release. Despite these inhomogeneities, an intact SCN maintains a very well-coordinated spatial circadian phase (time) coherence [3] which is vital for sustaining various circadian rhythms for mammals, and this coherence is achieved by action potential (AP)-mediated neural network as well as diffusive cell-cell coupling. Due to technical difficulties and limitations in experiments, however, so far very little information is available about the morphology of

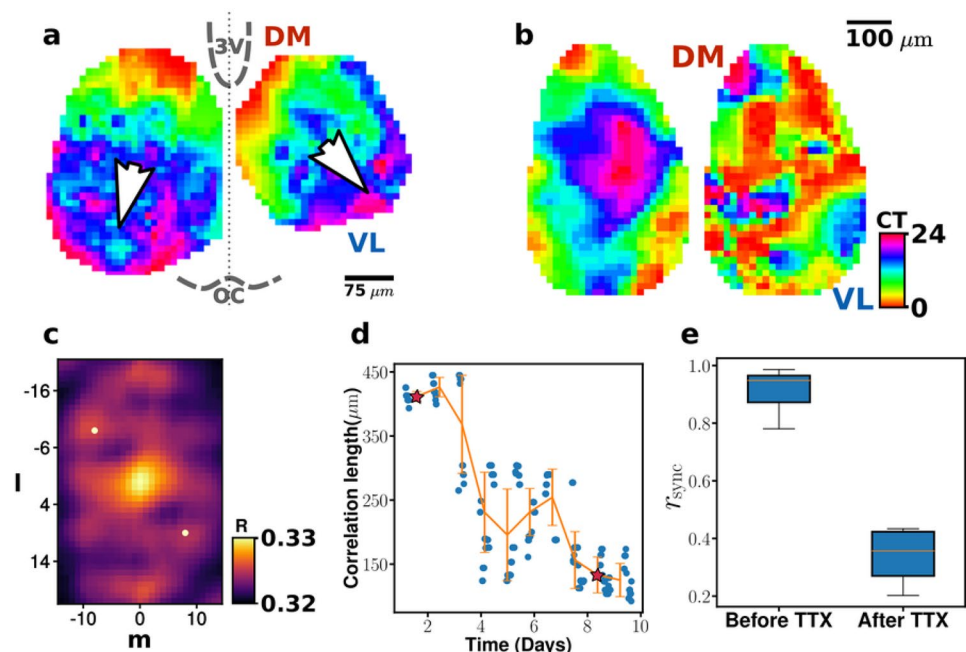
the connectivity among ~ 10,000 clock cells [4]. Building upon this limited amount of information, recently we have exhaustively and systematically explored a large pool (~ 25,000) of various model network morphologies to come up with some realistic network features of rat SCN neural networks. All candidates under consideration reflect an experimentally obtained ‘indegree distribution’ as well as a ‘physical range distribution of afferent clock cells’. Then, importantly, with a set of multitude criteria based on the properties of SCN circadian phase waves in extrinsically perturbed as well as in their natural states, we select out appropriate model networks: Some important measures are, 1) level of phase dispersal and direction of wave propagation, 2) phase-resetting ability of the model networks subject to external circadian forcing, and 3) decay rate of perturbation induced ‘phase-singularities’.

The successful, realistic networks thus identified have several common features: 1) “indegree” and “outdegree” should have a positive correlation; 2) the cells in the SCN ventrolateral region (core) have a much larger total degree than that of the dorsal medial region (shell); 3) The number of intra-core edges is about 7.5 times that of intra-shell edges; and 4) the distance probability density function for the afferent connections fits well to a beta function. Interestingly, the network morphologies that carry those features also recapitulate the seasonal response (variation) of the SCN phase dynamics that are subsequent to the external seasonal light/dark photo-period modulation.

## References

- Klein DC, Moore RY, Reppert SM. Suprachiasmatic Nucleus: The Mind’s Clock. 1st ed. Oxford University Press; 1991.
- Güldner F-H. Numbers of neurons and astroglial cells in the suprachiasmatic nucleus of male and female rats. *Experimental Brain Research*. 1983; 50–50.
- Jeong B, Hong JH, Kim H, Choe HK, Kim K, Lee KJ. Multi-stability of circadian phase wave within early postnatal suprachiasmatic nucleus. *Scientific Reports*. 2016; 6: 21463
- Min C, Kim H, Choi W, Lee KJ. Diversity in the structure of action potential-mediated neural connectivity within rat supra chiasmatic nucleus. *European Journal of Neuroscience*. 2019; 50: 2814–2829.

**Fig. 1** Circadian phase waves supported by mouse SCNs and their phase disintegration in the presence of TTX



**P52 High-dimensional topological analysis of BOLD sliding window correlations**

Emil Dmitruk<sup>\*1</sup>, Christoph Metzner<sup>2</sup>, Volker Steuber<sup>3</sup>, Shabnam Kadir<sup>4</sup>

<sup>1</sup>University of Hertfordshire, School of Engineering and Computer Science, Hatfield, United Kingdom

<sup>2</sup>Technische Universität Berlin, Department of Software Engineering and Theoretical Computer Science, Berlin, Germany

<sup>3</sup>University of Hertfordshire, Biocomputation Research Group, Hatfield, United Kingdom

<sup>4</sup>University of Hertfordshire, Centre for Computer Science and Informatics Research, Hatfield, United Kingdom

\*Email: e.dmitruk@herts.ac.uk

In recent years, topological insights into neuroscience have brought more understanding about the functional and structural connectivity of the brain [1, 2]. There is evidence that topological properties of brain connectomics are different for schizophrenia subjects and healthy controls [3, 4] but also that the topology can be used to reveal the brain state trajectories [5]. Inspired by those studies we aim to further investigate the brain dynamics and turn our attention to the dynamics of brain pathological states.

In this work we aim at establishing the framework for analysis of brain functional dynamics by studying the evolution of its higher-dimensional topological properties. We use Midnight Scan Club's [6] fMRI recordings acquired during motor task execution, and

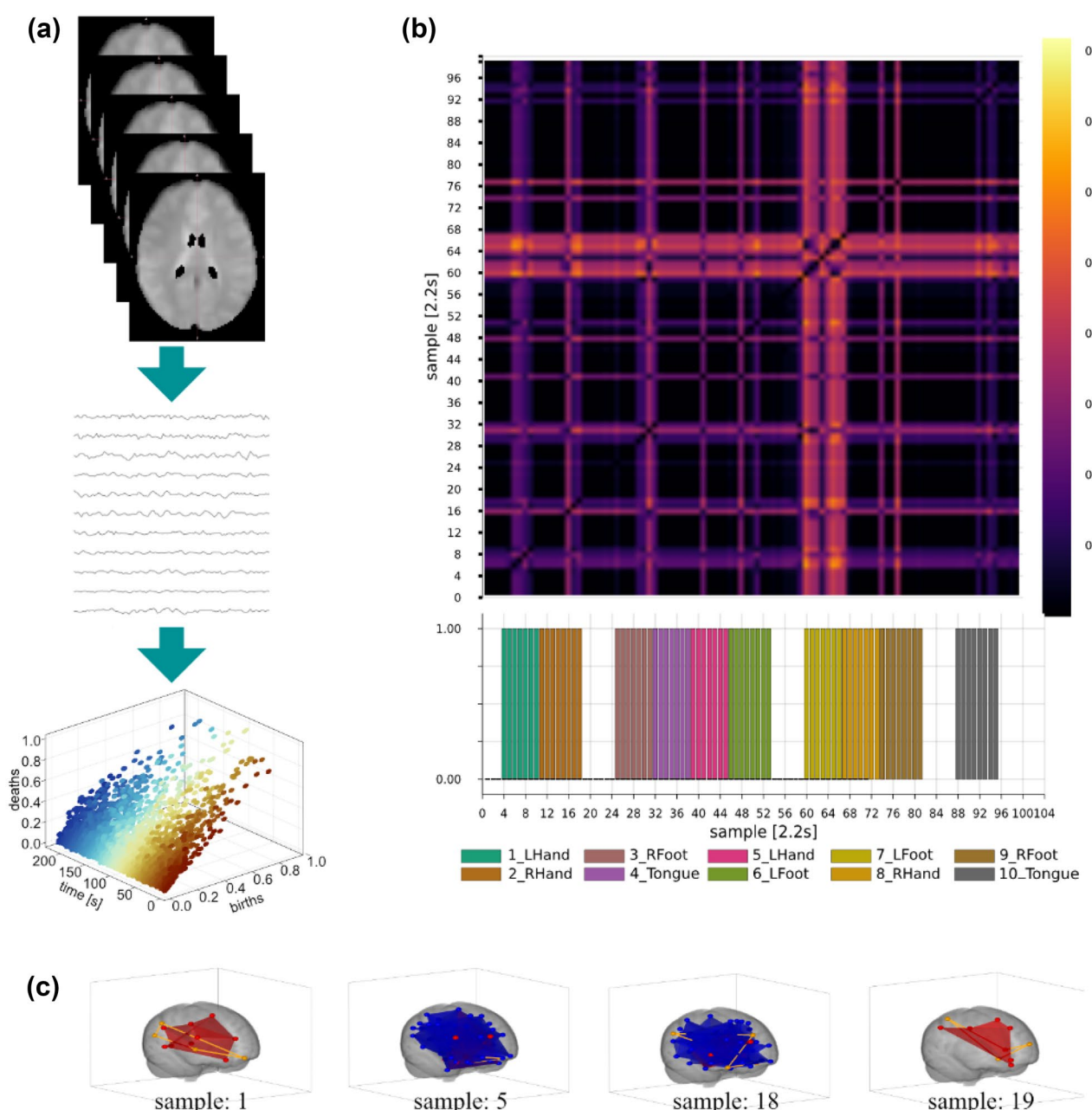


**Fig. 1** **a** Genesis of sequence of birth–death diagrams; **b** Example of Wasserstein matrix with related task information; **c** visualization of maximal simplicial complexes

investigate the topological properties of sliding window correlations [7]. Namely, in each individual single session recording, we compute average signals for each of the brain regions defined in the AAL2 [8] atlas and then compute sliding window correlations. For each correlation window, we derive a clique filtration [9] and obtain a birth–death diagram, representing brain topological properties—persistence of the cycles [10]. In the final step, we compute the Wasserstein distance for all pairs of such birth–death diagrams to investigate how the topological properties are evolving through time during task execution. The resulting Wasserstein distance matrix (Fig. 1) reveals interesting patterns of brain activity – our initial results indicate that some of the task transitions are correlated in time with the occurrence of higher-ordered topological structures. We hypothesize that those high-dimensional topological structures are related to the brain state transitions. What we found surprising are the facts that: (1) not all transitions are accompanied by immediate formation of those structures and (2) the consecutive simplicial complexes are strikingly different. Our method is the first application of high-dimensional topological properties in the study of dynamics of the brain activity. Our novel approach focuses on analysis of the functional connectomics of individuals using just a single recording, while traditional approaches for fMRI studies are designed to work with population averaged data. This approach should allow us to get a better understanding of the differences between individuals’ brain functional connectivities.

Once we learn more about the dynamic connectomics in the healthy population such as in the MSC data-set, this should provide a ‘ground truth’ with which to compare differing dynamic information processing topologies emerging from diseased brain states.

## References

1. M. Saggar, O. Sporns, J. Gonzalez-Castillo, P. A. Bandettini, G. Carlsson, G. Glover, and A. L. Reiss. Towards a new approach to reveal dynamical organization of the brain using topological data analysis. *Nature Communications*. 2018; 9(1): 1–14
2. A. Sizemore, C. Giusti, A. Kahn, J. M. Vettel, R. F. Betzel, and D. Bassett. Cliques and cavities in human connectome. *Journal of Computational Neuroscience*. 2018; 115–145
3. B. Stoltz, T. Emerson, S. Nahkuri, M. A. Porter, and H. A. Harrington. Topological Data Analysis of Task-Based fMRI Data from Experiments on Schizophrenia. Sep. 2018; arXiv:1809.08504v2
4. E. Dmitruk, C. Metzner, V. Steuber, and S. Kadir. Larger inter-individual variability of large-scale brain organization in schizophrenia revealed by topological data analysis. *Journal of Computational Neuroscience*. Dec. 2021; 49(1): S22–S24.
5. B. Rieck, T. Yates, C. Bock, K. Borgwardt, G. Wolf, N. Turk-Browne, and S. Krishnaswamy. Uncovering the Topology of Time-Varying fMRI Data using Cubical Persistence. Oct 2020; arXiv:2006.07882
6. E. M. Gordon et. al. Precision Functional Mapping of Individual Human Brains. *Neuron*. 2017. 95(4): 791–807.
7. R. H. R. Pruim, M. Mennes, D. van Rooij, A. Llera, J. K. Buitelaar, and C. F. Beckmann. ICA-AROMA: A robust ICA-based strategy for removing motion artifacts from fMRI data. *NeuroImage*. 2015; 112: 267–277
8. E. T. Rolls, M. Joliot, and N. Tzourio-Mazoyer. Implementation of a new parcellation of the orbitofrontal cortex in the automated anatomical labeling atlas. *NeuroImage*. 2015; 122: 1–5

## P53 Measuring Functional Connectivity Changes with Simultaneous Transcutaneous Vagus Nerve Stimulation (tVNS) and Magnetoencephalography (MEG)

**Charlotte Keatch**<sup>\*1</sup>, Elisabeth Lambert<sup>2</sup>, Will Woods<sup>3</sup>, Tatiana Kameneva<sup>4</sup>

<sup>1</sup>Swinburne University of Technology, Biomedical Engineering, Melbourne, Australia

<sup>2</sup>Swinburne University of Technology, School of Health Sciences, Department of Health and Medical Sciences, Melbourne, Australia

<sup>3</sup>Swinburne University of Technology, Faculty of Health Arts and Design, Melbourne, Australia

<sup>4</sup>Swinburne University of Technology, School of Science, Computing and Engineering Technologies, Melbourne, Australia

\*Email: ckeatch@swin.edu.au

Functional connectivity is an important part of the analysis of brain dynamics which looks at the connections between brain areas that may be functionally linked but spatially separate. Functional connectivity has been found to be altered in many different conditions such as schizophrenia and depression. Successful treatment of these conditions is often associated with improvement of connectivity.

Transcutaneous vagus nerve stimulation (tVNS) is a type of non-invasive brain stimulation that is used increasingly in the treatment of different conditions; however, there is little conclusive evidence as to the optimal parameters of stimulation and whether it can affect functional connectivity. In addition, there are relatively few studies that have combined tVNS with a neuroimaging method such as magnetoencephalography (MEG) due to the presence of large stimulation artifacts produced by the electrical current in tVNS.

In MEG, functional connectivity can be determined by looking at the brain signals originating from different areas of the brain and calculating whether they are correlated. We selected a phase-based method, Weighted Phase Lag Index (WPLI) which looks at the instantaneous phase difference between two signals from separate sources and estimates connectivity between regions. This method compensates for spatial leakage and other volume conduction issues that typically occur with other connectivity methods using MEG data that result in positive bias. We compared functional connectivity in response to two different frequencies of tVNS; 24 Hz and 1 Hz. Data was collected using MEG imaging concurrently with tVNS from 17 healthy participants. An interpolation method was applied to the data to remove stimulation artifacts, and functional connectivity was calculated using the WPLI method. We analyzed both whole-head and region of interest (ROI) connectivity. Regions of interest were selected based on three sub-networks; the Default Mode Network (DMN), the Salience Network (SN) and the Central Executive Network (CEN) to investigate whether tVNS could lead to changes in connectivity in a number of regions and networks that have been implicated in the pathology of depression. Results suggest that different frequencies of stimulation lead to changes in functional connectivity across a number of regions across the head, including areas involved in the pathology of depression. Altered connectivity was observed both within and between the three sub-networks (DMN, SN and CEN) that have been implicated in depression, as well as other cortical and sub-cortical brain areas.

The findings from this study suggests that different stimulation frequencies of tVNS can be utilized to alter connectivity in different areas of the brain, and further investigation may lead to the development of personalized stimulation protocols for the targeted treatment of different conditions.

#### P54 Modelling stimulation and inhibition of retinal ganglion cells during nanoparticle-enhanced infrared neural modulation

James Begeng<sup>\*1</sup>, Wei Tong<sup>2</sup>, Michael Ibbotson<sup>3</sup>, Paul Stoddart<sup>4</sup>, Tatiana Kameneva<sup>1</sup>

<sup>1</sup>Swinburne University of Technology, School of Science, Computing and Engineering Technologies, Melbourne, Australia

<sup>2</sup>National Vision Research Institute, Melbourne, Melbourne, Australia

<sup>3</sup>University of Melbourne, Melbourne, Victoria, Australia

<sup>4</sup>Swinburne University of Technology, ARC Training Centre in Biodevices, Melbourne, Australia

\*Email: jbegeng@swin.edu.au

The leading cause of blindness in industrialized countries is retinal degeneration, a class of neurodegenerative retinopathies characterized by the death of photoreceptors and lower-level retinal neurons. A retinal prosthesis can be used to restore visual sensation by stimulating the extant higher-level neurons, typically through an implanted electrode array. These devices have a low stimulus resolution due to current spread and electrode design limitations, and furthermore have no capacity for selective stimulation of different cell types which precludes acute image recognition. In particular, the selective stimulation of ON-type retinal ganglion cells (RGCs) and inhibition of OFF-type RGCs is thought to be essential to the restoration of high-acuity vision and represents a long-standing challenge in retinal prosthesis design. Nanoparticle-enhanced infrared neural modulation (NINM) is an optical neuromodulation technique which uses pulsed infrared light to deliver sharp thermal transients to neural tissue by nanoplasmonic heating of proximal gold nanorods. Short, high-power pulses generate large thermal gradients which induce large capacitive currents capable of evoking robust stimulation, whilst longer pulses can inhibit spontaneous action potentials via thermal block. This dual capacity for stimulation and inhibition may be uniquely well-suited to retinal prosthesis applications, for the purpose of selective stimulation of ON-type RGCs and inhibition of OFF-type RGCs. In this study, a single-compartment Hodgkin-Huxley-type model was simulated in a NEURON environment, consisting of leak, sodium, potassium, calcium and low-voltage-activated calcium currents based on published data [1, 2]. We further incorporate a temperature-dependent Q10 model for key sodium and potassium channels necessary for simulating thermal block during NINM [3], and a dT/dt dependent capacitive current based on GCS theory [4].

Our results show key differences in the response between ON- and OFF-type RGCs in response to NINM. Preliminary patch-clamp recordings from rat retinal explants are presented which confirm the presence of this difference in responses. These findings may have important implications for future NINM-driven retinal prostheses [5]. Predicted stimulation and inhibition thresholds for NINM in RGCs are also presented and compared with preliminary patch-clamp recordings from rat retinal explants.

#### References

1. Fohlmeister JF, Miller RF. Impulse encoding mechanisms of ganglion cells in the tiger salamander retina. *Journal of Neurophysiology*. 1997; 78: 1935–1947.
2. Wang X-J, Rinzel J, Rogawski M. A model of the T-type calcium current and the low-threshold spike in thalamic neurons. *Journal of Neurophysiology*. 1991; 66: 839–850.
3. Ganguly M, Jenkins MW, Jansen ED, Chiel HJ. Thermal block of action potentials is primarily due to voltage-dependent potassium currents: a modeling study. *Neural Eng*. 2019; 16: 036020.
4. Eom K, Byun KB, Jun SB, Kim SJ, Lee J. Theoretical Study on Gold-Nanorod-Enhanced Near-Infrared Neural Stimulation. *Biophysical Journal*. 2018; 115: 1481–1497.
5. Nelidova D, Morikawa RK, Cowan CS et al. Restoring light sensitivity using tunable near-infrared sensors. *Science*. 2020; 368(6495): 1108–1113.

#### P55 Self-organized neuronal subpopulations and network morphology underlying superbursts

In Hoi Jeong<sup>1</sup>, Kyoung Jin Lee<sup>\*1</sup>, Byoungsoo Kim<sup>1</sup>

<sup>1</sup>Korea University, Department of Physics, Seoul, South Korea

\*Email: kyoung@korea.ac.kr

Neural bursts are an important phenomenon that needs to be understood for their relevance to many different neurological diseases as well as neural computations. While there are different types of neuronal bursts, in this study we investigate the nature of population (as opposed to intrinsic cell-level) bursts, in particular, superbursts that are a small (~ 100 ms) packet of several population bursts [1, 2]. It has been suggested that neuronal population bursts occur when there exists a delicate balance of system-wide excitation and inhibition and when recurrent excitation loops exist in the network. However, there has been no rigorous investigation on the relation between network morphology and (super)burst dynamics. Here we investigate the important issue based on a well-established Izhikevich network model of integrate-fire neurons. We have employed the overall conduction delay as our control parameter for tuning network morphology as well as its matching burst dynamics. Interestingly, we found that initially identical neurons self-organize to develop several distinct neuronal subpopulations, which are characterized by different spike firing patterns as well as local network properties. Moreover, a few different motifs of superburst emerge according to a distinct mixture of neuronal subpopulations that, on average, fire at slightly different phases. Our analyses suggest that recurring motifs of different superbursts reflect complex yet organized modular structures of different subpopulations.

#### References

1. J. H. Choi, J. H. Kim, R. Heo, K. J. Lee, *Physical review Letters*. 2012; 108: 138103
2. Byoungsoo Kim and Kyoung J Lee, *New Journal of Physics*. 2022; 24 043047

#### P56 Efficient gradient descent by implementing eventProp in GeNN

Thomas Nowotny<sup>\*1</sup>, James Knight<sup>2</sup>

<sup>1</sup>University of Sussex, School of Engineering and Informatics, Brighton, United Kingdom

<sup>2</sup>University of Sussex, Department of Informatics, Brighton, United Kingdom

\*Email: t.nowotny@sussex.ac.uk

In a recent seminal work [1], Pehle and Wunderlich introduced the EventProp algorithm for calculating exact gradients for spiking neural network models. This algorithm determines the exact gradient of a loss function in a network of leaky integrate-and-fire (LIF) neurons by integrating a hybrid system of ordinary differential equations (ODEs) describing the dynamics of adjoint variables with jumps backward in time. This is the exact same type of computation that calculates the forward dynamics of the LIF neurons' membrane potential with jumps at threshold crossings.

GeNN [2, 3] is the GPU enhanced neuronal networks framework developed at Sussex that was designed to accelerate spiking neural network models of this type. Users provide the code describing the hybrid system, typically in terms of a simple forward Euler algorithm for the ODE and a spiking threshold and membrane potential reset for the jumps. GeNN transforms this description into efficient code running on GPUs.

Due to the striking similarities in the forward integration of the network dynamics and the backward integration for calculating the gradient of a loss function, we were able to implement EventProp in a very efficient way using GeNN, with simultaneous calculations of forward and backward dynamics and minimal changes to GeNN itself.

In this presentation, we show how EventProp is implemented in GeNN, and discuss results of testing it on standard benchmark problems, including the YingYang dataset [4], latency encoded MNIST [5], and the spiking Heidelberg digits [6]. We find that the classification performance of the GeNN EventProp implementation is comparable to the published benchmark results [1] and similar to those observed for the e-prop algorithm [7] and a back-propagation-through-time based solution. However, in terms of training and inference speed, EventProp in GeNN is between 4× and 10× faster than the other solutions.

### Acknowledgments

This work was funded by the EPSRC (Brains on Board project, Grant Number EP/P006094/1, ActiveAI project, Grant Number EP/S030964/1, Unlocking spiking neural networks for machine learning research, Grant Number EP/V052241/1), and the European Union's Horizon 2020 research and innovation programme under Grant Agreement 945539 (HBP SGA3).

### References

1. Wunderlich TC, Pehle C. Event-based backpropagation can compute exact gradients for spiking neural networks. *Scientific Reports*. 2021; 11: 12829.
2. Yavuz E, Turner J, Nowotny T. GeNN: A code generation framework for accelerated brain simulations. *Scientific Reports*. 2016; 6: 18854.
3. GeNN repository. Github. <https://github.com/genn-team/genn>
4. Kriener L, Gölz J, Petrovici M. The Yin-Yang dataset. arXiv. 2022; 2102.08211.
5. Lecun Y, Bottou L, Bengio Y, Haffner P. Gradient-based learning applied to document recognition. *Proceedings of the IEEE*. 1998; 86: 2278–2324.
6. Cramer B, Stradmann Y, Schemmel J, Zenke F. The Heidelberg Spiking Data Sets for the Systematic Evaluation of Spiking Neural Networks. *IEEE Transactions on Neural Networks and Learning Systems*. 2020; 1–14.
7. Bellec G, Scherr F, Subramoney A, Hajek E, Salaj D, Legenstein R, Maass W. A solution to the learning dilemma for recurrent networks of spiking neurons. *Nature Communications*. 2020; 11: 3625.

### P57 Modelling the effect of ephaptic coupling on spike propagation in peripheral nerve fibres

Helmut Schmidt<sup>1</sup>, Thomas R. Knösche<sup>\*2</sup>

<sup>1</sup>The Czech Academy of Sciences, Institute of Computer Science, Prague, Czechia

<sup>2</sup>Max Planck Institute for Human Cognitive and Brain Sciences, Brain Networks, Leipzig, Germany

\*Email: knoesche@cbs.mpg.de

Experimental and theoretical studies have shown that ephaptic coupling leads to the synchronisation and slowing down of spikes propagating along the axons within peripheral nerve bundles. The main focus thus far has been on a small number of identical axons [1–3], whereas realistic peripheral nerve bundles contain numerous axons with different diameters. Here, we present a computationally efficient spike propagation model, which captures the essential features of propagating spikes and their ephaptic interaction, and facilitates the theoretical investigation of spike volleys in large, heterogeneous fibre bundles [4]. The spike propagation model describes an action potential, or spike, by its position on the axon, and its velocity. The velocity is primarily defined by intrinsic features of the axons, such as diameter and myelination status, but it is also modulated by changes in the extracellular potential. These changes are due to transmembrane currents that occur during the generation of action potentials. The resulting change in the velocity is appropriately described by a linearized coupling function, which is calibrated with a biophysical model.

We first lay out the theoretical basis to describe how the spike in an active axon changes the membrane potential of a passive axon. These insights are then incorporated into the spike propagation model, which is calibrated with a biophysically realistic model based on Hodgkin-Huxley dynamics. The fully calibrated model is then applied to fibre bundles with a large number of axons and different types of axon diameter distributions. The computational efficiency of the spike propagation model enables a detailed investigation of how the structural parameters affect spike propagation and synchronisation. One key insight of this study is that the heterogeneity of the axonal diameters has a dispersive effect, and that with increasing level of heterogeneity the ephaptic coupling strength has to increase to achieve full synchronisation between spikes. Another result of this study is that in the absence of full synchronisation, the slowest spikes pertaining to the smallest axons form synchronised clusters. This partial entrainment can be explained by the effect of axon diameter on the amplitude of ephaptic coupling, which is larger between smaller axons [5]. If combined with forward models for the generation of electric fields at skin electrodes, these findings may help interpret the results of non-invasive experiments on the electrophysiology of peripheral nerves.

### References

1. JH Goldwyn, J Rinzel. Neuronal coupling by endogenous electric fields: cable theory and applications to coincidence detector neurons in the auditory brain stem. *Journal of Neurophysiology*. 2016; 115:2033–2051
2. H Schmidt, TR Knösche. Action potential propagation and synchronisation in myelinated axons. *PLOS Computational Biology*. 2019; 15:e1007004

3. H Sheheitli, VK Jirsa. A mathematical model of ephaptic interactions in neuronal fiber pathways: Could there be more than transmission along the tracts? *Network Neuroscience*. 2020; 4:595 – 610
4. H Schmidt, G Hahn, G Deco, TR Knösche. Ephaptic coupling in white matter fibre bundles modulates axonal transmission delays. *PLOS Computational Biology*. 2021; 17:e1007858
5. H Schmidt, TR Knösche. Modelling the effect of ephaptic coupling on spike propagation in peripheral nerve fibres. *Biol Cybern* (accepted)

#### P58 Estimating the neural dynamics from the evoked local field potentials in the primary auditory cortex of awake monkeys

Vincent S.C. Chien<sup>1</sup>, Peng Wang<sup>1</sup>, Yonatan I. Fishman<sup>2</sup>, Burkhard Maess<sup>1</sup>, Thomas R. Knösche<sup>\*1</sup>

<sup>1</sup>Max Planck Institute for Human Cognitive and Brain Sciences, Brain Networks, Leipzig, Germany

<sup>2</sup>Albert Einstein College of Medicine, Departments of Neurology and Neuroscience, New York, United States of America

\*Email: knoesche@cbs.mpg.de

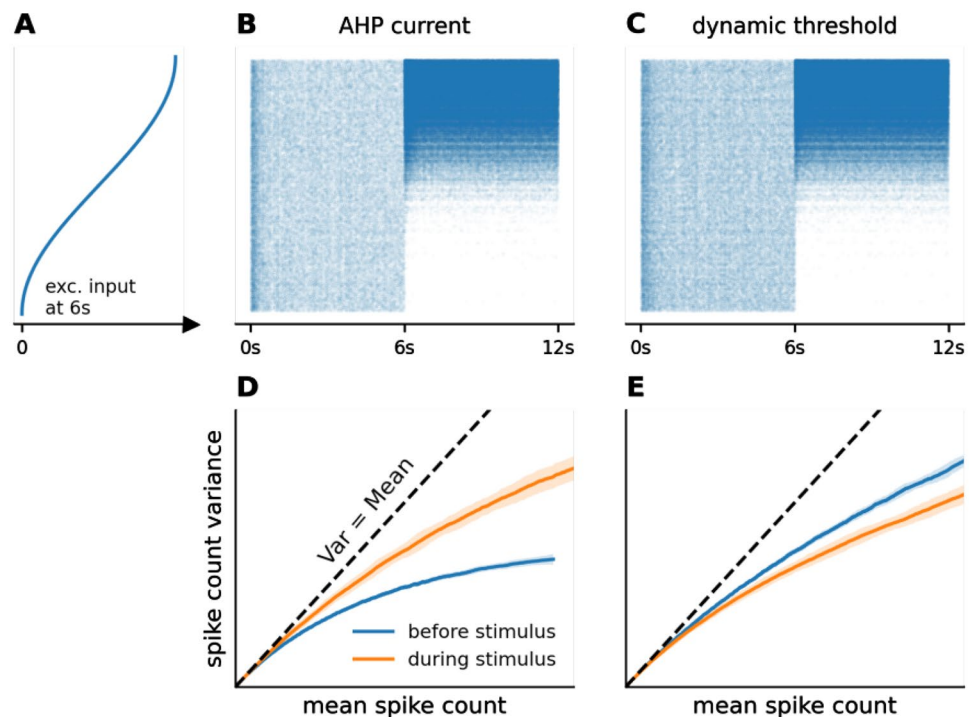
Parvalbumin-expressing (PV) and somatostatin-expressing (SOM) interneurons are distinct in their morphology, targeting locations, plasticity, spiking rates, time constants, and afferent inputs. How such differences contribute to their different functional roles in sensory coding, such as frequency discrimination, is still an open question. In this study, we attempt to estimate the neural dynamics of evoked responses by fitting a rate-based model to local field potentials (LFPs) recorded via multi-contact electrodes which sampled neural activity at 16 laminar depths simultaneously. Recordings include neural population responses to best-frequency (BF) and non-BF tones (intensity 60 dB SPL; duration 200 ms) at two representative sites in primary auditory cortex (A1) of awake monkeys. The column model considers three types of neural populations, including excitatory, PV, and SOM populations across

layers 2/3, 4, and 5/6. The model's state variables include the firing rates, postsynaptic potentials (PSPs), and synaptic efficacy reflecting short-term plasticity (STP). The model parameters include network connection strengths (default settings based on [1-4]), synaptic time constants, and STP rates. We fitted a two-column model (where the two columns laterally inhibit each other with E-to-SOM connections) to the laminar profiles of multi-unit activity (MUA) and current source density (CSD) derived from the recorded LFPs. The fitting procedure was carried out iteratively to find similar solutions (i.e., scaling factors on default connection strengths) for the two sites. The results show distinct estimated PV and SOM activities in response to BF and non-BF tones. In particular, PV firing rates are higher in BF than in non-BF responses, mainly due to different strengths of tonotopic thalamic input, whereas SOM firing rates are higher in non-BF than in BF responses due to lateral inhibition. This is consistent with a hypothetical functional role of PV-SOM interaction mentioned in [5], whereby tonotopic input and lateral inhibition can result in a switch between a disinhibited state (i.e., PV inhibiting SOM in BF responses) and an inhibited state (i.e., SOM inhibiting PV in non-BF responses). Future work will focus on adding data and constraints for consistent solutions, as well as the dynamic analysis of the fitted model.

#### References

1. Billeh, Yazan N., et al. Systematic integration of structural and functional data into multi-scale models of mouse primary visual cortex. *Neuron*. 2020; 106:3:388–403
2. Dura-Bernal, Salvador, et al. Data-driven multiscale model of macaque auditory thalamocortical circuits reproduces *in vivo* dynamics. *bioRxiv*. 2022
3. Ji, Xu-ying, et al. Thalamocortical innervation pattern in mouse auditory and visual cortex: laminar and cell-type specificity. *Cerebral Cortex*. 2016; 26:6: 2612–2625
4. Kato, Hiroyuki K., Samuel K. Asinof, and Jeffry S. Isaacson. Network-level control of frequency tuning in auditory cortex. *Neuron*. 2017; 95:2: 412–423
5. Hahn, Gerald, et al. Computational properties of the visual microcircuit. *bioRxiv*. 2020

**Fig. 1** **A** After 6 s of purely background activity, neurons in a recurrent neural network (8000 excitatory, 2000 inhibitory, 5% connection probability) receive an additional excitatory input. The input strength differs for different neurons. **B**, **C** Raster plots of the excitatory neurons, two different SFA mechanisms. **C**, **D** We calculated the response variance for each neuron, before and during stimulus



## P59 Spike frequency adaptation mechanism leading to variability quenching in recurrent neural networks

Tomas Barta<sup>\*1</sup>, Lubomir Kostal<sup>1</sup>

<sup>1</sup>Institute of Physiology, Czech Academy of Sciences, Laboratory of Computational Neuroscience, Prague, Czechia

\*Email: tomas.barta@fgu.cas.cz

Neural variability quenching is a decrease of trial-to-trial variability of neural response evoked by a stimulus. This phenomenon has been observed across many scales in the brain including the membrane potential of individual cells [1] and firing activity [2]. Monier et al. [1] suggested that the decrease of membrane potential variability is due to an increase in inhibitory activity associated with the stimulus onset. However, the origins of the decrease of firing activity variability (Fano factor) as well as its utility, are still unclear.

Our theoretical study demonstrated that increased inhibitory input to a neuron may decrease the membrane potential variability, despite increasing the variability of the input current [3]. Moreover, we showed that the spike frequency adaptation mechanism (SFA) of the neuron affects whether the neuron will fire spikes more or less regularly with higher inhibitory input.

In our continued effort we show that our previous results are relevant in classical models of recurrent neural networks with excitatory and inhibitory subpopulations, where the feedforward input in the network is purely excitatory and the inhibitory input is determined by the network properties. We used a recurrent neural network of exponential integrate-and-fire neurons with SFA [4]. Each neuron responded to a stimulus with different intensity (Fig. 1A-C), mitigating the effect of preferred and non-preferred stimuli. When the SFA was implemented by after-hyperpolarization current the Fano factor increased after the stimulus onset (Fig. 1D), while in networks with SFA implemented by voltage-gated sodium channel inactivation (dynamic firing threshold) the Fano factor decreased (Fig. 1E), even for neurons whose firing rate did not change upon stimulus onset. Next, we analyze to which

extent the differences between the SFA mechanisms affect information transmission properties.

Our work provides one of the possible mechanisms that can lead to neural variability quenching and analyzes its possible utility by evaluating information transmission capabilities.

## References

1. C. Monier, F. Chavane, P. Baudot, L. J. Graham, and Y. Frégnac. Orientation and Direction Selectivity of Synaptic Inputs in Visual Cortical Neurons. *Neuron*. 2003; 37(4):663–680, 2
2. M. M. Churchland et al., Stimulus onset quenches neural variability: a widespread cortical phenomenon. *Nature Neuroscience*. 2010; 13(3):369–78, 3
3. T. Barta and L. Kostal. Regular spiking in high-conductance states: The essential role of inhibition. *Physical Review E*. 2021; 103(2):022408, 2
4. Y. Zerlaut, S. Chemla, F. Chavane, and A. Destexhe. Modeling mesoscopic cortical dynamics using a mean-field model of conductance-based networks of adaptive exponential integrate-and-fire neurons. *Journal of Computational Neuroscience*. 2017; 44(1):45–61, 2

## P60 Joint tensor decomposition of neural activity across consecutive sessions reveals rich multiscale and behaviorally relevant dynamics in mouse V1

Lazaros Mitskopoulos<sup>\*1</sup>, Arno Onken<sup>1</sup>, Nina Kudryashova<sup>1</sup>

<sup>1</sup>University of Edinburgh, School of Informatics, Edinburgh, United Kingdom

\*Email: lazaro@smits@gmail.com

Neuronal population activity is remarkably adaptive in response to changing environmental or internal variables. Sensory processing even in the primary visual cortex has been shown to be modulated by behavior, spatial navigation signals and reward associations [1].

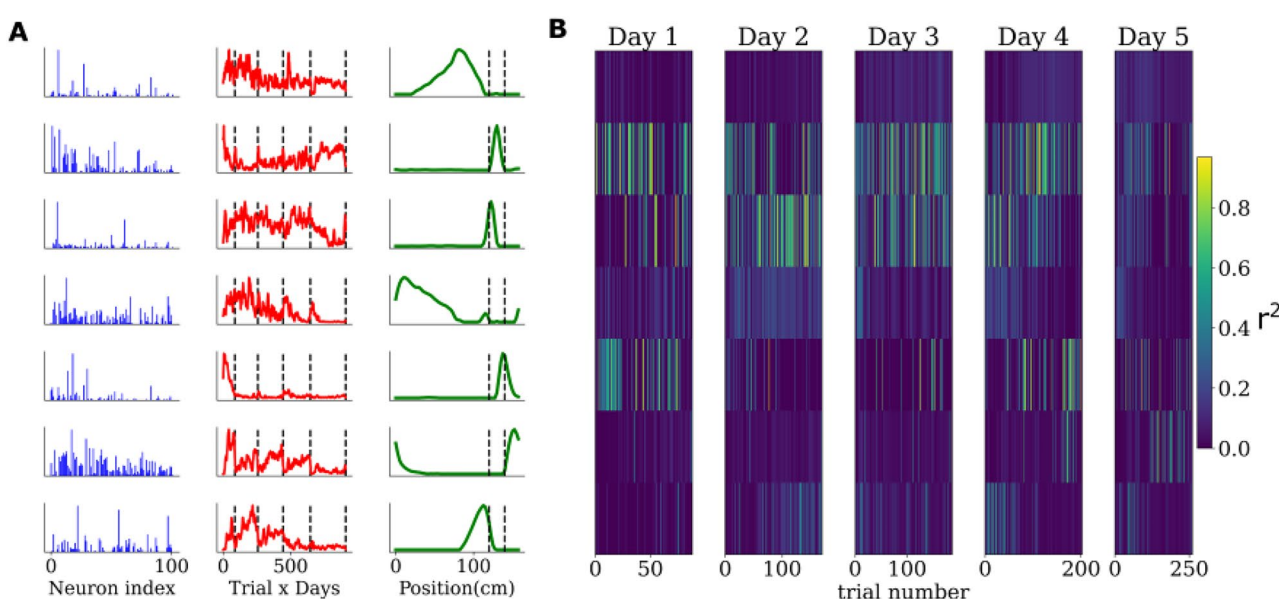


**Fig. 1** A NNTD of mouse V1 responses across recordings on 5 days. Example of 7 factors with neural (blue bars), trial-by-days (red lines), day change denoted by vertical dashed lines) and within-trial position

(cm) components (green lines). Reward zone was between 120 and 140 cm (dashed vertical lines). **B** Color plots for  $r^2$  values from linearly regressing lick counts in each trial on position components

Such adaptive changes can take place at multiple scales, ranging from fast dynamics unfolding within single trials to slow dynamics across days. In order to track these changes especially in the case of different recording sessions across days, one can leverage shared latent low dimensional structure that underlies population activity. Tensor decomposition methods such as PARAFAC [2] have shown considerable success in uncovering latent low dimensional descriptions of neural activity with components corresponding to cell assemblies, trial-to-trial gain modulation and within trial dynamics. However, PARAFAC assumes that each neural assembly is associated with only one within-trial dynamical component, and only one across-trial component. This can be restricting as cell assemblies might participate in multiple dynamical patterns. In contrast, Tucker-3 decomposition allows for such interactions through a core tensor that contains coefficients for linearly combining components. In this study we conducted non-negative Tucker-3 decomposition (NNTD) of neural responses in mouse V1 during navigation in a virtual reality environment (data from [3]). In these experiments, over the course of 5 days, mice learnt to lick at a specific location along a virtual corridor in order to receive a reward. We tracked changes in population responses by jointly decomposing data from all 5 days. Adding the non-negativity constraint allowed for a parts-based and biologically interpretable low dimensional description. To our knowledge, NNTD has never before been applied to neural recordings from multiple days. Our results demonstrate a rich picture of fast and slower collective processes operating in the population and interacting with one another. Some of the within-trial components (Fig. 1A shown in green) were tightly related to behavioral variables (Fig. 1B) despite the algorithm using only spiking data. Moreover, trial-by-days components (Fig. 1A, shown in red) displayed both dynamics spanning multiple days as well as distinct trajectories across trials of the same day, in spite of no explicit indication of day change in the fitting procedure. Importantly, our results were similar in all 4 animals included in the experiments, demonstrating robust discovery of behaviorally relevant neural dynamics.

## References

1. Flossmann, T., & Rochefort, N. L. Spatial navigation signals in rodent visual cortex. *Current opinion in neurobiology*. 2021; 67: 163–173.
2. Williams, A. H., Kim, T. H., Wang, F., Vyas, S., Ryu, S. I., Shenoy, K. V., Schnitzer, M., Kolda, T.G & Ganguli, S. Unsupervised discovery of demixed, low-dimensional neural dynamics across multiple timescales through tensor component analysis. *Neuron*. 2018; 98(6): 1099–1115.
3. Henschke, J. U., Dylida, E., Katsanevakis, D., Dupuy, N., Currie, S. P., Amvrosiadis, T., Pakan, J.M. & Rochefort, N. L. Reward association enhances stimulus-specific representations in primary visual cortex. *Current Biology*. 2020; 30(10): 1866–1880.

## P61 Brain state space reconstruction using LSTM

Yueyang Liu<sup>\*1</sup>, Artemio Soto-Breceda<sup>2</sup>, Mark Cook<sup>3</sup>, David Grayden<sup>2</sup>, Yun Zhao<sup>1</sup>, Phillipa Karoly<sup>2</sup>, Daniel Schmidt<sup>1</sup>, Levin Kuhlmann<sup>1</sup>

<sup>1</sup>Monash University, Department of Data Science and AI, Melbourne, Australia

<sup>2</sup>University of Melbourne, Department of Biomedical Engineering, Melbourne, Australia

<sup>3</sup>University of Melbourne, Department of Medicine, Melbourne, Australia

\*Email: [yueyang.liu@monash.edu](mailto:yueyang.liu@monash.edu)

Tracking the state and parameters of models is of great importance in the area of brain modelling. Normally, tracking is done via a

semi-analytical Kalman filtering derived specifically for NMMs (Neural Mass Model), for which an analytical solution is typically required [1]. We present an alternative, data-driven methodology for tracking the state and parameters of neural mass models from electromagnetic brain activity using deep learning techniques, specifically LSTM (Long Short-Term Memory) networks. Using this approach there is no need to guess the initial state, or determine, for example, the analytical solution to the Kalman gain and covariance, as would be needed in state and parameter estimation based on Kalman filtering.

The training data for the LSTM was the simulated electroencephalographic (EEG) data generated by an NMM given a wide range of parameters, to ensure that the LSTM model was trained with enough simulated data with different amplitude, frequency and shape [2]. The LSTM model was trained using a customized loss function, which forces the training to minimize not only the mean squared error between the prediction and the truth, but also the error between LSTM prediction and the model estimation [3, 4]. As a result, the trained model can simultaneously estimate the NMM state and parameters directly from EEG signals.

The testing result using simulation data over a wide range of the parameter space yielded an average R-squared between the true and estimated variables of approximately 0.97, while the Kalman filter had a negative R-squared due to fixed initialization. Additionally, the time efficiency is largely improved vis-à-vis Kalman filtering, as the average time to process a 110 s recording is around 0.3 s compared to 13 s using Kalman Filter. The same methodology was applied to other NMM to demonstrate the applicability of the methodology across different models. We have also applied it to real epileptic seizure EEG data. The results demonstrate the potential to detect or predict epileptic seizures, as the connectivity strength parameters vary significantly at the beginning of the seizure onset.

The proposed methodology has provided a novel approach to estimate the brain model state within a desired state space. It can provide time efficient estimation without considering the initial state or the analytical solution. On the other hand, we can apply other models as well, as long as it can generate enough training data. These methods enable the efficient tracking of NMM parameters and could potentially be used to determine the current dynamical state of an individual's brain from EEG data by determining where in the NMM bifurcation space the current brain activity lies.

## References

1. P. J. Karoly, L. Kuhlmann, D. Soudry, D. B. Grayden, M. J. Cook, and D. R. Freestone. Seizure pathways: A model-based investigation. *PLoS Computational Biology*. 2018 Oct; 14(10):e1006403
2. O. David and K. J. Friston. A neural mass model for MEG/EEG: coupling and neuronal dynamics. *NeuroImage*. 2003 Nov; 20(3): 1743–1755
3. J. F. Haderlein, I. M. Y. Mareels, A. Peterson, P. Z. Eskikand, A. N. Burkitt, and D. B. Grayden, ‘On the benefit of overparameterization in state reconstruction’, arXiv:2104.05775 [math], Apr. 2021, Accessed: Feb. 05, 2022. [Online]. Available: <http://arxiv.org/abs/2104.05775>
4. M. Raissi, P. Perdikaris, and G. E. Karniadakis, Physics-informed neural networks: A deep learning framework for solving forward and inverse problems involving nonlinear partial differential equations. *Journal of Computational Physics*. 2019 Feb; 378: 686–707.

## P62 Reproducing the macroscopic property of foraging behaviour using deep homeostatic reinforcement learning

Naoto Yoshida<sup>\*1</sup>, Yasuo Kuniyoshi<sup>2</sup>

<sup>1</sup>The University of Tokyo, Information Science and Technology, Tokyo, Japan

<sup>2</sup>The University of Tokyo, Department of Mechano-Informatics, Tokyo, Japan

\*Email: n-yoshida@isi.imi.i.u-tokyo.ac.jp

This study addresses the following question. "Using homeostasis as a computational principle, can macroscopic behavioral properties such as those exhibited by natural animals be realized from the motor control level?".

To tackle this problem, we specifically focus on the macroscopic behavior of animals in terms of the Geometric Framework (GF). GF is an experimental framework in nutritional ecology for assessing the animal's nutritional behavior [1-2]. A common setting of GF uses synthetic foods with different nutrient ratios (e.g., carbohydrate vs. protein), animals are allowed to eat them at will, and then the total amounts of the nutrient intake are recorded. In a theory of GF, if the agent is motivated to minimize the deviation from a nutritional target, the theory expects that there is a specific nonlinear relationship between the total amounts of the nutrient intake and the nutritional ratio [2]. In this study, we constructively show that this macroscopic property can be reproduced by using an autonomous agent with continuous motor control, which is optimized for homeostasis.

We took the following steps in the study: 1) We developed a specific method to scale up the Homeostatic reinforcement learning (HRL, explained below) framework, in which the applicability to high-dimensional problems was limited in previous studies [3]. 2) Using our method we trained agents in a foraging environment. We verified the behavioral homeostasis of trained agents in a test environment. 3) And then we evaluated the behavior of the agent by using a condition suggested in GF.

HRL is a computational framework, in which the reward function of RL is constructed to minimize the deviation of the internal physiological state of the body from its setpoint [3]. For step 1), we extended our previous method [4] to use deep convolutional architecture to enable the HRL agent to efficiently treat the vision inputs. For step

2), we trained our agent in the classical two-resource problem with continuous motor control (TRP, Figure-left) [4]. TRP is a simulation environment constructed using a physics simulator, which includes randomly-distributed two types of food resources with different nutritional settings in the arena. After the optimization, we conducted the behavioral experiment in which the agent's interoception is clamped at various nutritional conditions. The result assures the agent's behavioral homeostasis. Finally, in step 3), we tested the trained agent under a similar condition as GF. We evaluated the individual growth of nutrient intakes of the agent at each nutritional ratio. The result (Figure-right) suggests that the relationship between the total amounts of nutrient intake and the nutritional ratio qualitatively agrees with that of the observation in GF.

## References

1. Simpson, Stephen J., and David Raubenheimer. *The Nature of Nutrition*. Princeton university press. 2012.
2. Simpson, S. J., and D. Raubenheimer. The geometric analysis of feeding and nutrition: a user's guide. *Journal of Insect Physiology* 41.7, 1995: 545–553.
3. Keramati, Mehdi, and Boris Gutkin. Homeostatic reinforcement learning for integrating reward collection and physiological stability. *Elife* 3, 2014: e04811.
4. Yoshida, Naoto, et al. Embodiment perspective of reward definition for behavioural homeostasis. Deep RL Workshop NeurIPS2021. 2021.

## P63 Inhibitory Networks Explain Selective Attention in Dragonfly Target Detecting Neurons

Bernard Evans<sup>\*1</sup>, Steven Wiederman<sup>2</sup>, Benjamin Lancer<sup>3</sup>

<sup>1</sup>The University of Adelaide, School of Biomedicine, Adelaide, Australia

<sup>2</sup>The University of Adelaide, Adelaide Medical School, Adelaide, Australia

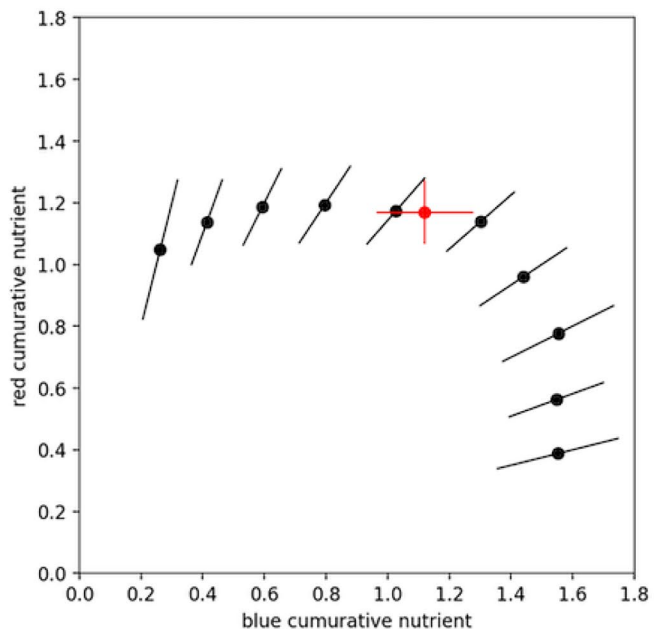
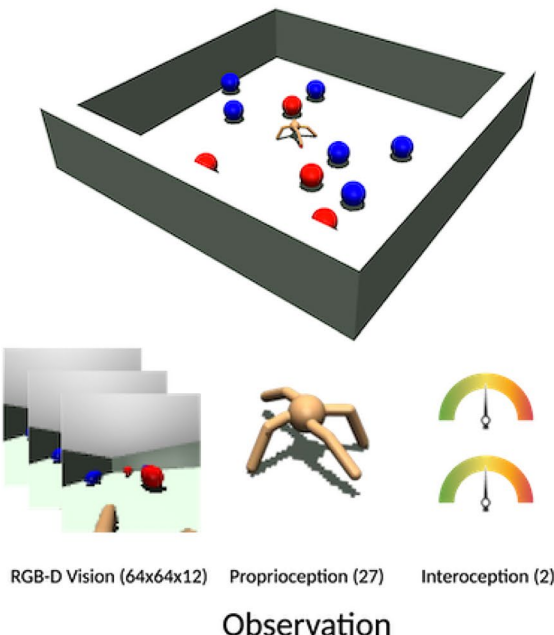


**Fig. 1** Left: The overview of our two-resource problem setting. Right: The result of the GF analysis of the agent after the training. Black points represent results with different nutrient ratios. The red point indicates the nutritional target of the agent when in the TRP

<sup>3</sup>The University of Queensland, Queensland Brain Institute, Brisbane, Australia

\*Email: bernard.evans@adelaide.edu.au

Aerial predators, such as the dragonfly, need to detect prey even when moving through complex, natural scenes. To do this, dragonflies must be able to distinguish desired prey items from potential distractors. This task is likely supported by a group of small target motion detector neurons (STMDs) found in the optic lobe of the dragonfly which respond to small moving features that subtend less than a few degrees. When presented with two or more targets, these neurons selectively attend to one, uninfluenced by the presence of other distractors [1]. Furthermore, these neurons can lock on to targets, ignoring more salient distractors while maintaining a lower overall response [2, 3]. Computational models which emulate the basic behavior of STMDs have been well established [4] but none yet account for selective attention. Here we present an elaborated STMD model using both excitatory reinforcement and inhibitory feedback mechanisms which reproduce the neuronal behaviors observed in dragonfly target detecting neurons. We further demonstrate that selective attention improves target discriminability in cluttered scenes. Our results provide insights into insect neurophysiology and demonstrate the potential of this algorithm for implementation in artificial visual systems and robotic applications geared to highly cluttered scenarios.

## References

- Wiederman SD, O'Carroll DC. Selective Attention in an Insect Visual Neuron. *Current Biology*. 2013; 23: 156–161
  - Lancer BH, Evans BJE, Fabian JM, O'Carroll DC, Wiederman SD. A target-detecting visual neuron in the dragonfly locks on to selectively attended targets. *Journal of Neuroscience*. 39 (43): 8497–8509.
  - Evans BJE, O'Carroll DC, Fabian JM, Wiederman SD. Dragonfly Neurons Attend to Targets within Natural Scenes. *Front. Cell. Neurosci.* 2022; 16: 857071
- Frequency coding is one of the basic forms of communication within the nervous system. It assumes that the frequency of the action potentials changes according to the stimulus intensity. In the simplest of the neuronal models, no saturation firing frequency exists, implying that the firing frequency would increase indefinitely with increasing stimulus intensity. This implication is in contrast with the experimentally observed behavior. Our work presents a comparison of the intrinsic saturation of firing frequency in four simple neuronal models: leaky integrate-and-fire model, leaky integrate-and-fire model with reversal potentials, two point leaky integrate-and-fire model, and a two point leaky integrate-and-fire model with reversal potentials. We observe that in the single compartment models, the reversal potential increases the slope of the "firing rate vs input" curve, limits the asymptotic voltage, but does not necessarily induce saturation of the firing frequency. The two compartment model without the reversal potential does not limit the firing frequency nor the asymptotic voltage. The case of excitatory inputs is considered first and followed by the case of both excitatory and inhibitory inputs. The two compartment model with the reversal potential, however, induces the saturation of

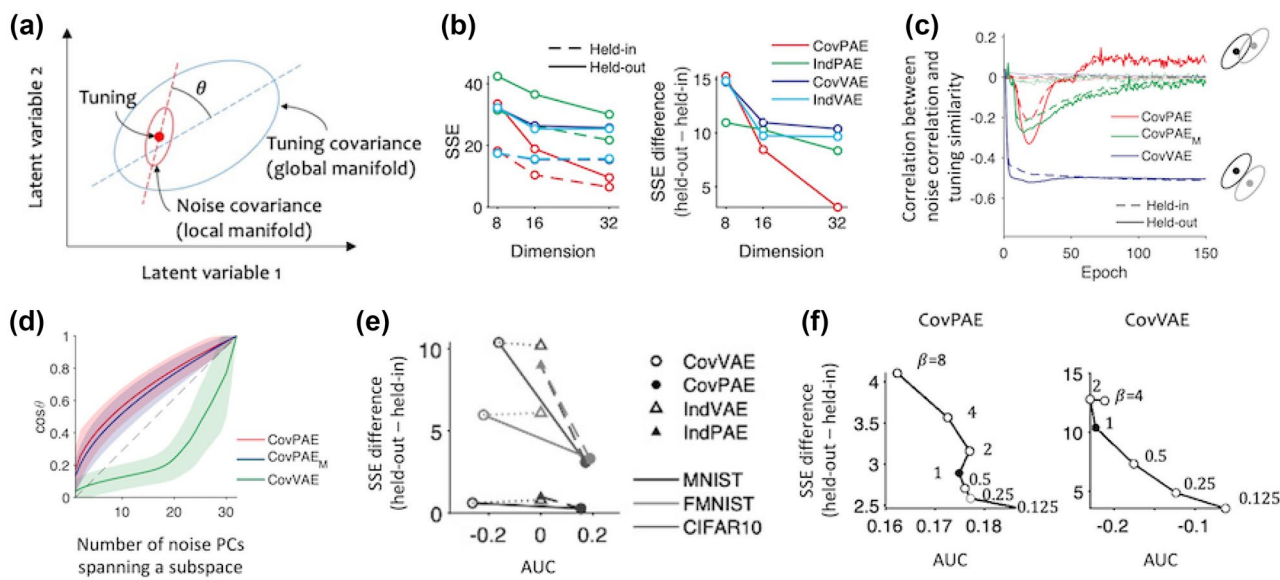


**Fig. 1** **a** Hypothesis. **b** Model performance. **c** Learned structure of noise correlation. **d** Noise-tuning alignment result. Shaded areas indicate across test stimuli. **e** Relationship between generalization perfor-

mance and area under curve – 0.5 (AUC). **f** Same as in (e), varying with the regularizer weight, beta. (**b–d, f**) Data from MNIST

## P64 Intrinsic firing frequency in single and multi-compartment neuronal models

Rimjhim Tomar<sup>\*1</sup>, Charles E Smith<sup>2</sup>, Petr Lansky<sup>3</sup>

<sup>1</sup>Second Medical Faculty, Charles University and Institute of Physiology, Czech Academy of Sciences, Prague, Czechia

<sup>2</sup>North Carolina State University, Department of Statistics, Raleigh, United States of America

<sup>3</sup>Institute of Physiology, Czech Academy of Sciences, Prague, Czechia

\*Email: rimjhimtomar28@gmail.com

Frequency coding is one of the basic forms of communication within the nervous system. It assumes that the frequency of the action potentials changes according to the stimulus intensity. In the simplest of the neuronal models, no saturation firing frequency exists, implying that the firing frequency would increase indefinitely with increasing stimulus intensity. This implication is in contrast with the experimentally observed behavior. Our work presents a comparison of the intrinsic saturation of firing frequency in four simple neuronal models: leaky integrate-and-fire model, leaky integrate-and-fire model with reversal potentials, two point leaky integrate-and-fire model, and a two point leaky integrate-and-fire model with reversal potentials.

We observe that in the single compartment models, the reversal potential increases the slope of the "firing rate vs input" curve, limits the asymptotic voltage, but does not necessarily induce saturation of the firing frequency. The two compartment model without the reversal potential does not limit the firing frequency nor the asymptotic voltage. The case of excitatory inputs is considered first and followed by the case of both excitatory and inhibitory inputs. The two compartment model with the reversal potential, however, induces the saturation of

firing frequency as well as of the asymptotic voltage. It is the simplest neuronal model with an intrinsic saturation of the firing frequency.

### Acknowledgments

This work was supported by the Czech Science Foundation project 20-10251S, Charles University project GA UK 373121 and by North Carolina State University.

### P65 Generalizable perceptual embedding with noise-tuning alignment

Jungwon Ryu<sup>\*1</sup>, Myoung Hoon Ha<sup>\*\*1</sup>, Sang Wan Lee<sup>1,2</sup>

<sup>1</sup>Korea Advanced Institute of Science and Technology, Center for Neuroscience-inspired AI, Daejeon, South Korea

<sup>2</sup>Korea Advanced Institute of Science and Technology, Department of Bio and Brain Engineering, Daejeon, South Korea

\*Email: rjungwon@gmail.com

\*\*Email: mh.ha.soar@gmail.com

Our perception of the external world is always limited and ambiguous, and the activities of sensory neurons are inherently noisy. Such exogenous and endogenous uncertainty factors pose a fundamental challenge for sensory coding. Despite the earlier studies for understanding how biological vision resolves these issues, little is known about how it can learn accurate and generalizable representations.

Two prominent computational approaches include identifying the underlying statistical regularities across the stimuli via dimensionality reduction and developing the model that encodes the stimulus probabilistically.

Here, adopting the perspective of the well-known requisite variety principle, we investigated the effect of the encoded uncertainty on the statistical structure of the stimuli that the model has learned. Specifically, we tested whether and how the global geometrical distribution of the latent variables is aligned with the local latent probability distribution that encodes the input stimulus. For this, we present a new computational model accommodating the noise-tuning alignment, which auto-encodes the input stimuli using the conditional latent distributions (Fig. 1A). We defined the tuning and noise covariances as the means and the covariances of the latent distributions, which specify the local manifold in the latent space for the given input. Whereas the tuning covariance is defined as the covariances of the tunings for the given mini-batch of stimuli, capturing the global structure of the latent manifold. Then we tested whether and how the local and global manifolds are aligned, and investigated their relationship with the generalization performance in image reconstruction tasks.

Simulations with three real-world benchmark datasets revealed that our models outperformed baseline probabilistic models such as variational autoencoders (Fig. 1B). To understand the learned noise covariance structure, we first computed the correlations between the noise covariances and the tuning similarity of the latent variable pairs. Interestingly, we found that the learning process of our model encourages non-negative correlation, as is often found in the primate visual cortex [1], but not in VAE models (Fig. 1C). When measuring the alignment angle between the tuning covariance and noise covariance, we found that two subspaces are more strongly aligned in our model, such that the primary noise principal components (PC) are more aligned with the primary tuning PC that explains stimulus variability, consistent with the recent single-cell studies [2]. On the contrary, these patterns were not identified in VAEs (Fig. 1S). Further, we found the amount of alignment is negatively correlated with the generalization error across datasets and models (Fig. 1E), and even within each model (Fig. 1F). Our findings suggest that noise-tuning alignment helps the stimulus

generalization, expanding the current understanding of the correlated neuronal noise [3–5].

### Acknowledgments

This work was supported by an IITP grant funded by the Korea government (MSIT) (No. 2019-0-01371, Development of brain-inspired AI with human-like intelligence), the National Research Foundation of Korea (NRF) grant funded by MSIT (NRF- 2019M3E5D2A0106626721), and a grant of the KAIST-KT joint research project through AI2XL Laboratory, Institute of Convergence Technology, funded by KT (No. 3, Genie Brain).

### References

- Smith MA, Kohn A. Spatial and temporal scales of neuronal correlation in primary visual cortex. *The Journal of Neuroscience*. 2008; 28(48):12591–603
- Montijn JS, Liu RG, Aschner A, Kohn A, Latham PE, Pouget A. Strong information-limiting correlations in early visual areas. *bioRxiv*. 2019; 842724
- Rumyantsev OI, Lecoq JA, Hernandez O, Zhang Y, Savall J, et al. Fundamental bounds on the fidelity of sensory cortical coding. *Nature*. 2020; 580(7801):100–105
- Valente M, Pica G, Bondanelli G, Moroni M, Runyan CA, et al. Correlations enhance the behavioral readout of neural population activity in association cortex. *Nature Neuroscience*. 2021; 1–12
- Moreno-Bote R, Beck JM, Kanitscheider I, Pitkow X, Latham P, Pouget A. Information-limiting correlations. *Nature Neuroscience*. 2014; 17(10):1410–17

### P66 Inferring effective networks of spiking neurons using a continuous-time estimator of transfer entropy

David Shorten<sup>1</sup>, Viola Priesemann<sup>2</sup>, Michael Wibral<sup>3</sup>, Joseph Lizier<sup>\*1</sup>

<sup>1</sup>The University of Sydney, Centre for Complex Systems, Sydney, Australia

<sup>2</sup>MPI for Dynamics and Self-Organization, Göttingen, Germany

<sup>3</sup>Georg-August-Universität, Campus Institut für Dynamik biologischer Netzwerke, Göttingen, Germany

\*Email: joseph.lizier@sydney.edu.au

When analyzing high-dimensional time-series datasets, the inference of effective networks has proven to be a valuable modelling technique. This technique produces networks where each target node is associated with a set of source nodes that are capable of providing explanatory power for its dynamics. Multivariate Transfer Entropy (TE) has proven to be a popular and effective tool for inferring these networks [1]. Recently, a continuous-time estimator of TE for event-based data such as spike trains has been developed which, in more efficiently representing event data in terms of inter-event intervals, is significantly more capable of measuring multivariate interactions [2]. The new estimator thus presents an opportunity to use TE for the inference of effective networks from spike trains, and we demonstrate in this paper for the first time its efficacy at this task. Using data generated from models of spiking neurons --- for which the ground-truth connectivity is known --- we demonstrate the accuracy of this approach in various dynamical regimes. We further show that it exhibits far superior performance to a pairwise TE-based approach at inference as well as a recently proposed convolutional neural network approach. Moreover, comparison with Generalised Linear Models (GLMs), which are commonly applied to spike-train data, showed clear benefits, particularly in cases of high synchrony. Finally, we demonstrate its utility in gleaning insight from recordings of *in vitro* spiking neurons, revealing

similar early lock-ins of information flow structure to directed functional networks [3], and at the same time identifying a higher proportion of links between nodes that are physically close together than in the corresponding directed functional networks.

## References

1. Novelli L., Wollstadt P., Mediano P., Wibral M., Lizier J. T. Large-scale directed network inference with multivariate transfer entropy and hierarchical statistical testing. *Network Neuroscience*. 2019; 3:827–847
2. Shorten D. P., Spinney R. E., Lizier J. T. Estimating transfer entropy in continuous time between neural spike trains or other event-based data. *PLoS Computational Biology*. 2021; 17:e1008054
3. Shorten D. P., Priesemann V., Wibral M., Lizier J. T. Early lock-in of structured and specialised information flows during neural development. *eLife*. 2022.

## P67 Electrophysiological models of right atrial ganglionic plexus principal neurons identified from transcriptomics data

Suranjana Gupta<sup>\*1</sup>, Adam J. H. Newton<sup>1</sup>, Alison Moss<sup>2</sup>, James S. Schwarber<sup>2</sup>, Rajanikanth Vadigepalli<sup>2</sup>, William W Lytton<sup>1</sup>

<sup>1</sup>SUNY Downstate Health Sciences University, Department of Physiology and Pharmacology, Brooklyn, NY, United States of America

<sup>2</sup>Thomas Jefferson University, Pathology, Anatomy and Cell Biology, Philadelphia, United States of America

\*Email: suranjana.gupta@ieee.org

The Right Atrial Ganglionic Plexus (RAGP), a component of the Intrinsic Cardiac Nervous System (ICNS), is a critical regulator of heart rate through control of sinoatrial node activity. The neurons of RAGP help control cardiac response to vagal activation. We developed single-compartment, biophysically-constrained computational models of RAGP principal neurons using ion-channel combinations that were derived from HT-qPCR (High Throughput quantitative Polymerase Chain Reaction) transcriptomics data of 405 single neurons of Yucatan minipig RAGP. Out of the 241 genes in the transcriptomics map, we identified 15 genes that encode ion channel proteins: voltage-gated sodium (Scn1a, Nav 1.1), voltage-gated potassium (Kcnc1, Kv 3.1;Kcn1, Kv 1.1), voltage-gated calcium [Cacna1a, Cav 2.1 (P/Q);Cacna1b, Cav 2.2 (N);Cacna1c, Cav 1.2 (L);Cacna1d, Cav 1.3 (L);Cacna1g, Cav 3.1 (T);Cacna1i,Cav 3.3 (T)], hyperpolarization activated (HCN1,HCN2,HCN3,HCN4) and inward rectifying potassium channels (Kcnj3, Kir 3.1). The corresponding Hodgkin-Huxley-based ion channel models were mined from several databases: ModelDB, Channelpedia, Ion Channel Genealogy, and PubMed. Comparative simulations were run on NetPyNE/NEURON software to shortlist a single model per gene that would best represent the channel's dynamic response in the assembled biophysical model of the RAGP neuron. After thresholding the transcriptomics map, 104 neurons with unique ion channel gene combinations emerged from the 405 cells. Our electrophysiological models elicited 3 distinct firing profiles in response to a current clamp stimulus: 65% elicited a single-spike phasic response, 2% elicited burst firing, and 21% elicited tonic firing (of which 33% continued firing post-stimulus).The firing frequencies increase by ~ 5 Hz for every 0.1 nA increase in the current clamp stimulus. The phasic, burst and tonic excitability profiles seen are comparable to those observed experimentally in minipig and rat. We next aim to expand our single cell models into a network and incorporate neuromodulatory inputs.

## Acknowledgements

We acknowledge the National Institutes of Health Common Fund SPARC Program (Grant OT2 OD030534) for funding our research work.

## P68 What determines the frequency and the duration of intermittent epileptic episodes in local cortical networks?

Nicolo Meneghetti<sup>\*1</sup>, Alberto Mazzoni<sup>1</sup>, Federico d'Alba<sup>2</sup>, Riccardo Mannella<sup>2</sup>

<sup>1</sup>Scuola Superiore Sant'Anna Pisa, The Biorobotics Institute and Department of Excellence for Robotics and AI, Pisa, Italy

<sup>2</sup>University of Pisa, Department of Physics, Pisa, Italy

\*Email: nicolo.meneghetti@santannapisa.it

Epilepsy is one of the most common brain disorders, causing serious disability and premature death worldwide. This disorder is generally thought to be due to an unbalance between inhibition and excitation leading to runaway activity. For instance, previous computational models [1] showed that a reduction of GABAergic transmissions in an asynchronous spiking network might lead to the emergence of seizure-like episodes, characterized by the surge of an excessive and synchronous neural activity. However, less is known about the dynamics of the transition between physiological asynchronous and pathological epileptic neuronal activity. Cortical models can contribute to shed light on the complex pathophysiological factors leading to epileptogenesis, helping the interpretation and possibly the prediction of epileptiform brain activity.

We developed a randomly connected network of leaky integrate-and-fire neurons simulating local visual cortex activity in epilepsy, starting from previous works describing a balanced condition of the same network [2]. As expected, progressively decreasing GABAergic conductances eventually led the network to display epileptic neural activity. However, for intermediate values, the network displayed a transition regime characterized by the coexistence of asynchronous and episodic seizure-like activity. We focused our analysis on this transition regime through both simulations and analytical analysis. The build-up phase of each sporadic episode of epileptic activity was composed by several cycles, observed as local maxima of the instantaneous population firing activity. In each cycles an increasing fraction of neurons fired, leading the average membrane potential to slowly increase. Once a population threshold of about 70% of excitatory neurons were fired, the build-up phase came to an end and a complete epileptic phase involving the whole network began. We found the duration of the build-up phase to be dependent on three factors: (i) the strength of GABA conductances; (ii) the external excitatory drive; (iii) the size of the network. The build-up phase duration was proportional to GABAergic synaptic strength and to the network size, while it was inversely proportional to the strength of the external excitatory drive. Furthermore, increasing the network size also led to a narrow range of GABA strength values displaying the transition regime. On the other hand, the duration of the epileptic episodes depended on the relative dynamics of excitatory and inhibitory synapses, as it depended on the built up of a strong inhibitory response. As a result, the network displayed epileptic activity until the inhibitory neurons managed to silence the excitatory ones, ending therefore the ictal regime. Coherently, decreasing the strength of the GABAergic synapses the inhibitory response lagged behind its glutamatergic counterpart, leading to an increase of both epileptic episodes' duration and frequency of occurrence.

## Acknowledgements

This work was funded by the Italian Ministry of Research (MIUR) through PRIN-2017 “PROTECTION” (project 20178L7WRS).

## References

1. F. Wendling, et al. Epileptic fast activity can be explained by a model of impaired GABAergic dendritic inhibition. *European J of Neuroscience*. 2002
2. Nicolas Brunel and Xiao-Jing Wang. What Determines the Frequency of Fast Network Oscillations With Irregular Neural Discharges? I. Synaptic Dynamics and Excitation-Inhibition Balance. *Journal of Neurophysiology*. 2003

## P69 Simulating Temporal Interference Stimulation

Joseph Tharayil<sup>\*1</sup>, Michael Reimann<sup>1</sup>, Esra Neufeld<sup>2</sup>, Felix Schürmann<sup>1</sup>, Henry Markram<sup>1</sup>

<sup>1</sup>École polytechnique fédérale de Lausanne (EPFL), Campus Biotech, Blue Brain Project, Geneva, Switzerland

<sup>2</sup>IT'IS Foundation, Computational Life Sciences Division, Zurich, Switzerland

\*Email: joseph.tharayil@epfl.ch

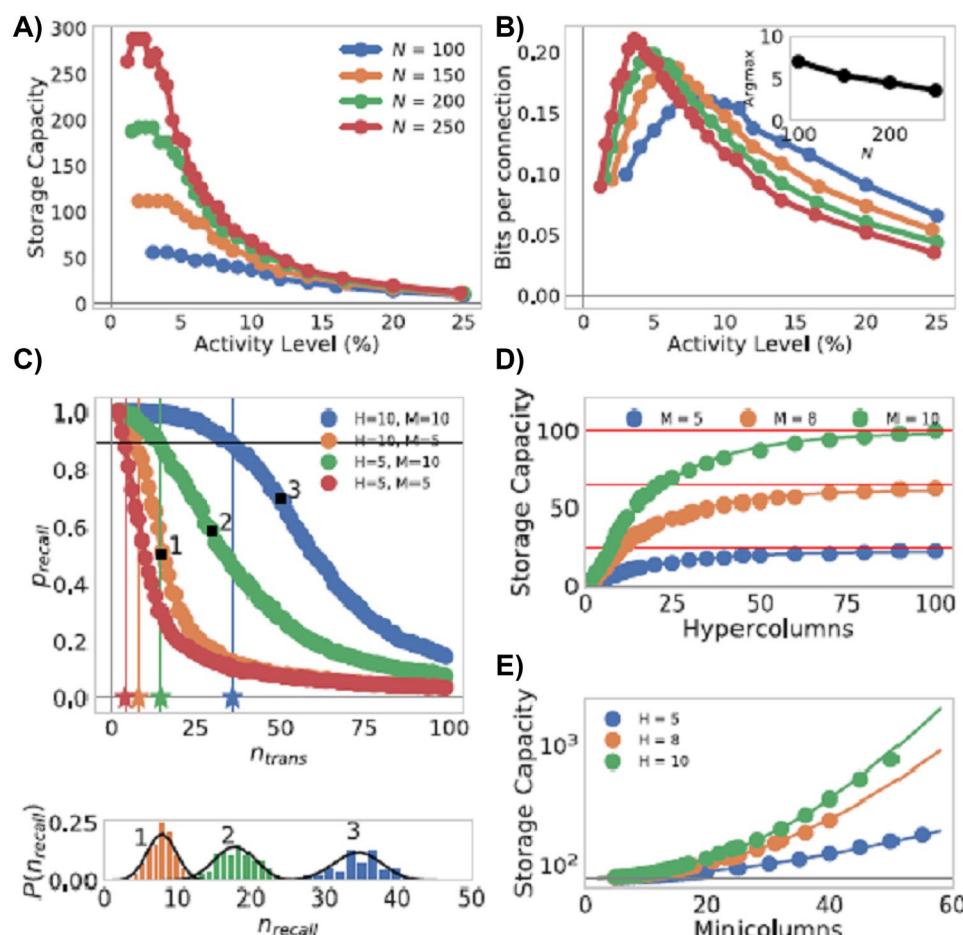
Temporal interference (TI) stimulation is a method of noninvasive brain stimulation, whereby two high-frequency currents, with

frequencies offset by a small amount, are applied transcranially. The superposition of the resulting fields has an envelope modulated at the offset frequency between the two current sources, with a modulation amplitude that varies spatially depending on the head anatomy and dielectric properties, and the positioning of the electrodes. While neurons are not believed to respond to the high frequency carrier signals, they are expected to respond to the lower-frequency amplitude modulation. By varying the offset frequency and the relative current scaling, TI can apply various stimulus patterns. The mechanism of action of TI stimulation is still debated; while TI is commonly believed to function via low-pass filtering of the TI signal by the neural membrane, others believe that ion-channel mediated rectification of the stimulus is required.

We simulate the impact, on individual neurons and neural circuits in the rat brain, of theta-burst stimulation applied using TI (TBS; 100 Hz pulses, 5 Hz repetition rate, two second duration). An MRI-derived finite element model of a detailed rat head anatomy is used to identify electrode combinations that produce peak envelope modulation amplitudes in selected regions of interest (cortex and striatum). The resulting extracellular fields are coupled with multi-compartment neuron models, and their simulated electrical activity was recorded. The neuron models were simultaneously subjected to realistic synaptic inputs, both excitatory and inhibitory.

We find that TBS is able to evoke spiking activity in our model, at realistic TI exposure strengths. We characterized the sensitivity to exposure strength and orientation, as well as to stimulus frequency and the level of background activity. Our results may help to provide mechanistic explanations for observed TBS neuromodulation, and to optimize stimulation parameters.

**Fig. 1** Storage capacity of an attractor memory model with BCPNN learning: **A** the effect of sparse activity; **B** information per synaptic connection; **C–E** the effect of the network architecture on the probability of recall for simple transitions (**C**) and storage capacity (**D, E**)



## P70 Storing long and overlapping sequences in an attractor memory network with Bayesian-Hebbian learning

Anders Lansner<sup>1</sup>, Paweł Herman<sup>\*2</sup>, Ramón Martínez<sup>3</sup>

<sup>1</sup>Stockholm University, KTH Royal Institute of Technology, Stockholm, Sweden

<sup>2</sup>KTH Royal Institute of Technology, Digital Futures, Stockholm, Sweden

<sup>3</sup>KTH Royal Institute of Technology, Computational Science and Technology, Stockholm, Sweden

\*Email: paherman@kth.se

Sequential dynamics is considered as one of the hallmarks of complex brain phenomena. In fact, many behavioral patterns and cognitive processes exhibit remarkable sequential characteristics, often reflected in neural activity. Although there are likely multiple biological mechanisms involved in generating sequential activity in the brain, we focus on functional implications of associative synaptic learning underlying sequence encoding at a network level. Despite many computational attempts at robust learning of multiple sequences of memory patterns, there has been relatively little emphasis on sequence disambiguation and on the capacity to store many long overlapping sequential memory patterns.

To address the challenge of robust sequence learning that deals with inherent noise and cross-talk between overlapping sequences we have devised, based on our previous work on synaptic learning in cortical attractor models [2], a parsimonious non-spiking attractor memory

network with the Hebbian-like Bayesian Confidence Propagating Neural Network (BCPNN) learning rule relying on synaptic traces with asymmetric temporal characteristics [1]. In particular, learning occurs through the accumulation of evidence for both independent and correlated activity of the network units and weighting these contributions against each other to estimate the strength of connecting weights. The sequential binding of static memory patterns into dynamic trajectories of quasi-stable attractors is then accomplished by the synaptic traces where contiguously active units develop excitatory connections in the direction of sequence propagation [1-2]. The remaining issue addressed in the work reported here is concerned with the scaling properties of this model framework and the resulting storage capacity parameterized by the network's modular architecture, synaptic properties and sparseness of neural representations. To investigate this question we first studied simple temporal transitions in the network (quantified by the probability of recall) and then generalized the computations and simulations for longer sequences. Since the configuration of network modularity was observed to play an important role in sequence disambiguation [1], we measured the storage capacity for sequential patterns at varying number of BCPNN hypercolumns and encapsulated units. Unsurprisingly, the larger the network the more sequences were reliably stored. With the increasing number of transitions imposed by longer sequences, the probability of recall of individual transitions gracefully decayed (Fig. 1C). Importantly, the key factor contributing to the network's scaling capabilities was the number of units per module (rather than modules themselves, Fig. 1D, E) and thus the sparseness of network's activity (Fig. 1A). Consequently, we demonstrated that the maximum information stored per projection was achieved by larger networks for lower levels of the network activity (Fig. 1B).

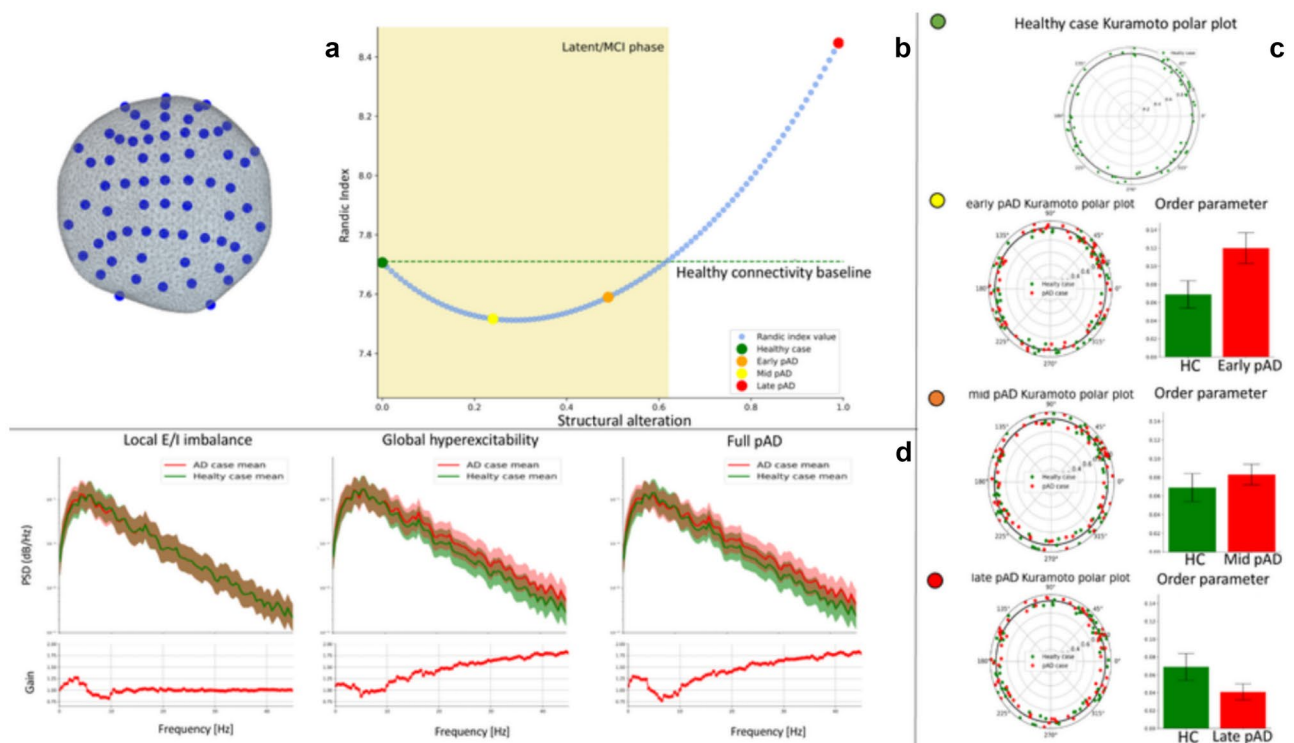


**Fig. 1** **a** Standard sensor grid utilized in the virtual brain. **b** Randic Index for 100 SC matrices, which portray disease progression through structural alterations. **c** FC calculations by means of Kuramato Index

of simulated EEG time series. **d** Power spectra distribution (PSD) for different pathological pAD effects (left, center) and full pAD case (right)

### Acknowledgments

Swedish Research Council: Swedish Research Links 2016-05871 and 2018-05360; Swedishe-Science Research Centre (SeRC); Erasmus Mundus EuroSPIN.

### References

1. Martinez, RH., Lansner, A., Herman, P. Probabilistic associative learning suffices for learning the temporal structure of multiple sequences. *PLoS ONE*. 2019; 14(8): e0220161
2. Tully, P., Lindén, H., Hennig, MH., Lansner, A. Spike-based Bayesian-Hebbian learning of temporal sequences. *PLOS Comp Biol*, 2016.

### P71 Insights on the dynamic origin of EEG pathological biomarkers of prodromic states of Alzheimer's Disease by using The Virtual Brain framework

Lorenzo Gaetano Amato<sup>1</sup>, Alberto Vergani<sup>\*2</sup>, Alberto Mazzoni<sup>2</sup>

<sup>1</sup>University of Pisa, Department of Physics, Pisa, Italy

<sup>2</sup>Scuola Superiore Sant'Anna Pisa, The Biorobotics Institute and Department of Excellence for Robotics and AI, Pisa, Italy

\*Email: albertoarturo.vergani@santannapisa.it

Alzheimer's disease (AD) is a neurological pathology constituting 60% of all cases of dementia. It impairs patients on multiple levels, altering both mesoscopic dynamics and macroscopic brain structures. These anomalies lead to biophysical hallmarks that are utilized to corroborate diagnosis in the overt phase. Due to the degenerative nature of AD, finding the signatures of the pathology before the onset is a crucial step: in fact, clinicians are interested in characterizing its prodromic phase (pAD), in which mild alterations of brain structures and functionalities are present even in the absence of evident symptoms [1]. In particular, there is no agreement on how the pAD condition could be estimated from non-invasive recordings as EEG. To find EEG biomarkers of pAD it is necessary to infer a direct relation between scalp recordings and brain degenerations.

Here we propose a The Virtual Brain model (TVB) [2] of pAD to estimate the associated EEG biomarkers. We modified the standard TVB model to take into account networks alterations known to be associated with pAD. For each of the alterations we assessed the specific effect on network dynamics and functional connectivity patterns. pAD alterations taken into account were: i) increase of the excitation/inhibition ratio (both global and localized in regions firstly affected by the disease), ii) decrease of long-range structural connectivity and relative neuroplastic adjustments [3].

In our analysis, we have been able to link global hyperexcitability to specific changes in EEG spectral components and in their functional connectivity (FC). FC was also heavily affected by structural alterations that caused a significant amount of rewiring. In particular we found that the Randic index [4] describes the relationship between functional to structural connectivity, allowing a classification for disease staging based on FC analysis.

In a context of invasive and high cost exams used for dementia diagnosis (e.g., PET and CSF), these results, instead, pave the way for the usage of low cost and portable devices as EEG to infer the neurodegeneration stage from FC patterns, combined with graph theoretical quantities as diagnostic meters for disease progression.

### Acknowledgments

This project is funded by Tuscany Region - PRredicting the EVolution of SubjectIvE Cognitive Decline to Alzheimer's Disease With machine learning – PREVIEW - CUP. D18D2000130.

### References

1. R. A. Sperling, J. Karlawish, and K. A. Johnson. Preclinical Alzheimer disease the challenges ahead. *Nature Reviews Neurology*. 2013; 9(1): 54–58
2. P. Sanz Leon, S. A. Knock, M. M. Woodman, L. Domide, J. Mersmann, A. R. McIntosh, and V. Jirsa. The virtual brain: a simulator of primate brain network dynamics. *Frontiers in Neuroinformatics*. 2013; 7:10
3. A. Fornito, A. Zalesky, and M. Breakspear. The connectomics of brain disorders. *Nature Reviews Neuroscience*. 2015; 16(3): 159–172
4. X. Li and Y. Shi. A survey on the randic index. *MATCH Communications in Mathematical and in Computer Chemistry*. 2008; 59(4): 127–156

### P72 SpikeDecoder: An explainable architecture for the temporal-spatial pattern extraction and position prediction

Yi Wang<sup>\*1</sup>, Roman Boehringer<sup>1</sup>, Thomas McHugh<sup>1</sup>

<sup>1</sup>RIKEN Center for Brain Science, Wako-shi, Japan

\*Email: yi.wang@riken.jp

Neural decoding is a powerful way to decipher and understand the links between neural activity and behavior, internal states, and brain mechanisms. Decoding the positions of mice using electrophysiological recordings in the hippocampus is one of the benchmark tasks due to the ‘internal–external’ corresponding relationship between place fields and physical locations. Recent studies have decoded the location from the large-scale processed, or sorted, electrophysiological data using unexplainable convolutional [1] and recurrent neural networks [2]. However, these models did not fully analyze and extract the characteristics in raw data, which limits their generalization. How to design an explainable and generalizable architecture that fully explores the temporal-spatial patterns embedded in the raw unsorted spike waveforms?

In our experiment, mice ( $n=4$ ) were implanted with an eight tetrode microdrive targeting the hippocampus. After recovery, the mice explored a 1.7 m linear track for 10 min. Spike waveforms were acquired via a Digital Lynx 4SX system, and an overhead camera tracked real-time position (Fig. 1A). Each raw unsorted spike waveform forms a channel  $\times$  time matrix. Waveforms from one tetrode form a tensor. There are eight tensors corresponding to the eight tetrodes. Each input sample is the collection of the eight sub-tensors cut by a random 1-s duration (Fig. 1B).

We proposed a two-stage ‘extraction-fusion’ architecture to benefit from the temporal-spatial structure of the waveforms and the separation by tetrodes. In the first stage (Fig. 1B), eight tetrode-specific pattern extractors detect temporal-spatial features in the waveforms. Specifically, in the dashed box, each 2-D waveform from tetrode one is fed into the temporal filtering layer, followed by the spatial filtering layer. In the second stage, a fusion layer fuses the information from different tetrodes, followed by dense layers to predict the current position.

Experiment results show that SpikeDecoder predicts the positions of the mice ( $n=4$ ) with an average Euclidian error of 24.8 cm, 17.2 cm, 17.8 cm, and 16.9 cm. The predictions correlate well with the true trajectory for a single mouse (Fig. 1c). Our model, which mines the raw spike waveform deeply with less spatial sampling (8 tetrodes), outperforms others that used 32-tetrode wavelet-preprocessed local field potentials [1] and 16-tetrodes sorted population vectors [2].

Finally, we analyze the decision of SpikeDecoder by occlusion analysis and Layer-wise Relevance Propagation. We could identify the tetrodes that contribute significantly, and the place fields captured by the model. We conclude that SpikeDecoder predicts

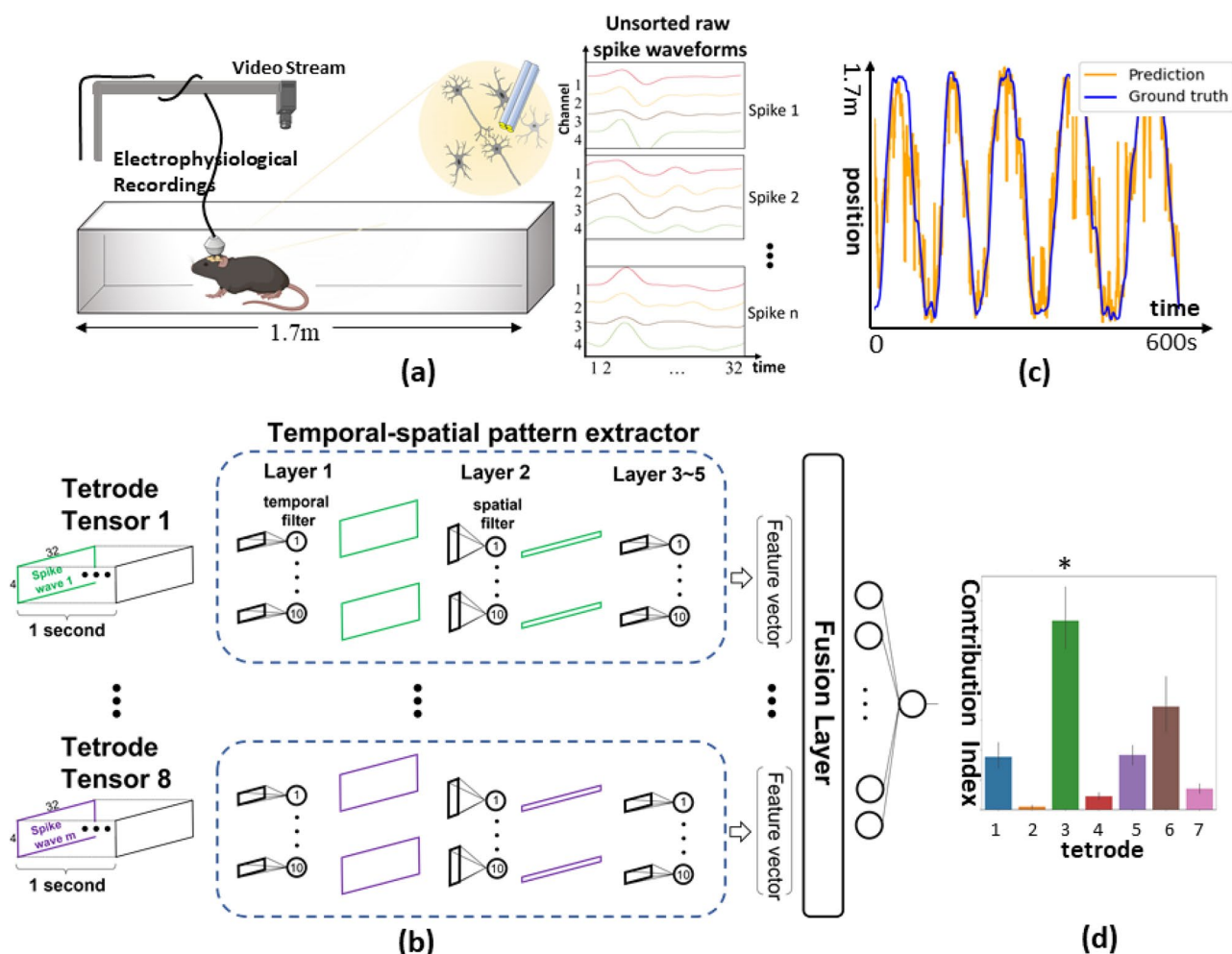


**Fig. 1** **a** The experiment setup and the raw waveforms, **b** The architecture of SpikeDecoder, **c** The position prediction, **d** The contribution of each tetrode by the network decision analysis

the positions mainly by the place fields of the place cells. Notably, it automatically uses unsorted data to complete spike sorting and ‘pattern-position’ matching. Moreover, it stems from, but is not limited, to position prediction. SpikeDecoder can be generalized to predict any behaviors or internal states that correlate with neural activities.

#### Acknowledgments

This work was support by a Grant-in-Aid for Scientific Research from MEXT (19H05646; T.J.M) and RIKEN CBS.

#### References

1. Frey M. Interpreting wide-band neural activity using convolutional neural networks. *Elife*. 2021; 10:e66551.
2. Tampuu A. Efficient neural decoding of self-location with a deep recurrent network. *PLoS computational biology*. 2019; 15(2):e1006822.

#### P73 Different behavioral strategies revealed by recurrent neural networks trained in multisensory integration tasks

Shirin Dora<sup>1</sup>, Amparo Gilhuis<sup>2</sup>, Cyriel Pennartz<sup>2</sup>, Jorge Mejias<sup>\*2</sup>

<sup>1</sup>Loughborough University, Department of Computer Science, Loughborough, United Kingdom

<sup>2</sup>University of Amsterdam, Swammerdam Institute for Life Sciences, Amsterdam, Netherlands

\*Email: jorge.f.mejias@gmail.com

Computational models based on recurrent neural networks (RNNs) have emerged as useful tools to understand the computations underlying perceptual and cognitive tasks [1–3]. When training RNNs on these tasks, the resulting network configuration strongly depends, however,

on the initial conditions of the network. This dependence of initial conditions is sometimes sorted out by averaging the results of the model over many network variants; hence such variability is often discarded. In this work, we explore an alternative hypothesis: that the variability in the solutions obtained by training RNNs reflects different ‘behavioral strategies’ which animals would potentially use to efficiently solve the task. To examine this hypothesis, we trained a large ( $N = 100$ ) number of RNNs to solve a classical multisensory decision-making task [4] and explore their different behavioral outputs. Networks were trained as in [2] and functioned by virtue of a balance between excitatory and inhibitory units. When examining the output of the trained RNNs, we observed a high level of variability in their psychometric and chronometric curves for unisensory and multisensory trials. We mapped quantitative features of these behavioral curves to estimate the decision speed, accuracy and precision of the networks to integrate uni- and multisensory stimuli and found that some networks always made slow but precise decisions, others made imprecise but fast decisions, and a few of them made fast and precise decisions. The fast and precise decisions were made mainly by networks integrating multisensory, rather than unisensory, stimulation. Behavioral variability also emerged when we considered other multisensory tasks (e.g., [5]). Our results show how variability across solutions in trained RNNs provides valuable information about possible behavioral strategies used by animals on perceptual and cognitive tasks and opens the door to use RNNs to investigate the structural neural basis of behavioral variability.

## References

1. Mante V, Sussillo D, Shenoy KV, Newsome WT. Context-dependent computation by recurrent dynamics in prefrontal cortex. *Nature*. 2013; 503 (7474): 78–84.
2. Song HF, Yang GR, Wang X-J. Training excitatory-inhibitory recurrent neural networks for cognitive tasks: a simple and flexible framework. *PLoS Computational Biology* 2016; 12(2): e1004792.
3. Yang GR, Joglekar MR, Song HR, Newsome WT, Wang X-J. Task representations in neural networks trained to perform many cognitive tasks. *Nature Neuroscience*. 2019; 22(2): 297–306.
4. Raposo D, Kaufman MT, Churchland AK. A category-free neural population supports evolving demands during decision-making. *Nature Neuroscience*. 2014; 17(12): 1784–1792.
5. Lohuis MNO, Pie JP, Marchesi P, Montijn JS, De Kock CPI, Pennartz CMA, Olcese U. Task complexity temporally extends the causal requirement for visual cortex in perception. *BioRxiv*, 2021.

## P74 Hierarchical decoupling of electromagnetic and haemodynamic cortical networks

Golia Shafiei<sup>\*1</sup>, Sylvain Baillet<sup>1</sup>, Bratislav Misic<sup>1</sup>

<sup>1</sup>McGill University, McConnell Brain Imaging Centre, Montreal Neurological Institute, Montreal, Canada

\*Email: golia.shafiei@mail.mcgill.ca

Large-scale functional architecture of the brain is commonly inferred from electromagnetic or haemodynamic activity. The former can be measured using electro- or magneto-encephalography (EEG/MEG), while the latter is measured using functional magnetic resonance imaging (fMRI). Although both modalities attempt to capture the same underlying biological process, they are sensitive to different

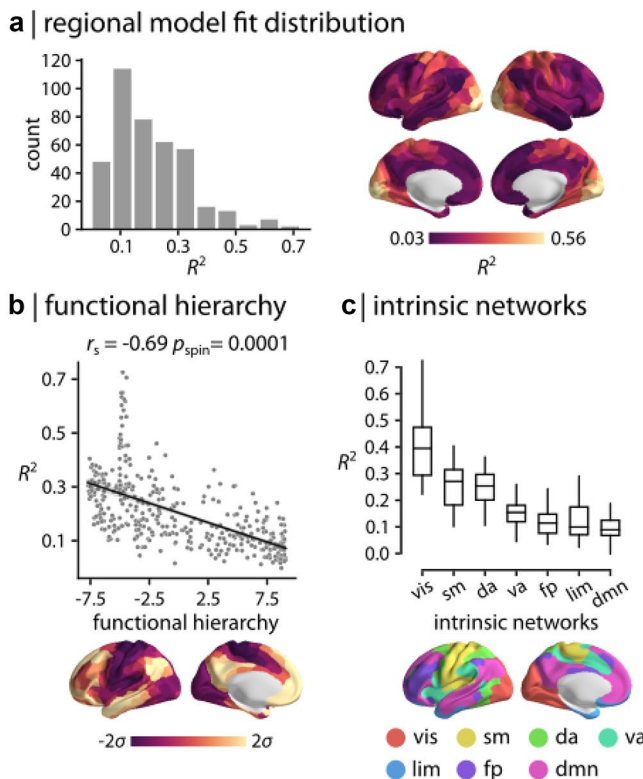


**Fig. 1** **a** Spatial organization of fMRI-MEG correspondence. The cross-modal correspondence is compared with **b** the functional hierarchical organization of cerebral cortex, **c** macro-scale intrinsic net-

works, and **d** cytoarchitectural variation of the cortex. **e** Dominance analysis is performed to quantify how MEG connectivity at different rhythms contribute to the cross-modal correspondence

physiological mechanisms and ultimately reflect neural activity at fundamentally different time scales [1]. Previous reports have found some, but not complete, global overlap between the two modalities [2]; however, less is known on how they can be mapped to one another at the regional level. We obtained resting-state fMRI and MEG data of  $n=33$  unrelated healthy young adults from Human Connectome Project (HCP [3]). The preprocessed fMRI data were used to construct functional connectivity networks as Pearson correlation coefficients between pairs of regional time-series. Resting state MEG data was preprocessed using Brainstorm [4]. Linearly constrained minimum variance (LCMV) beamformers were used to obtain source activity. Source-level time-series were then used to estimate functional connectivity as amplitude envelope correlations between all pairs of regions at six canonical electrophysiological frequency bands. Finally, a multi-linear regression model was used to map regional MEG connectivity to regional fMRI connectivity. The relationship between fMRI and MEG functional connectivity was highly heterogeneous across the cortex suggesting a close correspondence in sensory regions and poor correspondence in transmodal areas (Fig. 1A). The spatial layout of cross-modal correspondence resembled the unimodal-transmodal cortical hierarchy observed in large-scale functional and microstructural brain organization. Indeed, the regional model fit was significantly correlated with the principal functional gradient (Fig. 1B;  $r=-0.69$ ,  $p=0.0001$ ). Interestingly, the model fit was also associated with cyto-architectural variation of the cortex, estimated from the BigBrain's cell staining intensity profiles [5], with the peak association observed at cortical layer IV with high density of granule cells (Fig. 1D). Moreover, dominance analysis indicated that haemodynamic connectivity reflects a superposition of electromagnetic connectivity in multiple rhythms, with the greatest contributions from slower bands (Fig. 1E). Collectively, our findings demonstrate that the superposition of MEG connectivity in multiple frequency bands manifests as highly structured patterns of fMRI functional connectivity. The association between the two modalities is regionally heterogeneous and systematically follows the cortical hierarchy, with close correspondence in unimodal cortex and poor correspondence in transmodal cortex.

## References

1. Hall et al. The relationship between MEG and fMRI. *Neuroimage*. 2014; 102: 80–91.
2. Brookes et al. Investigating the electrophysiological basis of resting state networks using magnetoencephalography. *PNAS*. 2011; 108(40): 16783–16788.
3. Van Essen et al. The WU-Minn human connectome project: an overview. *Neuroimage*. 2013; 80: 62–79.
4. Tadel et al. Brainstorm: a user-friendly application for MEG/EEG analysis. *Computational Intelligence and Neuroscience*. 2011.
5. Paquola et al. The BigBrainWarp toolbox for integration of Big-Brain 3D histology with multimodal neuroimaging. *eLife*. 2021; 10:e70119.

## P75 Resting state fMRI meta-networks improve identifiability: a hierarchical functional connectivity study

Wei Zhang<sup>\*1</sup>, Maia Lazerwitz<sup>1</sup>, Pratik Mukherjee<sup>1</sup>

<sup>1</sup>University of California San Francisco, Department of Radiology and Biomedical Engineering, San Francisco, CA, United States of America

\*Email: wei.zhang4@ucsf.edu

Spatially hierarchical functional architecture of the human brain [1–3] has been recently revealed by novel fMRI functional connectivity reconstruction methods such as Low-to High-Dimensional Independent Components Analysis (LHDICA), Deep Sparse Matrix Factorization (DSMF),

and Deep Linear/Nonlinear Matrix Fitting (DMF/DNMF) [4–7]. This study investigates the spatial scale of the state-invariant blood oxygenation level-dependent (BOLD) functional connectivity signal related to human brain identifiability [8]. In other words, which of the hierarchically organized brain connectivity networks (BCNs) enables the identification of a particular individual from a group? Van De Ville et al. proposed a dynamic brain fingerprint technique to investigate the temporal dependence of brain identifiability at a connectome scale [9].

The fundamental scheme we employed for analyzing identifiability using hierarchical BCNs was: 1) Collect and organize a dataset including 100 subjects' test-retest resting state BOLD fMRI scans, in this case all children ages 8–12 years; 2) Compare DMF with DNMF for mapping hierarchical BCNs from the 100 subjects' test-retest fMRI signals, using identifiability as the metric of interest for revealing neurobiological information.

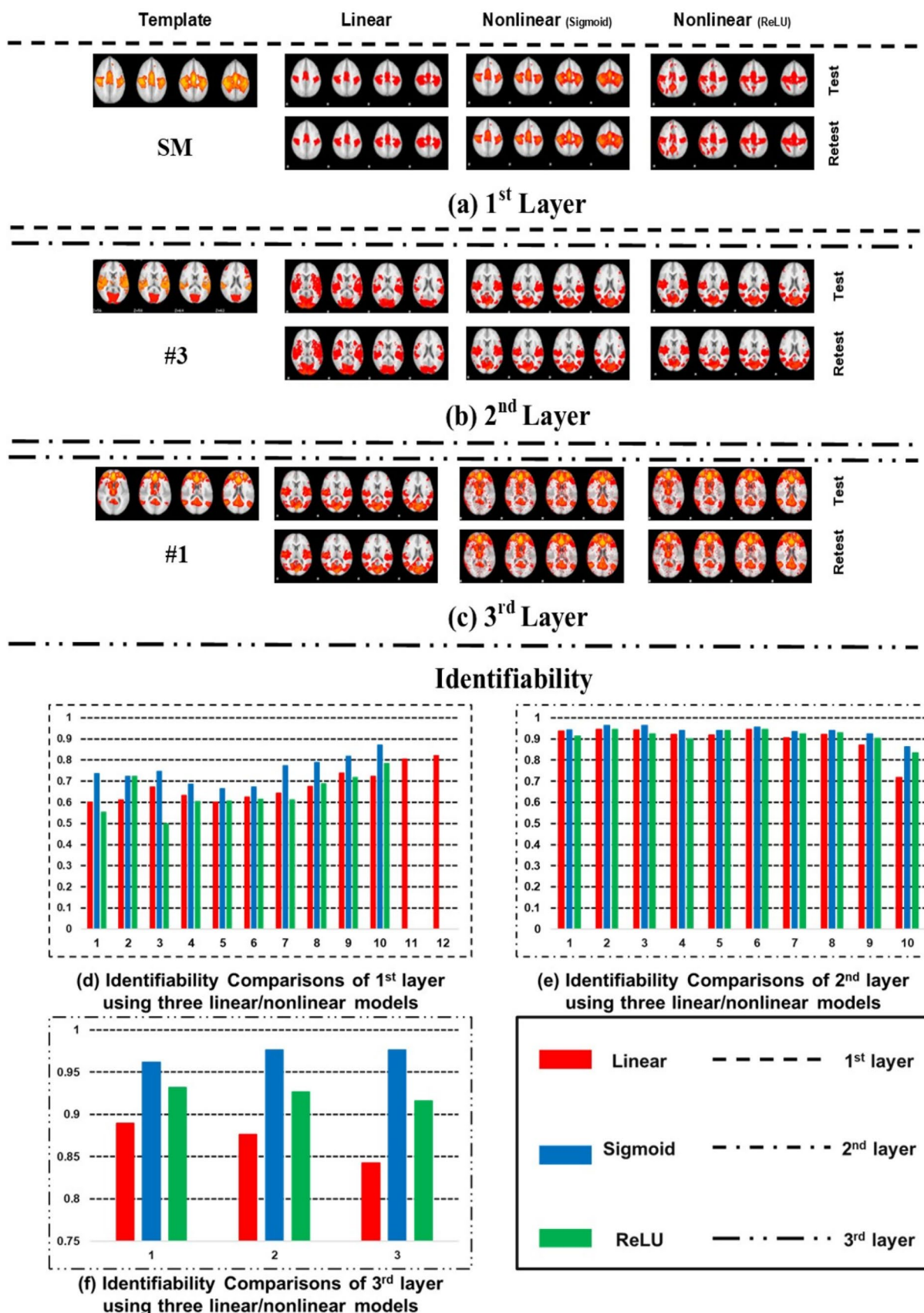
All identical test and retest resting state fMRI acquisitions of each individual, both of 6 min duration, were performed during the same scan session on a Siemens Prisma 3 T using multiband (MB) gradient echo echoplanar imaging using top-up from FSL software. In addition, other pre-processing steps are also applied to fMRI data [10]. The linear Deep MF model (DMF) and nonlinear Deep MF model (DNMF) are described in detail by Zhang et al. in 2020 and 2021, respectively [6, 7]. For DNMF, we compare the two nonlinear activation functions most widely used in Deep Neural Networks (DNNs) [10], specifically the Sigmoid function and the rectified linear unit (ReLU), to map hierarchical BCNs.

The qualitative results of hierarchical BCNs revealed via the Deep Linear/Nonlinear Model of the test vs. retest scans of SPIN fMRI data used in our identification analysis have been presented in our previous work [7]. This work concentrates on functional identification analytics using the derived hierarchical BCNs from the first to the third layers of the DMF and DNMF with Sigmoid and ReLU. Figure 1(A-C) shows example BCNs from the 1st to the 3rd layers using linear DMF and non-linear DNMF, with higher-level BCNs representing “meta-networks” often combining nodes of different lower-level BCNs. Figure 1(D-F) are quantitative comparisons of the 1st to the 3rd layer identification metrics. The main result is that the 2nd and 3rd layer BCNs enable greater identifiability than the lower-level BCNs.

In this work, the results demonstrate that Deep MF and Deep NMF enable the mapping of the human brain's reproducible hierarchical functional connectivity networks. Moreover, all hierarchical BCNs computed via linear and nonlinear models indicate that all three spatially hierarchical layers contribute to identifiability. Crucially, the identifiability increased from 0.60 to 0.97 from first-order BCNs to second-order BCNs, verifying our hypothesis that the deeper hierarchical “meta-networks” contain more of the state-invariant but trait-dependent BOLD functional connectivity information that improves identifiability.

## References

1. Bullmore, E., Sporns, O. Complex brain networks: graph theoretical analysis of structural and functional systems. *Nature Reviews Neuroscience*. 2009; 10:186–198.
2. Power, J. D., Cohen, A. L., Nelson, S. M., Wig, G. S., Barnes, K. A., Church, J. A., ... & Petersen, S. E. Functional network organization of the human brain. *Neuron*. 2011; 72:65–678.
3. Stam, C. J. Modern network science of neurological disorders. *Nature Reviews Neuroscience*. 2014; 15:683.
4. Wylie, K. P., Kronberg, E., Legget, K. T., Sutton, B., & Tregellas, J. R. Stable Meta-Networks, Noise, and Artifacts in the Human Connectome: Low-to High-Dimensional Independent Components Analysis as a Hierarchy of Intrinsic Connectivity Networks. *Frontiers in Neuroscience*. 2021; 15.
5. Sahoo, D., & Davatzikos, C. Learning Robust Hierarchical Patterns of Human Brain across Many fMRI Studies. *Advances in Neural Information Processing Systems*. 2021; 34.



◀Fig. 1 a, b, and c show representative BCNs identified via Linear DMF, Sigmoid DNMF, and ReLU DNMF models in the three layers. Figure 1d–f show the identifiability metric calculated via the linear and other two nonlinear models in the three layers, where 1.0 represents correct identification of individuals across test and retest scans in 100% of cases

6. Zhang, W., Palacios, E. M., & Mukherjee, P. Deep Linear Modeling of Hierarchical Functional Connectivity in the Human Brain. *BioRxiv*, 2020.
7. Zhang, W., Cai, T., Wren-Jarvis, J., Lazerwitz, M., Bourla, I., Mukherjee, P. Deep Nonlinear Modeling Extracts Reproducible Hierarchical Functional Networks from BOLD fMRI. Organization for Human Brain Mapping (OHB), 2022.
8. Finn ES, Shen X, Scheinost D, Rosenberg MD, Huang J, Chun MM, Papademetris X, Constable RT. Functional connectome fingerprinting: identifying individuals using patterns of brain connectivity. *Nat Neurosci*. 2015 Nov; 18(11): 1664–71.
9. Van De Ville, D., Farouj, Y., Preti, M. G., Liégeois, R., & Amico, E. When makes you unique: Temporality of the human brain fingerprint. *Science advances*. 2021; 7(42), eabj0751.
10. Zhang, S., Dong, Q., Zhang, W., Huang, H., Zhu, D., & Liu, T. Discovering hierarchical common brain networks via multimodal deep belief network. *Medical image analysis*, 2019; 54, 238–252.

#### P76 Compact Representation of Brain Structure and Dynamics via Eigenmodes and Resonances

Peter Robinson<sup>\*1</sup>, Tahereh Babaie-Janvier<sup>2</sup>, Rawan El-Zghir<sup>1</sup>, Natasha Gabay<sup>2</sup>, Xiao Gao<sup>3</sup>, James Henderson<sup>1</sup>, Brandon Munn<sup>4</sup>, Kevin Aquino<sup>1</sup>, Eli Muller<sup>4</sup>

<sup>1</sup>The University of Sydney, School of Physics, Sydney, Australia

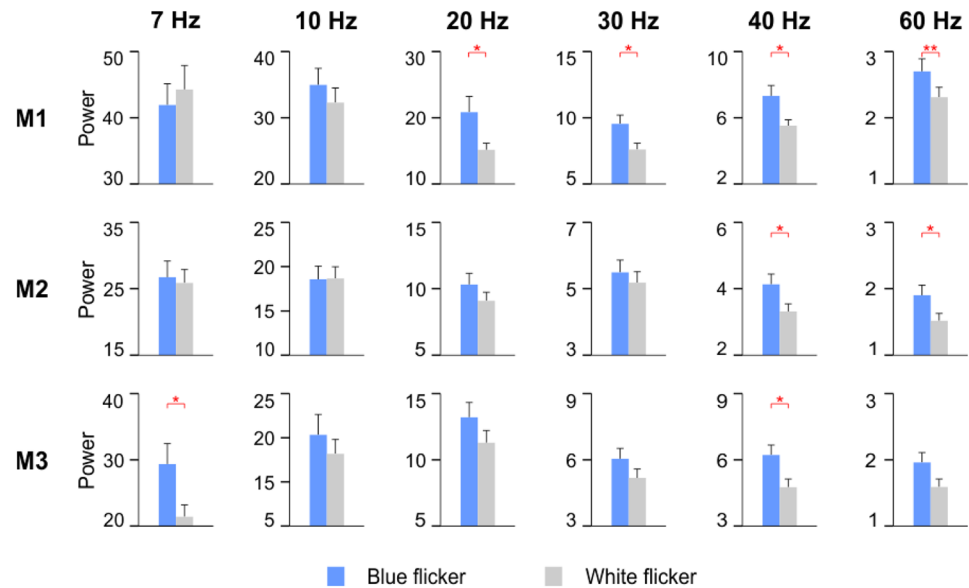
<sup>2</sup>The University of Sydney, School of Physics, Complex Systems, Sydney, Australia

<sup>3</sup>University of Melbourne, Department of Biomedical Engineering, Parkville, Australia

<sup>4</sup>The University of Sydney, Brain and Mind Centre, Sydney, Australia

\*Email: peter.robinson@sydney.edu.au

**Fig. 1** Non-normalized spectral power values (computed with SLT) at stimulation frequency for blue and white flicker stimuli. Individual mice are labelled M1, M2, M3. Statistical significance of the differences is highlighted with red. Error bars show standard error of the mean



Complex brain structure and dynamics are observed at tens to thousands of locations by MRI or electroencephalography. Analysis of these observations often relies on statistical analysis of time series and connectivity matrices (CMs) of two-point correlations of activity. Various steps of parcellation, thresholding, and statistical processing of data are applied to decimate the results to compact form. These steps commonly result in 4–20 activity patterns, often termed microstates, resting state networks (RSNs), or gradients, but the details depend on data processing steps and assumptions.

All brain data are generated by the physical brain in a mutually consistent way, so the approach here is to base analysis on the brain itself, using established methods from analysis of other physical systems. This results in a simultaneous description of brain structure and the dynamics it supports in terms of natural modes of oscillation and their spatial patterns and temporal frequencies. Data analysis and prediction are then done in ways that respect the system characteristics. Specifically, spectral analysis is used to decompose observed brain activity into a sum of natural modes, analogously to how the vibration of a violin string can be decomposed into notes. Each mode has simple characteristic spatial structure and a few frequency resonances. Brain modes and resonances are calculated via neural field theory (NFT), which averages over microscopic structure and dynamics to obtain equations for brain activity. These predict brain activity, correlations, and functional conductivity at scales of millimeters and above and, together with cortical geometry, determine the properties of the natural modes. Each mode has a simple spatial structure and macroscopic brain activity can be compactly represented in terms of the leading modes – usually about 10. Temporal dynamics of each mode are dominated by slow, alpha, and beta resonances, so dynamics can be tracked via the coefficients of these modes and resonances. In particular, evoked activity can be represented by just a few superposed damped oscillations, thereby avoiding the use of phenomenological evoked components. Likewise, structural and functional CMs are well approximated by about 10 modes, thus giving a physically-based alternative to RSNs and other statistically derived patterns.

Overall, we show that spectral decomposition in terms of natural modes and resonances achieves the long-sought goal of obtaining a compact description of brain dynamics and structure that is independent of investigator choices of parcellation, thresholding, and data analysis. This allows connectivity and activity to be represented in a unified way that relates to observed patterns and resonances, and to underlying

physical structure and dynamics. Qualitatively, modes are analogous to the musical notes produced by violin, while statistically robust patterns such as RSNs are the analogs of frequently played chords.

#### P77 Blue flicker stimulation enhances gamma rhythms in mouse visual cortex

Ana-Maria Ichim<sup>\*1</sup>, Harald Bârzan<sup>1</sup>, Vasile Vlad Moca<sup>2</sup>, Koen Vervaeke<sup>3</sup>, Raul Muresan<sup>1</sup>

<sup>1</sup>Transylvanian Institute of Neuroscience, Department of Experimental and Theoretical Neuroscience, Cluj-Napoca, Romania

<sup>2</sup>Transylvanian Institute of Neuroscience, Cluj-Napoca, Romania

<sup>3</sup>University of Oslo, Institute of Basic Medical Sciences, Oslo, Norway

\*Email: ich.annamaria@gmail.com

Jan Purkinje pioneered streaming rhythmic light, using flicker-induced phosphenes in humans [1]. Since then, understanding how diffuse flickering light entrains oscillatory activity has remained challenging. Clear evidence emerged about entrainment at different stimulation frequencies [2]. Recent clinical studies employ flicker as a non-conventional treatment for Alzheimer's disease (AD) and cognitive dysfunction in the ischemic brain. For example, GENUS therapy [3] uses exposure to 40-Hz white flicker light, entraining gamma oscillations to reduce the  $\beta$ -amyloid load in murine AD models. What has been little explored, however, is how the entrained gamma oscillations behave in response to different colors of the flicker light.

We investigated the effect of white flicker versus blue flicker in isoflurane anesthetized C57/BL6J adult mice ( $n=3$ ). Flicker was delivered monocularly for 6 s using two LED panels (white and 460 nm blue), with pulsed light at different frequencies (7, 10, 20, 30, 40, and 60 Hz; 50% duty cycle). Pooling across multiple recordings, we obtained 40 trials for each stimulation frequency (10 trials / frequency / recording, 240 total trials). Recordings were interleaved (blue-white-blue-white). LED luminance was 280 lx and was normalized across different colors by modulating driver voltage. In vivo electrophysiology data was acquired @32 kSamples/s from the primary visual cortex using a 32-channel linear silicon probe. To obtain the local field potentials (LFP), the data was low-pass filtered @300 Hz, downsampled to 1 kHz, and high-pass filtered @0.1 Hz. To remove line noise and harmonics, notch filters @50 and @100 Hz were applied. We used the Superlet Transform (SLT) [4, 5] to measure LFP power at each stimulation frequency. The difference between LFP power to white vs blue light was statistically assessed using Student's t-test and reported separately across the three animals used.

We found a marked increase in LFP power in response to blue stimulation compared to white, across the frequency range. This difference was significant for the 40 Hz flicker across all three animals. These results are especially relevant for GENUS therapy, which uses 40 Hz flicker stimuli. Our findings suggest that blue light may represent an improvement over the currently used white flickering for this protocol. Further analyses using different kinds of stimuli (e.g., drifting bars or sinusoidal gratings) with white vs blue light are necessary to determine the usefulness of blue light in visual stimulation paradigms.

#### Acknowledgements

The research leading to these results has received funding from: NO Grants 2014–2021, under Project contract number 20/2020 (RO-NO-2019-0504), four grants from the Romanian National Authority for Scientific Research and Innovation, CNCS-UEFISCDI (codes PN-III-P2-2.1-PED-2019-0277, PN-III-P3-3.6-H2020-2020-0109, ERA-Net NEURON UNSCRAMBLY, ERA-Net FLAG-ERA

ModelDXConsciousness), and a H2020 grant funded by the European Commission (grant agreement 952096, NEUROTWIN).

#### References

1. Rule, M., Stoffregen, M. and Ermentrout, B. A model for the origin and properties of flicker-induced geometric phosphene. *PLoS Computational Biology*. 2011; 7(9): pp.e1002158.
2. Wacker, M., Galicki, M., Putsche, P., Milde, T., Schwab, K., Haueisen, J., Ligges, C. and Witte, H. A time-variant processing approach for the analysis of alpha and gamma MEG oscillations during flicker stimulus generated entrainment. *IEEE Transactions on Biomedical Engineering*. 2011; 58(11): pp.3069–3077.
3. Chan, D., Suk, H.J., Jackson, B., Milman, N.P., Stark, D., Beach, S.D. and Tsai, L.H. Induction of specific brain oscillations may restore neural circuits and be used for the treatment of Alzheimer's disease. *Journal of Internal Medicine*. 2021; 290(5): pp.993–1009.
4. Moca, V.V., Bârzan, H., Nagy-Dăbăcan, A. and Mureșan, R.C. Time–frequency super-resolution with superlets. *Nature communications*. 2021; 12(1): pp.1–18.
5. Bârzan, H., Moca, V.V., Ichim, A.M. and Muresan, R.C. Fractional superlets. In 2020 28th European Signal Processing Conference (EUSIPCO). 2021, January; pp. 2220–2224. IEEE.

#### P78 Gaze lateralization bias during free visual exploration of faces

Emanuela Loredana Dan<sup>\*1</sup>, Vasile Vlad Moca<sup>2</sup>, Mihaela Dînșoreanu<sup>3</sup>, Raul C. Mureșan<sup>1</sup>

<sup>1</sup>Transylvanian Institute of Neuroscience, Department of Experimental and Theoretical Neuroscience, Cluj-Napoca, Romania, Romania

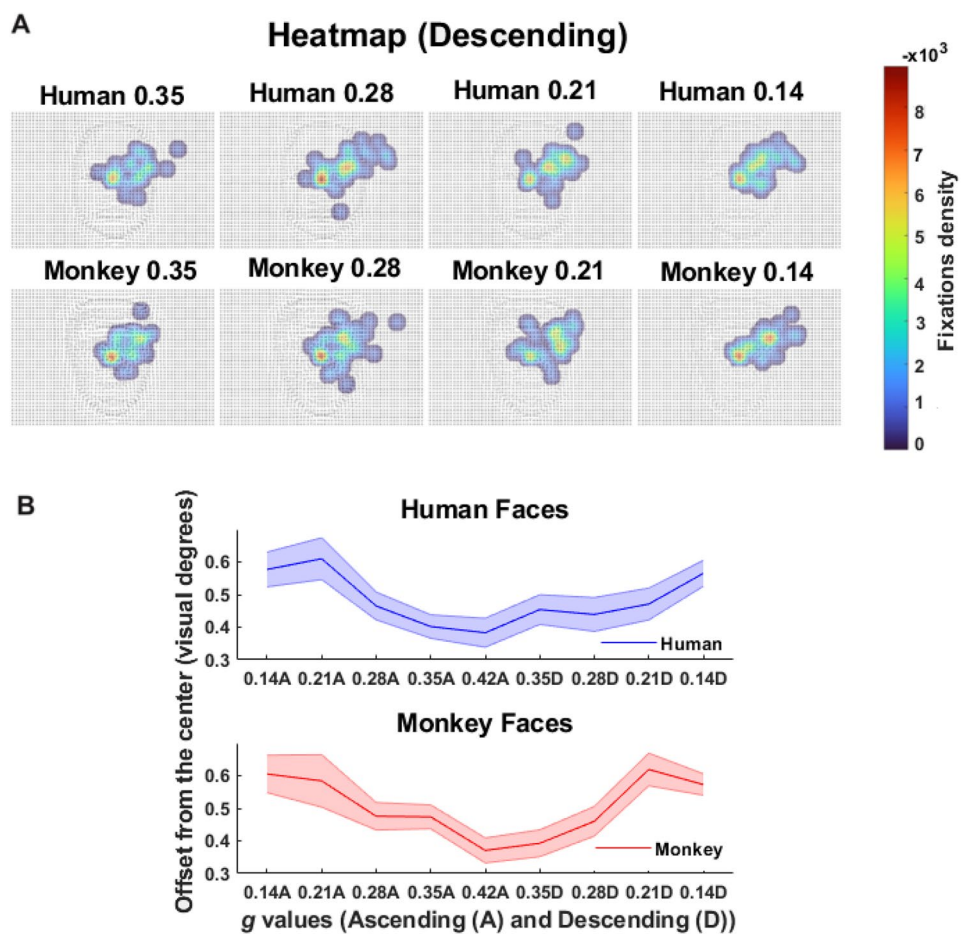
<sup>2</sup>Asociatia Transylvanian Institute of Neuroscience, Cluj-Napoca, Romania

<sup>3</sup>Technical University of Cluj-Napoca, Cluj-Napoca, Romania, Romania

\*Email: danemanuelaloredana@gmail.com

In humans, visual sampling of face images exhibits a lateral gaze bias that is wider for conspecifics, probably due to behavioral social interaction [1]. Stimulus properties, such as spatial frequency, may also influence visual behavior engaging central and/or peripheral pathways. It is likely that low spatial frequency information (coarse details), is better conveyed by the magnocellular pathway (parasol ganglion cells whose density is correlated to eccentricity [2]), leading to a functional lateralization of visual cortex [3] that may be involved in face perception. Here, we assessed if the conspecific lateralization bias is maintained during an eye-tracking free visual exploration experiment, when basic image features are removed, and only low spatial frequency information is retained. Eye-tracking measurements were recorded (50 Hz) during the presentation of “Dots” images of human and monkey faces with different levels of visibility [4], in ascending (low-to-high) and descending (high-to-low) order of visibility ( $n=7$  subjects;  $t=180$  trials). Lateralization gaze bias was quantified as the offset from image center to the fixations' center of mass, in visual degrees, as a function of visibility. Heatmaps (Fig. 1A) and lateralization quantification indicate a significant right gaze bias, estimated for each stimulus category by comparing the data to chance level using a 2-tailed Wilcoxon Signed Rank test [ $p(x \leq Z)$ ]. Because data was normally distributed or moderately violated normality (Shapiro–Wilk test), parametric tests were considered robust to compare lateralization bias per condition. Significant differences were found between the offsets of the smallest and the largest visibility levels, for both face conditions ( $p$  values  $> \alpha$ ) (Fig. 1B). However, comparing

**Fig. 1** Right lateralization bias. **A** Heatmap (e.g., one subject; “Descending” stimulus presentation order, different visibility levels/g values) displaying a right gaze bias. **B** Lateral asymmetry quantification. Error bands represent s.e.m. The U-shaped curve emphasizes a lateralization bias influenced by the g values (higher offset values at lower visibility/smaller g values)



human and monkey face offsets (considering ascending and descending visibility order), no significant differences were found ( $p$  values  $> \alpha$ ) (Welch's t-tests).

To conclude, visibility levels influence the lateralization gaze bias (offset magnitude depends on visual difficulty), which may reflect a perceptual optimization mechanism, i.e., increased reliance on peripheral vision maximizing integration of low spatial-frequency information in “Dots” images. However, lateralization is not influenced by face conditions (human vs. monkey faces), implying that conspecific gaze bias [1] may require high spatial frequency image components.

#### Acknowledgments

The research has received funding from: NO Grants 2014–2021, 20/2020 (RO-NO-2019-0504); CNCS-UEFISCDI (PN-III-P2-2.1-PED-2019-0277, PN-III-P3-3.6-H2020-2020-0109, ERA-Net NEURON UNSCRAMBLY, ERA-Net FLAG-ERA ModelDXConsciousness); European Commission H2020 (GA 952096, NEUROTWIN).

#### References

- Guo, Kun, et al. Left gaze bias in humans, rhesus monkeys and domestic dogs. *Animal cognition*. 2009; 12.3: 409–418.
- Kauffmann, Louise, et al. The neural bases of spatial frequency processing during scene perception. *Frontiers in integrative neuroscience*. 2014; 8: 37.
- Paz-Alonso, Pedro M., et al. A parvocellular-magnocellular functional gradient in human visual cortex. *bioRxiv*. 2022.
- MOCA, Vasile V., et al. Visual exploration and object recognition by lattice deformation. *PloS one*. 2011; 6.7: e22831.

#### P79 Efficient training of sparse SNN classifiers with structural plasticity using GeNN

James Knight<sup>\*1</sup>, Thomas Nowotny<sup>1</sup>

<sup>1</sup>University of Sussex, School of Engineering and Informatics, Department of Informatics, Brighton, United Kingdom

\*Email: j.c.knight@sussex.ac.uk

In recent years, significant advances have been made in training spiking neural networks (SNNs) to solve real world tasks using backpropagation through time (BPTT) [1] or more biologically-plausible gradient-based local learning rules such as e-prop [2].

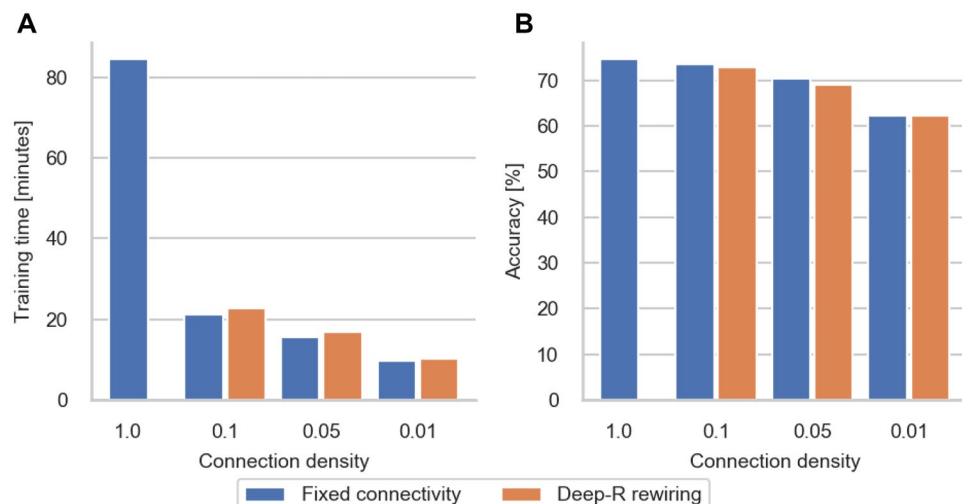
We have shown previously that, using GeNN — our GPU-accelerated SNN simulator [3, 4] — we can use e-prop to train recurrent SNNs which perform comparably to LSTMs but are up to  $7\times$  faster when performing inference on the same GPU hardware [5].

However, like the majority of work in this area, we thus far only looked at densely connected SNNs whereas, in biology, synaptic connectivity is typically sparse.

GeNN is designed to exploit sparse connectivity so, replacing the dense recurrent connectivity with fixed sparse 1% connectivity, reduces the time taken to train a classifier model on the Spiking Heidelberg Digits (SHD) dataset [6] using e-prop by over  $8\times$  although it also results in a reduction in classification accuracy.

In biological brains, alongside the changes to the strength of existing synapses driven by synaptic plasticity, structural plasticity prunes

**Fig. 1** **A** Training time and **B** accuracy of a model with a single recurrently connected hidden layer of 256 ALIF neurons with varying levels of sparsity on the recurrent connections and those connecting the input to the hidden layer, trained on Spiking Heidelberg Digits for 50 epochs on a V100 GPU



unused synapses and forms new ones. The Deep-R learning rule [7] provides a framework for combining gradient-based learning with structural plasticity while maintaining a fixed total number of synapses. In this framework, neurons are either excitatory or inhibitory which is reflected in the sign of their efferent synaptic weights. When weight changes produced by the gradient-based learning rule would cause a synapse's weight to change sign, Deep-R removes the synapse and replaces it with another — leading to efficient sampling of network configurations and enforcing Dale's rule.

Here we combine Deep-R with e-prop and demonstrate that augmenting a SHD classifier implemented in GeNN with a simple, single-threaded Python implementation of Deep-R only has a negligible effect on the training time but allows sparse networks to be trained to respect Dale's rule with only excitatory neurons in the input layer and an 80:20 ratio of excitatory to inhibitory neurons in the recurrent layer. In the future, parts of the Deep-R algorithm could be parallelized on the GPU to further reduce the training overheads.

#### Acknowledgments

This work was funded by the EPSRC (Brains on Board grant EP/P006094/1, ActiveAI grant EP/S030964/1, and Unlocking spiking neural networks for machine learning research, grant EP/V052241/1). Compute time was provided by the EPSRC (grant EP/T022205/1).

#### References

1. Zenke F, Vogels T. The Remarkable Robustness of Surrogate Gradient Learning for Instilling Complex Function in Spiking Neural Networks. *Neural Computation*. 2021; 33(4): 899–925
2. Bellec G, Scherr F, Subramoney A, et al. A solution to the learning dilemma for recurrent networks of spiking neurons. *Nature Communications*. 2020; 11(1):3625
3. Yavuz E, Turner J, Nowotny T. GeNN: A code generation framework for accelerated brain simulations. *Scientific Reports*. 2016; 6:18854
4. GeNN repository. Github. <https://github.com/genn-team/genn>
5. Knight J, Nowotny T. Efficient GPU training of LSNNs using eProp. *Neuro-Inspired Computational Elements Conference*. 2022
6. Cramer B, Stradmann Y, Schemmel J, et al. The Heidelberg Spiking Data Sets for the Systematic Evaluation of Spiking Neural Networks. *IEEE Transactions on Neural Networks and Learning Systems*. 2020; 1–14
7. Bellec G, Kappel D, Maass W, et al. Deep rewiring: Training very sparse deep networks. *6th International Conference on Learning Representations*. 2018; 1–24

#### P80 Forecasting psychogenic non-epileptic seizure likelihood from ambulatory EEG and ECG

Wenjuan Xiong<sup>\*1</sup>, Tatiana Kameneva<sup>2</sup>, Elisabeth Lambert<sup>3</sup>, Mark Cook<sup>4</sup>, Ewan Nurse<sup>5</sup>

<sup>1</sup> Swinburne University of Technology, School of Software and Electrical Engineering, Melbourne, Australia

<sup>2</sup> Swinburne University of Technology, Telecommunication Electrical Robotics and Biomedical Engineering, Melbourne, Australia

<sup>3</sup> Swinburne University of Technology, School of Health Sciences, Department of Health and Medical Sciences, Melbourne, Australia

<sup>4</sup> University of Melbourne, Department of Medicine, Melbourne, Australia

<sup>5</sup> Seer Medical, Melbourne, Australia

\*Email: wxiong@swin.edu.au

The neural and cardiovascular system may exhibit critical slowing, a phenomenon preceding transitions to seizures, which is measured by an increase in variance and autocorrelation of the system [1]. Critical slowing features have been used to forecast epileptic seizures [2]. Psychogenic non-epileptic seizures (PNES), opposite to epileptic seizures, are not usually associated with abnormal electrical discharges in brain activity and are considered to be due to psychological distress. This study examines the existence of cycles of PNES in brain and cardiac activity in electroencephalogram (EEG) and electrocardiography (ECG) data and test whether PNES can be forecasted.

EEG and ECG data from 10 patients with non-epileptic seizures, and no background of epilepsy were used. The mean period of recordings was 150 h, with an average of 9 non-epileptic seizures per patient. Five cycles (5-min, 1-h, 6-h, 12-h, 24-h) of EEG and ECG critical slowing features were extracted. The relationship between seizure onset times and phases of each cycle of critical slowing features was investigated. Forecasting models were developed using combinations of critical slowing features at each cycle length. Seasonal Autoregressive Integrated Moving Average (SARIMA) model was used to forecast critical slowing cycles. The projection of the forecasted cycles was used to calculate the probability of seizures based on the pre-determined seizure probability given phases of each cycle. The best forecasters with the highest area under the receiver-operator curve (AUC) were selected.

PNES events occurred in the rising phases of EEG feature cycles of 12-h and 24-h at a rate significantly above chance. The proposed forecasters achieved performance better than chance in 60% of patients, and the mean sensitivity, false-positive rate (FPR), area under the curve (AUC), and forecasting horizon of the best forecaster across patients were 83%, 0.49/h, 0.77 and 33 min, respectively. In 80% of patients the best forecaster used cycles longer than 6-h.

The study suggests that cyclic EEG biomarkers of non-epileptic seizures exist and opens the potential of seizure forecasting beyond epilepsy.

## References

1. Scheffer et al. Early-warning signals for critical transitions. *Nature*. 2009
2. Maturana et al. Critical slowing as a biomarker for seizure susceptibility. *Nature Communication*. 2020

## P81 Neurally-informed modelling of ageing effects on the speed-accuracy trade-off

Elaine Corbett<sup>\*1</sup>, Cian Judd<sup>1</sup>, Jessica Dully<sup>1</sup>, Simon Kelly<sup>2</sup>, David McGovern<sup>3</sup>, Redmond O'Connell<sup>1</sup>

<sup>1</sup>Trinity College Dublin, Trinity College Institute of Neuroscience, Dublin, Ireland

<sup>2</sup>University College Dublin, Electrical and Electronic Engineering, Dublin, Ireland

<sup>3</sup>Dublin City University, Psychology, Dublin, Ireland

\*Email: corbetel@tcd.ie

When instructed to prioritize speed over accuracy in perceptual decision making, older adults tend to make smaller adjustments to their choice behavior compared to younger adults. Behavioral modelling suggests this may be due to less pronounced adjustment of decision bounds across conditions and a general preference for a more cautious response style. However, this work has relied on standard models which overlook important algorithmic elements and adjustments that have been identified in recent neurophysiological research. The current study aimed to leverage neurally-informed modelling to investigate ageing's effects on speed-accuracy adaptation. Thirty older adults and 30 young adult controls underwent EEG recordings while performing a random dot-motion task in which the number of points awarded for choice accuracy versus speed was manipulated across the two regimes. Both groups adapted their behavior in response to speed pressure, with young adults showing a more substantial reduction in response time. However, there was no group difference in the number of points scored. Consistent with previous modelling studies, both groups exhibited increased starting levels of motor preparation under speed pressure, but the adjustments were significantly smaller in the older group. These pre-stimulus motor adjustments were used to constrain a sequential sampling model which also included dynamic within-trial time-dependent bound reductions ('urgency') based on the observation that motor preparation exhibited substantial build-up prior to evidence onset in both groups. This neurally-constrained model indicated that only young adults significantly adapted their urgency rate across conditions. Taken together, these results point to the larger behavioral adjustments to time pressure of the young group being underpinned by greater static and dynamic bounds adjustments among younger adults. However, most previous studies did not provide their participants with explicit feedback on speed-accuracy tradeoffs. Here, we show that while older adults maintained more consistent bound settings across conditions, this did not actually come at a cost to the points earned. We also report an exploratory, model-based approach for accounting

for behaviorally-irrelevant differences in EEG signal amplitudes when comparing decision signals between groups. Overall, the project highlights the potential exciting applications of neurally constrained modeling for enabling more accurate group comparisons.

## Acknowledgements

This study was funded by the European Union's Horizon 2020 research and innovation program under the European Research Council Consolidator Grant IndDecision – 865474 and the Marie Skłodowska-Curie grant agreement No 842143, and the Irish Research Council (GOIPG/2019/808).

## P82 Automating dynamic community detection by optimizing scalefreeness

Italo Ivo Lima Dias Pinto<sup>\*1</sup>, Kanika Bansal<sup>1</sup>, Javier Omar Garcia<sup>1</sup>

<sup>1</sup>US DEVCOM Army Research Laboratory, Columbia University, Humans in Complex Systems Division, Department of Biomedical Engineering, New York, United States of America

\*Email: italoivo@gmail.com

The science of complex systems has been deployed to investigate the properties in which many constituents of a system give rise to complex behavior, quantifying the strength of elementwise interactions and investigating the rules that govern overall system behavior. Understanding neurodynamics through the lens of complex systems has proven a fruitful endeavor facilitating the field of network neuroscience that probes how heterogeneous regions of the brain interact under different constraints, contextual circumstances, and task demands. A fundamental property of brain networks is to reconfigure rapidly to enable human's unique ability to adapt, resiliently operating whilst responding to various stimuli and events. This natural "elasticity" is arguably a critical feature to general intelligence, and the rapid reconstructions of networks within the brain are only possible due to the rich dynamical interactions occurring between the neural components across a large range of temporal and spatial scales, usually described as the "scale freeness" of brain dynamics. One way to tap into the brain's rich dynamics is to define interactions within and between networks that evolve over time via the appearance and disappearance of community structures. Extracting such community structures and their temporal evolution is non-trivial and has led to the development of multiple computational methods; one such widely popular method is the generalized Louvain algorithm, which groups nodes in communities such that structures are coherent across time by maximizing a quality function called modularity. However, in the dynamic implementation of this algorithm, we must optimize computational resolution parameters to target the appropriate spatial and temporal scales of the system for the extraction of meaningful and informative community structures. This optimization has largely been in the estimation of modularity (e.g., variance, differences to a "null" community structure) across these parameters but often still requires a subjective choice on "scale" and some a priori hypotheses. Building on the findings that the elastic nature of the brain leads to dynamical processes characterized by scale freeness, we present a procedure to automate the parameter optimization. We propose an iterative procedure to minimize the skewness of the community size distribution towards large or small communities in order to determine the spatial resolution parameter. For the time resolution parameter, we propose to choose a value which allows for the scale-free distribution of temporal intervals that network nodes have between switching communities. We present findings from neural measures that vary in temporal and spatial resolutions (e.g., fMRI, EEG) and validate with common

benchmarks and understood behavior. Future research will provide parameter optimization for multiplexed networks and an expansion of the selection criteria for the resolution parameters to allow for a variety of contexts and complex systems.

#### P83 AnalySim: A web platform for collaborative data sharing and analysis for research

Anca Doloc-Mihu<sup>1</sup>, Cengiz Gunay<sup>\*1</sup>, Ryan Gambrell<sup>1</sup>, Ahkeelah Lindo<sup>1</sup>, Joseph Ongchangco<sup>1</sup>

<sup>1</sup>Georgia Gwinnett College, School of Science and Technology, Lawrenceville, GA, United States of America

\*Email: cengique@users.sf.net

AnalySim is an open-source website project for hosting data and performing analysis for various types of datasets. AnalySim aims to help with data sharing, data hosting for publications, interactive visualizations, collaborative research, and crowdsourced analysis. Special support is planned for datasets with many changing parameters and recorded measurements, such as those produced by neuronal parameter search studies with large number of simulations. However, AnalySim is not limited to this type of data and allows running custom analysis code. Currently, it has a proof-of-concept demonstration of analysis capabilities by embedding JavaScript notebooks provided from ObservableHQ.com. Python Jupyter notebooks are being currently implemented.

AnalySim was one of the INCF Google Summer of Code (GSoC) projects in 2021 and this program several new features, such as forking, were added. In this poster, we will review some of these features and talk about the current advances in this year's GSoC plans. Offering advanced features on an interactive web platform improves visibility of one's research and helps the paper review process by allowing to reproduce others' analyses. In addition, it fosters collaborative research by providing access to others' public datasets and analysis, creating opportunities to ask novel questions, guide one's research, and start new collaborations or join existing teams. AnalySim can be said to provide a "social scientific environment", which include features such as forking or cloning existing projects to customize them and tagging or following researchers and projects. In addition, one can filter datasets, duplicate analyses and improve them, and then publish findings via interactive visualizations. In summary, AnalySim is a Github-like tool specialized for scientific problems - especially when datasets are large and complex as in parameter search. Our poster will present work in progress of this website.

#### P84 A small-world network model for species-specific cortical circuits

Seungdae Baek<sup>\*1</sup>, Youngjin Park<sup>1</sup>, Se-Bum Paik<sup>1</sup>

<sup>1</sup>Korea Advanced Institute of Science and Technology, Department of Bio and Brain Engineering, Daejeon, South Korea

\*Email: seung7649@kaist.ac.kr

Long-range horizontal connections (LRCs) are extraordinarily long wirings that are distinguished from the local connections of the short

lateral spread [1] observed in the primary visual cortex (V1) of various mammalian species. Observations across species with [2, rats] or without [3, mice] LRCs imply that LRCs play a distinct role in visual processing, depending on the species-specific conditions of V1. However, details of how LRCs develop and what functions they play remain elusive. Here, we suggest that the development of LRCs can organize a "small-world network" in V1 [4] and that this enables an efficient integration of information at each network size. We found that a "small-world" network, which minimizes the average "global" distance between distant nodes while maximizing "local" interactions between adjacent nodes with a limited number of connections, can be achieved by a combination of dense local connections and sparse long shortcuts, as observed in species with a large V1. Using a model simulation of convergent networks with retino-cortical projections, we show that the organization of a small-world network in V1 may fulfill the requirements of a well-functioning visual system, which can encode visual information on a wide spectrum range, from local to global scales. Particularly for a large V1 circuit, we found that local connections alone cannot properly integrate information on a global scale, but adding sparse LRCs can make the entire V1 circuitry as a small world that can recognize and classify images on a fairly wide visual spectrum range. We also found that LRCs may not contribute in a small V1 where local connections suffice, which may explain the species-specific emergence of LRCs. For a simulation of the model, we designed a three-layer neural network with lateral connections and convergence feedforward connectivity as a simplified model of the visual pathway. Lateral connections were implemented following the connectivity distribution data observed in the brain. To test the contribution of LRCs to visual object recognition, we used stimulus image sets with local features only (letter shape), global features only (location of two dots), and both features to train the model network and examined the classification performance while varying the ratio of LRCs in the circuit. As a result, we found that the addition of LRCs significantly increases the classification accuracy for images with global features, particularly for a large network model. Notably, the performance of the network was maximized at a specific portion of the LRCs, suggesting that sparse LRCs added to dense local connections can organize an optimal structure of networks to encode visual stimuli in various spectra. Finally, we found that this optimal condition can be predicted by estimating the small-world degree of each network circuit from the observed correlation between the network performance and the corresponding connectivity parameters — clustering coefficient, average path length, and small-worldness — with variations of the stimulus features and the network size. Overall, our results suggest that a combination of distinct types of cortical connectivity induces a mathematically optimal profile of circuitry, thus providing a better understanding of the species-specific existence of LRCs in mammalian species.

#### References

1. Voges, N. A modeler's view on the spatial structure of intrinsic horizontal connectivity in the neocortex. *Progress in Neurobiology*. 2010; 92: 277–292.
2. Rumberger, A. Intra- and inter-areal connections between the primary visual cortex V1 and the area immediately surrounding V1 in the rat. *Neuroscience*. 2001; 102: 35–52.
3. Seeman, S. C. Sparse recurrent excitatory connectivity in the microcircuit of the adult mouse and human cortex. *eLife*. 2018; 7: 1–27.
4. Watts, D. J. & Strogatz, S. H. Collective dynamics of 'small-world' networks. *Nature*. 1998; 393: 440–442.

## P85 Comparison of visual quantities in untrained deep neural networks

Hyeonsu Lee<sup>\*1</sup>, Woochul Choi<sup>1</sup>, Dongil Lee<sup>1</sup>, Se-Bum Paik<sup>1</sup>

<sup>1</sup>Korea Advanced Institute of Science and Technology, Department of Bio and Brain Engineering, Daejeon, South Korea

\*Email: hslee9305@kaist.ac.kr

The ability to compare two quantities is essential for animals to survive. Interestingly, a sense of quantity comparison is widely observed even in visually naïve animals, implying that this function can emerge innately in the absence of learning. Remarkably, neuronal activities selective to a specific proportion represented in non-symbolic numerical visual stimuli are observed in monkeys [1] and in humans [2], which may provide the basis for the development of functional circuits for quantity comparisons. However, details of how the brain achieves this ability remain elusive. Here, using a model simulation of biologically inspired deep neural networks and a set of visual stimuli that represent different proportions and differences between a number of white and black dots, we found that neuronal units that selectively respond to different proportions and differences between two quantities can emerge spontaneously in untrained deep neural networks. Using a randomly initialized AlexNet [3], we found that neuronal tuning to proportion and difference, two metrics by which a pair of non-symbolic numerical quantities can be compared, arise in the complete absence of training. The observed selectivity is robust across conditions of various visual features, such as the total area, size, and/or the convex hull of visual stimuli. We also found that these instances of neuronal selectivity enable the network to perform a quantity comparison task and that various behavioral and neuronal characteristics in the brain, such as the distance effect and response modulation across correct/incorrect trials, were reproduced by these tuned activities. Next, to understand how units selective to a specific proportion or difference in quantity can emerge spontaneously, we hypothesized an adapted model of summation coding [3], in which proportion/difference tuning arises from the summation of monotonically increasing or decreasing responses as the proportion or difference increases. Observations from our model simulation validated our hypothesis — an analysis of feedforward projections shows that units of increasing and decreasing responses provide a biased input to the proportion/difference selective units, but not to non-selective units, and an ablation test shows that silencing those increasing and decreasing responses significantly reduces the number of the proportion/difference-selective units. In addition, we found that the nonlinearity of increasing and decreasing response profiles can determine whether the connected unit encodes the proportion or difference. Specifically, unit response fitted to a power function is likely to induce proportion selectivity, while that fitted to an exponential function generates a difference tuning. We confirmed that this specific connection was essential for the emergence of a distinct type of comparison tuning — the ablation of power-like units significantly reduces the number of proportion units, and vice versa. In summary, our findings suggest that diverse cognitive functions can originate from the biased projections of random feedforward circuits; this provides advanced insight into the mechanisms underlying the development of innate functions in the brain.

## References

1. Vallentin D, Nieder A. Behavioral and prefrontal representation of spatial proportions in the monkey. *Current Biology*. 2008; 18(18): 1420–1425.
2. Jacob S.N, Nieder A. Tuning to non-symbolic proportions in the human frontoparietal cortex. *European Journal of Neuroscience*. 2009; 30(7): 1432–1442.
3. Kim G, Jang J, Baek S, Song M, Paik S.B. Visual number sense in untrained deep neural networks. *Science Advances*. 2021; 7(1): eabd6127.

## P86 Emergence of symmetry recognition requires visual experience

Jaeyoung Lew<sup>\*1</sup>, Min Song<sup>1,2</sup>, Se-Bum Paik<sup>1,2</sup>

<sup>1</sup>Korea Advanced Institute of Science and Technology, Department of Bio and Brain Engineering, Daejeon, South Korea

<sup>2</sup>Korea Advanced Institute of Science and Technology, Program of Brain and Cognitive Engineering, Daejeon, South Korea

\*Email: lewpa64@kaist.ac.kr

The ability to detect symmetry of a visual object is crucial for social animals in various situations, such as mate selection, hunting, and perceptual grouping. This ability is thought to originate from neuronal responses that selectively respond to symmetry [1], but the developmental mechanism underlying this selectivity in the brain remains elusive. Recent model studies have suggested that higher-order visual cognition processes, such as face detection [2] or number selectivity [3], can arise solely from random feedforward connections in an untrained deep neural network (CNN), which raises a relevant question of whether visual symmetry sense can arise spontaneously. Here, using a convolutional neural network model of the ventral visual stream (AlexNet), we show that symmetry sense, in the form of selective tuning at a single-unit level, arises spontaneously after training on natural images. First, we tested how networks trained on natural images can utilize symmetry information for image classification, finding that symmetry is an important feature contributing to performance accuracy. The responses of readout units in a network trained to natural images were significantly correlated with the symmetry index of the input images, and the level of such correlation was greater than that of other low-level visual features, including luminance, contrast and complexity of the image, while such results do not appear in an untrained network. This implies that symmetry sense is an essential visual function for image classification that can emerge through the learning of natural image statistics. Next, to assess the extent to which network training accounts for the emergence of symmetry sense, we searched for symmetry channels in randomly initialized untrained networks. While we found a small number of symmetry channels in untrained networks, their responses were not strong enough to convey the information about symmetry to the deeper layers. This result is in contrast with the observation that certain higher-order visual functions such as face detection can arise spontaneously in untrained networks, with the level of selectivity comparable to those in pretrained networks and even the biological brain [2]. This implies that a certain class of visual function, such as symmetry tuning, while being a simple mathematical function, cannot arise in neural networks without extensive training on visual images. Lastly, we investigated the detailed developmental process of symmetry tuning. We observed that the weight matrices of feedforward projections become symmetric during training and assumed that these symmetric weight matrices could provide a basis for symmetry-selective channels. We validated this idea by defining a weight symmetry index (WSI), which represents the degree of symmetry in weights. We found that the weights of the symmetry channels in pretrained networks had significantly higher WSI values than those of non-selective channels. In contrast, no channel could attain a WSI outcome that was significantly higher than the chance level in an untrained network, explaining the absence of symmetry sense. Our findings provide advanced insight for those seeking to understand the neuronal-level mechanisms of symmetry sense and

augment our understanding of the development of cognitive functions that spontaneously arise from visual experience.

## References

1. Sasaki Y, Vanduffel W, Knutsen T, et al. Symmetry activates extrastriate visual cortex in human and nonhuman primates. *Proceedings of the National Academy of Sciences of the U.S.A.* 2005; 102(8):3159–3163.
2. Baek S, Song M, Jang J, et al. Face detection in untrained deep neural networks. *Nature Communications.* 2021; 12(1):1–15.
3. Kim G, Jang J, Baek S, et al. Visual number sense in untrained deep neural networks. *Science Advances.* 2021; 7(1):eabd6127.

## P87 Effect of temperature and geometry on action potential propagation failure at axonal branch points in sympathetic preganglionic neurons

Yuxuan Wu<sup>1</sup>, Mallika Halder<sup>2</sup>, Alan Sokoloff<sup>2</sup>, Yaqing Li<sup>3</sup>, Michael Sawchuk<sup>2</sup>, Shawn Hochman<sup>3</sup>, **Astrid A. Prinz**<sup>\*1</sup>

<sup>1</sup>Emory University, Department of Biology, Atlanta, GA, United States of America

<sup>2</sup>Emory University, Department of Cell Biology, Atlanta, GA, United States of America

<sup>3</sup>Emory University, Department of Physiology, Atlanta, GA, United States of America

\*Email: astrid.prinz@emory.edu

We combine anatomical and electrophysiological data obtained in an ex vivo adult mouse preparation with computational modeling to examine potential factors that modulate and control signal processing and gain at the interface of spinal sympathetic preganglionic neurons (SPNs) and their synaptic targets, postganglionic neurons in the sympathetic ganglion chain that regulate blood flow to distributed organ systems such as muscle and skin. This central-peripheral circuit is intimately involved in modulation of stress, metabolism, blood distribution and thermoregulation. Despite being a physiologically critical area in vertebrate neuroscience, it is little explored. Here, we focus on axon and axonal branch point geometry and temperature (T) as two interacting factors that influence the success or failure of action potential propagation at branch points. As SPN axons are predominantly unmyelinated and show variations in diameter and branching, reliability of conduction at their branch points is expected to be T-sensitive and modifiable by hypo- and hyperthermia.

We have constructed a conductance-based multi-compartment model of an axonal branch point consisting of a parent axon (P) which branches into two daughter axons (D1 and D2). The model is implemented in Python and contains three membrane currents – fast sodium INa, delayed rectifier IKd, and leak. Parameters of INa and IKd are adapted from our previous model of postganglionic neurons [1]. Temperature is modeled through its influence on ionic reversal potentials via the Nernst equation and on ion channel gating time constants using a Q10=3, typical for channels.

Figure 1 shows results from our model pilot studies on the effects of axon and branch point geometry and T on branch point failure. To investigate the effect of T and its interactions with branch point geometry, we used the model in two configurations that are identical except for the diameter of D2– 0.3 mm (left) vs. 0.1 mm (right). P, D1, and D2 are each 1 mm long and a spike is initiated in P. As T is increased, both model configurations exhibit a transition from faithful spike propagation in D1 and D2, to failure in one branch, to failure in both. In the model at left (0.3 mm D2), this transition occurs between the

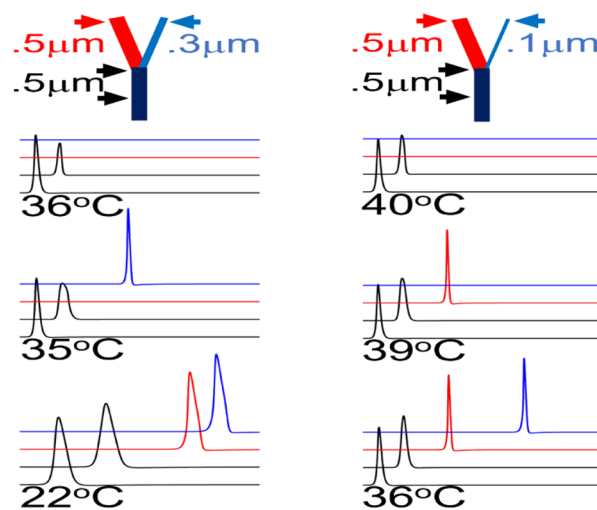


**Fig. 1** Influence of T on branch point failure. Two model configurations (top) differ in D2 diameter (blue). Voltage traces show membrane potential at different Ts for locations indicated by arrows. Both configurations transition from no failure, to one branch failing, to both branches failing, as T increases. Left: wider branch fails first. Right: narrower branch fails first

T frequently used in most experiments (22 °C), including our electrophysiological studies in the sympathetic chain that assessed magnitude of SPN signal divergence, and mouse body T (36 °C). This illustrates how fever or hyperthermia can affect sympathetic and other neural system function. Interestingly, in the left model the wider D1 (red) fails first as T increases, while at right, the narrower D2 (blue) fails first. This indicates two different failure mechanisms that can be explained by interactions between axon geometry and T-dependent spike duration, which will be explored in detail in further work using this model. Our study supports that computational modeling can be a crucial complement to experimental studies in circuits where details of current flows and potential changes are not experimentally accessible, as at the spinal-to-sympathetic chain interface.

## Acknowledgements

Supported by NIH grant 5R01NS102871 (MPI: Hochman, Prinz).

## References

1. McKinnon ML, Tian K, Li Y, Sokoloff AJ, et al. Dramatically Amplified Thoracic Sympathetic Postganglionic Excitability and Integrative Capacity Revealed with Whole-Cell Patch-Clamp Recordings. *eNeuro.* 2019; 6(2): 0433–18.

## P88 A mathematical perspective on edge-centric brain functional connectivity

Leonardo Novelli<sup>\*1</sup>, Adeel Razi<sup>2</sup>

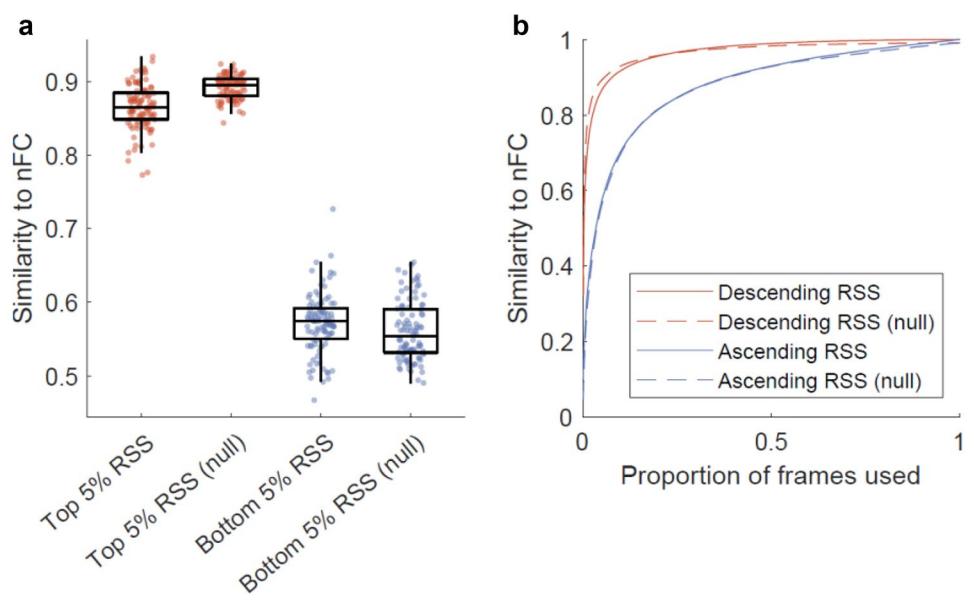
<sup>1</sup>Monash University, Monash Biomedical Imaging, Australia

<sup>2</sup>Monash University, Melbourne, Australia

\*Email: leonardo.novelli@monash.edu

Edge time series are increasingly used in brain functional imaging to study the node functional connectivity (FC) dynamics at the finest

**Fig. 1** The null model can reproduce the results published in [1, Fig. 1D], despite the arbitrary timing of the high-amplitude cofluctuations. Only a small fraction of frames exhibiting the largest cofluctuations root-sum-of-squares (RSS) are required to explain a significant fraction of variance in the FC



temporal resolution while avoiding sliding windows [1, 2]. Although the new technique has generated excitement in the field, its potential and limitations are matters of current investigation. We contribute to the ongoing dialogue with a statistical perspective and a criticism of the edge-centric approach as applied to fMRI datasets to date. Our central argument is that the existing findings based on edge time-series can be derived more simply from the static FC under a i.i.d. Gaussian null hypothesis that accounts for the observed static spatial correlations but not the temporal ones. Under this strong stationarity assumption, the edge time series variability is described by the sampling distribution of the static correlation matrix, known as the Wishart distribution. We can thus take a statistical perspective and use analytic derivations to predict the edge-centric features from the static FC. These predictions are tested on resting-state fMRI data of 100 unrelated participants from the Human Connectome Project (HCP) [3]. We show analytically that the edge FC, the edge communities, the large co-fluctuations, and the corresponding spatial brain activity patterns can all be predicted from the static FC. When tested on fMRI data from the HCP, the predictions based on the null model are sufficient to replicate the main edge-centric features both qualitatively and quantitatively (one example in Fig. 1). The inability to reject the null hypothesis on most of the HCP 100 unrelated participants does not support the conclusion that edge time-series and edge-centric metrics provide additional information beyond the static FC. These results are not an attempt to disprove the existence of finely timed neural events—they just warn that the evidence provided by fMRI data may not be sufficient to reject simpler explanations for the edge-centric features studied in [1] and [2]. In fact, previous influential studies have warned about the dangers of extracting structure from noise in the context of time-varying FC, also using minimal null models to reproduce existing results [4]. However, it would be premature to conclude that the edge-centric approach has no merit, and we acknowledge the fast progress in its development and applications. It would also be unreasonable to assume that the null hypothesis of i.i.d. variables is a good description of the BOLD signal, which is slowly-varying and highly autocorrelated. Thus, the fact that such null model is able to replicate the edge-centric features in [1] and [2] indicates that the temporal structure of the edge time series has not been exploited to the fullest. We encourage future work to focus on dynamic measures that cannot be easily explained by minimal null models.

## References

1. F.Z. Esfahlani et al. High-amplitude cofluctuations in cortical activity drive functional connectivity. *Proceedings of the National Academy of Sciences*. 2020; 117: 28393
2. J. Faskowitz et al. Edge-centric functional network representations of human cerebral cortex reveal overlapping system-level architecture. *Nature Neuroscience*. 2020; 23: 1644
3. Van Essen et al. The WU-Minn Human Connectome Project: An overview. *Neuroimage*. 80; 62–79
4. R. Liégeois et al. Interpreting temporal fluctuations in resting-state functional connectivity MRI. *NeuroImage*. 2017; 163; 437

## P89 A model of REM-NREM sleep state cycling with application to infancy

Lachlan Webb<sup>1</sup>, Andrew Phillips<sup>2</sup>, James A Roberts<sup>3</sup>

<sup>1</sup>QIMR Berghofer Medical Research Institute, Australia

<sup>2</sup>Monash University, Turner Institute for Brain and Mental Health, Melbourne, Australia

<sup>3</sup>QIMR Berghofer, Computational Biology, Brisbane, Australia

\*Email: lachlan.webb@qimrberghofer.edu.au

Sleep is divided into distinct sleep states, most notably rapid-eye movement (REM) and non-REM (NREM) sleep. In infancy, due to different cortical and physical manifestations of sleep, the REM and NREM equivalent sleep states are often referred to as Active and Quiet sleep, respectively. Other key differences in REM-NREM cycling for infants include more rapid cycling, and the commencement of sleep in the equivalent REM state, instead of the NREM state (Wake-REM-NREM vs. the mature Wake-NREM-REM). We are interested in understanding the physiological mechanisms underlying developmental changes in sleep state cycling from infancy to early childhood.

The physiologically based sleep-wake model developed by Phillips and Robinson (2007) [1] has been used as a standard model for understanding adult sleep/wake behaviors [2, 3, 4], but it has yet to be extended to modelling sleep states.

We extended the model to include a REM-on/active group and REM-off group [5, 6] with mutual inhibition providing the basis for REM-NREM cycling. The REM-NREM cycling is driven by a REM sleep homeostatic process, similar to other models that have been proposed [7].

We found parameter combinations that produce REM-NREM cycling, including sleep cycles observed in infancy. Varying the values of the parameters in the REM-NREM mutual inhibition relationship resulted in changing which is the initial sleep state, which can be modulated by the parameters governing the dynamics of the REM homeostatic drive. Through varying these parameters, the model is able to reproduce both adult Wake-NREM-REM and infant Wake-REM-NREM behaviors. We have thus identified a plausible mechanism for the immature ultradian sleep state cycling observed in infants. Our work provides a new tool for understanding developmental sleep patterns.

## References

- Phillips AJK, Robinson PA. A Quantitative Model of Sleep–Wake Dynamics Based on the Physiology of the Brainstem Ascending Arousal System. *Journal of Biological Rhythms*. 2007; 22(2):167–179.
- Skeldon AC, Derkx G, Dijk DJ. Modelling changes in sleep timing and duration across the lifespan: Changes in circadian rhythmicity or sleep homeostasis? *Sleep Medicine Reviews*. 2016; 28:96–107.
- Puckeridge M, Fulcher BD, Phillips AJK, et al. Incorporation of caffeine into a quantitative model of fatigue and sleep. *Journal of Theoretical Biology*. 2011; 273(1):44–54.
- Phillips AJK, Robinson PA, Kedziora DJ, et al. Mammalian Sleep Dynamics: How Diverse Features Arise from a Common Physiological Framework. *PLOS Computational Biology*. 2010; 6(6):e1000826.
- Saper CB, Fuller PM, Pedersen NP, et al. Sleep state switching. *Neuron*. 2010; 68(6):1023–42.
- Héricé C, Patel AA, Sakata S. Circuit mechanisms and computational models of REM sleep. *Neuroscience Research*. 2019; 140:77–92.
- Booth V, Diniz Behn CG. Physiologically-based modeling of sleep-wake regulatory networks. *Mathematical Biosciences*. 2014; 250:54–68.

## P90 Modeling of chirps in seizures

Shrey Dutta<sup>\*1</sup>, Michael Breakspear<sup>2</sup>, James A Roberts<sup>3</sup>

<sup>1</sup>QIMR Berghofer Medical Research Institute, University of Queensland, Faculty of Medicine, Brisbane, Australia

<sup>2</sup>The University of Newcastle, School of Psychology, School of Medicine and Public Health, Hunter Medical Research Institute, Newcastle, Australia

<sup>3</sup>QIMR Berghofer, Computational Biology, Brisbane, Australia

\*Email: shrey.dutta@qimrberghofer.edu.au

A commonly observed feature of epileptic seizures is slowing chirps of their fundamental frequency and harmonics as seizures approach termination. Here, employing a network of Hodgkin-Huxley neurons augmented with K+, Na+, and O2 dynamics, we show that different types of seizures --- from dominating in lower frequencies to exhibiting instantaneous chirps --- emerge spontaneously in the model (without stimulation), with their morphology depending on the availability of ionic and metabolic resources. Using stereoelectroencephalography (SEEG) data from epilepsy patients, we find that the model is able to quantitatively reproduce clinically-observed frequency slowing, variable seizure durations, and periods of post-ictal suppression following seizure termination. The estimated locations of data seizures in the model parameter space provide new insights into the individualized degree of pathology in energy demand and supply, and open new avenues for studying the epileptic brain.

## P91 Assessing the electromotor neural network topology through modeling and genetic algorithm optimization

Angel Lareo<sup>\*1</sup>, Pablo Varona<sup>2</sup>, Francisco B Rodriguez<sup>2</sup>

<sup>1</sup>Universidad Autónoma de Madrid, Madrid, Spain

<sup>2</sup>Universidad Autónoma de Madrid, Ingeniería Informática, Madrid, Spain

\*Email: angel.lareo@estudiante.uam.es

Pulse Mormyridae generates electrical pulses to communicate and to obtain information from the environment. Ethological studies have related specific sequences of pulse intervals (SPIs) in the signal of these fish to distinct behaviors (e.g., advertisement signals) [1, 3]. Accelerations, scallops, rasps, and cessations are four distinct reported SPI patterns, each showing characteristic temporal structures. The timing of pulse generation is controlled by the electromotor system, a neural network in the central nervous system.

The role of the topology of the electromotor system to generate distinct SPI patterns is assessed here using a computational network model adjusted to reproduce nucleus characteristics and known information of the network as described by previous studies [1, 2]. A genetic algorithm (GA) was developed and applied to tune the synaptic parameters to reproduce the whole set of recorded SPI patterns using the same internal network configuration [4, 5, 6]. The topology of this model is based on a simplified representation of the network with four nuclei: VPd, DP, PCN, and CN. Both nuclei DP and PCN constitute different excitatory pathways to the CN nucleus. CN is the output of the model, and its activation also excites VPd through a corollary discharge pathway (CDP). Finally, VPd inhibits both DP and PCN, so the activation of CN triggers an inhibitory feedback loop in the network.

To address how different pathways in the network contribute to the variability of SPI patterns showed by the mormyrids electromotor system, specific synapses were removed to build two alternate topologies: (TP1) a model without CDP, deactivating the inhibitory feedback loop; and (TP2) a model without PCN activation pathway, so CN only received activation through DP. The GA was then applied to TP1 and TP2 to adjust the synaptical parameters. Fitting results from alternate topologies were consistently worse than those obtained from the original model. In TP1, the absence of a CDP makes the SPIs not to be reproduced. In TP2, reducing to one the activation pathways to CN, the variability of SPIs was reduced: scallops are not reproduced, while accelerations and rasps became indistinguishable.

These results remark the importance of the network dynamical balance to reproduce the variability of behavioral sequential patterns exhibited by the electromotor system.

## Acknowledgements

Funded by AEI/FEDER PID2020-114867RB-I00, and PGC2018-095895-B-I00.

## References

- Caputi, A. A., Carlson, B. A., and Macadar, O. Electric organs and their control. In *Electroreception*, pages 410–451. Springer. 2005
- Carlson, B. A. Neuroanatomy of the mormyrid electromotor control system. *Journal of Comparative Neurology*. 2002; 454(4): 440–455
- Carlson, B. A. and Hopkins, C. D. Stereotyped temporal patterns in electrical communication. *Animal Behaviour*. 2004; 68(4): 867–878
- Lareo, A. and Rodriguez, F. B. Sequential Information Processing in Electroreception: A Modelling Approach. In *Dynamic Days in Latin America and the Caribbean*, Puebla, México. 2016
- Lareo, A., Varona, P., and Rodriguez, F. Evolutionary Tuning of a Pulse Mormyrid Electromotor Model to Generate Stereotyped

- Sequences of Electrical Pulse Intervals. In International Conference on Artificial Neural Networks. Springer. 2018; 359–368
6. Lareo, Á., Varona, P., and Rodriguez, F. B. Modeling the variability of the electromotor command system of pulse electric fish. *bioRxiv*. 2021; pages 2020–06

#### P92 Closed-loop stimulation protocol driven by flexible neural codes based on Victor-Purpura distance

Alberto Ayala<sup>1</sup>, Angel Lareo<sup>\*1</sup>, Pablo Varona<sup>1</sup>, Francisco B Rodriguez<sup>1</sup>

<sup>1</sup>Universidad Autónoma de Madrid, Ingeniería Informática, Madrid, Spain

\*Email: angel.lareo@estudiante.uam.es

Coding and processing of temporal information occur in neural systems with inherent temporal variability. In this regard, feedback loops in these systems are important for processing temporal information. Thus, closed-loop experimental designs, in which the system is stimulated based on certain events of its ongoing activity, are suitable to study such coding, although considering the variability of these events is not an easy task.

An implementation of a real-time closed-loop stimulation protocol to study flexible neural codes is presented here. This implementation is based on the Temporal Code-Driven Stimulation (TCDS) [1–3] protocol which acquires a neural signal with the required precision and binarizes it. After the detection of a predetermined temporal code in the binarized signal, the protocol stimulates the system in a code dependent manner. However, given the structure of the predetermined code time sequence, neural systems typically emit similar codes with certain variability in their temporal sequence. Thus, a flexible code detection metric, the Victor-Purpura distance [4], has been added to the functionality of the TCDS protocol to search for specific patterns and establish similarities between the temporal structure of neural codes. In addition, relevant events in which the information is coded in neural systems usually occur within or below the millisecond scale and consequently closed-loop operations must be performed with this required precision. Accordingly, this protocol has been developed using the Real-Time eXperiment Interface tool [5], which is an open-source hard real-time data acquisition and control framework for biological and neuroscientific research widely used by many laboratories. To validate this approach, closed-loop experiments were carried out using a hardware implementation of a Hindmarsh-Rose neuron model. In these experiments, performance was analyzed by measuring latencies of the closed-loop tasks under different computational stress conditions, as well as the correct performance of the protocol.

Based on the latency results, the implemented stimulation protocol complies with the required temporal constraints. The experimental results showed that the implemented protocol and Victor-Purpura metric adequately considered the temporal variability in the system's sequential activity to establish the code-driven stimulation closed-loop.

#### Acknowledgements

Funded by AEI/FEDER PID2020-114867RB-I00, and PGC2018-095895-B-I00.

#### References

1. A Lareo, CG Forlim, RD Pinto, P Varona, FB Rodriguez. Temporal code-driven stimulation: definition and application to electric fish signaling. *Frontiers in Neuroinformatics*. 2016; 10:41
2. A Lareo, CG Forlim, RD Pinto, P Varona, FB Rodriguez. Analysis of Electroreception with Temporal Code-Driven Stimulation. *Lecture Notes in Computer Science*. 2017; 10305:101–111.
3. A Ayala, A Lareo, P Varona, FB Rodriguez. Closed-loop temporal code-driven stimulation implemented and tested using Real-Time eXperimental Interface (RTXI). 30th Annual Computational Neuroscience Meeting: CNS\*2021. *Journal of Computational Neuroscience*. 2021; 49, 3–208: 153–586.
4. JD Victor, KP Purpura. Nature and precision of temporal coding in visual cortex: a metric-space analysis. *Journal of neurophysiology*. 1996; 76(2):1310–1326.
5. YA Patel, A George, AD Dorval, JA White, DJ Christini, RJ Butera. Hard real-time closed-loop electrophysiology with the Real-Time eXperiment Interface (RTXI). *PLOS Computational Biology*. 2017; 13(5):e1005430.

#### P93 Fine temporal patterning of partial synchronization of gamma rhythms

Quynh-Anh Nguyen<sup>1</sup>, Leonid Rubchinsky<sup>\*2</sup>

<sup>1</sup>Indiana University Purdue University Indianapolis, Mathematical Sciences, Indianapolis, IN, United States of America

<sup>2</sup>Indiana University Purdue University Indianapolis and Indiana University School of Medicine, Department of Mathematical Sciences and Stark Neurosciences Research Institute, Indianapolis, IN, United States of America

\*Email: lrubchin@iupui.edu

Synchronization of neural activity in the gamma frequency band is associated with various cognitive phenomena. Abnormalities of gamma synchronization may underlie symptoms of several neurological and psychiatric disorders, such as schizophrenia and autism spectrum disorder [1, 2]. Properties of gamma band neural oscillations are known to critically depend on the synaptic properties of circuits expressing this activity. The present study explores how synaptic properties in pyramidal-interneuronal circuits affect not only the fine temporal patterning of neural synchrony, that is the variability of the neural synchronization on very short timescales. If two signals show only moderate synchrony strength, it may be possible to consider these dynamics as transitions between synchronized and desynchronized states. This patterning of the synchronized dynamics may be independent of the average synchronization strength [3, 4].

Following previous studies with minimal inhibitory-excitatory circuits [5], we use models of connected circuits expressing pyramidal-interneuronal gamma (PING) activity to explore the temporal patterning of synchronized and desynchronized episodes. Changes in the synaptic strength may alter the temporal patterning of synchronized dynamics (even if the average synchrony strength is not changed). Larger values of both excitatory and inhibitory synapses between excitatory and inhibitory neurons tend to promote short desynchronizations; larger values of synapses between inhibitory interneurons tend to promote longer synchronizations. Furthermore, we show that circuits with different patterning of synchronization in time may have different sensitivity to synaptic input.

Our results show that synaptic changes may affect not only average synchrony strength, but also the temporal patterning of gamma synchronization. Our observation of networks with different temporal dynamics of synchronization having different sensitivity to common synaptic input provides one potential functional mechanism for different temporal patterning of synchronization. Thus, the synaptic changes, which affect gamma oscillations and result in different properties of

information processing in the brain (and its abnormalities in several neurological and neuropsychiatric disorders), may mediate physiological properties of neural circuits not only via change in the average synchrony level, but also via change of how synchrony is patterned in time over very short time scales.

### Acknowledgements

This work was supported by NSF grant DMS 1813819.

### References

- Uhlhaas PJ and Singer W. Oscillations and neuronal dynamics in schizophrenia: the search for basic symptoms and translational opportunities. *Biological Psychiatry*. 2015; 77:1001–1009.
- Spellman TJ and Gordon JA. Synchrony in schizophrenia: a window into circuit-level pathophysiology. *Current Opinion in Neurobiology*. 2015; 30:17–23.
- Ahn S, Rubchinsky LL. Potential mechanisms and functions of intermittent neural synchronization. *Frontiers in Computational Neuroscience*. 2017; 11:44.
- Ahn S, Zauber SE, Witt T, Worth RM, Rubchinsky LL. Neural synchronization: Average strength vs. temporal patterning. *Clinical Neurophysiology*. 2018; 129:842–844.
- Nguyen Q-A, Rubchinsky LL. Temporal patterns of synchrony in a pyramidal-interneuron gamma (PING) network. *Chaos*. 2021; 31:043134.

### P94 A computational model of the thalamocortical interactions resulting in the mixed selectivity of prefrontal cortical cells

Sima Mofakham<sup>\*1,3</sup>, Jessica Phillips<sup>2</sup>, Chen Cui<sup>3</sup>, Kurt Butler<sup>3</sup>, Marzieh Ajirak<sup>3</sup>, Jordan Saadon<sup>4</sup>, Charles Mikell<sup>1</sup>, Petar Djuric<sup>3</sup>, Yuri Saalmann<sup>2</sup>

<sup>1</sup>Stony Brook University Hospital, Neurological Surgery, Stony Brook, United States of America

<sup>2</sup>University of Wisconsin-Madison, Psychology, Madison, United States of America

<sup>3</sup>Stony Brook University, Electrical and Computer Engineering, Stony Brook, United States of America

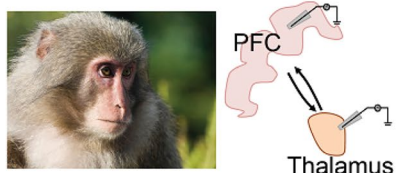
\*Email: Sima.Mofakham@stonybrookmedicine.edu

Despite the critical need to understand the neural bases of higher-order cognitive functions such as working memory, we lack a comprehensive theoretical framework to describe these phenomena at the cellular and network level. Single-cell recordings from the prefrontal cortex of

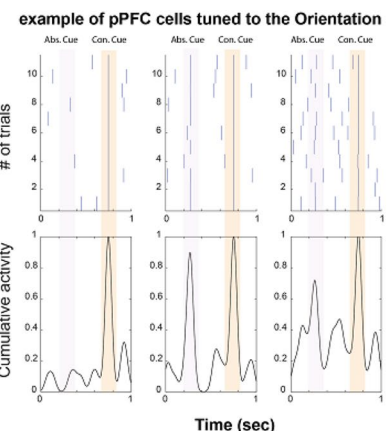
non-human primates and rodents during working memory behavioral tasks have demonstrated tuning of these cells, reflected in their firing rate, to different aspects of the behavioral task. The “tuned” cells encode and maintain the information presented to accomplish the task. However, these experimental recordings have revealed that most cells had been tuned to multiple aspects of the task with a *mixed selectivity*. It has been proposed that this *mixed selectivity* of cortical cells during working memory tasks enables cognitive flexibility, whereby multiple different behavioral responses could be readily read out from the high-dimensional neural representations. However, the underlying mechanisms giving rise to *mixed selectivity* have never been fully explained [1]. Here, we attempt to provide a data-grounded computational model of working memory that explains how: 1) working memory is stored in cortical representations, 2) thalamus shapes these cortical representations, 3) mixed selectivity arises from thalamocortical interactions, while the signal remains robust. To accomplish this goal, we analyzed local field potential (LFP) and single-cell recordings from the anterior and posterior prefrontal cortex and mediodorsal thalamus (MD) during a working memory task performed by macaques. In this task, the monkey must initially select and remember the correct visual features (context), then the correct rule, and finally respond. We used a data-driven, machine-learning approach to evaluate the direction of information flow within the circuit. We used experimental recordings from cortical and thalamic regions and machine learning causality techniques to dynamically track the direction of connectivity between cortical and thalamic regions at different task epochs. Then, we developed a reduced layer-specific thalamocortical model using the leaky integrate-and-fire spiking model to shed light on the underlying mechanism supporting working memory (Fig. 1). Here, the cortical representations associated with working memory are formed and maintained within and across cortical areas by thalamic projections from “core” and “matrix” MD cells [2]. The *core* cells maintain the *context* and the *presented rule* throughout the task, while the *matrix* cells mediate the selection and signal transmission across cortical regions. The interplay of these two mechanisms (local computation and long-distance communication) results in the *mixed selectivity* observed in single-cell recordings without negatively affecting specificity and selectivity in task performance. Mixed selectivity optimizes the cortical network’s performance in this context by allowing dynamic encoding and decoding of cortical representations. This model replicates many aspects of our experimental observations and leads to specific predictions. Working memory is one of the building blocks of our higher-order cognitive functions. This model could have important implications in cases when working memory is disrupted and can be used to pave the way to develop the next generation of therapeutic approaches.

**Fig. 1** We used experimental data simultaneously recorded from the thalamus and superficial/deep prefrontal cortex (PFC) layers (left panel) to build a model that describes how *mixed selectivity* arises from thalamocortical interactions. The right panel shows examples of posterior PFC cells without (plot on the left) and with *mixed selectivity* (middle and right plots)

#### Fine-grained experimental monkey recordings



#### Simulating neural activity during the working memory



## References

1. V. Mante, D. Sussillo, K.V. Shenoy, W. T. Newsome. Context-Dependent Computation by Recurrent Dynamics in Prefrontal Cortex. *Nature*. 2013; 503 (7474): 78–84.
2. Schmitt, L. Ian, R.D. Wimmer, M. Nakajima, M. Happ, S. Mofakham, M.M. Halassa. Thalamic Amplification of Cortical Connectivity Sustains Attentional Control. *Nature*. 2017; 545 (7653): 219–23.

## P95 Determinants of input amplitude and slope detection in bursting neurons

Rebecca Miko<sup>\*1</sup>, Volker Steuber<sup>1</sup>, Michael Schmuker<sup>1</sup>

<sup>1</sup>University of Hertfordshire, Biocomputation Research Group, Hatfield, United Kingdom

\*Email: r.miko@herts.ac.uk

Turbulence in natural environments causes a rich temporal structure in gas stimuli, which contains information that may aid in gas-based navigation [1, 2]. Research has suggested that animals exploit this structure to locate odour sources [3] and that some of this information lies in the temporal dynamics of the signals [2]. Furthermore, a study found that particular spatial and temporal features in neuronal inputs trigger bursts [4], which would suggest that these firing patterns represent a particular form of neural code. We investigated if and to what extent a bursting neuron that implements the Izhikevich differential equations [5] can detect amplitudes and slopes of a naturalistic input signal. The input signal was injected directly into each neuron as Gaussian white noise (sampling rate  $f_s = 400$  Hz,  $\mu = 0.003$ , and  $\sigma = 0.005$ ) with a 25 Hz Butterworth low-pass filter. We recorded bursts which we defined as having < 10 ms intervals between spikes.

We then recorded the lengths of the bursts, for example, 2- or 3-spike bursts, to understand the distribution of burst density over the amplitudes and the slopes in the signal. From there, we created receiver operator characteristic (ROC) curves for the 2- and 3-spike burst distributions. Our fitness function was the area under the curve (AUC), where higher AUC values tell us that the neuron is more successful at distinguishing between different slopes or amplitudes.

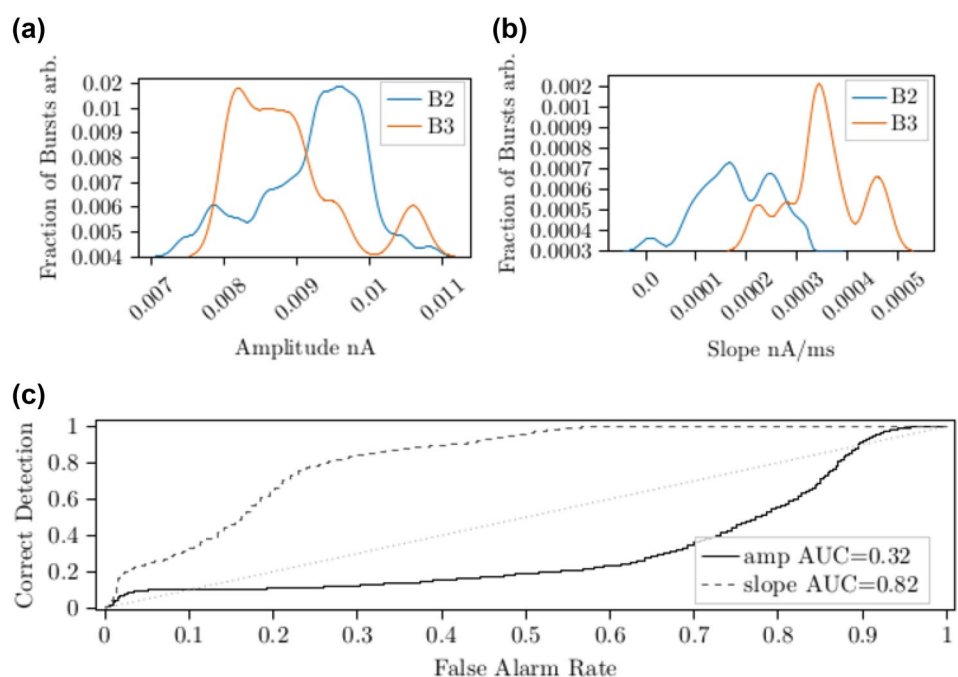
We found that, depending on the parameters, the neurons can detect either the slope of the signal (Fig. 1), or the amplitude, or both.

These neurons were successful when presented with a generated naturalistic input signal. We plan to extend this research by investigating if and to what extent these neurons can detect amplitudes and slopes of an input signal which has been recorded directly from a neuromorphic sensor called an electronic nose (e-nose) within a real-world environment. Wind conditions, temperature and sensor time lags are some of the biggest challenges we will face. It would be interesting to see how our neurons perform in these conditions and what adjustments need to be made in order to be successful at detecting signal slopes and amplitudes with real-world data.

## References

1. Celani, A., Villermaux, E. and Vergassola, M.: Odor landscapes in turbulent environments. *Physical Review X*. 2014; 4(4): p.041015.
2. Schmuker, M., Bahr, V. and Huerta, R.: Exploiting plume structure to decode gas source distance using metal-oxide gas sensors. *Sensors and Actuators B: Chemical*. 2016; 235: pp.636–646
3. Jacob, V., Monsempès, C., Rospars, J.P., Masson, J.B. and Lucas, P.: Olfactory coding in the turbulent realm. *PLoS Computational Biology*. 2017; 13(12): p.e1005870
4. Kepcs, Adam, Xiao Jing Wang, and John Lisman. Bursting neurons signal input slope. *Journal of Neuroscience*. 2002; 22.20, pp. 9053–9062
5. Izhikevich, Eugene M. Simple model of spiking neurons. *IEEE Transactions on Neural Networks*. 2003; 14.6: pp. 1569–1572

**Fig. 1** An analysis of a neuron's response to a given input signal. **A** the distribution of burst density over the signal amplitudes. **B** the distribution of burst density over the slopes of the signal. **C** the ROC curves showing discriminability between 2- and 3-spike distributions. These results show that different burst lengths correspond to different slopes



**P96 Entropy, free energy, symmetry and dynamics in the brain**Viktor Jirsa<sup>1</sup>, Hiba Sheheitli<sup>\*2</sup>

<sup>1</sup>INSERM & Aix-Marseille Université, Theoretical Neuroscience Group, Institut De Neurosciences Des Systèmes, Marseille, France  
<sup>2</sup>Aix-Marseille Université, Institut de Neurosciences des Systèmes, Marseille, France

\*Email: hs497@cornell.edu

Neuroscience is home to concepts and theories with roots in a variety of domains including information theory, dynamical systems theory, and cognitive psychology. Not all of those can be coherently linked, some concepts are incommensurable, and domain-specific language poses an obstacle to integration. Still, conceptual integration is a form of understanding that provides intuition and consolidation, without which progress remains unguided. This paper is concerned with the integration of deterministic and stochastic processes within an information theoretic framework, linking information entropy and free energy to mechanisms of emergent dynamics and self-organization in brain networks. We identify basic properties of neuronal populations leading to an equivariant matrix in a network, in which complex behaviors can naturally be represented through structured flows on manifolds establishing the internal model relevant to theories of brain function. We propose a neural mechanism for the generation of internal models from symmetry breaking in the connectivity of brain networks. The emergent perspective illustrates how free energy can be linked to internal models and how they arise from the neural substrate.

**P97 Whole brain comparison of effective cortical micro-connectome**

Kouki Matsuda<sup>1</sup>, Arata Shirakami<sup>1</sup>, Ryota Nakajima<sup>1</sup>, Yuki Yamaguchi<sup>1</sup>, Masanori Shimono<sup>\*1</sup>

<sup>1</sup>Kyoto University, Graduate School of Medicine and Faculty of Medicine, Kyoto, Japan

\*Email: nori417@gmail.com

The cortex is an evolutionarily new component of the brain that supports the high intelligence of mammals. In the brain, each cortical region should have some degree of homology, but should also require different local circuits for each function it performs to achieve its specific purpose. Until now, microconnectome studies have focused on an individual brain region, observing the characteristics of local circuits. This study extended the analytical techniques that had been used only for an individual brain region to encompass all the cortical regions of

mice [Fig. 1A], and we systematically compared among cortical brain regions having topologies of the local circuits that are designed for specific functional demands. Prior to the comparison of topologies, we report information about basic physiological parameters, such as firing rate and layer thickness, that had not been fully known in past studies. It has been generally believed that inhibitory neurons, which are relatively less in number than excitatory neurons, are able to keep the activity level balanced, so they do not become either silent or epileptic in the activity of the excitatory neurons due to their high firing rate. As a result, first, we found that although the frontal region is known to be a hub region with connections to many regions in the brain's wide-area network, even viewed as an isolated local circuit, its centrality is confirmed to be high in k-core centrality [Fig. 1b]. These findings provide new insight into separate brain regions, and provide important complementary information that has not been discovered in many studies of the whole-brain network.

**P98 Network properties of the medial prefrontal cortex altered by chronic social stress in mice**

Yuki Yamaguchi<sup>1</sup>, Takeshi Hase<sup>2</sup>, Arata Shirakami<sup>1</sup>, Ryota Shinohara<sup>3</sup>, Shihō Kitaoka<sup>4</sup>, Tomoyuki Furuyashiki<sup>3</sup>, Masanori Shimono<sup>\*1</sup>

<sup>1</sup>Kyoto University, Graduate School of Medicine and Faculty of Medicine, Kyoto, Japan

<sup>2</sup>Tokyo Medical and Dental University, Medical Data Sciences Office, Bunkyo-ku, Japan

<sup>3</sup>Kobe University, Graduate School of Medicine, Kobe, Japan

<sup>4</sup>Hyogo Medical University, School of Medicine, Kobe, Japan

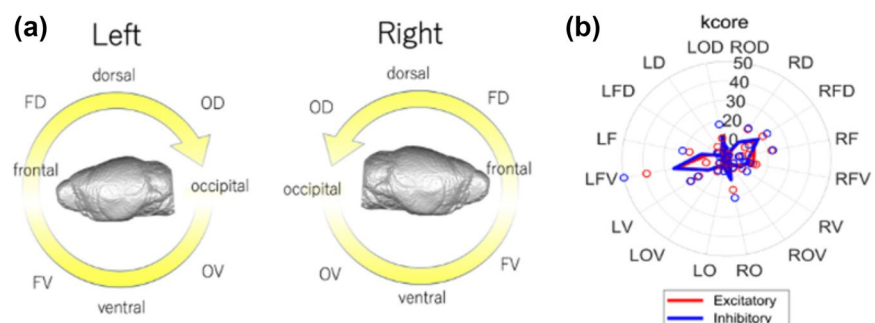
\*Email: nori417@gmail.com

Chronic social stress causes emotional and cognitive disturbances and increases the risk of mental illness such as depression. Many studies have revealed that an extraordinarily high number of neurons constitute a complex local network for their functions in the brain. The analysis of such complex networks will better illustrate mental illness pathophysiology than that of individual neuron types, but this has not been reported.

This study elucidates neuronal network alterations associated with chronic social stress-induced depressive-like behaviors in mice. We analyzed complex neuronal networks in the medial prefrontal cortex, a brain region whose structure and functions chronic stress impairs to cause depression, in naïve mice and stressed mice, as follows.

Step 1: We constructed datasets of neural networks consisting of 50 neurons from naïve and stressed mice, respectively, including all cortical layers of the medial prefrontal cortex. We used information obtained from electrical spikes in neurons to estimate links between network nodes.

**Fig. 1** **A** Expression of brain classification in 16 categories and their abbreviated names. **B** Radar chart of k-core centralities at individual brain regions. In panel (B), red and blue lines show features of excitatory and inhibitory neurons respectively, and individual data samples correspond with black dots



Step 2: We applied the Neural Network Embedding technology to extract low-dimensional features from the neural networks [1].  
 Step 3: Based on the low-dimensional features from Step 2 and XGBoost algorithm, we built classifiers between naïve and stressed mice.

Finally, we identified the physiological characteristics of disease by giving (independently defined) physiological labels on the neurons that play important roles in this classification.

## References

- Shirakami, Arata, Takeshi Hase, and Yuki Yamaguchi. "Neural network embedding of functional microconnectome." bioRxiv. 2021.

## P99 Neuromodulatory influence over cortico-thalamic basal ganglia function

Natasha Taylor<sup>\*1</sup>, Eli Muller<sup>1</sup>, Brandon Munn<sup>1</sup>, Gabriel Wainstein<sup>1</sup>, James Shine<sup>1</sup>

<sup>1</sup>The University of Sydney, Brain and Mind Centre, Camperdown, Sydney, Australia

\*Email: natasha.taylor@sydney.edu.au

The basal ganglia is a complex subcortical system involving an array of different nuclei that are both functionally and anatomically segregated. The basal ganglia includes a number of distinct sub-circuits, such as the direct, indirect and hyper-direct pathways, each of which integrates cortical and thalamic projections across the brain in order to mediate motor, cognitive and limbic functions. Classically, dopamine has been viewed as the primary neuromodulator for this circuit, as it facilitates activity in the direct pathway, but inhibits activity in the indirect pathway. Unfortunately, the simplicity of the dopaminergic influence of the basal ganglia circuitry inherently misses the complexity of other neuromodulatory influences of the basal ganglia. For instance, the cholinergic system provides major inputs to the basal ganglia, and typically causes effects that oppose the dopaminergic system. Serotonin and noradrenaline also have similarly important effects on the circuit. Despite these links, we currently do not know how different combinations of neuromodulatory ligands effects the emergent oscillatory activity of the basal ganglia and its connections with the thalamus and cortex.

To remedy this problem, we extended a working neural mass model of the cortico-thalamic basal ganglia system [1] by incorporating parameters that mimicked the impact of dopaminergic, cholinergic, serotonergic modulation on the cortico-thalamic basal ganglia model. Specifically, to mimic the modulation of the cholinergic system in the cortico-thalamic basal ganglia model, we manipulated the cortico-striatal coupling D1 nuclei (reducing direct pathway) and firing rate (to mimic 'bursty' activity) of the D2 nuclei of the indirect pathway. To model the serotonergic modulation of the cortico-thalamic basal ganglia model, we manipulated the firing rate of the sub-thalamic nucleus (reduced) and globus pallidus internus (increased). In order to assess the role of different neuromodulatory system influence of the basal ganglia, we measured the population gain of each nuclei output from the cortico-thalamic basal ganglia system, the steady state and the summary population gain of the direct, indirect and hyper-direct pathway. Our results provide the first systematic exploration of the complex neuromodulatory state-space that impacts the dynamics of the cortico-thalamic basal ganglia system.

Our future work will attempt to interrogate the different neuromodulatory influences over the basal ganglia system, by mimicking pathological states of Parkinson's disease. In particular we will attempt to understand the contributions of pathology to the cholinergic, serotonergic and dopaminergic systems on overall cortico-thalamic basal ganglia function.

Therefore, we have highlighted an advantage of using neural population models of the cortico-thalamic basal ganglia system to elucidate the complexity of neuromodulatory influence and their impact in pathological states.

## References

- E. J. Müller and P. A. Robinson. Quantitative theory of deep brain stimulation of the subthalamic nucleus for the suppression of pathological rhythms in Parkinson's disease. *PLOS Computational Biology*. 2018; 14(5): 1–20.

## P100 EEG tracking using neural field theory distinguish unconscious and disconnection across arousal states

Vicente Medel<sup>\*1</sup>, Eli Müller<sup>1</sup>, Cameron Casey<sup>2</sup>, Brandon Munn<sup>1</sup>, Robert Sanders<sup>3</sup>, James Shine<sup>1</sup>

<sup>1</sup>The University of Sydney, Brain and Mind Centre, Sydney, Australia

<sup>2</sup>University of Wisconsin, Department of Anesthesiology, Madison, United States of America

<sup>3</sup>The University of Sydney, Department of Anaesthetics, Sydney, Australia

\*Email: vicente.medel@gmail.com

How conscious experience becomes disconnected from the environment, or disappears, across arousal states is unknown. We sought to identify the neural biophysical substrates of sensory disconnection and unconsciousness using a novel serial awakening paradigm and a neural modeling strategy. Here we use neural field model of the brain, a powerful technique for constructing physiologically based models of the brain that can predict large-scale measures of brain activity, which can be fitted to experimental data to infer the underlying biophysical mechanisms of brain states. Subjects were recruited for sedation with dexmedetomidine -a powerful noradrenergic-based anaesthetic-, and underwent serial awakenings to establish whether subjects were in states of disconnected consciousness or unconsciousness in the preceding 20 s. We show EEG brain tracking can inform novel and previously hidden biophysical properties of conscious states related to sensory disconnection and unconsciousness induced by dexmedetomidine anesthesia. We discuss our results with noradrenergic-related modulations of neural dynamics, and the role of brainstem neuromodulatory effect in the corticothalamic system.

## P101 Modeling the dynamics of arbitrary partially known biochemical systems via hybrid mass action and neural kinetics endowed ODEs

Domas Linkevicius<sup>\*1</sup>, Angus Chadwick<sup>1</sup>, Melanie I. Stefan<sup>2</sup>, David C. Sterratt<sup>1</sup>

<sup>1</sup>University of Edinburgh, Institute for Adaptive and Neural Computations, School of Informatics, Edinburgh, United Kingdom

<sup>2</sup>Medical School Berlin, Faculty of Medicine, Berlin, Germany

\*Email: d.linkevicius@sms.ed.ac.uk

All cells in the brain contain large and complex chemical reaction networks (CRNs). Accurate dynamical models of these CRNs would allow for detailed predictions under experimental manipulations, such as malfunctioning proteins or addition of novel drugs. One of the standard approaches to modeling the dynamics of CRNs is via the assumption of mass action kinetics and then numerically solving

the system of induced polynomial ordinary differential equations (ODEs). This approach is unfeasible for the large CRNs in the brain due to a dearth of data on reaction structure and reaction rates. However, there are a number of experimentally constrained CRN models of parts of the neural biochemical networks, which are a source of information on their dynamics.

We describe a novel method that utilizes existing models of CRNs in order to fit the dynamics of CRNs whose reaction structure and rates are not fully known. Specifically, we augment an existing mass action CRN model with latent species, a matrix of parameters representing the reaction structure and a neural network serving as the rate function for the reactions over latent species. We merge the two parts via bridge species where specific mechanistic assumptions are made on how the bridge species interact with the real species from the existing CRN. We use the framework of neural ODEs [3] to fit the reaction structure matrix and the rate function to empirically observable dynamical data. To demonstrate our approach, we use a hybrid model which utilizes existing models of calcium buffering [1], CaMKII dynamics [5] and Stargazin-AMPA phosphorylation and lateral movement [6]. Using this partial model of synaptic dynamics, we attempted to reproduce the results on high frequency CaMKII-dependent forms of synaptic plasticity [2, 3].

Very few studies have tried restricting a machine learning model via a specific ODE model, rather than general physical laws. Our approach is a significant step in the construction of detailed, interpretable dynamical models of complex phenomena such as synaptic plasticity. Most importantly, it bypasses the prohibitive requirement of knowing thousands of reaction rates and reaction structures that comprise CRNs, such as the ones contained in synapses. Our work may be more generally adaptable to systems for which there are good sub-models.

## References

- Bartol, T. M., et al. Computational reconstitution of spine calcium transients from individual proteins. *Frontiers in Synaptic Neuroscience*. 2015; 7:1–24.
- Bayazitov, I. T., et al. Slow presynaptic and fast postsynaptic components of compound long-term potentiation. *Journal of Neuroscience*. 2007; 27; 11510–11521.
- Chen, R. T., et al. Neural ordinary differential equations. *Advances in Neural Information Processing Systems* 2018-Decem. 2018; 6571–6583.
- Incontro, S., et al. The camkii/nmda receptor complex controls hippocampal synaptic transmission by kinase-dependent and independent mechanisms. *Nature Communications*. 2018; 9:2069.
- Michalski, P. J., and Loew, L. M. Camkii activation and dynamics are independent of the holoenzyme structure: An infinite subunit holoenzyme approximation. *Physical Biology*. 2012; 9:6.
- Urakubo, H., et al. Requirement of an allosteric kinetics of nmda receptors for spike timing-dependent plasticity. *Journal of Neuroscience*. 2008; 28; 3310–3323.

## P102 Clustered stimuli and oscillations can improve pattern recognition in a detailed model of cerebellar cortex

Ohki Kataura<sup>\*1</sup>, Reinoud Maex<sup>2</sup>, Shabnam Kadir<sup>1</sup>, Volker Steuber<sup>2</sup>

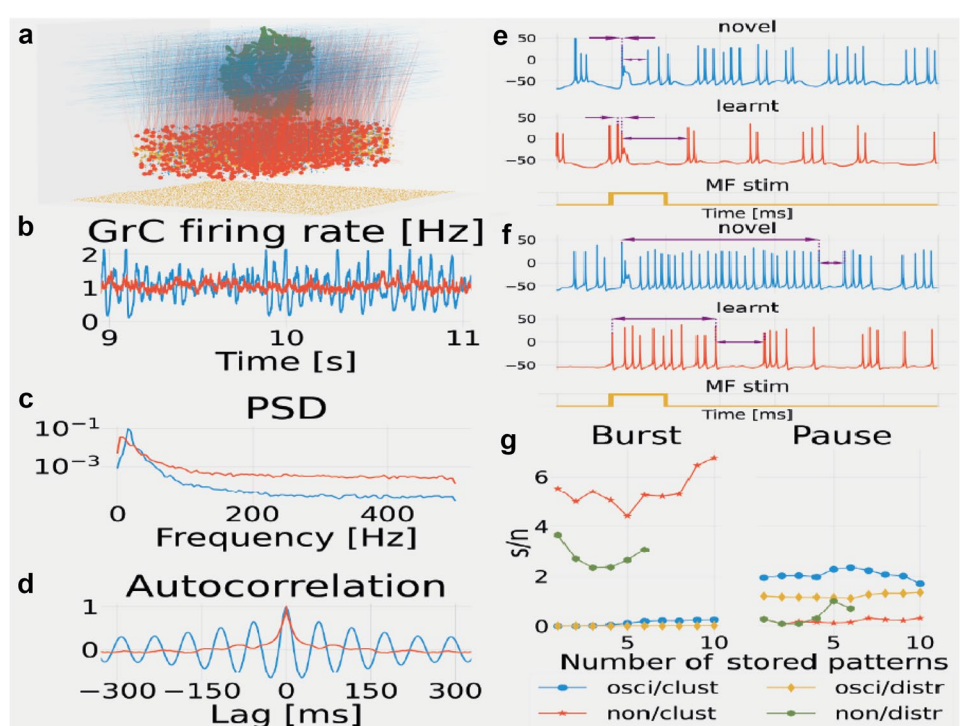
<sup>1</sup>University of Hertfordshire, Centre for Computer Science and Informatics Research, Hatfield, United Kingdom

<sup>2</sup>University of Hertfordshire, Biocomputation Research Group, Hatfield, United Kingdom

\*Email: cns@neuronapail.com

The cerebellum plays essential roles in motor control and timing. Based on its anatomy and physiology, it has been hypothesized that the cerebellar cortex can operate as a simple perceptron, and that its capacity is maximized by expanding mossy fiber (MF) input patterns into high-dimensional granule cell (GrC) activity patterns. Many lines of research have supported this theory; however, it needs to be reconciled with recent experimental findings. For example, imaging studies indicate that a wide range of GrCs are spontaneously active within a certain time

**Fig. 1** **a** Model overview. **b** Population firing rate of GrCs in two network states. **c, d** Power spectral density and autocorrelation of GrCs. **e, f** Membrane potential of PC in oscillatory and non-oscillatory network. Arrows indicate burst and pause. **g** The s/n ratio for the PC response as a function of the number of stored patterns. Clustered and distributed stimuli in the two states are compared



window. Other studies have reported that input to the cerebellar cortex is clustered and that populations of GrCs can show oscillatory activity. Potential computational roles of the clustering and oscillations are still open questions. In this study, we constructed a biologically detailed model of the cerebellar cortex, which includes multi-compartmental models of Golgi and Purkinje cells (GoCs and PCs), point models of GrCs, and Poisson spike generators associated with MFs and stellate cells (Fig. 1A). The model reflects spatial input effects and channel-dependent dynamics: the ascending segments of the GrC axons allow strong activation of the neighboring PC; the parallel fibers activate a large extent of the network and cause lateral inhibition through GoCs; and the PC can generate complex spike like responses to strong excitation. The model showed that sparser connections between GrCs and GoCs suppressed the spontaneous oscillation of GrCs (Fig. 1B-D). We stimulated a population of MFs and compared the pattern response of the PC. In the oscillatory network, the PC showed a short burst and a pause in spiking in response to the stimuli (Fig. 1E). However, in the non-oscillatory network, the PC responded with a long burst without any pause in spiking (Fig. 1F). We trained the network with long-term depression (LTD) complemented by long-term potentiation (LTP) of the GrC - PC synapses and compared the pattern response to novel and learnt stimuli using a signal-to-noise ratio (s/n) for the initial pattern-response burst and after-burst pause. The s/n for the burst was higher in the non-oscillatory network whereas the s/n for the pause was higher in the oscillatory network (Fig. 1G), indicating that the readout mechanism for pattern recognition in the cerebellum depends on the network state. Finally, we trained and stimulated both networks with clustered and distributed MFs and compared their pattern responses. In both network states, the s/n was higher for clustered stimuli (Fig. 1G). These findings suggest computational advantages of clustered input and oscillatory activity in the cerebellum. Future work will analyze tasks involving temporal patterns and modified learning algorithms.

#### P103 Homeostatic structural and synaptic plasticity both contribute to the repair of peripherally-lesioned balanced networks

Ankur Sinha<sup>1</sup>, Christoph Metzner<sup>2</sup>, Neil Davey<sup>3</sup>, Rod Adams<sup>3</sup>, Michael Schmuker<sup>3</sup>, Volker Steuber<sup>\*3</sup>

<sup>1</sup>University College London, Department of Neuroscience, Physiology, and Pharmacology, London, United Kingdom

<sup>2</sup>Technische Universität Berlin, Department of Software Engineering and Theoretical Computer Science, Berlin, Germany

<sup>3</sup>University of Hertfordshire, Biocomputation Research Group, Hatfield, United Kingdom

\*Email: v.steuber@herts.ac.uk

A number of peripheral lesion experiments have shown that structural plasticity causes large scale changes in brain networks [1-3]. Our understanding of the mechanisms underlying structural plasticity, however, remains limited. Structural plasticity modifies network connectivity over long periods of time at slower rates than synaptic plasticity by the formation and removal of synapses. Since alterations in network connectivity are expected to affect network function, the study of resulting functional consequences of structural plasticity remains an important area of research.

We have previously developed a novel model of peripheral lesioning and subsequent repair in a balanced cortical Asynchronous Irregular (AI) spiking network [4]. By selectively activating homeostatic structural and synaptic plasticity mechanisms in our simulations, we investigate their contributions to network repair following deafferentation. In our simulations, inhibitory synaptic plasticity alone re-balances neurons outside the Lesion Projection Zone (LPZ) by increasing the

strength of their inhibitory inputs. However, it fails to restore activity in the deprived neurons inside the LPZ even after small peripheral lesions. Homeostatic inhibitory synaptic plasticity reduces the conductances of inhibitory synapses projecting onto neurons in the LPZ but this resulting loss in inhibition is insufficient to reactivate them. Strengthening of IE synapses by Spike-timing Dependent Plasticity (STDP), on the other hand, stabilizes the activity of neurons outside the LPZ. Therefore, the network achieves a state where the neurons outside the LPZ retain their functionality, but the LPZ is effectively lost.

Simulations where only homeostatic structural plasticity was enabled also failed to re-establish the balanced state of the network following deafferentation. In these simulations, the activity of the deprived neurons in the LPZ was initially restored back to pre-lesion levels but the network did not stabilize to the desired low firing rate regime. Instead, it continued to reconfigure and eventually exhibited abnormally high firing rates. Thus, our simulations predict that both homeostatic processes contribute to successful repair. We suggest that structural plasticity is required for larger changes in network connectivity and synaptic plasticity for the fine tuning of conductances. Our results are coherent with the idea that multiple plasticity mechanisms together sustain functional brain networks.

#### References

1. Rasmusson, D. D. Reorganization of raccoon somatosensory cortex following removal of the fifth digit. *Journal of Comparative Neurology*. 1982; 205:313–326
2. Keck, T., Mrsic-Flogel, T. D., Afonso, M. V., Eysel, U. T., Bonhoeffer, T. & Hübener, M. Massive restructuring of neuronal circuits during functional reorganization of adult visual cortex. *Nature Neuroscience*. 2008; 11:1162–1167
3. Keck, T., Scheuss, V., Jacobsen, R. I., Wierenga, C. J., Eysel, U. T., Bonhoeffer, T., et al. Loss of sensory input causes rapid structural changes of inhibitory neurons in adult mouse visual cortex. *Neuron*. 2011; 71:869–882
4. Sinha, A., Metzner, C., Davey, N., Adams, R., Schmuker, M. & Steuber, V. Growth rules for the repair of Asynchronous Irregular neuronal networks after peripheral lesions. *PLOS Computational Biology*. 2021; 17:1–35

#### P104 Changes in age-related neurochemicals in the anterior cingulate cortex following brief mindfulness intervention

Rongxiang Tang<sup>1</sup>, Changho Choi<sup>2</sup>, Yi-Yuan Tang<sup>\*3</sup>

<sup>1</sup>University of California San Diego, San Diego, United States of America

<sup>2</sup>University of Texas Southwestern Medical Center, Advanced Imaging Research Center, Dallas, United States of America

<sup>3</sup>Arizona State University, Phoenix, AZ, United States of America

\*Email: yiyan@asu.edu

Mindfulness intervention (MI) has shown promise in reducing the risk of Alzheimer's disease and related dementias (ADRD). MI fosters attention and awareness of present moment experiences and improves cognition, emotion, and psychological health. MI also alters brain functional and structural plasticity, suggesting its potential as a preventive intervention targeting cognitive and brain aging. Neurochemical changes in brain metabolites are signatures of both healthy and pathological aging. Yet, it remains unknown whether brief MI could induce changes in the neurobiochemical system, particularly in brain metabolites implicated in aging. Here, we conducted the first pilot study using a noninvasive 3 T proton magnetic resonance spectroscopy

(<sup>1</sup>H-MRS) to measure brain metabolism in vivo in the anterior cingulate cortex (ACC), a key brain region implicated in MI and aging. Twenty-two meditation-naïve college students underwent ten 60-min consecutive online sessions using integrative body-mind training (IBMT), a form of open monitoring and effortless MI, which has shown positive effects on the brain, physiology, and behavior in a series of RCTs [1, 2]. All participants were assessed before and after IBMT using <sup>1</sup>H-MRS and behavioral measures. Single-voxel point-resolved spectroscopy (PRESS) was conducted for estimating the metabolite concentrations (TR 2 s, TE 90 ms, sweep width 2.5 kHz, 1024 sampling points, and 256 signal averages). Water suppression and B0shimming up to second-order were performed with the vendor-supplied tools. Reference water signal was acquired for eddy current compensation, multi-channel combination, and metabolite quantification. Spectral fitting was performed with LCModel software using in-house basis spectra of 18 metabolites which were calculated incorporating the PRESS slice selective RF and gradient pulses. The spectral fitting was performed between 0.5–4.0 ppm. After correcting the LCModel estimates of metabolite signals for the T2 relaxation effects, the millimolar concentrations of metabolites were calculated with reference to water at 42 M [3, 4]. We detected a significant increase in glutamate and N-acetylaspartate in the rostral ACC, a decrease in myo-inositol in the dorsal ACC post-intervention, significant increases in trait mindfulness, positive affect, and cognitive reappraisal, and decreases in negative affect and perceived stress post-intervention. Our findings indicated that brief MI induced neurochemical changes in the ACC, and the directionality of metabolite changes following MI was in the opposite direction to the trends typically observed in aging and ADRD, which often exhibited decreases in glutamate and N-acetylaspartate levels and increase in myo-inositol.

## References

1. Tang YY. The neuroscience of mindfulness meditation: How the body and mind work together to change our behavior. Springer. 2017.
2. Tang YY, et al. Effortless training of attention and self-control: Mechanisms and applications, Trends in Cognitive Sciences. 2022; 26(7): 567–577
3. Provencher SW. Estimation of metabolite concentrations from localized in vivo proton NMR spectra. Magnetic Resonance in Medicine. 1993; 672–679.
4. Ganji SK et al. T2 measurement of J-coupled metabolites in the human brain at 3 T. NMR Biomed. 2012; 523–529

## P105 Thalamic clustering coefficient moderates vigor-sleep quality relationship

Xiaoqian Ding<sup>1</sup>, Qingmin Li<sup>1</sup>, Yi-Yuan Tang<sup>\*2</sup>

<sup>1</sup>Liaoning Normal University, Dalian, China

<sup>2</sup>Arizona State University, Phoenix, AZ, United States of America

\*Email: yiyuan@asu.edu

Poor sleep has detrimental effects on psychological and physical health, it is critical to understand the factors that can improve sleep quality. Some studies have shown positive affect such as high vigor is related to better sleep efficiency and quality, but others showed contradictory results [1, 2]. Considering that individual vigor is regulated by nerve signals transmitted by the thalamus, and the thalamus and the peripheral cortex constitute a sleep circuit that jointly acts the sleep process, we hypothesize that the thalamus and its network may regulate both vigor and sleep quality.

In this study, we applied resting-state functional magnetic resonance imaging (fMRI) and graph theory methods, specifically the thalamic clustering coefficient to explore the relationship between vigor and

sleep quality. Totally 116 healthy college students were recruited, and brain images were acquired on a 3 T Philips Achieva MRI system using an echo-planar imaging sequence in 36 slices (repetition time = 2000 ms, echo time = 30 ms, flip angle = 801, the field of view = 23 cm, matrix = 64 × 64, 4-mm thickness, and 0-mm gap). Images preprocessing and further analysis were performed by SPM8 ([www.fil.ion.ucl.ac.uk/spm](http://www.fil.ion.ucl.ac.uk/spm)) and resting-state fMRI data analysis toolkit (<http://resting-fmri.sourceforge.net>). The functional connectivity of the whole brain network in each subject was detected by using the 90-Parcel AAL template. We investigated network properties (sparsity threshold ranged from 0.09 to 0.3, with an increment of 0.01), and calculated the regional topological characteristics - the left and right thalamic clustering coefficients [3]. The Profile of Mood States was used to measure vigor scores, and the Pittsburgh Sleep Quality Index (PSQI) was used to assess sleep quality.

Our results have shown that the vigor score is significantly negatively correlated with the left thalamic clustering coefficient and the PSQI score respectively, and the left thalamic clustering coefficient is significantly positively correlated with the PSQI score. Moreover, the left thalamic clustering coefficient significantly moderates the relationship between vigor and sleep quality. In the group with a high left thalamic clustering coefficient, the higher individual vigor indicates the poorer sleep quality. Whereas in the group with a low left thalamic clustering coefficient, the relationship between vigor and sleep quality is not significant. The right thalamic clustering coefficient is not significantly correlated with vigor or PSQI score and does not regulate the relationship between vigor score and PSQI score.

In sum, vigor may serve as a predictor of individual sleep quality. The relationship between vigor and sleep quality is heterogeneous between populations with high or low left thalamic clustering coefficient. The findings may shed light on the development of personalized interventions for people with poor sleep or sleep disorders.

## References

1. Pressman et al. The whole is not the sum of its parts: Specific types of positive affect influence sleep differentially. Emotion. 2017; 17: 778–793.
2. Ong AD, Kim S, Young S, Steptoe A. Positive affect and sleep: A systematic review. Sleep Med Rev. 2017; 35: 21–32
3. Xue S, Tang YY, Posner MI. Short-term meditation increases network efficiency of the anterior cingulate cortex. Neuroreport. 2011; 22: 570–4.

## P106 Deep generative adversarial network capturing spiral waves in disinhibited circuits of the cortex

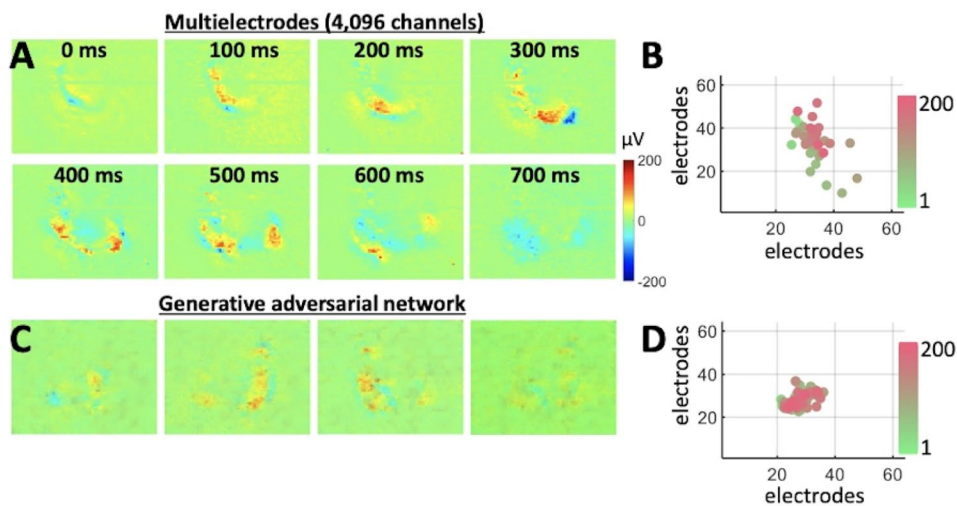
Megan Boucher-Routhier<sup>\*1</sup>, Jean-Philippe Thivierge<sup>1</sup>

<sup>1</sup>University of Ottawa, School of Psychology, Ottawa, Canada

\*Email: mrout092@uottawa.ca

In cortical circuits, disinhibited states of activity are characterized by complex spatiotemporal patterns including spiral waves [1]. These waves arise during interictal epileptic events and consist of neural activity that rotates around a center of mass. While dimensionality reduction techniques have accounted for neuronal population activity based on a limited number of dimensions [2], it is unclear whether low-dimensional models are sufficient to account for disinhibited cortical states where patterns of activity cannot be described by broad features such as oscillations or shared patterns of fluctuation. Here, we investigated the dimensionality of neural activity in both healthy and disinhibited networks as well as deep neural networks. Neural activity from acute rodent cortical slices was recorded using a high-density multielectrode array. Cortical disinhibition was induced

**Fig. 1** Capturing cortical spiral waves with a generative adversarial network. **A** Temporal evolution of a single spiral wave. **B** Spatial distribution of center-of-mass across 200 waves. **C** Single wave generated by a conditional adversarial network (cGAN). **D** Center-of-mass distribution across 200 waves generated by cGAN



by perfusing slices with a pro-epileptiform artificial cerebrospinal fluid solution containing a potassium channel blocker 4-Aminopyridine (4-AP), decreased magnesium, and increased potassium. The data collected revealed spiral waves (Fig. 1A) that were characterized by a spatially delimited center of mass (Fig. 1B), a broad distribution of instantaneous phases across individual electrodes, and a decrease in voltage near the center of mass. Principal components analysis revealed a broad distribution of eigenvalues whose dimensionality could not be accounted for by low-rank fluctuations. A deep conditional generative adversarial network (cGAN) [3] was trained on spiral waves extracted from the experimental recordings (Fig. 1C). This network captured key features of the data including the tight center of mass (Fig. 1D), broad eigenvalue distribution, spatial correlations, and dimensionality of spiral waves. By adjusting the input of the cGAN, the model generated new samples that deviated in systematic ways from the experimental data, thus allowing the exploration of a broad range of states from healthy to pathologically disinhibited neural networks. Results revealed that the dimensionality of population activity served as a marker of neural activity along a continuum from healthy to disinhibited brain states. These results open avenues

for employing cGANs to replicate the dynamics of cortical seizures and accelerate the design of optimal neurostimulation aimed at suppressing pathological brain activity.

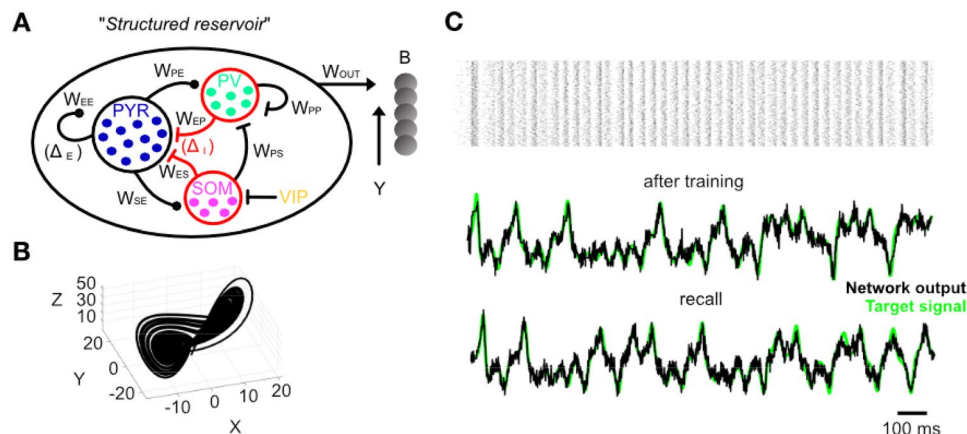
#### Acknowledgements

This work was supported by a Discovery Grant to J.P.T from the Natural Sciences and Engineering Council of Canada (NSERC Grant No. 210977).

#### References

- Huang, X., Troy, W. C., Yang, Q., Ma, H., Laing, C. R., Schiff, S. J., and Wu, J.-Y. Spiral waves in disinhibited mammalian neocortex. *Journal of Neuroscience*. 2004; 24(44): 9897–9902.
- Engel, T. A., and Steinmetz, N. A. New perspectives on dimensionality and variability from large-scale cortical dynamics. *Current Opinion in Neurobiology*. 2019; 58: 181–190.
- Mirza, M., and Osindero, S. Conditional generative adversarial nets. *ArXiv*. 2014.

**Fig. 1** Reservoir computing model with inhibitory subtypes. **A** Canonical circuit with PYR, PV, SOM, and VIP neurons. Weighted connections ( $W$ ) represent interaction strength. **B** Lorenz attractor. **C** Top: spike raster of a network generating a chaotic attractor during training (target signal on). Middle: trained network output. Bottom: network output during recall (target signal off)



## P107 Key role of neuronal diversity in structured reservoir computing

Jean-Philippe Thivierge<sup>1</sup>, Éloïse Giraud<sup>\*1</sup>, Annie Théberge Charbonneau<sup>1</sup>

<sup>1</sup>University of Ottawa, School of Psychology, Ottawa, Canada

\*Email: egira024@uottawa.ca

The ability of brain regions to regulate sensory, cognitive, and motor processes stems from an intricate and precisely organized network architecture. Reservoir computing models capture these emergent abilities and learn complex functions by training the output weights of recurrent networks [1]. These models, however, are typically limited to randomly connected networks of homogeneous units. Here, we propose a new class of structured reservoir models that incorporate a diversity of cell types and their known connections (Fig. 1A). In a first version of this model, the reservoir was composed of mean-rate units separated into pyramidal (PYR), parvalbumin (PV), somatostatin (SOM) and vasoactive intestinal peptide-expressing (VIP) cells. Linear stability analysis of this model revealed two distinct dynamical regimes, namely (i) an inhibition-stabilized network (ISN) where strong recurrent excitation was balanced by strong inhibition; and (ii) a non-ISN network where weak excitation did not require inhibition to maintain stability [2]. Next, these results were extended by developing a leaky integrate-and-fire model that captured different cell-types along with their network architecture and connection probabilities. The performance of this network was assessed in a task where the model was trained to generate a chaotic Lorenz attractor (Fig. 1B). Output weights were adjusted using a least-squares method [3]. After training, weights remained frozen while the network recalled the learned pattern (Fig. 1C). The contribution of each cell type was tested by graded stimulation of targeted neurons within the population. ISN networks yielded decreased accuracy with both activation and deactivation of PYR, SOM, and PV neurons. This sensitivity to perturbations was explained by the ISN networks operating in a regime near the limits of stability. By comparison, non-ISN networks were robust to perturbations, with the activation of SOM and PV neurons yielding the largest decrease in performance. In both ISN and non-ISN networks, the impact of briefly deactivating PV cells persisted over extended time scales. In sum, the effect of perturbations on network performance was intimately dependent on the neuronal subtype targeted, the strength of the stimulation, and the regime of the recurrent network. The proposed framework of structured reservoir computing opens avenues for exploring the role of neuronal diversity and connectivity motifs on learning complex temporal sequences.

### References

1. Vincent-Lamarre P, Calderini M & Thivierge J-P. Learning Long Temporal Sequences in Spiking Networks by Multiplexing Neural Oscillations. *Frontiers in Computational Neuroscience*. 2020; 14: 78.
2. Sanzeni A, Akitake B, Goldbach H C, et al. Inhibition stabilization is a widespread property of cortical networks. *eLife*. 2020; 9: e54875.
3. Boucher-Routhier M, Zhang B L F & Thivierge J-P. Extreme neural machines. *Neural Networks*. 2021; 144: 639–647.

## P108 Evaluating functional vision for simulated visual prostheses using gait analysis

Daniel Petrovski<sup>\*1</sup>, Tatiana Kameneva<sup>1</sup>, Christopher McCarthy<sup>1</sup>, Oren Tirosh<sup>2</sup>

<sup>1</sup>Swinburne University of Technology, School of Science, Computing and Engineering Technologies, Melbourne, Australia

<sup>2</sup>Swinburne University of Technology, School of Health Sciences, Melbourne, Australia

\*Email: dpetrovski@swin.edu.au

Retinitis Pigmentosa is a genetic eye disorder that causes photoreceptor cells in the retina to die slowly, leading to partial vision loss that progressively worsens over time and eventually results in complete blindness. However, many retinal ganglion cells that convey visual information from the photoreceptor cells to the brain via the optic nerve remain functional. Retinal prostheses aim to restore vision to patients affected by Retinitis Pigmentosa by stimulating remaining retinal ganglion cells through an implantable electrode array placed close to the retina. Visual inputs from a camera or photodiodes are computationally processed where subsequent electrodes are activated, stimulating the retinal ganglion cells. However, the restored vision is only rudimentary and in very low resolution. To improve the efficacy of retinal prostheses, it is important to understand visual neuroscience signal processing and how electrical stimulation affects neural responses and functional outcomes. The performance of retinal prostheses and the resulting restored vision is often measured through means that assess visual function and do not directly consider patient outcomes. Therefore, there is a need to develop assessment methods that evaluate functional vision leading to better patient outcomes. A critical functional outcome of vision is the ability to navigate environments safely and confidently. Under reduced vision conditions, confidence in an individual's perception of the environment is reduced and affects gait as a more cautious walking strategy is implemented. We propose gait as a predictor of confidence which links to better functional outcomes in visual prostheses.

This study conducted a gait analysis of subjects navigating an obstacle course under different visual representations. These visual representations were achieved with goggles that simulate varying levels of vision loss. Participants with fully functional vision and no physical injuries that would affect gait were selected. Gait parameters were measured in 3D using motion capture with 12 infrared cameras and infrared-reflective markers placed on the participants.

Our preliminary results showed the feasibility of using gait parameters such as stride length, walking speed, obstacle clearance, and swing phase as a proxy for confidence in an individual's perception of the environment with simulated vision loss. Therefore, it is feasible to use gait to evaluate functional vision, where this methodology can then be applied to assess functional vision in patients with visual prostheses.

## P109 Influence of electrical coupling in shaping time intervals and dynamical invariants of central pattern generator sequences

Pablo Sánchez-Martín<sup>\*1</sup>, Alicia Garrido-Peña<sup>2</sup>, Blanca Berbel<sup>1</sup>, Francisco B Rodriguez<sup>3</sup>, Rafael Levi<sup>2</sup>, Pablo Varona<sup>3</sup>

<sup>1</sup>Universidad Autónoma de Madrid, Departamento de Ingeniería Informática, Madrid, Spain

<sup>2</sup>Universidad Autónoma de Madrid, Grupo de Neurocomputación Biológica (GNB), Madrid, Spain

<sup>3</sup>Universidad Autónoma Madrid, Ingeniería Informática, Madrid, Spain

\*Email: pablo.sanchez@inv.uam.es

Central pattern generators (CPG) typically contain electrically coupled cells and mutually inhibited neurons by chemical synapses, which result in stereotyped sequences of neural activations. CPG rhythmic activity display dynamical invariants consisting of robust linear relationships between intervals building those sequences that are preserved cycle-by-cycle. The duration of the sequence time intervals help to balance

flexibility and robustness for the coordination of the motor rhythms [1, 2] but it is not clear how the electrical coupling contributes to this balance.

Long recordings were obtained from the bursting activity of the stomatogastric pyloric CPG of *Carcinus maenas* crabs showing distinct degrees of synchronization among the electrically coupled cells. The activity of the lateral pyloric (LP) neuron was detected from an extracellular recording and the two electrically coupled pyloric dilator (PD) neurons were recorded with intracellular electrodes.

We assessed the characterization of the synchronization degree between the CPG electrically coupled cells and its relationship with excitability, the duration of time intervals that build up the sequences and overall coordination of the intervals to shape the CPG rhythm and build dynamical invariants. In particular, we used raster plots of the intraburst spiking activity of the electrically coupled cells, box plots illustrating the variability of the time intervals, representations of the synchronization level against different metrics that characterize the excitability, and the representation of the cycle-by-cycle sequence interval relationships that reflect the temporal coordination of the CPG. Our results illustrate the existing dynamic synchronization, the decrease of excitability with stronger synchronization and the influence of the coupling level in the time intervals that shape distinct dynamical invariants. We also show that existing models of CPG neurons and synapses do not display the interval variability observed in the experiments. These results contribute to the understanding of the intrinsic coordination of central pattern generators that help to design novel autonomous robotics paradigm including those used for rehabilitation tasks.

#### Acknowledgments

This work was funded by AEI/FEDER PGC2018-095895-B-I00 and PID2020-114867RB-I00.

#### References

1. Elices I, Levi R, Arroyo D, Rodriguez FBFB, Varona P. Robust dynamical invariants in sequential neural activity. *Scientific Reports*. 2019; 9:9048
2. Garrido-Peña A, Elices I, Varona P. Characterization of interval variability in the sequential activity of a central pattern generator model. *Neurocomputing*. 2021; 461: 667–78.

#### P110 Dynamical principles of functional neural sequences validated in hybrid robots built with living central pattern generators

Pablo E. Soëtard<sup>1</sup>, Rodrigo Amaducci<sup>2</sup>, Pablo Sánchez-Martín<sup>3</sup>, Manuel Reyes-Sánchez<sup>2</sup>, Alicia Garrido-Peña<sup>2</sup>, Rafael Levi<sup>2</sup>, Francisco B Rodriguez<sup>1</sup>, Pablo Varona<sup>\*1</sup>

<sup>1</sup>Universidad Autónoma de Madrid, Ingeniería Informática, Madrid, Spain

<sup>2</sup>Universidad Autónoma de Madrid, Grupo de Neurocomputación Biológica, Madrid, Spain

<sup>3</sup>Universidad Autónoma de Madrid, Departamento de Ingeniería Informática, Madrid, Spain

\*Email: pablo.varona@uam.es

Hybrots are hybrid robots built with living neural systems and engineered robotic designs [1–3]. They are a promising tool for experimental neuroscience and an essential step towards future hybrid neuroethologies.

We have designed two robotic platforms to validate motor coordination arising from the balance between robustness and flexibility in neural sequences produced by living central pattern generators (CPG). This balance is achieved by the presence of dynamical invariants in the form

of strong linear relationships between some of the time intervals that build such sequences while other intervals remain flexible and independent [4]. In our experiments we used the crustacean pyloric CPG and intracellular recordings of the LP and PD neurons. The first robot modulated the oscillation of its three pairs of legs using the dynamical invariants of the living CPG and modified its locomotion during environmental light changes by providing robotic sensory feedback to the living neural circuit. A second bipedal robot coordinated its joint actuators using the mentioned sequence time intervals and maintained an upright posture by sending feedback to the living CPG according to its gyroscope sensors. A wireless connection over WiFi or Bluetooth was established to allow online bidirectional information flow between the biological CPG and the robots.

In our validation examples, the robot locomotion relied exclusively on the dynamical invariants from the sequential signaling of the nervous system. The locomotion was modulated by environmental changes sensed by the robot and informed as current injection feedback to the living circuit. Tracking of the robot motion and information from the robot motors was used to validate the transformation of the dynamical invariants observed in the living CPG to the actual movement of the robot under the different environmental changes. Motor coordination was sustained at all times independently of the locomotion speed and sensory feedback.

Our results show that hybrots are useful to validate dynamical principles observed in living central pattern generators and to provide new design paradigms for autonomous robotics. They also illustrate future directions towards hybridization of brain and robotic technologies that can be applied in neurorehabilitation and exoskeleton design.

#### Acknowledgments

Funded by AEI/FEDER PGC2018-095895-B-I00 and PID2020-114867RB-I00 P.E.S. and R.A. contributed equally to this work.

#### References

1. Potter SM. Hybrots: hybrid systems of cultured neurons + robots, for studying dynamic computation and learning. *Proc. 2002 Simul. Adapt. Behav. 7 Work. Mot. Control Humans Robot. Interplay Real Brains Artif. Devices*, Edinburgh: 2002.
2. Murugan M, Du DHC. Hybrot: Towards improved performance in hybrid SLC-MLC devices. *Proc. 2012 IEEE 20th Int. Symp. Model. Anal. Simul. Comput. Telecommun. Syst. MASCOTS 2012*, 2012.
3. Ando N, Kanzaki R. Insect-machine hybrid robot. *Current Opinion in Insect Science*. 2020; 42: 61–9.
4. Elices I, Levi R, Arroyo D, Rodriguez FB, Varona P. Robust dynamical invariants in sequential neural activity. *Scientific Reports* 2019; 99048.

#### P111 Model-based analysis of frequency-rich BOLD fMRI

Ashish Raj<sup>1</sup>, Benjamin Sipes<sup>\*1</sup>, Parul Verma<sup>1</sup>

<sup>1</sup>University of California, San Francisco, Radiology and Biomedical Imaging, San Francisco, CA, United States of America

\*Email: benjamin.sipes@ucsf.edu

The synchronized spontaneous low-frequency fluctuations in the brain's resting-state neural activity are routinely measured with blood oxygen level-dependent (BOLD) contrast functional MRI (fMRI). Conventionally, fMRI data is bandpass filtered from 0.01–0.08 Hz to eliminate high BOLD frequencies considered to be noise, yet some evidence suggests that BOLD frequencies as high as 0.25 Hz contain valuable information [1]. A possible reason why frequency-dependent interpretations of fMRI data is not currently used is that there is no reasonable signal generation model that can benefit from frequency

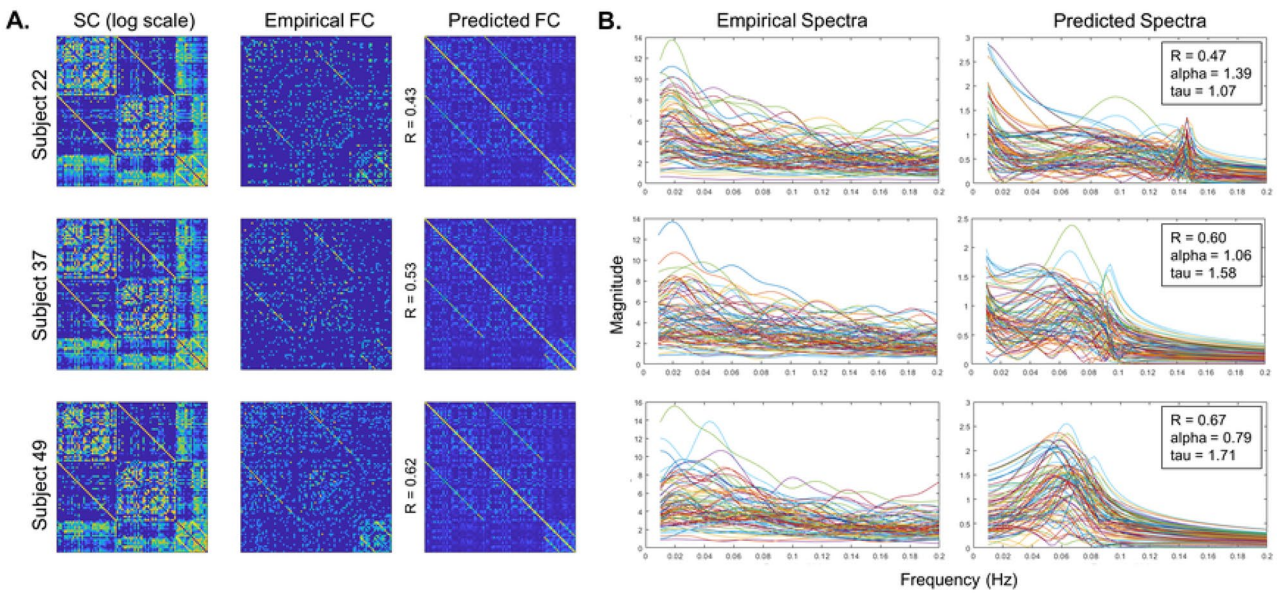


**Fig. 1** **A** Spectral Graph Model (SGM) predictions for functional connectivity (FC), showing first the SC (log-scale for visualization), the empirical FC, and the predicted FC, with Pearson's R along the

y-axes. **B** Empirical fMRI power spectral densities on the left with SGM predictions for fMRI spectra on the right. All data shown were selected from three subjects in our dataset with varying parameters

content. In this study we propose a simple yet powerful signal generation model for fMRI that relies upon and extends emerging spectral graph approaches [2].

We use T1-weighted, T2\*-weighted fMRI (TR = 2 s), and 30-direction diffusion (d)MRI data from 56 healthy controls. We parcellated the whole brain by the Desikan-Killiany 86-region atlas [3]. We derived functional connectivity (FC) as the maximum cross-correlation across all time lags between each pair of regional timeseries. We obtain fMRI power spectral densities (PSD) directly from the regional timeseries from 0.01–0.2 Hz. We derived structural connectivity (SC) with probabilistic tractography and quantified regional connections as the number of probabilistic-weighted streamlines between them.

We propose a generative model for fMRI signal spread based on the SC network, similar to our past work [2], with fMRI BOLD signal. In our equation, fMRI signal between any two regions is controlled by an inverse of the common characteristic time constant, tau, and signal flow between these regions are scaled by the SC strengths connecting them. The global coupling parameter, alpha, acts as a controller of weights given to long-range white-matter connections. We use the SC Laplacian to generalize to the entire brain network. We take the Fourier transform of this generalized equation to model the fMRI signal as an estimate of the fMRI's empirical PSD.

For each subject, we simultaneously fit the two global parameters, alpha and tau. We used cost functions that maximized the FC correlation and mean spectral correlation across regions, then we took the sum of these as our total cost.

Across all subjects, the prediction between empirical and predicted FC and spectra had a mean (std) Pearson's R of 0.49 (0.047) and 0.56 (0.075), respectively. Thus, we find that this linear signal generation model accurately predicts the cross-correlation FC matrix (Fig. 1A) and the mean fMRI PSD (Fig. 1B) using these two global parameters. The Laplacian eigenvectors used by our model demonstrate their ability to predict fMRI spectra at high BOLD frequencies, thus providing evidence that meaningful BOLD signals at high frequencies emerge from the brain's underlying anatomy.

## References

- Yuen N, Osachoff N, Chen J. Intrinsic frequencies of the resting-state fmri signal: The frequency dependence of functional connectivity and the effect of mode mixing. *Frontiers of Neuroscience*. 2019; 13: 900.
- Verma P, Nagarajan S, Raj A. Spectral graph theory of brain oscillations—revised and improved. *NeuroImage*. 2022; 249: 118919.
- Desikan R, Ségonne F, Fischl B, et al. An automated labeling system for subdividing the human cerebral cortex on MRI scans into gyral based regions of interest. *NeuroImage*. 2006; 31(3): 968–980.

## P112 Reflected fractional Brownian motion in 3d-brain shapes: insights into the distribution of serotonergic axons

Skirmantas Janusonis<sup>\*1</sup>, Ralf Metzler<sup>2</sup>, Thomas Vojta<sup>3</sup>

<sup>1</sup>University of California, Santa Barbara, Department of Psychological and Brain Sciences, Santa Barbara, CA, United States of America

<sup>2</sup>University of Potsdam, Institute of Physics and Astronomy, Potsdam-Golm, Germany

<sup>3</sup>Missouri University of Science and Technology, Department of Physics, Rolla, MO, United States of America

\*Email: janusonis@ucsb.edu

The immediate neighborhood of virtually every brain neuron contains thin, meandering axons that release serotonin (5-HT). These axons, also referred to as serotonergic fibers, are present in nearly all studied nervous systems (both vertebrate and invertebrate) and appear to be a key component of biological neural networks. In the mammalian brain, they create dense mesh works that are macroscopically described by densities. It is not known how these densities arise from the trajectories of individual fibers, each of which resembles a unique random-walk path. This poses interesting theoretical questions, solving which will advance our understanding of brain plasticity and regeneration. For example, serotonin-associated psychedelics have recently been shown

to promote global brain integration in depression [1], and serotonergic fibers are nearly unique in their ability to robustly regenerate in the adult mammalian brain [2].

We have recently introduced a conceptual framework that treats the serotonergic axons as “stochastic axons.” Stochastic axons are different from axons that support point-to-point connectivity (often studied with graph-theoretical methods) and require novel theoretical approaches. We have shown that serotonergic axons can be potentially modeled as paths of fractional Brownian motion (FBM) in the super-diffusive regime (with the Hurst exponent  $H > 0.5$ ). Our supercomputing simulations demonstrate that particles driven by reflected FBM (rFBM) accumulate at the border enclosing the shape [3]. Likewise, serotonergic fibers tend to accumulate at the border of neural tissue, in addition to their general similarity to simulated FBM paths [4].

This work expands our previous simulations in 2D-brain-like shapes by considering the full 3D-geometry of the brain. This transition is not trivial and cannot be reduced to independent 2D-sections because increments of FBM trajectories exhibit long-range correlation. Supercomputing simulations of rFBM ( $H > 0.5$ ) were performed in the reconstructed 3D-geometry of a mouse brain at embryonic day 17 (serotonergic fibers are already well developed at this age and begin to invade the cortical plate). The obtained results were compared to the actual distribution of fibers in the mouse brain. In addition, we obtained preliminary results by simulating rFBM with a region-dependent  $H$ . This next step in complexity presents challenges (e.g., it can be highly sensitive to mathematical specifications), but it is necessary for the predictive modeling of interior fiber densities in heterogenous brain tissue.

### Acknowledgements

This research was funded by an NSF-BMBF CRCNS grant (NSF #2112862 to SJ & TV; BMBF #STAXS to RM), an NSF CRCNS grant (NSF #1822517 to SJ), an NSF grant (#OAC-1919789 to TV), and a Cottrell SEED award (to TV).

### References

1. Daws RE, Timmermann C, Giribaldi B, et al. Increased global integration in the brain after psilocybin therapy for depression. *Nature Medicine*. 2022; 28:844–851
2. Jin Y, Dougherty SE, Wood K, et al. Regrowth of serotonin axons in the adult mouse brain following injury. *Neuron*. 2016; 91:748–762
3. Vojta T, Halladay S, Skinner S, et al. Reflected fractional Brownian motion in one and higher dimensions. *Physical Review E*. 2020; 102: 032108
4. Janusonis S, Detering N, Metzler R, Vojta T. Serotonergic axons as Fractional Brownian Motion paths: Insights into the self-organization of regional densities. *Frontiers in Computational Neuroscience*. 2020; 14: 56.

### P113 Neuromodulation of striatal D1 cells shapes BOLD fluctuations in anatomically connected thalamic and cortical regions

Marija Markicevic<sup>\*1</sup>, Oliver Sturman<sup>2</sup>, Johannes Bohacek<sup>2</sup>, Markus Rudin<sup>3</sup>, Valerio Zerbi<sup>4</sup>, Ben Fulcher<sup>5</sup>, Nicole Wenderoth<sup>4</sup>

<sup>1</sup>ETH Zurich, Zurich, Switzerland

<sup>2</sup>ETH Zurich, Department of Health Sciences and Technology, Laboratory of Molecular and Behavioral Neuroscience, Zurich, Switzerland

<sup>3</sup>ETH Zurich, Institute for Biomedical Engineering, Zurich, Switzerland

<sup>4</sup>ETH Zurich, Department of Health Sciences and Technology, Neural Control of Movement Lab, Zurich, Switzerland

<sup>5</sup>The University of Sydney, School of Physics, Sydney, Australia

\*Email: marija.markicevic@hest.ethz.ch

Understanding how the brain’s macroscale dynamics are shaped by underlying microscale mechanisms is a key problem in neuroscience. In animal models, we can now investigate this relationship in unprecedented detail by directly manipulating cellular-level properties while measuring the whole-brain response using resting-state fMRI. Here we focused on understanding how blood-oxygen-level-dependent (BOLD) dynamics, measured within a structurally well-defined striato-thalamo-cortical circuit, are shaped by chemogenetically exciting or inhibiting D1 medium spiny neurons (MSNs) of the right dorsomedial striatum (CPdm).

Excitatory, inhibitory Designer Receptors Exclusively Activated by Designer Drugs (DREADDs) and control viral vectors were used to target right dmCP (D1 excitation  $n = 13$ , D1 inhibition  $n = 15$ , D1 control  $n = 10$ ). Four weeks later, rsfMRI measurements were acquired with a 7 T Bruker scanner following well-established pipelines for animal handling, anesthesia and data acquisition. An GE-EPI sequence was used with repetition time of 1 s and echo time of 15 ms with 2280 volumes for a total scan time of 38 min. Clozapine (30 µg/kg) was intravenously injected 15 min after the start of the fMRI scan session to activate the DREADD. RsfMRI data was preprocessed using an already established pipeline to remove artefacts. The structural connectome of the mouse brain was used to map out the regions that constitute striato-thalamo-cortical circuit. BOLD time series dynamics of local regions were quantified using a machine-learning approach that leverages 7702 time-series features using ‘highly comparative time series analysis’ toolbox. Specifically, a linear support vector machine (using tenfold stratified cross validation averaged over 50 repeats) was used to assess changes in BOLD dynamics upon DREADD activation. Statistical significance was estimated using a permutation test, controlling the false discovery rate across the multiple hypothesis tests.

We found that CPdm neuromodulation alters BOLD dynamics within thalamic subregions that project back to CPdm, leading to slower and more autocorrelated fluctuations of the time series signal. In the cortex, the strongest changes in local dynamics were observed in unimodal regions, i.e., regions that process information from a single sensory modality, while changes in the local dynamics weakened along a putative cortical hierarchical gradient towards transmodal regions. In contrast, a decrease in functional connectivity was observed only for cortico-striatal connections after D1 excitation. Our results provide a comprehensive understanding of how targeted cellular-level manipulations affect both local dynamics and interactions at the macroscale, revealing the influence of structural characteristics of a circuit and hierarchical cortical gradients in shaping those dynamics. Furthermore, we provide causal evidence into how regional dynamics change after neuromodulation shaping the temporal autocorrelation of distributed but connected regions at the macroscale. Our findings contribute to ongoing attempts to understand the influence of structure–function relationships in shaping inter-regional communication at subcortical and cortical levels. The results reported here could help in developing, refining, and validating dynamical models for the brain’s distributed dynamics.

### P114 Estimating the phase resetting curve of basal ganglia neurons from responses to pulsed noise and sine wave currents

Erick Olivares<sup>\*1</sup>, Charles Wilson<sup>1</sup>

<sup>1</sup>Universidad de Texas at San Antonio, Department of Biology, San Antonio, TX, United States of America

\*Email: erickolivaresb@gmail.com

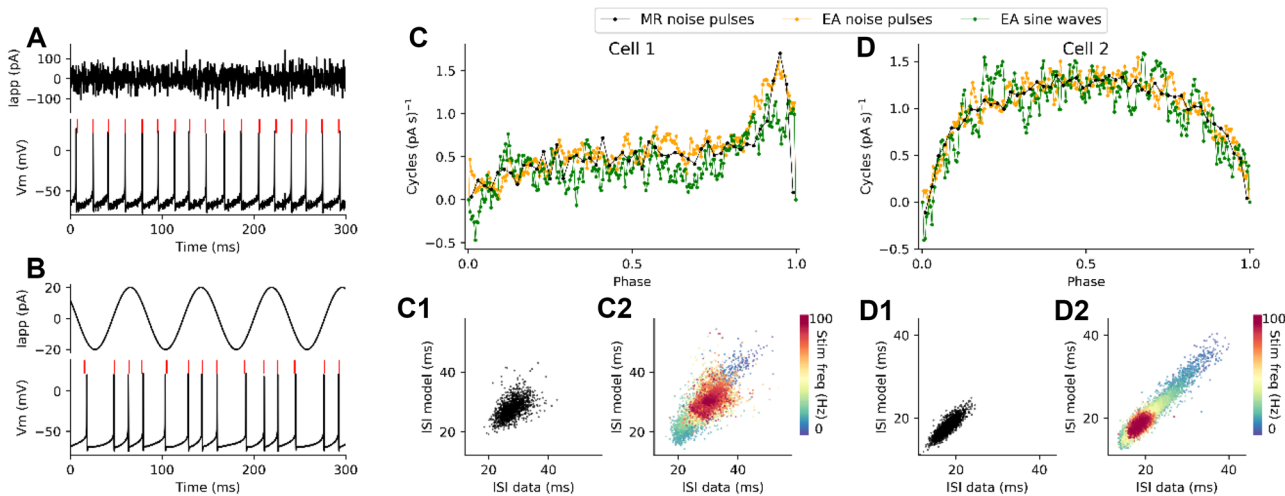


**Fig. 1** Spike times predictions from the phase model. **A, B** Examples of noise pulses and sine wave stimulation protocol. Actions potentials predicted by the phase model in dashed red lines on top of voltage traces. **C, D** PRC retrieved using the multiple regression and the EA method in both stimulation protocols. **C1-D1** Experimental ISIs

The globus pallidus is populated by oscillatory neurons. Parvalbumin-positive neurons in the external globus pallidus (GPe-Parv) fire autonomously at rates that range from 10 to 70 Hz [1]. In addition to forming the main efferent pathway GPe-Parv neurons are interconnected by local axon collaterals, creating an active local inhibitory network that acts as a hub in the indirect pathway of the basal ganglia [2]. An accurate model of the local network of GPe-Parv neurons requires a model for the single neuron that can predict the behavior of the neurons and also represent the intrinsic heterogeneity in their firing rate and responses to inputs.

The spiking of oscillatory neurons can be predicted by the phase resetting model [3]. In this model, the phase resetting curve (PRC) characterizes the sensitivity of the oscillator to a given stimulus depending on its time of arrival in the inter-spike interval (ISI). The PRC can be estimated experimentally and together with the neuron intrinsic rate, can capture the neuron heterogeneity inside a neuronal population. Traditionally, the PRC is estimated by analyzing the perturbation produced by a brief pulse of current during the ISI [4]. This method can be improved by delivering a barrage of brief pulses with random amplitudes and making use of multiple regression to fit the PRC from the charge delivered in the binned ISI and its effect on ISI length [5]. In principle, any broad bandwidth stimulation can carry the information necessary to retrieve a PRC, but, as far as we know, there is no general method. In this work, we used an evolutionary algorithm (EA), an assumption-free method to extract the PRC that predicts the perturbations in spike timing created from any broadband stimulus. The EA is effective in minimizing non-linear functions in high dimensional spaces. We designed an EA to find the PRC that minimizes the difference of the predicted and experimental spike timing in response to broadband noise or to sine wave stimuli over a range of frequencies. We validated the EA approach in the barrage of brief noise pulses, the PRCs obtained with the EA were similar to the ones obtained using the multiple regression method. Then, we evaluate the EA method in a different stimuli protocol consisting of pure sine waves from 1 to 100 Hz in recording sweeps of 10 s each. While the multiple regression method shows to be numerically unstable in this stimuli protocol, the EA method showed to be robust. GPe-Parv cells exhibit a wide variety of PRC shapes that presumably reflect different styles of synaptic

from the noise pulses protocol versus ISIs predicted using the EA-PRC from sine wave data. C2-D2) Experimental ISIs from the sine wave protocol versus ISIs predicted using the EA-PRC from noise pulses data, colors depict the stimuli frequency at which the ISIs were obtained

integration. PRCs obtained using noise pulses closely resembled those calculated using sine wave stimuli in the same cell (Fig. 1). Moreover, the PRC calculated from one stimulation protocol could be used to predict spike times observed in response to other stimulus waveforms.

## References

- Mercer, J. N., Chan, C. S., Tkatch, T., Held, J., & Surmeier, D. J. Nav1.6 sodium channels are critical to pacemaking and fast spiking in globus pallidus neurons. *Journal of Neuroscience*. 2007; 27(49): 13552–13566.
- Olivares, E., Higgs, M. H., & Wilson, C. J. Local inhibition in a model of the indirect pathway globus pallidus network slows and deregularizes background firing, but sharpens and synchronizes responses to striatal input. *Journal of Computational Neuroscience*. 2022; 50(2): 251–272.
- Wilson, C. J. Predicting the response of striatal spiny neurons to sinusoidal input. *Journal of neurophysiology*. 2017; 118(2): 855–873.
- Achuthan, S., & Canavier, C. C. Phase-resetting curves determine synchronization, phase locking, and clustering in networks of neural oscillators. *Journal of Neuroscience*. 2009; 29(16): 5218–5233.
- Netoff, T., Schwemmer, M. A., & Lewis, T. J. Experimentally estimating phase response curves of neurons: theoretical and practical issues. In *Phase response curves in neuroscience*. 2012; pp. 95–129. Springer, New York, NY.

## P115 Spiking neural networks as finite state transducers for temporal pattern recognition

Yaqoob Muhammad<sup>\*1</sup>, Volker Steuber<sup>2</sup>, Borys Wróbel<sup>3</sup>

<sup>1</sup>University of Hertfordshire, Computer Science, Hatfield, United Kingdom

<sup>2</sup>University of Hertfordshire, Biocomputation Research Group, Hatfield, United Kingdom

<sup>3</sup>Adam Mickiewicz, University in Poznan, Evolving Systems Laboratory, Poznan, Poland

\*Email: m.yaqoob3@herts.ac.uk

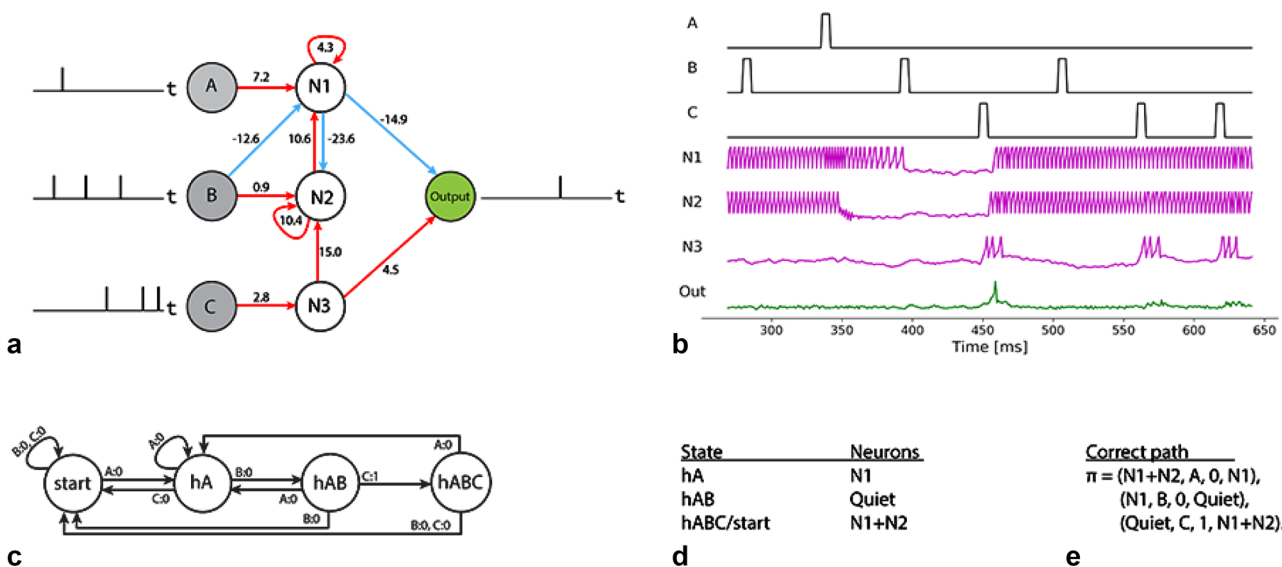


**Fig. 1** **a** Minimal spiking neural network evolved to recognise a pattern of three signals. **b** The behaviour of the network receiving a random input stream. **c** Finite state transducer maps input string ABC to

Spiking neural networks (SNNs) have been studied extensively to understand and reproduce the capabilities of the human brain. Models of finite automata [1] have been used previously to model individual neurons [2]. In our work, we use the theoretical framework of finite automata to describe and analyze the behavior of small *networks* of spiking neurons. Having a formal computational model of spiking neural networks will help in understanding the relationship between the underlying structure and the corresponding behavior. We suggest a formal model of a finite state transducer (FST) to describe the functioning of minimal SNNs evolved to perform temporal pattern recognition [3]. The operation and the constituents of the evolved SNNs are found to have a one-to-one correspondence with the 6 tuple of a FST that maps the input string ABC to the output string {0,1} [3]. Thus, a spiking neural network recognizing a temporal pattern of three signals can be formalized as a 6 tuple machine,  $SNN = (Q, \Sigma, \Delta, q_0, F, \sigma)$ , where Q is the finite set of network states, the spiking of interneurons in the interval following an input signal describes a network state = {start, hA, hAB, hABC},  $\Sigma$  is the finite set of input channels = {A, B, C},  $\Delta$  represents the finite set of spiking behaviors of the output neurons {spiking, quiet},  $q_0$  is the starting state of the network (the spiking behavior of interneurons when the network receives a signal in the wrong order), F is the finite set of final states (when the network receives signals in the correct order ABC) = {hABC}, and  $\sigma$  defines transitions between network states  $\sigma \subseteq Q \times \Sigma \times \Delta \times Q$ . The evolved network receives a continuous input stream and produces spike(s) in the output neuron only if the signals are received in the correct order (Fig. 1a). A segment of the spiking activity in the network is shown in Fig. 1b. Before the onset of the first correct signal (around 350 ms), the network is in the start state (continuous spiking of neurons N1 and N2). When the network receives the first target signal A, N1 speeds up and shuts down N2 – transforming the network to hA state, represented by continuous spiking of N1. The persistent spiking of N1 also prevents the output neuron from spiking. Subsequently, when the network receives a signal on channel B, it shuts down N1 and transforms to the hAB state, enabling the output neuron to spike when receiving the last target signal C. The analysis of the evolved SNNs revealed that these transitions between network states accomplish temporal pattern recognition. Moreover, we demonstrate that the behavior of a spiking neural network can be formalized as a finite state

output string {0,1}. **d** Network states with corresponding active neurons. **e** The correct path in the network, from starting start (spiking of N1 and N2) to the accepting state (the output spikes)

transducer. In future, we plan to wire minimal SNNs together to build larger systems that can recognize complex patterns.

## References

1. R. Alur and D. L. Dill. A theory of timed automata. *Theoretical computer science*. 1994; 126(2):183–235.
2. E. De Maria, C. Di Giusto, and L. Laversa. Spiking neural networks modelled as timed automata: with parameter learning. *Natural Computing*. 2020; 19(1):135–155.
3. M. Yaqoob and B. Wróbel. Robust very small spiking neural networks evolved with noise to recognise temporal patterns. In ALIFE 2018: Conference on Artificial Life – MIT Press, pages 665–672. 2018.

## P116 Fractal correlation patterns of cognitive processing in working memory tasks

Paweł Oświecimka<sup>\*1</sup>, Anna Ceglarek<sup>2</sup>, Jeremi Ochab<sup>3</sup>, Marcin Wątorek<sup>3</sup>

<sup>1</sup>Institute of Nuclear Physics Polish Academy of Sciences, Kraków, Poland

<sup>2</sup>Jagiellonian University, Kraków, Poland

<sup>3</sup>Jagiellonian University, Institute of Theoretical Physics, Kraków, Poland

\*Email: pawel.oswiecimka@uj.edu.pl

False memories are a topic that has enjoyed decades of fascinating research. With the advance of experimental techniques, insight into cognitive processes of short-term memory distortions has become possible. One such technique allowing to measure neural activity while a person is memorizing and retrieving information is functional magnetic resonance imaging (fMRI). However, fMRI data have a non-trivially associated auto-correlation and cross-correlation signal structure and are notoriously challenging to analyze due to their very low temporal resolution (of the order seconds).

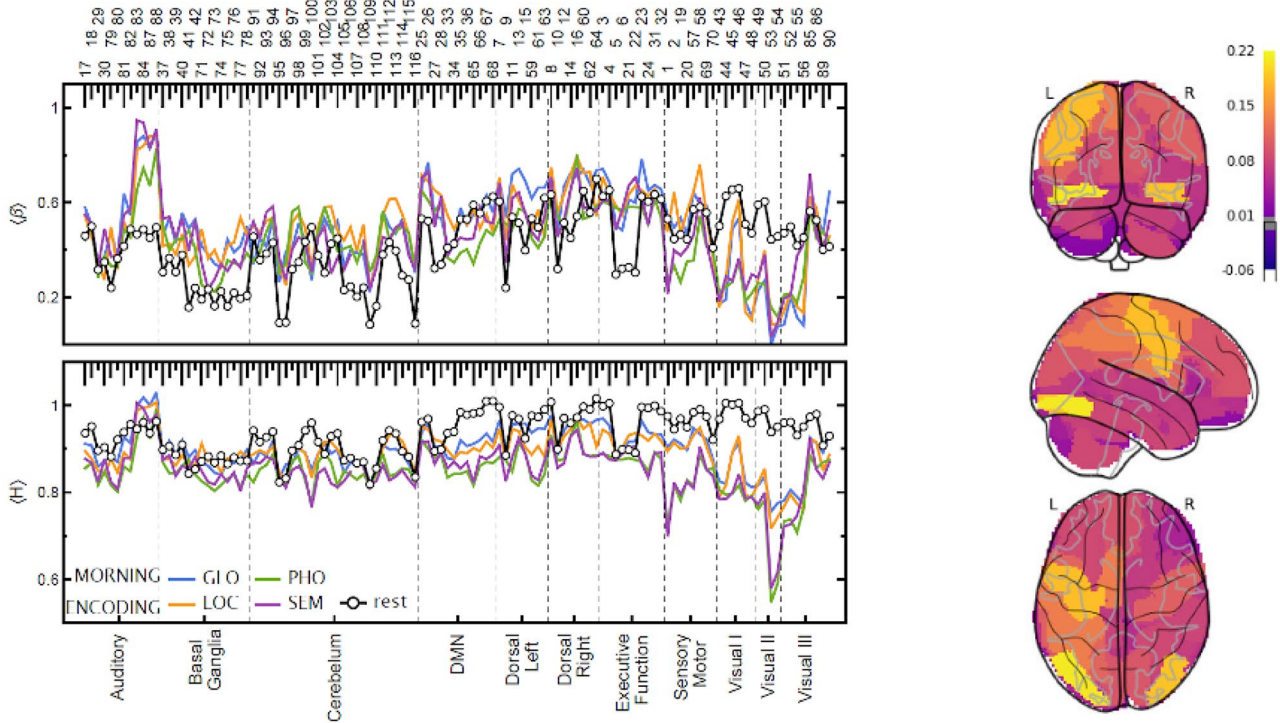


**Fig. 1** (Left panel) Plots of the spectral, and Hurst,  $H$ , scaling exponents estimated for time series in the encoding phase. The exponents were calculated for each ROIs and ordered on the plot according to

the AAL atlas (top) and resting-state networks. (Right panel) Glass brain plot of  $\langle H \rangle$  differences between verbal (PHO, SEM) and non-verbal (LOC, GLO) tasks rendered with nilearn

In our study, we applied fractal analysis to investigate fMRI data representing a diurnal variation of working memory in four types of experimental tasks: two visual-verbal (based on lists of semantically or phonetically associated words) and two non-verbal (pictures of similar objects). The regional brain activity was quantified with the Hurst exponent and detrended cross-correlation coefficients. Our analyses clearly show that the fMRI data obtained from most brain areas can be regarded as  $1/f$ . Moreover, the obtained characteristics of the signals in specific occipital lobe areas depend not only on the type of experimental tasks but also on the stage of the experiment, i.e. memorizing the stimuli or information retrieval.

A particularly apparent difference is visible between memorization in verbal and non-verbal tasks. In the former case, for some brain regions in the Visual II resting-state network, the Hurst exponents assume values very close to 0.5, indicating a lack of linear temporal correlations in the signals. In contrast, we observe more persistent behavior in the latter. The reduction of persistent behavior in tasks relative to the spontaneous brain activity (resting state) is statistically significant in many brain areas, as presented in Fig. 1.

The cross-correlations between brain areas are, too, indicative of differences in the processing of tasks and experimental stages. Uncovering such regionally coordinated changes involves comparing distributions of correlation matrices' eigenvalues. We strengthen these results by grouping eigenvalues according to their eigenvector similarity rather than their natural order. The detrended correlations turn out to be more sensitive than Pearson correlations, showing the greatest differences between the resting state and other tasks, between memorization and retrieval and between verbal and non-verbal tasks, as well as other subtler results.

#### Acknowledgments

The study was supported by the Foundation for Polish Science co-financed by the European Union under the European Regional

Development Fund in the POIR.04.04.00-00-14DE/18-00 project is carried out within the Team-Net program.

#### P117 Chronic cannabis use effects on brain structural connectivity: A connectome analysis

Suzan Maleki<sup>1\*</sup>, Chao Suo<sup>2</sup>, Stuart Oldham<sup>1</sup>, Yann Chye<sup>3</sup>, Karen Caeyenberghs<sup>4</sup>, Rebecca Segrave<sup>3</sup>, Karyn Richardson<sup>3</sup>, Sam Hughes<sup>3</sup>, Edouard Kayayan<sup>3</sup>, Joseph Pitt<sup>3</sup>, Warda Syeda<sup>5</sup>, Murat Yucel<sup>2</sup>

<sup>1</sup>Monash University, Clayton, Australia

<sup>2</sup>Monash University, BrainPark, Turner Institute for Brain and Mental Health, School of Psychological Science, Melbourne, Australia

<sup>3</sup>Monash University, Psychological Sciences, Clayton, Australia

<sup>4</sup>Deakin University, School of Psychology, Australia

<sup>5</sup>University of Melbourne, Psychological Sciences, Melbourne, Australia

\*Email: suzan.maleki@monash.edu

Cannabis is the most commonly illicit substance used, with approximately 180 million users globally. According to the literature, regular cannabis use causes deficits in memory, learning, executive functions, and also is associated with depression and anxiety. Neuroimaging studies using magnetic resonance imaging (MRI) have attempted to investigate the effects of regular cannabis use on cortical and subcortical structures with heterogeneous findings [1]. While white matter (WM) integrity is less examined, diffusion studies to date have reported altered WM tracts connecting hippocampus, frontal regions, and cerebellum [2]. However, most diffusion studies used basic parameters (e.g., fractional

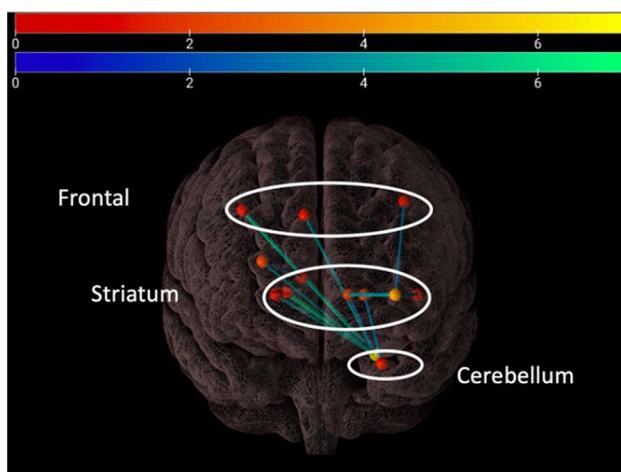


**Fig. 1** Significant group differences of structural connectivity observed between chronic cannabis users and healthy controls across 14 nodes and 13 edges including three clusters of frontal, striatum, and cerebellum

anisotropy (FA)), therefore, more advanced analysis approaches are needed to better characterize cannabis induced WM impairments. We pre-processed anatomical T1 and diffusion weighted MRI data from 47 regular cannabis users and 39 healthy controls collected at Monash Biomedical Imaging (MRI protocol, T1: TR = 2300 ms, TE = 2.07 ms, voxel size = 1 mm<sup>3</sup>; diffusion: 60 directions, b = 3000 s/mm<sup>2</sup>, TR = 8800 ms, TE = 110 ms, voxel size = 2.5 mm<sup>3</sup>). Then we estimated WM fiber orientation distribution (FOD) images from upsampled pre-processed diffusion data using single-shell 3-tissue constrained spherical deconvolution (ss3t-CSD) method. Next, we performed anatomically constrained tractography (ACT) using “iFOD2” probabilistic algorithm to generate 20 M tracts at whole brain level using MRtrix3tissue and FSL softwares. We then filtered reconstructed tractograms using spherical-deconvolution informed filtering of tractograms. Finally, we performed connectome analysis by generating individual connectivity matrices from filtered ACT tractograms and FreeSurfer parcellations (84

nodes using Desikan-Killiany atlas). Network based statistics software used to statistically test the group differences.

We observed significant group differences of structural connectivity between chronic cannabis users and healthy controls. Our findings indicate that cannabis users had reduced structural connectivity across 14 nodes and 13 edges (connections) compared to healthy non-users (two-sample t-test,  $p = 0.017$ , permutations = 5000). The observed network differences can be classified into three main clusters of frontal regions, striatum (putamen and pallidum), and cerebellum (Fig. 1).

To our knowledge, this is one of the first studies to use advanced structural connectome analysis on chronic cannabis users. Our results align with previous literature on volumetric, morphometric and basic diffusion measurements [2]. Future work will examine whether the affected regions are associated with cognitive deficits in chronic cannabis users.

## References

1. Lorenzetti, Valentina, Yann Chye, Pedro Silva, Nadia Solowij, and Carl A. Roberts. Does Regular Cannabis Use Affect Neuroanatomy? An Updated Systematic Review and Meta-Analysis of Structural Neuroimaging Studies. *European Archives of Psychiatry and Clinical Neuroscience*. 2019; 269: 59–71
2. Chye, Yann, Rebecca Kirkham, Valentina Lorenzetti, Eugene McTavish, Nadia Solowij, and Murat Yücel. Cannabis, Cannabinoids, and Brain Morphology: A Review of the Evidence. *Biological Psychiatry: Cognitive Neuroscience and Neuroimaging*. 2021; 6(6): 627–635

## P118 Analysis of multipoint activity in the mouse brain based on flocking algorithm

Margarita Zaleshina<sup>\*1</sup>, Alexander Zaleshin<sup>2</sup>

<sup>1</sup>Moscow Institute of Physics and Technology, Russia

<sup>2</sup>Institute of Higher Nervous Activity and Neurophysiology, Moscow, Russia

\*Email: zaleshina@gmail.com

Artificial neural networks are usually suitable for describing connections and processes occurring in the brain. However, the methods used

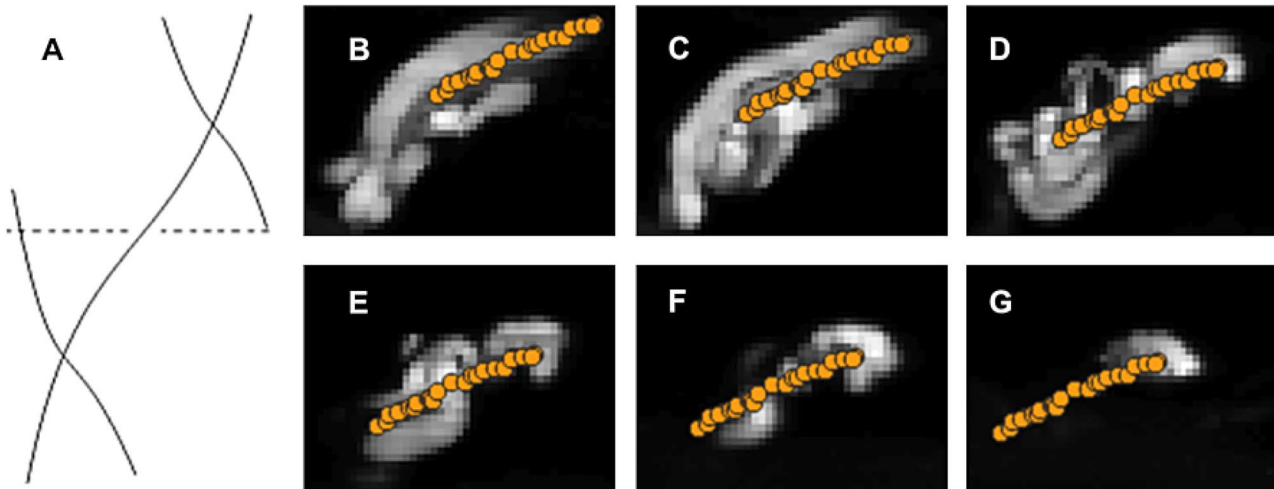


**Fig. 1** **A** Spreading of optogenetics luminosity along neural circuits. **B–F** Displacement of centroids of neural networks on neighboring slices of a multipage TIFF file. The orange dots show the centroids for 21 adjacent slices

to calculate the behavior of animals in a flock can also be extended to model neural networks [1]. We assume that the topological properties of the distribution of individuals in a moving flock are able to represent information about the environment in the same way as it is realized by a network of neurons. When the network's topological structure is rebuilt, the results of information processing change. The spread of activation in nearby neural circuits can occur in one area of the brain, with further extent of activation in different areas of the brain. The trace activity of neural circuits can affect the parameters of subsequent activation of neurons occurring in the same locations.

In this work, we processed sets of in the mouse brain images obtained by the light-sheet fluorescence microscopy method. Recognition of multipoint activity and spatial analysis of the distribution of cells according to fluorescence microscopy datasets was performed based on data packages published in an open repository (<https://ebrains.eu> [2, 3]). In our study 60 fluorescence microscopy datasets obtained from 23 mice ex vivo and represented in multi-page TIFF files were analyzed.

Individual elements in fluorescence microscopy records were selected based on their brightness in grayscale mode. The spatial distributions of individual cells at the same moment of measurement were calculated during the analysis. The centroids of different cells' ensembles are calculated for groups of fluorescence-activated cells.

Location variations of neural circuit activities were studied on the basis of the flocking algorithm. The displacement trajectories of multipoint activity were revealed for various sets of analyzed ensembles. All calculations were performed on the basis of the characteristic features of neural circuit trajectories, such as common intersections and overlapping buffer zones of different tracks. Additionally, the "spatial areas of the trajectories" (zones of their location) were determined and the trajectory blurring corridors were calculated.

Spreading of optogenetics luminosity along neural circuits with closure and divergence of individual sets of trajectories is presented in Fig. 1A. The displacements of the collective activity of the "flock" of neurons were traced by the centroids and by the blurring of areas of multipoint neural activity (Fig. 1B–F).

In this work we demonstrated the usability of flocking algorithm in analysis of spatiotemporal distribution of multipoint neuronal activity of fluorescence-activated cells. We have shown that geoinformation applications for calculating spatial relationships in fluorescence microscopy datasets enrich the possibilities of processing connectivity and neighborhood in neural networks. In the future, the methods of flock analysis can be used to detect the interdependence of the spatial–temporal distribution of different ensembles of neurons in multifactorial studies.

## References

1. Battersby S. News Feature: The cells that flock together. PNAS. 2015; 112(26):7883–5.
2. Silvestri L, et al. Whole brain images of selected neuronal types. HBP Neuroinformatics Platform. 2019.
3. Silvestri L, et al. Whole-brain images of different neuronal markers. HBP Neuroinformatics Platform. 2020.

## P119 A method for improving regression and correlation coefficient estimates in the presence of noise

Jason Pina<sup>\*1</sup>, Joel Zylberberg<sup>2</sup>

<sup>1</sup>York University, Department of Physics and Astronomy, Toronto, Canada

<sup>2</sup>York University, Centre for Vision Research and Department of Physics and Astronomy, Toronto, Canada

\*Email: jay.e.pina@gmail.com

A key challenge in neuroscience is estimating relationships between biological, behavioral, or cognitive variables in the presence of noise. Such noise, or measurement error, arises from uncertainties due to either recording device limitations or intrinsic biological variability, both of which are ever-present in neuroscience experiments. This noise can greatly reduce estimated linear regression and correlation coefficients, as well as the fraction of explained variance (or  $R^2$  value), compared to their true values. Despite the large impact this *regression dilution* can have on downstream inferences that result from these reported estimates, it is seldom accounted for in neuroscience. However, in many neuroscience experiments, data that can be leveraged to eliminate this bias is already collected, as the relevant variables are often averages of multiple observations. We present a simple, easy-to-implement method that utilizes these multiple measurements to estimate the noise variance and allow for the regression dilution effect to be removed. Using simulated data, we show that the confidence intervals from our unbiased estimator indeed consistently capture the underlying regression and correlation coefficients, in sharp contrast with those from the uncorrected estimates. This demonstrates that our estimator is directly applicable to any linear regression analysis in neuroscience for which the variables are based off of averages, using data collected from a broad set of potential observation modalities. Such modalities include spike counts, fMRI, EEG, and PET scans, from which common regression analyses such as noise and signal correlations, inter-subject correlations (ISCs), functional connectivity analyses, and representational similarity matrices (RSMs) can be computed. All of these analyses can involve averaging at some stage of the process, such as over subjects, space (pixels/neurons), or time.

As a specific example of how our estimator can lead to new neuroscientific insights, we apply our method to 2-photon calcium imaging data from recent experimental work. In the experiment, neuronal responses to two classes of novel stimuli were compared across separate recording sessions in the same neurons to determine whether changes consistent with learning were observable. Detecting these changes required ruling out regression coefficients equal to one (corresponding to no change), which standard methods are unable to do: due to regression dilution, the coefficients estimated from noisy data will be less than one even when the neural responses do not change. In contrast, our approach successfully identified several conditions with low uncorrected regression coefficients as being consistent with a true, underlying regression coefficient of  $\sim 1$ , while ruling out several others as indeed having true coefficients well below 1, findings that better delineate the experimental conditions under which individual neuronal changes occur. Thus, our simple method to account for the effects of noise on estimates of correlation and linear regression coefficients sheds light on learning in the context of novel stimuli, an active area of interest in neuroscience.

## P120 Computational modeling of neuron-astrocyte interactions in large neural populations using the NEST simulator

Jugoslava Acimovic<sup>\*1</sup>, Han-Jia Jiang<sup>2</sup>, Tiina Manninen<sup>1</sup>, Jonas Stampanis<sup>2,4</sup>, Mikko Lehtimäki<sup>1</sup>, Marja-Leena Linne<sup>3</sup>, Markus Diesmann<sup>2,4</sup>, Sacha van Albada<sup>2,4</sup>

<sup>1</sup>Tampere University, Faculty of Medicine and Health Technology, Tampere, Finland

<sup>2</sup>Jülich Research Centre, Institute of Neuroscience and Medicine, Jülich, Germany

<sup>3</sup>Tampere University, Medicine and Health Sciences, Tampere, Finland

<sup>4</sup>Jülich Research Centre, Institute for Advanced Simulation, Jülich, Germany

\*Email: jugoslava.acimovic@tuni.fi

Astrocytes, the most abundant glial type in the cortex, interact with neighboring synapses, neurons and glia through complex cellular machinery [1]. Astrocytes form mostly nonoverlapping microdomains, and a single such microdomain can be reached by several hundreds of neurons and as many as ~100,000 synapses [3]. Experimental studies have demonstrated coordinated neuronal and astrocytic activity *in vivo* [2]. Computational methods can help to integrate the data on cellular mechanisms and structural organization of the cortical tissue, and to explore how neuron-astrocyte interactions modulate population-level activity.

In the past two decades, the number of published computational models that include some form of neuron-astrocyte interaction has been steadily increasing [4, 5]. The majority of the published models was implemented in custom made code that is often not publicly available. Implementing these models in well-established open-source simulation tools improves reproducibility of the results and sharing of the models [4, 5]. Two earlier efforts to develop open-source tools for simulation of neuronal and glial networks include Arachne [6], and an implementation in the Brian simulator [7].

We developed a new solution for efficient simulation of large heterogeneous populations of neurons and astrocytes implemented as a module in the NEST simulator (<https://www.nest-simulator.org/>). We first extended the concept of a synapse in NEST to include interaction between three compartments, pre- and postsynaptic neurons and the neighboring astrocytic compartment. Next, we developed new method to establish efficiently interactions within a large heterogeneous cellular population of neurons and astrocytes. Finally, we tested the new tool by analyzing spontaneous activity regimes in medium-size networks composed of several hundreds of cells.

In summary, we present a new module for NEST simulator that supports reproducible, open access and efficient development of

computational models for large heterogeneous populations of neurons and astrocytes.

### Acknowledgements

The study received funding as a Partnering Project to the European Union's Horizon 2020 Framework Programme for Research and Innovation under the Specific Grant Agreement No. 945539 (Human Brain Project SGA3). The work is also supported by the Academy of Finland (decision Nos. 326494, 326495, and 345280).

### References

1. Bazargani N, Attwell D. Astrocyte calcium signaling: the third wave. *Nature Neuroscience*. 2016; 19(2):182–9.
2. Lines J, et al. Astrocytes modulate sensory-evoked neuronal network activity. *Nature Communications*. 2020; 11:3689.
3. Zisis E, et al. Digital Reconstruction of the Neuro-Glia-Vascular Architecture. *Cerebral Cortex*. 2021; 00:1–18.
4. Manninen T, et al. Computational Models for Calcium-Mediated Astrocyte Functions. *Frontiers in Computational Neuroscience*. 2018; 12:14.
5. Manninen T, Aćimović J, et al. Challenges in Reproducibility, Replicability, and Comparability of Computational Models and Tools for Neuronal and Glial Networks, Cells, and Subcellular Structures. *Frontiers in Neuroinformatics*. 2018; 12:20.
6. Aleksić SG, et al. ARACHNE: A neural-neuroglial network builder with remotely controlled parallel computing. *PLoS Computational Biology*. 2017; 13(3): e1005467.
7. Stimberg M, Goodman DFM, Brette R, De Pittà M. Modeling neuron–glia interactions with the Brian 2 simulator. In: De Pittà M, Berry H (eds) *Computational glioscience*. Springer, Cham. 2019; 471–505.

**Publisher's Note** Springer Nature remains neutral with regard to jurisdictional claims in published maps and institutional affiliations.